SMALL VESSEL FUNCTION & MICROINFARCTS: ZOOMING IN ON CEREBRAL SMALL VESSEL DISEASE WITH MRI

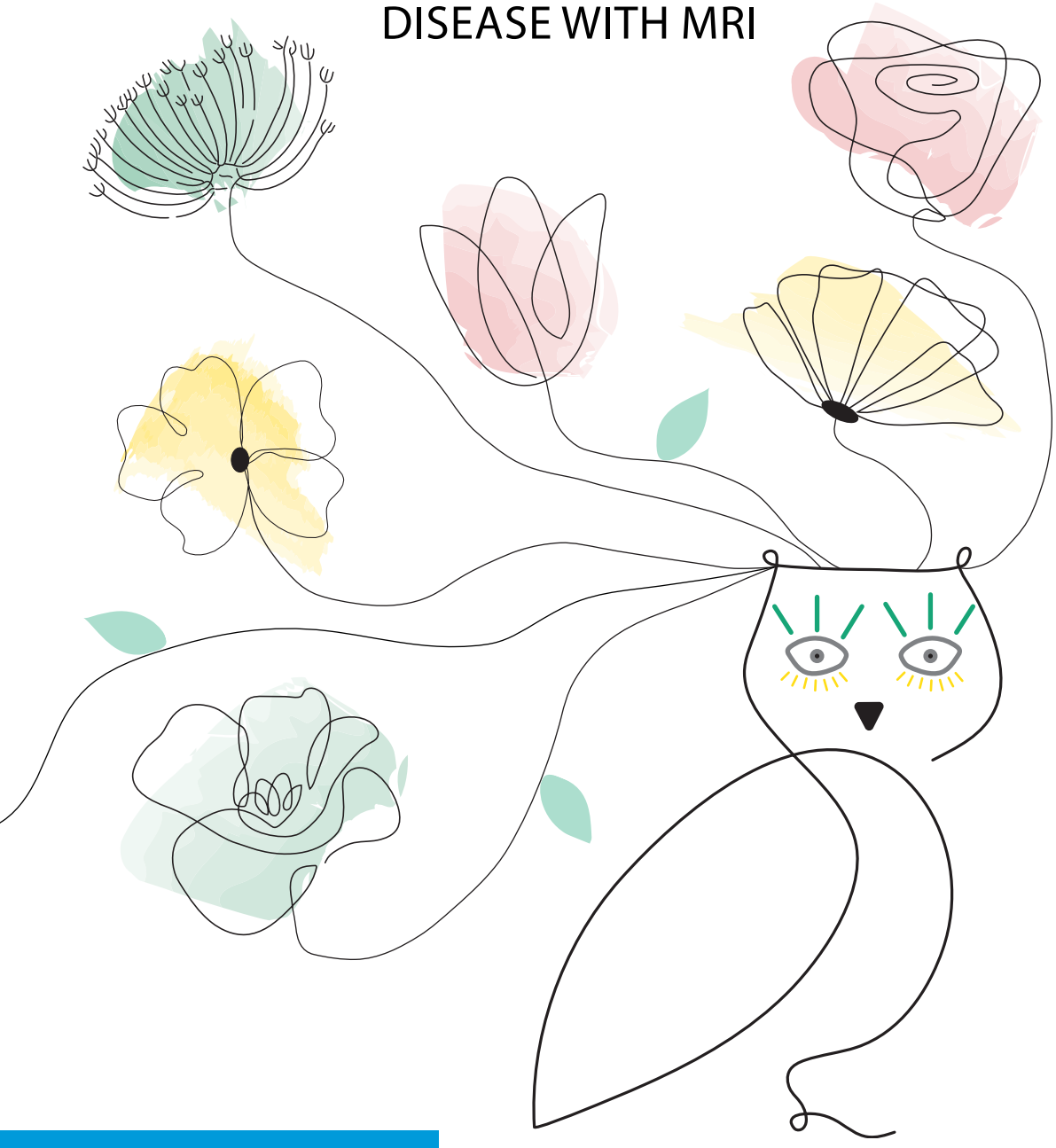

UMC Utrecht Brain Center

Hilde van den Brink

Small vessel function & microinfarcts: zooming in on cerebral small vessel disease with MRI

Hilde van den Brink

ISBN:	978-94-6458-907-8
Printing:	Ridderprint | www.ridderprint.nl
Cover design:	Hilde van den Brink
Layout and design:	Wiebke Keck, persoonlijkproefschrift.nl

Financial support by the Dutch Heart Foundation and Alzheimer Nederland (Amersfoort) for the publication of this thesis is gratefully acknowledged.

The research described in this thesis was supported by a grant of the Dutch Heart Foundation (CVON 2018-28 & 2012-06 Heart Brain Connection), the Netherlands Organisation for Scientific Research (NWO Vici grant 918.16.616) and the European Union's Horizon 2020 (SVDs@target 666.881).

Small vessel function & microinfarcts: zooming in on cerebral small vessel disease with MRI

Inzoomen op oorzaken en gevolgen van ziektes van de kleine hersenbloedvaten met MRI
(met een samenvatting in het Nederlands)

Proefschrift

ter verkrijging van de graad van doctor aan de
Universiteit Utrecht
op gezag van de
rector magnificus, prof.dr. H.R.B.M. Kummeling,
ingevolge het besluit van het college voor promoties
in het openbaar te verdedigen op

donderdag 16 maart 2023 des middags te 12.15 uur

door

Hendrikje van den Brink

geboren op 1 december 1991
te Harderwijk

Promotor:
Prof. dr. G.J. Biessels

Copromotoren:
Dr. J.J.M. Zwanenburg
Dr. J.C.W. Siero

Beoordelingscommissie:
Prof. dr. H.B. van der Worp
Prof. dr. E.M. Hol
Prof. dr. B.K. Velthuis
Prof. dr. M.W. Vernooij
Prof. dr. E.T. van Bavel

“Nobody cares how much you know
until they know how much you care”

Theodore Roosevelt

Table of Contents

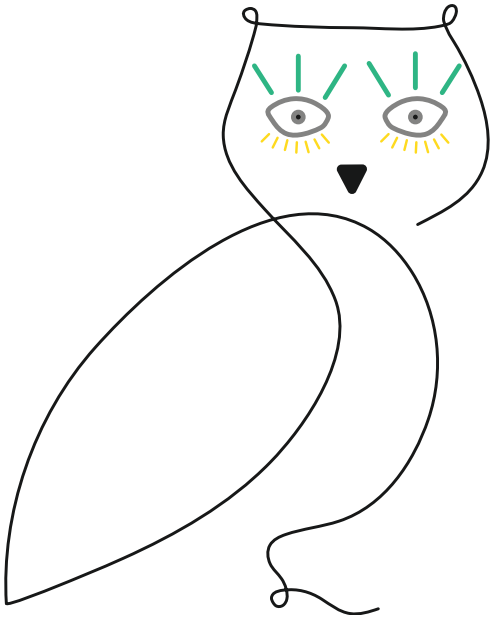

1

General introduction

Cerebral small vessel disease (cSVD) refers to pathological processes that affect the perforating arteries, arterioles, capillaries and venules of the brain, with both monogenic as well as sporadic causes.[1] cSVD is known to lead to widespread tissue injury in the brain, which gives rise to functional impairment.[1] cSVD causes about one quarter of all strokes and contributes to about half of all dementias through which it has a profound health impact.[2] Despite these serious consequences, apart from generic vascular risk factor management, there still is no specific treatment available. This likely has to do with the fact that underlying disease mechanisms leading to parenchymal injury and functional impairment are not entirely clear yet (see Figure). In Chapter 2 we describe a case study of identical twins which in my view clearly illustrates that our understanding of the causative factors in cSVD is still far from complete.

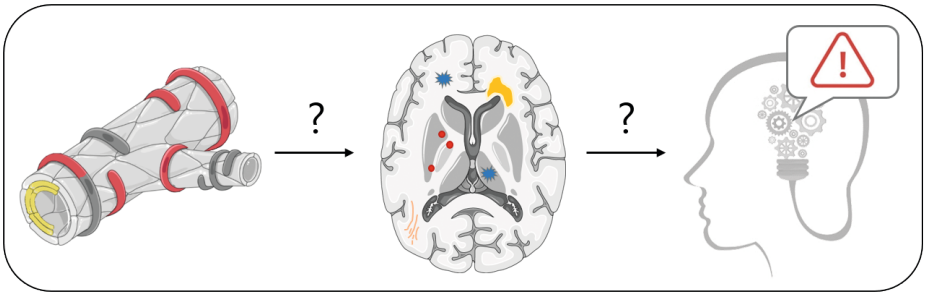

Figure: Graphical impression of cSVD pathology (left), parenchymal injury (middle) and functional impairment (right). The question marks indicate that we are yet unsure through which disease mechanisms these events are linked.

When imaging cSVD in humans *in vivo* we mostly make use of magnetic resonance imaging (MRI).[3] Despite the wide range of available MRI markers for cSVD, there are two important limitations of the currently available markers. First, it is very difficult to study the disease at the level of the affected small vessels, given the small diameter of the affected blood vessels in cSVD and the limited resolution of MRI scanners. This hampers the study of underlying disease mechanisms at the core of the disease, the small vessels themselves (question mark 1 in the Figure). So far, cSVD has therefore mostly been studied through markers of parenchymal injury, such as white matter hyperintensities, microbleeds, lacunes and enlarged perivascular spaces, which are essentially downstream consequences of cSVD.[4] These lesions represent the end-stage of pathological processes and are largely irreversible. A second limitation of the available MRI markers in cSVD is that, even though these markers have a fair specificity for cSVD and relate to important clinical outcomes (e.g. cognitive decline and dementia), they together cannot explain the full burden of cSVD-related functional impairment.[5,6] The lesion load of established markers does not fully predict the severity of sypmtoms in individual patients (question mark 2 in the Figure). We are thus likely missing injury that is contributing to clinical symptoms.

There is thus a clear need for biomarkers that capture cSVD at the level of the small vessels themselves, as well as new markers to better capture tissue injury in cSVD. Continuous developments on ultra-high field imaging and translation of new measures to clinical MRI scanners provide new options to address these knowledge gaps.[3] I will focus on two of these developments in this thesis. The overarching aim of my thesis is to **characterize new *in vivo* MRI markers of cerebral small vessel disease, in particular small vessel function and cerebral microinfarcts**.

Small vessel function

With the development of ultrahigh field imaging at 7T-MRI in humans, we can now image the small vessels themselves *in vivo*. Individual small perforating arteries were first visualised with MRI in cSVD 12 years ago, revealing that patients with cSVD showed fewer lenticulostriate arteries than controls.[7–9] From studies in experimental animal models, we know that the neuropathological changes in the small vessels affect the functioning of the small vessels as well.[10–13] Therefore, in an effort to capture even earlier pathological alterations, research over recent years aimed to find ways to study the function of small vessels in humans. At the start of my PhD project, we had several novel measures available on 7T-MRI to assess small vessel function *in vivo* in humans. Our first measure concerns the assessment of blood flow velocity and pulsatility in small perforating arteries.[14,15] Blood flow pulsatility is of particular interest in cSVD, because small vessel pathology is hypothesized to cause stiffened vessels walls that are insufficiently capable of dampening arterial pulse pressure, leading to transmission of higher pulsatility in arterioles where it causes additional damage.[1] On our Philips 7T-MRI system in Utrecht, we use a 2D single-slice velocity phase contrast sequence to measure blood flow velocity during the cardiac cycle in small perforating arteries that pass through the centrum semiovale and the basal ganglia. From these blood flow velocity measures we can calculate velocity pulsatility, as: (peak systolic velocity – peak diastolic velocity)/mean velocity. The first proof of principle study in six young subjects was published in 2016,[14] after which the technique was further optimized to improve estimates of velocity and pulsatility in perforating arteries with a sub-voxel size diameter, temporal resolution to attain reasonable scan time for use in elderly and optimize automatic detection of perforating arteries.[15,16] Test-retest agreement was found to be good in elderly[15] and a first explorative study in patients with stroke due to cSVD showed increased pulsatility compared with healthy controls.[17]

The second small vessel function measure concerns the assessment of small vessel reactivity. Vascular reactivity is a vital component of vascular function that enables the adjustment of blood flow to the brain when needed by altering vessel tone and diameter.[1] Small vessel pathology is known to alterations in the small vessel walls, among which reduced elasticity of the vessel wall. This small vessel stiffness is, among others, thought to reduce vasodilatory and constrictive capacity, thereby decreasing small vessel reactivity.[1,18] This capacity for small vessel reactivity can be tested by applying a stimulus

that triggers vessel reactivity and measuring the increase in blood flow to (specific parts of) the brain, for example, with the use of arterial spin labelling (ASL) or blood oxygenation level-dependent (BOLD) MRI.[19] There are varying methods to provoke vasodilation, each assessing different aspects of reactivity. Task-based methods, such as motoric and visual stimulation, are often used. Neuronal activation triggers neurovascular coupling and induces vasodilation through the capillaries in the feeding pre-capillary, parenchymal and penetrating arterioles to increase blood flow to the motor or visual cortex.[18] Additionally, there are neurovascular coupling *in*dependent methods that trigger vasodilation by directly affecting the vessel wall, for example by increasing CO_2 levels in the blood through breath-holding or by administering CO_2, or by administering vasodilatory medication such as acetazolamide.[19,20] Administration of CO_2 was found to be a consistent stimulus with good tolerability in cSVD patients.[21] The increase in CO_2 levels in the blood causes relaxation of vascular smooth muscle cells mostly at the level of the arterioles, thereby causing direct small vessel vasodilation.[22] These methods of assessing vascular reactivity have been used on 3T-MRI before, with findings suggestive of a relationship between decreased vascular reactivity and cSVD.[19,23,24] The advantage of applying these methods on ultra-high field imaging is that 7T-MRI provides a sensitivity and temporal and spatial resolution that was not possible before.[25] Additionally, the use of BOLD MRI on 7T-MRI has specific benefits. The BOLD signal on 7T-MRI is larger due to a higher sensitivity to the magnetic susceptibility effect of deoxyhemoglobin, and is weighted more toward signal from the cerebral small vessels than on lower field strengths.[25] These factors permit better separation of signal that originates from small vessels rather than larger draining veins.[25] To my knowledge, no previous studies have applied such measures of small vessel reactivity on 7T-MRI in patients with cSVD.

In the first part of this thesis, we study these novel measures of small vessel function as potential biomarkers in patients with cSVD. Specifically I aim to:

- Determine if novel measures of small vessel function on 7T-MRI can detect disease effects at the level of the small vessels themselves in patients with monogenic and sporadic cSVD
- Identify which aspects of small vessel function on 7T-MRI are altered in patients with monogenic and sporadic cSVD
- Assess how small vessel function alterations relate with markers of tissue injury and cognitive function

These measures are assessed in patients with cSVD in the ZOOM@SVDs study. Specifically, we assess basal ganglia and centrum semiovale perforating artery blood flow velocity and pulsatility, vascular reactivity to a short visual stimulus in the occipital cortex, and reactivity to hypercapnia throughout different areas of the brain. ZOOM@SVDs is a prospective observational cohort study in patients with monogenic and sporadic cSVD. The rationale and design of the study are described in Chapter 3 of this thesis.

Measures of small vessel function have a high potential to improve understanding of underlying disease mechanisms in cSVD and to be potential surrogate outcome markers in treatment trials that target the small vessels. However, we do not yet know if their signal-to-noise is high enough to detect any disease effects and if so, which aspects of small vessel function on 7T-MRI are altered. I address these topics in Chapter 4 and 5 for monogenic and sporadic cSVD respectively. In these chapters we also relate small vessel function measures with conventional MRI markers of tissue injury in cSVD and with cognitive function. In Chapter 6 we extend this focus by using whole-brain and voxel-level associations of small vessel function with white matter integrity to study if small vessel function could be causally related with tissue injury in cSVD. In this chapter we assess white matter integrity with diffusion MRI, which is currently the most sensitive method for studying tissue injury in cSVD.[26,27]

Cerebral microinfarcts

Cerebral microinfarcts are small brain lesions that are presumed to be ischemic and are a common neuropathological finding in patients with stroke and cognitive decline.[28,29] In fact, these lesions may comprise the most widespread form of vascular tissue injury.[30–32] Cerebral microinfarcts could be an important component in explaining the pathway between cSVD-related tissue injury and clinical symptoms, especially because they likely disrupt brain structure and function beyond their lesion boundaries.[28,33,34] With diffusion-weighted imaging, cerebral microinfarcts as small as 1-2mm in diameter can be detected in the acute phase. However, an important disadvantage of diffusion-weighted imaging is that the signal contrast fades over two weeks,[35] thereby allowing for very short time window for microinfarct detection. For a long time, cerebral microinfarcts in their chronic state were considered to be too small to be seen *in vivo*.[30] However, after microinfarcts were first visualized in the cortex with 7T-MRI, the relatively larger ones can now also be studied on widely available 3T-MRI.[36] This opened up the opportunity to study these chronic lesions, albeit only in the cortex, on a much larger scale and evaluate their value as a potential biomarker. An extensive review from 2017 described the progress that was made regarding understanding the detection, frequency, risk factors and functional consequences of cerebral microinfarcts.[28] A substantial number of remaining uncertainties remained, however. In the second part of this thesis we study two areas that required further research. Specifically I aim to:

- Improve understanding of underlying mechanisms of cerebral cortical microinfarcts, in particular the role of cerebral amyloid angiopathy and hypoperfusion
- Assess the prognostic value of cerebral microinfarcts for long-term clinical outcome

Causes of cerebral microinfarcts are known to be heterogeneous and are associated not only with small vessel disease, but also with large vessel disease and cardiac disease. There are also multiple possible underlying mechanisms that explain these relations:

small vessel disease pathology (e.g. cerebral amyloid angiopathy, arteriolosclerosis), microemboli and hypoperfusion.[28]

Cerebral amyloid angiopathy (CAA) is characterized by β-amyloid deposition in the walls of small arterioles and capillaries in the cerebral cortex and meninges, known to lead to haemorrhagic, but likely also ischemic lesions.[37,38] Neuropathological studies have shown an association between cerebral microinfarcts and CAA.[39–41] Interestingly, the particular location where cerebral microinfarcts are observed seems relevant to the underlying pathology. In a neuropathology study in community-dwelling individuals, it were particularly the cortical, not subcortical, cerebral microinfarcts that were associated with CAA pathology.[42] In another study, only microinfarcts in the occipital cortex, but not the frontal cortex or hippocampus, were related to local CAA pathology.[43] In this thesis, we study microinfarcts in CAA *in vivo*. We studied the frequency of cortical cerebral microinfarcts in patients with CAA, the incidence of new microinfarcts after one year and how the microinfarcts relate with other MRI correlates of CAA in Chapter 7.

Different observations suggest that hypoperfusion may also be a possible underlying mechanism of microinfarcts. First of all, in neuropathology studies cortical microinfarcts are observed in watershed areas, border zones between cerebral vascular territories where tissue is furthest from arterial supply and thus is most vulnerable to reduced perfusion.[44–46] Also, a previous study found that cortical microinfarct presence related to reduced global brain perfusion in a memory clinic population.[47] Patients from the memory clinic, however, likely have multiple aetiologies contributing to their cerebral pathologies. Therefore the question remains whether the observed association was causal or just reflected shared risk factors. In previous studies in mice, hypoperfusion induced by carotid stenosis led to microinfarcts.[48] In this thesis, we studied cortical microinfarcts in humans with an internal carotid artery occlusion as a model for cerebral hemodynamic compromise in Chapter 8. We studied the frequency and location of cortical microinfarcts with reference to the occlusion, as well as the association of cortical microinfarcts with the severity of collateral steno-occlusive disease and cerebral blood flow.

Cerebral microinfarcts thus relate to several disease processes, and they may therefore also mark a clinically relevant outcome in cSVD. Indeed a growing body of evidence shows a cross-sectional relation between microinfarct presence and cognitive decline, both in neuropathology and *in vivo* studies.[28,29] Importantly, with *in vivo* microinfarct detection, we can also assess if microinfarcts predict future outcomes during life. In Chapter 9 we study the presence of acute microinfarcts in patients from a memory clinic and we study if their presence predicts clinical outcome (i.e. marked cognitive decline, major vascular event, institutionalization and death).

Apart from the markers that I studied in this thesis, during my PhD additional progress in imaging markers for cSVD has been made. In Chapter 10 we provide a review of

developments in advanced neuroimaging markers for cSVD on MRI, with a focus on clinical and research applications. Finally, in Chapter 11 I will conclude with a general discussion where I reflect upon the findings of this thesis and how they answer the key aims that I set in this introduction, as well as which questions I think should be addressed next.

References

1. Wardlaw JM, Smith C, Dichgans M. Small vessel disease: mechanisms and clinical implications. *Lancet Neurol*. 2019;18(7):684-696.
2. Debette S, Schilling S, Duperron MG, Larsson SC, Markus HS. Clinical Significance of Magnetic Resonance Imaging Markers of Vascular Brain Injury: A Systematic Review and Meta-analysis. *JAMA Neurol*. 2019;76(1):81-94.
3. Zwanenburg JJM, Van Osch MJP. Targeting cerebral small vessel disease with MRI. *Stroke*. 2017;48(11):3175-3182.
4. Wardlaw JM, Smith EE, Biessels GJ, et al. Neuroimaging standards for research into small vessel disease and its contribution to ageing and neurodegeneration. *Lancet Neurol*. 2013;12(8):822-838.
5. Nitkunan A, Barrick TR, Charlton RA, Clark CA, Markus HS. Multimodal MRI in cerebral small vessel disease: Its relationship with cognition and sensitivity to change over time. *Stroke*. 2008;39(7):1999-2005.
6. Patel B, Markus HS. Magnetic resonance imaging in cerebral small vessel disease and its use as a surrogate disease marker. *Int J Stroke*. 2011;6(1):47-59.
7. Kang CK, Park CA, Park CW, Lee YB, Cho ZH, Kim YB. Lenticulostriate arteries in chronic stroke patients visualised by 7 T magnetic resonance angiography. *Int J Stroke*. 2010;5(5):374-380.
8. Seo SW, Kang CK, Kim SH, et al. Measurements of lenticulostriate arteries using 7T MRI: New imaging markers for subcortical vascular dementia. *J Neurol Sci*. 2012;322(1-2):200-205.
9. Ling C, Fang X, Kong Q, et al. Lenticulostriate arteries and basal ganglia changes in cerebral autosomal dominant arteriopathy with subcortical infarcts and leukoencephalopathy, a high-field mri study. *Front Neurol*. 2019;10:1-9.
10. Schreiber S, Bueche CZ, Garz C, et al. The pathologic cascade of cerebrovascular lesions in SHRSP: Is erythrocyte accumulation an early phase. *J Cereb Blood Flow Metab*. 2012;32(2):278-290.
11. Jandke S, Garz C, Schwanke D, et al. The association between hypertensive arteriopathy and cerebral amyloid angiopathy in spontaneously hypertensive stroke-prone rats. *Brain Pathol*. 2018;28(6):844-859.
12. Joutel A, Monet-leprêtre M, Gosele C, et al. Cerebrovascular dysfunction and microcirculation rarefaction precede white matter lesions in a mouse genetic model of cerebral ischemic small vessel disease. *J Clin Invest*. 2010;120(2):433-445.
13. Dabertrand F, Krøigaard C, Bonev AD, et al. Potassium channelopathy-like defect underlies early-stage cerebrovascular dysfunction in a genetic model of small vessel disease. *Proc Natl Acad Sci*. 2015;112(7):E796-E805.
14. Bouvy WH, Geurts LJ, Kuijf HJ, et al. Assessment of blood flow velocity and pulsatility in cerebral perforating arteries with 7-T quantitative flow MRI. *NMR Biomed*. 2015;29(9):1295-1304.
15. Geurts L, Biessels GJ, Luijten P, Zwanenburg J. Better and faster velocity pulsatility assessment in cerebral white matter perforating arteries with 7T quantitative flow MRI through improved slice profile, acquisition scheme, and postprocessing. *Magn Reson Med*. 2018;79(3):1473-1482.
16. Arts T, Siero JCW, Biessels GJ, Zwanenburg JJM. Automated Assessment of Cerebral Arterial Perforator Function on 7T MRI. *J Magn Reson Imaging*. 2021;53(1):234-241.

17. Geurts L, Zwanenburg JJM, Klijn CJM, Luijten PR, Biessels GJ. Higher Pulsatility in Cerebral Perforating Arteries in Patients With Small Vessel Disease Related Stroke, a 7T MRI Study. *Stroke*. 2019;50(1):62-68.

18. Iadecola C. The Neurovascular Unit Coming of Age: A Journey through Neurovascular Coupling in Health and Disease. *Neuron*. 2017;96(1):17-42.

19. Blair GW, Doubal FN, Thrippleton MJ, Marshall I, Wardlaw JM. Magnetic resonance imaging for assessment of cerebrovascular reactivity in cerebral small vessel disease: A systematic review. *J Cereb Blood Flow Metab*. 2016;36(5):833-841.

20. Chabriat H, Pappata S, Ostergaard L, et al. Cerebral hemodynamics in CADASIL before and after acetazolamide challenge assessed with MRI bolus tracking. *Stroke*. 2000;31(8):1904-1912.

21. Stringer MS, Blair GW, Shi Y, et al. A Comparison of CVR Magnitude and Delay Assessed at 1.5 and 3T in Patients With Cerebral Small Vessel Disease. *Front Physiol*. 2021;12:644837.

22. Ainslie PN, Duffin J. Integration of cerebrovascular CO2 reactivity and chemoreflex control of breathing: Mechanisms of regulation, measurement, and interpretation. *Am J Physiol - Regul Integr Comp Physiol*. 2009;296(5):R1473-R1495.

23. Sam K, Conklin J, Holmes KR, et al. Impaired dynamic cerebrovascular response to hypercapnia predicts development of white matter hyperintensities. *NeuroImage Clin*. 2016;11:796-801.

24. Sam K, Crawley AP, Conklin J, et al. Development of White Matter Hyperintensity Is Preceded by Reduced Cerebrovascular Reactivity. *Ann Neurol*. 2016;80(2):277-285.

25. Siero JCW, Bhogal A, Jansma JM. Blood oxygenation level-dependent/Functional Magnetic Resonance Imaging: Underpinnings, Practice, and Perspectives. *PET Clin*. 2013;8(3):329-344.

26. Pasi M, Van Uden IWM, Tuladhar AM, De Leeuw FE, Pantoni L. White Matter Microstructural Damage on Diffusion Tensor Imaging in Cerebral Small Vessel Disease: Clinical Consequences. *Stroke*. 2016;47(6):1679-1684.

27. Baykara E, Gesierich B, Adam R, et al. A Novel Imaging Marker for Small Vessel Disease Based on Skeletonization of White Matter Tracts and Diffusion Histograms. *Ann Neurol*. 2016;80(4):581-592.

28. van Veluw SJ, Shih AY, Smith EE, et al. Detection, risk factors, and functional consequences of cerebral microinfarcts. *Lancet Neurol*. 2017;16(9):730-740.

29. Brundel M, Bresser J De, Dillen JJ Van, Kappelle LJ, Biessels GJ. Cerebral microinfarcts: a systematic review of neuropathological studies. *J Cereb Blood Flow Metab*. 2012;32(3):425-436.

30. Smith EE, Schneider J a, Wardlaw JM, Greenberg SM. Cerebral microinfarcts: the invisible lesions. *Lancet Neurol*. 2012;11(3):272-282.

31. Auriel E, Westover MB, Bianchi MT, et al. Estimating Total Cerebral Microinfarct Burden From Diffusion-Weighted Imaging. *Stroke*. 2015;46(8):2129-2135.

32. Westover MB, Bianchi MT, Yang C, Schneider JA, Greenberg SM. Estimating cerebral microinfarct burden from autopsy samples. *Neurology*. 2013;80(15):1365-1369.

33. Auriel E, Edlow BL, Reijmer YD, et al. Microinfarct disruption of white matter structure: A longitudinal diffusion tensor analysis. *Neurology*. 2014;83(2):182-188.

34. Ferro DA, Kuijf HJ, Hilal S, et al. Association between Cerebral Cortical Microinfarcts and Perilesional Cortical Atrophy on 3T MRI. *Neurology*. 2022;98(6):E612-E622.

35. Lansberg MG, Thijs VN, O'Brien MW, et al. Evolution of apparent diffusion coefficient, diffusion-weighted, and T2-weighted signal intensity of acute stroke. *Am J Neuroradiol*. 2001;22(4):637-644.

36. van Veluw SJ, Zwanenburg JJM, Engelen-Lee J, et al. In vivo detection of cerebral cortical microinfarcts with high-resolution 7T MRI. *J Cereb blood flow Metab*. 2013;33(3):322-329.

37. Vinters H V. Cerebral Amyloid Angiopathy A Critical Review. *Stroke*. 1987;18(2):311-324.

38. Chen Y wei, Lee M jen, Smith EE. Cerebral amyloid angiopathy in East and West. *Int J stroke*. 2010;5:403-411.

39. Lauer A, Veluw SJ Van, William CM, et al. Microbleeds on MRI are associated with microinfarcts on autopsy in cerebral amyloid angiopathy. *Neurology*. 2016;87(14):1488-1492.

40. Kövari E, Herrmann FR, Hof PR, Bouras C. The relationship between cerebral amyloid angiopathy and cortical microinfarcts in brain ageing and Alzheimer's disease. *Neuropathol Appl Neurobiol*. 2013;39(5):498-509.

41. Ringman JM, Sachs MC, Zhou Y, Monsell SE, Saver JL, Vinters H V. Clinical predictors of severe cerebral amyloid angiopathy and influence of APOE genotype in persons with pathologically-verified Alzheimer's disease. *JAMA Neurol*. 2014;7(71):878-883.

42. Arvanitakis Z, Capuano AW, Leurgans SE, Buchman AS, Bennett DA, Schneider JA. The Relationship of Cerebral Vessel Pathology to Brain Microinfarcts. *Brain Pathol*. 2017;27(1):77-85.

43. Kövari E, Herrmann FR, Gold G, Hof PR, Charidimou A. Association of cortical microinfarcts and cerebral small vessel pathology in the ageing brain. *Neuropathol Appl Neurobiol*. 2017;43(6):505-513.

44. Suter O christina, Sunthorn T, Kraftsik R, et al. Cerebral Hypoperfusion Generates Cortical Watershed Microinfarcts in Alzheimer Disease. *Stroke*. 2002;33(8):1986-1992.

45. Kapasi A, Leurgans SE, James BD, et al. Neurobiology of Aging Watershed microinfarct pathology and cognition in older persons. *Neurbiology of aging*. 2018;70:10-17.

46. Strozyk D, Dickson DW, Lipton RB, et al. Contribution of vascular pathology to the clinical expression of dementia. *Neurbiology of aging*. 2010;31(10):1710-1720.

47. Ferro DA, Mutsaerts HJJM, Hilal S, et al. Cortical microinfarcts in memory clinic patients are associated with reduced cerebral perfusion. *J Cereb Blood Flow Metab*. 2020;40(9):1869-1878.

48. Okamoto Y, Yamamoto T, Kalaria RN, et al. Cerebral hypoperfusion accelerates cerebral amyloid angiopathy and promotes cortical microinfarcts. *Acta Neuropathol*. 2012;123(3):381-394.

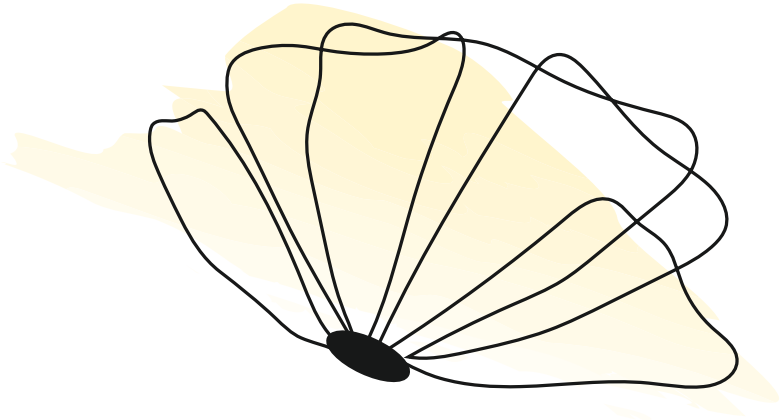

2

A case of sporadic cerebral small vessel disease in an identical twin

Hilde van den Brink, Nick. A. Weaver, Geert Jan Biessels

Case Reports in Neurology: 2020;12(3):416-421

Abstract

Sporadic cerebral small vessel disease (cSVD) is primarily attributed to heritability and vascular risk factors. Still, our understanding of the causative factors in cSVD lesion burden in the brain is far from complete. This is exemplified by this case of identical twins with remarkably similar vascular risk profiles, where one twin had developed severe cSVD on neuroimaging with cognitive deficits, while the other twin had no cSVD. This case highlights the need to search for further causes of cSVD, also beyond genetic and conventional vascular risk factors. Identification of other potential risk factors or disease mechanisms should be a priority for cSVD research to improve our understanding, prevention and treatment of this common cause of vascular brain injury with major clinical consequences.

Introduction

Cerebral small vessel disease (cSVD) is an important cause of stroke and cognitive impairment. Both single gene disorders (e.g. CADASIL) and sporadic forms of cSVD exist. Genetics also contribute to sporadic forms of cSVD, which is supported by twin and pedigree studies showing heritability rates between 52-78%.[1] In addition, vascular risk factors for sporadic cSVD are well-established, but do not explain the full burden and occurrence of cSVD either.[2,3] Here we present a unique case of identical twins with remarkably similar vascular risk profiles, where one twin had developed severe cSVD on neuroimaging with concomitant cognitive deficits, while the other twin had no cSVD and was cognitively unimpaired.

Case Report

A 62-year-old man was referred to our memory clinic with a 2-year history of slowly progressive behavioral and cognitive changes. His family noticed that he was apathetic, had a shorter temper and was more emotional than before. Also, they noticed that his speech was notably slower and less fluent, and he had difficulty keeping focus in busy surroundings. He had a 1-year known history of hypertension, was a former smoker (1.5 pack years) and was obese (BMI: 31). Neurological examination revealed mild balance problems. Blood tests showed a slightly elevated LDL-cholesterol; no other abnormalities were found in the basic metabolic panel (including blood count, electrolytes, glucose, thyroid, vitamin B12 and liver and kidney functions). There was no family history of cardiovascular disease or dementia. Neuropsychological examination objectified most profound impairment of processing speed, executive functioning and verbal long-term memory, as well as more subtle deficiencies in word fluency and focused attention. Brain MRI showed beginning confluent white matter hyperintensities (Fazekas 2) (see Figure 1). Multiple lacunes were observed in the periventricular and deep white matter of bilateral cerebral hemispheres, and in the pons and bilateral cerebellum. Furthermore, cerebral microbleeds were seen in both sides of the putamen, both sides of the thalamus and the bilateral temporal, parietal and occipital lobes. There was mild cortical atrophy, but no hippocampal atrophy. Based on these findings, the patient was diagnosed with multi-domain mild cognitive impairment due to cerebral small vessel disease, with hypertension as a possible contributing factor.

Interestingly, the patient has an identical twin who participated in a research study as healthy volunteer, for which he underwent clinical assessment, brain MRI, and neuropsychological testing. He also had a 1-year known history of hypertension and was overweight (BMI: 29), but otherwise his medical history was unremarkable. Brain MRI of the healthy twin showed very minimal signs of cSVD for his age (see Figure 1), and cognitive testing and neurological examination were normal. Laboratory tests showed a slightly elevated LDL-cholesterol. Table 1 provides an overview of demographics and vascular risk factors of the twins.

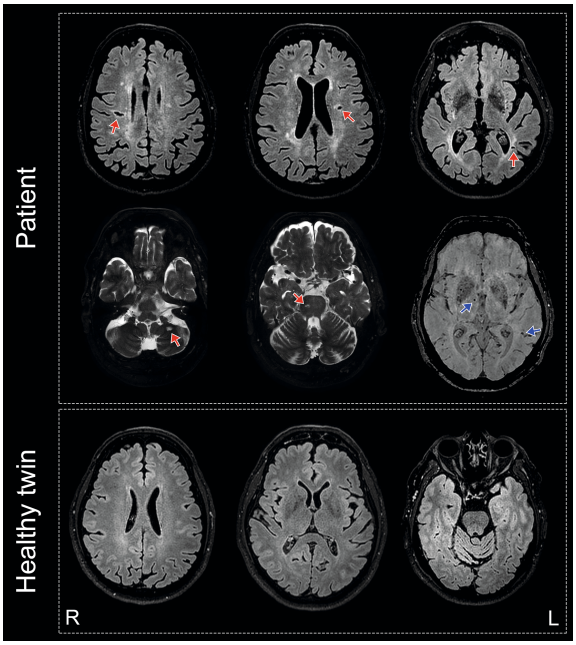

Figure 1: Brain MRI for the patient and healthy twin (age 62 years). Representative axial slices are shown. Fluid-attenuated inversion recovery sequences are shown for the patient (top row) and healthy twin (bottom row), and T2-weighted (middle row, left and center image) and susceptibility-weighted sequences (middle row, right image) are shown for the patient. Red arrows indicate lacunar infarcts and blue arrows indicate cerebral microbleeds. R = right, L = left.

Table 1: Demographics, vascular risk factors and medication use for the patient and his identical healthy twin

	Patient	**Healthy twin**
Demographics		
Education	Higher secondary education	Higher secondary education
Profession	Industrial buyer	Financial controller
Vascular risk factors		
Hypertension	Yes, since 1 year	Yes, since 1 year
Current blood pressure	123/81 mmHg	136/92 mmHg
Hypercholesterolemia	LDL-cholesterol 3.8	LDL-cholesterol 3.9
Diabetes mellitus	No	No
Smoking	Former, 1.5 pack years	Never
Alcohol	Yes, 1-2 per week	Yes, 1-2 per week
BMI	31	29
Medication		
	Lisinopril 10 mg Amlodipine 5 mg Hydrochloorthiazide 12.5 mg	Lisinopril 10 mg

Discussion

Here we present a case of identical twins of whom one developed severe cSVD with cognitive deficits, while the other twin showed no signs of cSVD and was cognitively unimpaired. The twins have a very similar vascular risk factor profile, with the only exception that the patient had a brief history of smoking and needed more antihypertensive medication to control blood pressure than his healthy brother.

Based on current knowledge it is hard to find a complete explanation for the discordant cSVD severity and consequent cognitive deficits in this pair of identical twins. We do not have genetic data available, but because the brothers are identical twins they should have a highly similar genome. It is therefore unlikely that genetic differences would fully explain the very different phenotypes. The discordant phenotype might be explained by different gene expression through epigenetics. It is however unknown what (environmental) factor would have triggered such epigenetic processes.

In addition, vascular risk factors are well known to contribute to sporadic cSVD, with hypertension recognized as a key risk factor.[2,4] Nevertheless, the minimal difference in blood pressure controllability (i.e. amount of medication needed) and the brief history of smoking of the patient seem insufficient to explain the large difference in cSVD severity and cognitive outcome. This is supported by earlier work that concluded that vascular risk factors together only explain a very limited part of variance (2%) in cSVD markers on MRI.[3] Current knowledge thus seems insufficient to identify all relevant risk factors in this case of sporadic cSVD.

In accordance with the current views in the cSVD research field,[5] this case emphasizes that known causes for cSVD seem to insufficiently explain cSVD occurrence and consequent cognitive impairment. This case highlights we are likely missing essential information on other potential risk factors or disease mechanisms that contribute to sporadic cSVD. Given the important impact of cSVD at the population level, through stroke, dementia and other forms of functional loss, it is clear that this knowledge gap needs to be addressed, in order to improve prevention and treatment. cSVD research has thus far often been rather descriptive, using mainly downstream markers of tissue injury to better understand the disease. There is clearly a need to identify specific modifiable molecular and cellular pathways that are fundamental to cSVD. These include molecular targets identified through rare cases of monogenetic forms of SVDs that may also be relevant to sporadic forms, but also processes like endothelial dysfunction, inflammation and increased blood brain barrier leakage.[5] We also need more specific cSVD biomarkers reflecting the condition of the small vessels themselves. These would be of value in future etiological studies, but can also be used as outcome measure to provide proof of efficacy for novel treatments targeting the small vessels. Such approaches are currently being tested in the H2020 program “SVDs@target”’ (https://www.svds-at-target.eu/).

This does not take away that treatment of known (vascular) risk factors according to current guidelines[6,7] is of utmost importance.

Acknowledgement

The authors would like to thank Paul J. Hop for his helpful review of the manuscript.

References

1. Choi JC. Genetics of Cerebral Small Vessel Disease. *J Stroke*. 2015;17(1):7–16.
2. Wardlaw JM, Smith C, Dichgans M. Mechanisms underlying sporadic cerebral small vessel disease: insights from neuroimaging. *Lancet Neurol*. 2013;12(5):70060–70067.
3. Wardlaw JM, Allerhand M, Doubal FN, Hernandez MV, Morris Z, Gow AJ, et al. Vascular risk factors, large-artery atheroma, and brain white matter hyperintensities. *Neurology*. 2014;82(15):1331–1338.
4. Staals J, Makin SDJ, Doubal FN, Dennis MS, Wardlaw JM. Stroke subtype, vascular risk factor , and total MRI brain small-vessel disease burden. *Neurology*. 2014;83:1228–1235.
5. Wardlaw JM, Smith C, Dichgans M. Small vessel disease: mechanisms and clinical implications. *Lancet Neurol*. 2019;18(7):684–696.
6. Smith EE, Saposnik G, Biessels GJ, Doubal FN, Fornage M, Gorelick PB, et al. Prevention of Stroke in Patients with Silent Cerebrovascular Disease: A Scientific Statement for Healthcare Professionals from the American Heart Association/American Stroke Association. *Stroke*. 2017;48(2):e44–e71.
7. Gorelick PB, Scuteri A, Black SE, DeCarli C, Greenberg SM, Iadecola C, et al. Vascular Contributions to Cognitive Impairment and Dementia: A Statement for Healthcare Professionals From the American Heart Association/American Stroke Association. *Stroke*. 2011;42(9):2672–2713.

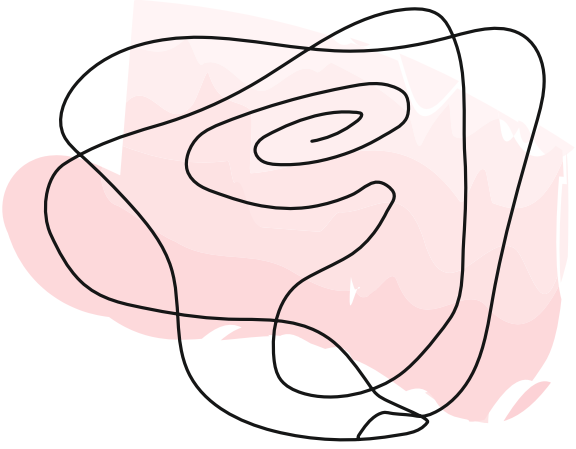

3

Zooming in on cerebral small vessel function in small vessel diseases with 7T MRI: Rationale and design of the "ZOOM@SVDs" study

Hilde van den Brink, Anna Kopczak, Tine Arts, Laurien Onkenhout, Jeroen C.W. Siero, Jaco J.M. Zwanenburg, Marco Duering, Gordon W. Blair, Fergus N. Doubal, Michael S. Stringer, Michael J. Thrippleton, Hugo J. Kuijf, Alberto de Luca, Jeroen Hendrikse, Joanna M. Wardlaw, Martin Dichgans, Geert Jan Biessels on behalf of the SVDs@target group

Cerebral Circulation – Cognition and Behaviour: 2021;2:100013

Abstract

Background

Cerebral small vessel diseases (SVDs) are a major cause of stroke and dementia. Yet, specific treatment strategies are lacking in part because of a limited understanding of the underlying disease processes. There is therefore an urgent need to study SVDs at their core, the small vessels themselves.

Objective

This paper presents the rationale and design of the ZOOM@SVDs study, which aims to establish measures of cerebral small vessel dysfunction on 7T MRI as novel disease markers of SVDs.

Methods

ZOOM@SVDs is a prospective observational cohort study with two years follow-up. ZOOM@SVDs recruits participants with Cerebral Autosomal Dominant Arteriopathy with Subcortical Infarcts and Leukoencephalopathy (CADASIL, N=20), sporadic SVDs (N=60), and healthy controls (N=40). Participants undergo 7T brain MRI to assess different aspects of small vessel function including small vessel reactivity, cerebral perforating artery flow, and pulsatility. Extensive work-up at baseline and follow-up further includes clinical and neuropsychological assessment as well as 3T brain MRI to assess conventional SVD imaging markers. Measures of small vessel dysfunction are compared between patients and controls, and related to the severity of clinical and conventional MRI manifestations of SVDs.

Discussion

ZOOM@SVDs will deliver novel markers of cerebral small vessel function in patients with monogenic and sporadic forms of SVDs, and establish their relation with disease burden and progression. These small vessel markers can support etiological studies in SVDs and may serve as surrogate outcome measures in future clinical trials to show target engagement of drugs directed at the small vessels.

Introduction

Cerebral small vessel diseases (SVDs) affect small arteries, capillaries and small veins in the brain.[1] SVDs account for most hemorrhagic strokes, a quarter of ischemic strokes, and at least 40% of dementia cases, alone or in combination with neurodegenerative pathology.[1] Roughly 70% of 65-year-old individuals and almost all 90-year-olds exhibit manifestations of SVDs on brain imaging.[2] Despite this profound impact, there is no specific treatment for SVDs with proven efficacy. Current management is limited to treatment of risk factors, foremost hypertension, which is clearly of fundamental importance, but is not sufficient to halt SVDs and their consequences. Better insight into the mechanisms underlying SVDs is urgently needed to support the development of targeted treatments.

Over the years there has been major progress in the development of SVD biomarkers. These include visible manifestations on MRI (i.e. lacunes, white matter hyperintensities, microbleeds, enlarged perivascular spaces[3]), more subtle microstructural white matter changes (measured with diffusion tensor imaging[4–6]) and blood-based biomarkers of neuro-axonal damage (serum neurofilament light[7]). All of these biomarkers primarily reflect SVDs-related parenchymal injury. This injury relates to important functional outcomes, in particular cognitive decline and dementia, but is essentially a downstream consequence of a disease that originates in the small cerebral vessels. In these vessels, SVDs manifest as loss of smooth muscle cells, fibrinoid necrosis, narrowing of the lumen, and thickening of the vessel wall.[1,8] This impacts vessel function, as observed in pial and parenchymal arteries in experimental animal models of both hereditary and sporadic forms of SVDs.[9,10] Emerging techniques at 7T MRI provide noninvasive measures of cerebral small vessel function in humans.[11] These measures allow SVDs to be studied at their core, the small vessels themselves, and have important potential as biomarker of SVDs to help unravel the pathophysiology and serve as surrogate outcome measures in treatment studies.

This paper presents the rationale and design of ZOOM@SVDs, part of the SVDs@target research program (see textbox). ZOOM@SVDs explores (1) which aspects of small vessel function on 7T brain MRI are affected in patients with Cerebral Autosomal Dominant Arteriopathy with Subcortical Infarcts and Leukoencephalopathy (CADASIL) and in patients with symptomatic sporadic SVD, and (2) how small vessel function relates to SVD severity at baseline and disease progression after two years.

SVDs@target (Small vessel diseases in a mechanistic perspective: Targets for Intervention – Affected pathways and mechanistic exploitation for prevention of stroke and dementia) (www.svds-at-target.eu). The program is funded by Horizon 2020 and includes three clinical studies: ZOOM@SVDs (current paper), INVESTIGATE-SVDs, and TREAT-SVDs. This textbox provides a summary on INVESTIGATE-SVDs and TREAT-SVDs.

INVESTIGATE-SVDs (Imaging NeuroVascular, Endothelial and STructural InteGrity in prepAration to TrEat Small Vessel Diseases.): PI Prof JM Wardlaw, Centre for Clinical Brain Sciences Edinburgh.

INVESTIGATE-SVDs is a three-centre (Edinburgh, Maastricht, Munich) observational study in 45 patients with sporadic SVDs and in 30 patients with CADASIL. The main objective is to advance knowledge of SVD pathophysiology by assessing the relationship between blood brain barrier integrity, cerebrovascular reactivity to CO_2, intracranial vascular and CSF pulsatility, blood pressure and its variability and clinical and structural features of SVD.

TREAT-SVDs (EffecTs of Amlodipine and other Blood PREssure Lowering Agents on Microvascular FuncTion in Small Vessel Diseases): PI Prof M Dichgans, Institute for Stroke and Dementia Research, Ludwig-Maximilians-Universität, Munich

TREAT-SVDs is a five-centre (Edinburgh, Maastricht, Munich, Oxford, Utrecht), randomized, open-label, crossover trial in 75 patients with sporadic SVDs and 30 patients with CADASIL. The primary objective is to test the hypothesis that the calcium channel blocker amlodipine has a beneficial effect on small vessel function in patients with symptomatic SVDs when compared to either the Angiotensin II type 1 receptor blocker losartan or the beta-blocker atenolol. The secondary objective is to test the hypothesis that losartan has a beneficial effect on small vessel function compared to atenolol.

Material and methods

Study design

ZOOM@SVDs is a prospective observational cohort study with a follow-up measurement after two years. The study is a collaboration between the University Medical Center Utrecht (UMCU) in the Netherlands and the Institute for Stroke and Dementia Research at Ludwig-Maximilians-Universität (LMU), Munich, Germany. At the UMCU, 60 patients with symptomatic sporadic SVD and 30 age and sex-matched controls are recruited. At the LMU, 20 patients with CADASIL and 10 age and sex-matched controls are recruited. Participants attend two baseline visits and one follow-up visit after two years, see Table 1 for an overview of the data collection per visit. The 7T MRI scan for all participants is performed at the UMCU. All other assessments for the patients with CADASIL and their controls are performed at the LMU.

Table 1: Overview of data collection per visit

	Baseline visit 1 Day 1	Baseline visit 2 Day 8-28	Follow-up 2 years
Informed consent	X		
Clinical assessment	X		X
Blood sampling	X		
Neuropsychological assessment	X		X
7-day blood pressure monitoring	X		
3T brain MRI	X		X
7T brain MRI		X	

Ethical approval

The Medical Ethics Review Committees of the UMCU and the LMU both approved the study (under number NL62090.041.17 and 17-088 respectively). The study is registered in the Nederlands Trial Register (under number NTR6265) and is conducted in accordance with the declaration of Helsinki and the European law of General Data Protection Regulation. Written informed consent is obtained from all participants prior to enrollment in the study.

Participants

Patients with symptomatic sporadic SVDs (N=60) are recruited from the stroke, rehabilitation and memory clinics of the UMCU, and from referring neighboring clinics (Diakonessenhuis Zeist and Utrecht). Patients with a diagnosis of CADASIL (N=20), either confirmed by molecular genetic testing of the *NOTCH3* gene or by skin biopsy, are recruited through the Institute for Stroke and Dementia Research at the LMU. The institute is a tertiary national referral center for patients with CADASIL in Germany. Controls are recruited among partners or relatives of the patients, and through flyer advertisement. Table 2 lists specific participant inclusion and exclusion criteria.

Table 2: Inclusion and exclusion criteria for patients with sporadic SVDs, CADASIL and healthy controls

General selection criteria for all groups	
Inclusion criteria	**Exclusion criteria**
- Age 18 years or older - Capacity to give written informed consent - Independent in activities of daily living (Modified Rankin score ≤ 3)	- Pregnant or breastfeeding women and women of childbearing age not taking contraception - Contraindication to MRI or unable to undergo MRI protocol due to physical condition - Other major neurological or psychiatric conditions affecting the brain and interfering with the study design (e.g. multiple sclerosis, Parkinson's disease) - Life expectancy <2 years
Additional selection criteria specific to patients with sporadic SVDs	
Inclusion criteria	**Exclusion criteria**
History of a clinical lacunar stroke in the last 5 years with a corresponding small subcortical infarct visible on MRI or CT, compatible with the clinical syndrome OR Cognitive impairment defined as visiting a memory clinic with cognitive complaints and objective cognitive impairment (based on a validated cognitive measurement tool such as, but not limited to, CAMCOG) with confluent white matter hyperintensities on MRI (defined as Fazekas ≥ 2)	- Evidence for a monogenic form of SVDs - In case of inclusion for clinical lacunar stroke: ≥50% luminal stenosis in large arteries supplying the infarct area Major-risk for cardioembolic source of embolism (defined as permanent or paroxysmal atrial fibrillation, sustained atrial flutter, intracardiac thrombus, prosthetic cardiac valve, atrial myxoma or other cardiac tumors, mitral stenosis, myocardial infarction in the last 4 weeks, left ventricular ejection fraction < 30%, valvular vegetations, or infective endocarditis) Other specific causes of stroke (e.g. arteritis, dissection, vasospasm, drug misuse)
Additional selection criteria specific to patients with CADASIL	
Inclusion criteria	**Exclusion criteria**
A diagnosis of CADASIL established by molecular genetic testing of the *NOTCH3* gene (presence of an archetypical, cysteine-affecting mutation) or the presence of granular osmiophilic material in ultrastructural, electron microscopy analysis of skin biopsy. *NB: thus both symptomatic and asymptomatic patients are included.*	Not applicable
Additional selection criteria specific to controls	
Inclusion criteria	**Exclusion criteria**
No additional inclusion criteria applicable	- A history of stroke or of cognitive complaints for which the person has previously sought medical advice - So-called "silent" SVDs defined as confluent white matter hyperintensities (Fazekas ≥ 2) or lacunes on the 3T brain MRI scan on baseline visit 1

Baseline assessment

Clinical assessment

The following measures are collected during the clinical assessment:

- Demographic factors, including age, sex and education level
- Medical history, including history of TIA, stroke, cognitive impairment and vascular risk factors (i.e. hypertension, hyperlipidemia, diabetes, smoking, BMI and alcohol use)
- Physical activity (i.e. EPIC Physical Activity Questionnaire[12]) and physical performance (i.e. SPPB[13])
- Physical examination, including a National Institute of Health Stroke Scale (NIHSS) examination[14] and blood pressure measurements
- Current medication

Blood sampling

Laboratory investigations are performed in blood from a venipuncture in order to document the cardiovascular risk profile, including total cholesterol, HDL-cholesterol, LDL-cholesterol, triglycerides, HbA1c, and C-reactive protein. In women of childbearing age, a pregnancy test is performed as a screening measure before undergoing MRI.

In addition to these laboratory tests, blood is obtained in two 8ml cell preparation tubes with sodium citrate (BD, 362782). Directly after collection, peripheral blood mononuclear cells are isolated and stored at -80 degrees Celsius,[15] with the aim to explore the contribution of immune cells to the severity of SVDs. This procedure is also performed in the other clinical studies of SVDs@target (i.e. INVESTIGATE-SVDs and TREAT-SVDs) and the analyses and findings will be combined for all three studies and addressed in separate work.

Blood pressure monitoring at home

At baseline, participants receive a telemetric blood pressure device to measure their blood pressure at home for seven days. The device (Tel-O-Graph® GSM Plus) has a CE 0044 label, has been validated according to the European standard ISO 81060-2:2009 and is graded A/A by the British Hypertension Society. Data are anonymously transferred via mobile phone networks (GPRS, General Packet Radio Service) to a central database for analysis. Participants measure the blood pressure three times daily: after waking, at noon and in the evening at bedtime. Participants are instructed to repeat the blood pressure measurements at each time point within 5 minutes. For data analyses, only the 2nd blood pressure measurement is used. If only one reading at a time point is available, that data will be used for the analysis. In addition to blood pressure, a pulse wave analysis is automatically performed with each blood pressure measurement to assess pulse wave velocity.

Neuropsychological assessment

All participants undergo a standardized neuropsychological assessment battery in a fixed order. The battery includes the Consortium to Establish a Registry for Alzheimer's Disease (CERAD) battery,[16] with the addition of the Trail Making Test,[17] phonemic fluency,[17] and digit span[18] to better assess processing speed and executive function (Table 3). The battery is consise, but still covers global cognition as well as specific cognitive domains. Individual test scores are standardized into *z*-scores using the control groups as a reference. Test *z*-scores are combined to represent specific cognitive domains (Table 3). Subsequently, global cognitive functioning is calculated as an average *z*-score across all domains. In addition, a clinical dementia rating scale (CDR) is obtained[19] and depressive symptoms are assessed with the Center for Epidemiologic Studies Depression Scale (CES-D).[20] The main cognitive outcome will be a compound score of the *z*-scores for the domains attention and processing speed, and executive function.

Table 3: Neuropsychological tests and questionnaires in fixed order.

Neuropsychological tests	**Cognitive function**	**Cognitive domain**
Category fluency (animals, 60s)	Verbal fluency, semantic memory	Executive function
Boston naming test (short version)	Word naming	Language
MMSE	Cognitive screening	-
Word List Learning		
Immediate recall	Episodic memory	Memory
Delayed recall	Episodic memory	Memory
Delayed recognition	Episodic memory	Memory
Constructional praxis		
Copy	Visuoconstruction	Visuoconstruction
Delayed recall	Visuospatial memory, visuoconstruction	Memory
Trail making test		
Part A	Attention and psychomotor speed	Attention and processing speed
Part B	Executive function	Executive function
Phonemic fluency (letter S, 60s)	Verbal fluency, executive function	Executive function
Digit span		
Forward	Attention and information processing speed	Attention and processing speed
Backward	Working memory	Executive function
Questionnaires	**Scope**	
Clinical Dementia Rating scale	Cognitive screening questionnaire	
CES-D questionnaire	Depressive symptoms questionnaire	

MMSE= Mini-Mental State Examination, CES-D= Center for Epidemiological Studies Depression Scale

3T brain MRI

3T brain MRI data are acquired on a Philips Achieva 3T scanner with an 8-channel SENSE head coil at UMCU (patients with sporadic SVD and controls) and on a Siemens Magnetom Skyra 3T scanner with a 64 channel head coil at the LMU (patients with CADASIL and controls). The scan protocol includes a 3D T1-weighted gradient echo, a 3D T2-weighted turbo spin echo, a 3D T2*-weighted gradient echo, and a 3D fluid-attenuated inversion recovery (FLAIR) scan. These sequences serve to assess conventional markers of SVDs and global brain volumes. In addition, the scan protocol includes diffusion imaging to measure white matter integrity. Table 4 summarizes all sequences and technical details for both sites.

SVD markers – i.e. lacunes, microbleeds and perivascular spaces - are visually rated on the 3T MRI scans by two trained raters according to the STRIVE criteria.[3] Differences between raters are resolved by consensus.

Volumetric measures are determined with established protocols at the individual study sites, to ensure that the data are analyzed with the best suiting software for the scanner systems and participant populations. At the UMCU, white matter hyperintensities (WMHs) are automatically segmented from T1-weighted and FLAIR images,[21,22] manually checked and, if necessary, edited. Lacunes are manually segmented using intensity-based seed-growing in an in-house built tool in MeVisLab (MeVis Medical Solutions AG, Bremen, Germany). T1-weighted images and FLAIR images are automatically segmented with the Computational Anatomy Toolbox (CAT12 http://www.neuro.uni-jena.de/cat/) to generate tissue probability maps from which gray matter (GM), white matter (WM) and cerebrospinal fluid (CSF) volumes are approximated. GM and WM volumes are normalized for intracranial volume. At the LMU, volumetric measures are assessed as previously published.[23] In short, WMHs are automatically segmented using a deep learning algorithm,[24,25] manually checked, and edited when necessary. Lacunes are manually segmented using intensity-based seed-growing in a custom 3D editing tool in MATLAB (R2016b, The MathWorks, Natick, MA). Total intracranial and brain volumes are approximated from tissue probability maps calculated from the T1-weighted images, using SPM (v12; Wellcome Department of Cognitive Neurology, London, UK; http://www.fil.ion.ucl.ac.uk/spm). GM and WM volumes are normalized for intracranial volume.

Table 4: 3T brain MRI protocol.

MR sequence	Acquired resolution mm^3	Time min:s	Parameters
Utrecht			
T1-weighted GE	1.0x1.0x1.0	05:39	FOV 256x232x192 mm^3; TR 8 ms; TI 955 ms; shot interval 2500 ms; flip angle 7°
T2-weighted TSE	0.7x0.7x0.7	07:37	FOV 250x250x190 mm^3; TR 2500 ms; TE 298 ms
T2*-weighted GE	0.8x0.8x0.8	02:22	FOV 230x192x144 mm^3; TR 69 ms; TE 29 ms; flip angle 23°
FLAIR	1.0x1.0x1.0	06:15	FOV 250x250x180 mm^3; TR 5000 ms; TE 253 ms; TI 1700 ms
Diffusion MRI	2.5x2.5x2.5	06:49	FOV 220x220x120 mm^3; TR 8185 ms; TE 73 ms; b-values 0 and 1200 s/mm^2; directions 45
BOLD rs-fMRI	2.9x2.9x3.5	05:00	FOV 200x235x146 mm^3; TR 2500 ms; 3 echos at TE 9.1, 25.3, and 41.4 ms [45]
Qflow	1.2x1.2x2.0	00:19	FOV 150x103 mm^2; TR 14 ms; TE 3.7 ms; flip angle 25°; Venc 100 cm/s
ASL	3.0x3.1x7.0	06:00	FOV 240x240x133 mm^3; pCASL; label duration 1800 ms; postlabeling delay 1800 ms; 40 dynamics
Munich			
T1-weighted GE	1.0x1.0x1.0	05:08	FOV 256x256x192 mm^3; TR 2500 ms; TE 4.37 ms; TI 1100 ms; flip angle 7°
T2-weighted TSE	0.9x0.9x0.9	03:42	FOV 263x350x350 mm^3; TR 3200 ms; TE 408 ms
T2*-weighted GE	0.9x0.9x2.0	05:56	FOV 230x160x187 mm^3; TR 35 ms; TE 5-30 ms; flip angle 15°
SWI	0.6x0.6x3.0	04:02	FOV 240x156x195 mm^3; TR 28 ms; TE 20 ms; flip angle 9°
FLAIR	1.0x1.0x1.0	06:27	FOV 250x250x176 mm^3; TR 5000 ms; TE 398 ms; TI 1800 ms
Diffusion MRI	2.0x2.0x2.0	07:47	FOV 240x150x240 mm^3; TR 3800 ms; TE 104.8 ms; b-values 0, 1000 and 2000 s/mm^2; 90 diffusion directions (30 for b=1000 s/mm2 and 60 for b=2000 s/mm2)

GE= gradient echo; TSE= turbo spin echo; FLAIR= Fluid attenuated inversion recovery; DTI= diffusion tensor imaging; BOLD= Blood oxygenation level-dependent; rs-fMRI= resting state functional magnetic resonance imaging; Qflow = quantitative flow; (pC)ASL= (pseudoContinuous) Arterial spin labeling; SWI= susceptibility weighted imaging; FOV= Field of view; TE= Echo Time; TI= Inversion Time; TR= Repetition Time.

7T brain MRI

All 7T brain MRI data are acquired on a Philips 7T scanner at the UMCU (Philips Healthcare, Best, The Netherlands) using a 32-channel receive head coil in combination with a quadrature transmit coil (Nova Medical, MA, USA). 7T MRI offers three main advantages over regular field strength imaging for studying small vessel function[26]: (1) higher signal to noise ratio allowing for high spatial and temporal resolution measurements, (2) higher sensitivity to the magnetic susceptibility effect of deoxyhemoglobin responsible for the blood oxygenation level-dependent (BOLD) MR contrast and (3) improved ability to discern the BOLD signal in the small vessels from that in larger draining veins.

In ZOOM@SVDs, we use three dedicated 7T protocols that can inform about small vessel function:

1. Blood flow velocity and flow pulsatility are assessed in perforating arteries in the basal ganglia and semioval centre with dedicated 2D phase-contrast velocity mapping.[27–29] These measures assess flow in the perforating arteries in a 2D slice at the level of the basal ganglia and semioval centre. The measures are influenced by the state of the perforating arteries, but also by up- and downstream flow regulation.

2. Small vessel reactivity in the visual cortex in response to a visual stimulus (i.e. neurovascular coupling) is assessed by means of the BOLD hemodynamic response. This is an ROI based measure in the visual cortex that assesses the parenchymal microvasculature. Neuronal activation triggers neurovascular coupling and induces vasodilation through the capillaries in the feeding pre-cappilary, parenchymal and penetrating arterioles to increase blood flow to the activated visual cortex.[30]

3. Whole-brain small vessel reactivity (cerebrovascular reactivity) to a hypercapnic stimulus (i.e. breathing 6% CO_2 in air) is measured with the BOLD response. This is a whole-brain measure from which more specific ROIs can be defined to assess the local parenchymal microvasculature. The hypercapnic stimulus causes relaxation of the vascular smooth muscle cells at the level of the arterioles, thereby causing direct small vessel vasodilation.[31]

The three protocols are complementary as they assess different small vessel populations, in different ROIs, either at rest or during stimulation with two different types of stimuli. The next three paragraphs describe the methods of these three 7T MRI protocols.

Blood flow velocity and pulsatility index in perforating arteries

Perforating artery flow data are acquired using two single-slice 2D phase-contrast acquisitions. Slices are placed at the level of the basal ganglia and the semioval centre using predefined anatomical landmarks[27]. A peripheral pulse unit is used for retrospective cardiac gating (Table 5 summarizes technical details). For post-processing, the ROI in the basal ganglia slice is manually delineated from the 2D phase-contrast magnitude image.

The ROI in the semioval centre slice is generated using an automatically delineated 2D white matter mask from a T1-weighted scan. The outside border of this mask (80 pixels = 14 mm) is excluded to be robust to subject motion between the acquisition of the T1-weighted and the 2D phase-contrast scan, which could lead to unsolicited inclusion of cortical vessels located in sulci. In these ROIs, perforating artery detection is performed with a previously developed method which automatically excludes perforating arteries in ghosting artefacts in the semioval centre[32] and perforating arteries in the basal ganglia that are oriented non-perpendicularly to the scanning plane. Additionally, apparent perforating arteries that are located within a 1.2mm radius from each other are excluded, as these mostly are 'false detections' of larger and non-perpendicular vessels. Subsequently, the perforating artery flow is assessed per subject as in earlier work.[27,29,33] The protocol is visually summarized in Figure 1.

Outcome measures, assessed separately for the basal ganglia and the semioval centre, are cerebral perforating artery density (number of perforating arteries/cm^2), mean blood flow velocity (the averaged mean velocity per subject in cm/s) and flow pulsatility index (PI). To determine PI, the perforating arteries' velocities over the cardiac cycle are first normalized and averaged. Then PI is calculated per subject as $(V_{max} - V_{min})/V_{mean}$ where V_{max}, V_{min} and V_{mean} are the maximum, minimum and mean of the normalized and averaged blood flow velocity over the cardiac cycle.[27,28] For ZOOM@SVDs we consider PI and mean blood flow velocity as primary outcome measures.

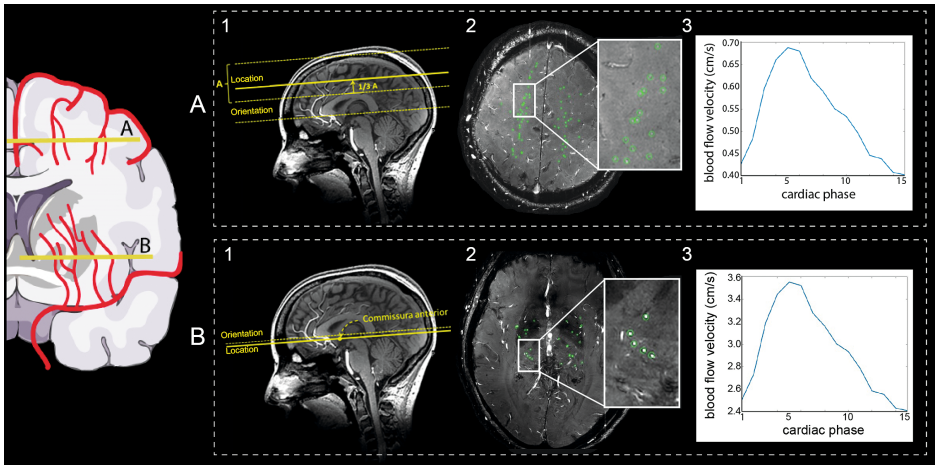

Figure 1: Overview figure of the single-slice 2D phase-contrast acquisitions. The schematic image on the left provides an impression of the perforating arteries that are assessed. Part A and B show examples of the (1) image acquisition, (2) 2D slice with the perforating arteries in green in the regions of interest, and (3) a blood flow velocity trace for the semioval centre (A) and the basal ganglia (B) respectively. From the blood flow velocity trace, an average blood flow velocity and flow pulsatility index are calculated.

Small vessel reactivity to a visual stimulus
Participants are presented with a strong visual stimulus to activate the visual cortex, and the subsequent increase in oxygenated blood to the activated brain is measured through a BOLD contrast weighted sequence. By making a fit of the average hemodynamic response function (HRF) in response to the stimulus, we can study the amplitude, and timing of small vessel reactivity in the cortex.

BOLD MRI data are acquired in eight slices in the visual cortex during a 10-minute experiment (Table 5 summarizes technical details of the sequence). The visual stimulus is an 8Hz blue-yellow reversing checkerboard, presented with Presentation software (Presentation® version 18.1, Neurobehavioral Systems, Inc). The stimulus train compromises a block design part to determine the region of interest, and an event-related design part to derive the HRF.[34] The experiment starts with the event-related design which consists of a baseline period of 45.1 seconds (= 51 volumes), a trigger period of 413.6 seconds (= 470 volumes) and another baseline period of 59.8 seconds (= 68 volumes). During the baseline period, a black screen with two red dots is presented to serve as a fixation point. During the trigger period, a total of 51 stimuli of 500 ms each are presented (2x2 125 ms opposing checkerboard frames). The inter-stimulus interval range is 3.3-18.7 seconds, sampled from an exponential distribution, and uniform jittering of ¼*TR is applied (yielding a sub-TR temporal resolution of 220 ms).[34,35] The block design consists of blocks of 16.72 seconds (=19 volumes) in which the fixation screen and reversing checkerboard are alternated over three blocks (total of 100.32 seconds = 114 volumes). Within the ROI we disentangle signal from the small vessels and from larger draining veins based on signal properties: large draining veins have a low signal and high signal variability wherefore we can calculate a temporal noise-to-signal ratio per voxel and then apply a single fixed value threshold above which the voxel represents signal from a large vein. The protocol is visually summarized in Figure 2A.

Outcome measures for the block design are ROI volume and BOLD amplitude. Outcome measures for the event-related design are four HRF characteristics: amplitude, full-width-at-half-maximum (FWHM), onset time and time-to-peak, separately for both the small vessels and the larger draining veins within the ROI. For ZOOM@SVDs we consider HRF amplitude and FWHM in the small vessels as primary outcome measures.

Small vessel reactivity to a hypercapnic stimulus
Whole-brain cerebrovascular reactivity was measured using BOLD contrast weighted MRI during a 10-minute experiment (Table 5 summarizes the sequence's technical details). The vasoactive stimulus is a hypercapnic challenge based on an earlier published protocol in SVDs.[36] In short, participants wear a face mask connected to a unidirectional breathing circuit. The participants breathe medical air and 6% CO_2 in air with a flow rate of 30L/min in alternating two-minute blocks: three two-minute blocks of medical air with two two-minute blocks of 6% CO_2 in air in between. Gasses are pre-mixed in medically

graded cylinders (Linde Gas, The Netherlands). Monitoring equipment records pulse rate (sampling rate = 500Hz) and end-tidal CO_2 ($etCO_2$, 40Hz,, CD3-A AEI Technologies, Pittsburgh, USA). The protocol is visually summarized in Figure 2B.

Outcome measures are the BOLD response amplitude in the cortical and subcortical GM, and total WM, NAWM and WMH. For ZOOM@SVDs, we consider the BOLD response amplitude in all these ROIs as primary outcome measures.

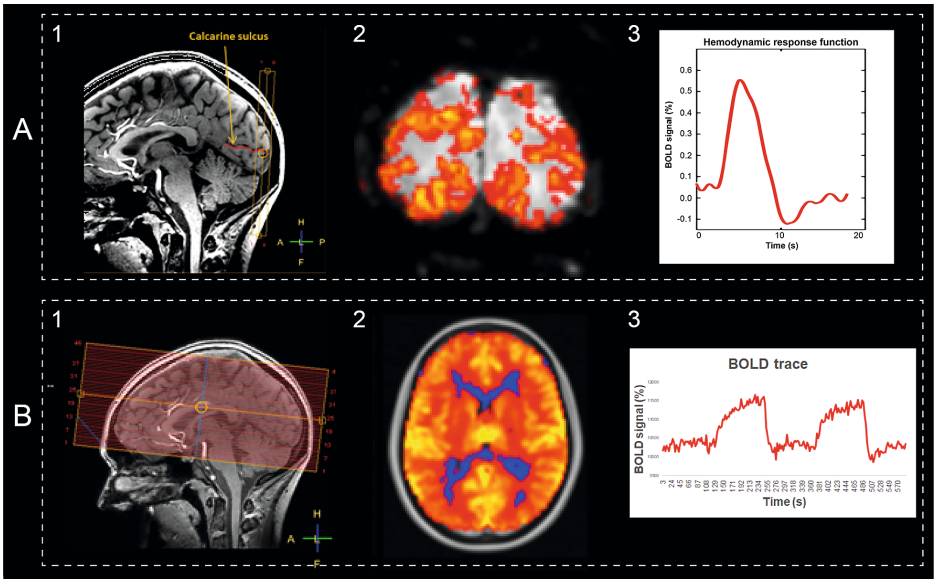

Figure 2: Overview figure of the BOLD acquisitions. Part A (visual stimulus) and B (hypercapnic stimulus) show examples of the (1) image acquisition, (2) voxelwise reactivity maps, and (3) BOLD signal curves over time for small vessel reactivity. For A, amplitude and full-width-at-half-maximum are extracted from the hemodynamic response function. For B, the average % of BOLD signal change to the hypercapnic stimulus is calculated, using the recorded $etCO_2$ trace as the input model for analysis.

Table 5: 7T brain MRI protocol in fixed order

MR sequence	Acquired resolution mm^3	Time min:s	Parameters
T1-weighted	1.0x1.0x1.0	01:59	FOV 250x250x190 mm^3; TR 4.2 ms; TI 1297 ms; shot interval 3000 ms; flip angle 5°
2D-Qflow CSO	0.3x0.3x2.0	03:24*	FOV 230x230 mm^2; reconstructed resolution 0.18x0.18mm^2 ; TR 29 ms; TE 16 ms; Venc 4 cm/s
T1-weighted[a]	1.0x1.0x1.0	00:47	FOV 250x250x190; TR 4.1 ms; TI 1253 ms; shot interval 3000; flip angle 5°
2D-Qflow BG	0.3x0.3x2.0	03:47*	FOV 170x170 mm^2; reconstructed resolution 0.18x0.18mm^2 ;TR 28 ms; TE 15 ms; Venc 20 cm/s
2D-Qflow M1	0.5x0.5x3.0	01:47*	FOV 250x200 mm^2; TR 12 ms; TE 4.3 ms; Venc 100 cm/s
T2* whole brain	0.6x0.6x0.6	03:02	FOV 239x191x100 mm^3; TR 77 ms; TE 27 ms; flip angle 20°
T2* visual cortex	0.6x0.6x1.0	02:21	FOV 160x169x29 mm^3; TR 1250 ms; TE 16 ms; flip angle 40°
BOLD fMRI visual cortex[b]	1.3x1.3x1.3	10:05	FOV 140x140x11 mm^3; TR 880 ms; TE 25 ms
T1-weighted[a]	1.0x1.0x1.0	00:47	FOV 250x250x190 mm^3; TR 4.1 ms; TI 1253 ms; shot interval 3000; flip angle 5°
BOLD fMRI whole-brain[c]	2.0x2.0x2.0	10:00	FOV 224x256x101 mm^3; TR 3000 ms; TE 25 ms

CSO= centrum semiovale; BG= Basal Ganglia; M1= first segment of the middle cerebral artery; BOLD= Blood oxygenation level-dependent; fMRI= functional magnetic resonance imaging; FOV= Field of view; TE= Echo Time; TI= Inversion Time; TR= Repetition Time. *Total scan time for a heart rate of 80bpm.

[a] A fast version of the T1-weighted sequence was added multiple times to assess potential subject motion during the scan, particularly after repositioning for attaching the mask for the hypercapnic challenge.

[b] The participant is presented with a visual stimulus.

[c] The participant undergoes a hypercapnic challenge.

Follow up assessment

Two years after the baseline visit, all participants are invited for follow-up. During this visit, the clinical assessment, neuropsychological assessment (same test versions as at baseline) and 3T brain MRI scan are repeated (see Table 1 and respective sections above). If participants are not able to undergo a visit in the hospital, a short evaluation is performed via a telephone interview. If there is doubt about the reliability of the patient report because of cognitive problems, additional information is gathered from next of kin. Study participation finishes after the follow-up visit.

Sample size considerations

With a sample size of 60 patients with sporadic SVDs and 30 age and sex-matched controls, we can detect baseline abnormalities of small vessel function on continuous outcome measures with an effect size of 0.5 or more between groups with a power of 80% at a 5% significance level. At two-year follow-up, we expect that the dropout rate will not exceed 20%. This means that we can detect associations between baseline small vessel function and lesion progression or cognitive decline over two years if the determinant explains 16% or more variance with a power of 80% at a 5% significance level.

Regarding the 20 CADASIL patients with their 10 age and sex-matched controls, we can detect abnormalities of small vessel function with an effect size of 0.96 or more between groups with a power of 80% at a 5% significance level. The average age of the CADASIL participants in the study is around 50 years. At this age, CADASIL patients already have marked manifestations of SVDs. In controls of this age, none or only very subtle manifestations of sporadic SVDs are to be expected. If CADASIL indeed manifests with abnormalities of small vessel function on 7T MRI, there should be substantial differences between the groups, for which the sample size should be sufficient.

Planned analyses

For the primary objective – to assess which aspects of small vessel function on 7T brain MRI are affected in patients versus controls –, cross-sectional analyses will be performed at baseline to compare patients with CADASIL or sporadic SVDs to their respective controls. Main outcome measures are compared between patients and controls with the appropriate parametric or non-parametric independent samples tests, adjusting for age and sex.

For the secondary objective – to assess how small vessel function relates to SVD disease severity at baseline and disease progression after two years –, analyses will primarily be performed within the patient groups. Measures of small vessel function will be related with baseline parenchymal SVD markers and cognitive functioning, and the progression of these indicators of disease severity at follow-up. Analyses will be performed with multiple regression and will be adjusted for age sex and vascular risk factors where approriate.

Timeline

The first participant was enrolled in March 2017. Participant enrolment for the CADASIL patients and their age and sex-matched controls was completed in July 2019. Enrolment for the patients with sporadic SVDs and controls is still ongoing. We expect to publish the first baseline results in 2021. Two-year follow-up visits are ongoing.

Discussion

ZOOM@SVDs will provide novel functional biomarkers of SVDs at the level of the small vessels themselves. We will assess cerebral perforating artery flow, and vascular reactivity to a visual and a hypercapnic stimulus with 7T MRI in patients with hereditary (i.e. CADASIL) and sporadic SVDs and controls. The different protocols in ZOOM@SVDs capture complementary aspects of small vessel function; in different types of small vessels, in different ROIs, both at rest and during stimulation with two different types of stimuli. We will determine which aspects of small vessel function are affected by SVDs and how this relates to disease severity and progression.

The small vessel functional measures in ZOOM@SVDs were chosen based on their relevance for SVDs and earlier research. We assess blood flow velocity and pulsatility index in perforating arteries in the basal ganglia and semioval centre. These perforating arteries are of particular interest given that, in SVDs, these are affected by arteriolosclerosis. We interpret pulsatility index as a measure of vascular stiffness, but the measure is also influenced by up- and downstream cerebral blood flow, pulse pressure and autoregulation. In earlier explorative work, we reported higher pulsatility in perforating arteries of patients with stroke attributable to SVD compared with controls, but similar blood flow velocity.[28] In ZOOM@SVDs, we will expand these observations in larger cohorts of highly phenotyped patients, including patients with CADASIL as a prototypic condition of pure and relatively severe SVD. In addition, we assess small vessel reactivity through neurovascular coupling in the visual cortex. Earlier studies with similar paradigms on 3T MRI have observed decreased vascular reactivity in response to a visual stimulus in patients with cerebral amyloid angiopathy (CAA).[37–41] In ZOOM@SVDs, we study CADASIL and sporadic SVDs that show largely subcortical lesions, but might have abnormal cortical small vessel reactivity as well. The strength of 7T MRI is that we will be able to carefully isolate the signal from the parenchyma, derived from changes in blood oxygen levels in the local capillaries and draining venules, in reponse to upstream arteriolar dilation. It is important to realize that, in order to represent neurovascular coupling and small vessel function, neuronal activation to the visual stimulus should be unaffected. We expect neuronal activation to be normal in CADASIL and sporadic SVD, as an earlier study reported normal cortical electrical potentials to a visual stimulus in patients with CADASIL and CAA.[39] Lastly, we assess small vessel reactivity with a hypercapnic stimulus that causes vasodilation in the arterioles.[31] Compared with the visual stimulus, the hypercapnic stimulus provides a whole-brain (rather than only cortical) measure of small vessel reactivity, that does not involve neurovascular coupling. Earlier studies used this paradigm on 3T MRI and observed that lower vascular reactivity was related to a higher burden of parenchymal SVD lesions in sporadic[42] and monogenic SVD.[43] In ZOOM@SVDs, we can capitalize on the high-resolution signal of 7T MRI to study local small vessel function, for example at the exact location of parenchymal lesions.

A strength of the ZOOM@SVDs study is that we will assess small vessel disease at its core, in the small vessels. By using three complementary measures across different brain regions we will be able to evaluate different aspects of small vessel function in different vessel subpopulations. By studying both monogenic and sporadic SVDs, we expect to find both shared and differential features of different forms of SVDs. Although downstream consequences of CADASIL and sporadic SVDs in the parenchyma show important similarities, there clearly are differences in the molecular and cellular pathways that affect the small vessels, likely with different signatures of vessel (dys)function. Moreover, in sporadic SVDs, vascular risk factors may differentially affect different vessel populations. Hypertension, for example, is known to most strongly affect the perforating arteries at the base of the brain, which are directly exposed to high pressure from the large arteries.[44] Finally, functional changes in different vessel populations may differentially affect the brain parenchyma. Therefore ZOOM@SVDs will also addess the interrelation between the nature of small vessel dysfunction and patterns of injury, also in longitudinal analyses. A limitation of ZOOM@SVDs is that, given the extensive protocol, there will likely be a relative overrepresentation of patients that are less affected (i.e. in earlier disease stages). Moreover, in order not to make the protocol too demanding, we prioritized detailed assessment of the primary parameters of interest. Consequently, some of the secondary clinical outcome measures are only assessed with screening tests with restricted sensitivity (e.g. assessment of motor performance and depression). Finally, 3T MRIs and their post-processing were performed at different centres for patients with CADASIL and sporadic SVDs. Importantly, the scans of the respective controls were always acquired on the same scanners as the patients. Although differences in scan acquisition and analysis may give rise to small differences in for example brain volume measurements, this should not impact the outcome of the study, because all primary analyses involving 3T parenchymal injury markers will be done within each patient group in comparison to their respective controls.

ZOOM@SVDs will characterize which small vessel function measures are affected in patients with CADASIL and sporadic SVDs compared with controls. Within the patient groups, we will establish which functional measures relate to disease severity (e.g. lesion burden and cognitive functioning). These markers could be well-suited to assist future etiological studies. In addition, the reversible nature of small vessel function makes the measures possibly potent outcome markers in intervention studies on candidate therapies that target the small vessels, thereby ultimately supporting the development of eagerly needed SVD treatment.

References

1. Wardlaw JM, Smith C, Dichgans M. Small vessel disease: mechanisms and clinical implications. *The Lancet Neurology.* 2019;18:684–696.
2. Debette S, Schilling S, Duperron MG, Larsson SC, Markus HS. Clinical Significance of Magnetic Resonance Imaging Markers of Vascular Brain Injury: A Systematic Review and Meta-analysis. *JAMA Neurology.* 2019;76:81–94.
3. Wardlaw JM, Smith EE, Biessels GJ, Cordonnier C, Fazekas F, Frayne R, et al. Neuroimaging standards for research into small vessel disease and its contribution to ageing and neurodegeneration. *The Lancet Neurology.* 2013;12:822–838.
4. Van Norden AGW, De Laat KF, Van Dijk EJ, Van Uden IWM, Van Oudheusden LJB, Gons RAR, et al. Diffusion tensor imaging and cognition in cerebral small vessel disease: The RUN DMC study. *Biochimica et Biophysica Acta - Molecular Basis of Disease.* 2012;1822:401–407.
5. Tuladhar AM, Van Norden AGW, De Laat KF, Zwiers MP, Van Dijk EJ, Norris DG, et al. White matter integrity in small vessel disease is related to cognition. *NeuroImage: Clinical.* 2015;7:518–524.
6. Baykara E, Gesierich B, Adam R, Tuladhar AM, Biesbroek JM, Koek HL, et al. A Novel Imaging Marker for Small Vessel Disease Based on Skeletonization of White Matter Tracts and Diffusion Histograms. *Annals of Neurology.* 2016;80:581–592.
7. Duering M, Konieczny MJ, Tiedt S, Baykara E, Tuladhar AM, van Leijsen E, et al. Serum neurofilament light chain levels are related to small vessel disease burden. *Journal of Stroke.* 2018;20:228–238.
8. Pantoni L. Cerebral small vessel disease: from pathogenesis and clinical characteristics to therapeutic challenges. *The Lancet Neurology.* 2010;9:689–701.
9. Dabertrand F, Krøigaard C, Bonev AD, Cognat E, Dalsgaard T, Domenga-Denier V, et al. Potassium channelopathy-like defect underlies early-stage cerebrovascular dysfunction in a genetic model of small vessel disease. *Proceedings of the National Academy of Sciences.* 2015;112:E796–E805.
10. Joutel A, Monet-leprêtre M, Gosele C, Baron-menguy C, Hammes A, Schmidt S, et al. Cerebrovascular dysfunction and microcirculation rarefaction precede white matter lesions in a mouse genetic model of cerebral ischemic small vessel disease. *The Journal of Clinical Investigation.* 2010;120:433–445.
11. Zwanenburg JJM, Van Osch MJP. Targeting cerebral small vessel disease with MRI. *Stroke.* 2017;48:3175–3182.
12. Pols M, Peeters PHM, Ocké MC, Slimani N, Bueno-de-mesquita HB, Collette HJA. Estimation of Reproducibility and Relative Validity of the Questions Included in the EPIC Physical Activity Questionnaire. *International Journal of Epidemiology.* 1997;26:181S – 189.
13. Guralnik JM, Simonsick EM, Ferrucci L, Glynn RJ, Berkman LF, Blazer DG, et al. A Short Physical Performance Battery Assessing Lower Extremity Function: Association With Self-Reported Disability and Prediction of Mortality and Nursing Home Admission. *Journal of Gerontology.* 1994;49:M85–M94.
14. Ortiz GA, Saaco RL. National Institues of Health Stroke Scale (NIHSS). In: *Wiley Encyclopedia of Clinical Trials*, 2008.
15. Hamot G, Ammerlaan W, Mathay C, Kofanova O, Betsou F. Method Validation for Automated Isolation of Viable Peropheral Blood Mononuclear Cells. *Biopreservation and Biobaking.* 2015;13:152–163.

16. Morris JC, Heyman A, Mohs RC, Hughes JP, Van Belle G, Fillenbaum G, et al. The Consortium to Establish a Eegistry for Alzheimer's Disease (CERAD). Part I. Clinical and Neuropsychological Assessment of Alzheimer's Disease. *Neurology.* 1989;39:1159–1165.
17. Lezak MD, Howieson DB, Bigler ED, Tranel D. *Neuropsychological Assessment*. New York: NY: Oxford University Press; 2012.
18. Wechsler D. *Wechsler Adult Intelligence Scale-Fourth Edition*. San Antonio, TX: Pearson; 2008.
19. Morris JC. The Clinical Dementia Rating (CDR): Current version and scoring rules. *Neurology.* 1993;43:2412–2412.
20. Lewinsohn PM, Seeley JR, Roberts RE, Allen NB. Center for Epidemiological Studies-Depression Scale (CES-D) as a screening instrument for depression among community-residing older adults. *Psychology and Aging.* 1997;12:277–287.
21. Camarasa R, Doué C, de Bruijne M, Dubost F. Segmentation of White Matter Hyperintensities with an Ensemble of Multi-Dimensional Convulational Gated Recurrent Units. 2018.
22. Kuijf HJ, Biesbroek M, de Bresser J, Heinen R, Andermatt S, Bento M, et al. Standardized Assessment of Automatic Segmentation of White Matter Hyperintensities and Results of the WMH Segmentation Challenge. *IEEE Transactions on Medical Imaging.* 2019;38:2556–2568.
23. Gesierich B, Tuladhar AM, ter Telgte A, Wiegertjes K, Konieczny MJ, Finsterwalder S, et al. Alterations and test–retest reliability of functional connectivity network measures in cerebral small vessel disease. *Human Brain Mapping.* 2020;41:2629–2641.
24. Ronneberger O, Fischer P, Brox T. U-Net: Convolutional Networks for Biomedical Image Segmentation. In: *International Conference on Medical Image Computing and Computer-Assisted Intervention*, 2015.
25. Long J, Shelhamer E, Darrell T. Fully convolutional networks for semantic segmentation. In: *2015 IEEE Conference onf Computer Vision and Patter Recognition (CVPR)*, 2015.
26. Siero JCW, Bhogal A, Jansma JM. Blood oxygenation level-dependent/Functional Magnetic Resonance Imaging: Underpinnings, Practice, and Perspectives. *PET Clinics.* 2013;8:329–344.
27. Bouvy WH, Geurts LJ, Kuijf HJ, Luijten PR, Kappelle LJ, Biessels GJ, et al. Assessment of blood flow velocity and pulsatility in cerebral perforating arteries with 7-T quantitative flow MRI. *NMR in Biomedicine.* 2015;29:1295–1304.
28. Geurts L, Zwanenburg JJM, Klijn CJM, Luijten PR, Biessels GJ. Higher Pulsatility in Cerebral Perforating Arteries in Patients With Small Vessel Disease Related Stroke, a 7T MRI Study. *Stroke.* 2019;50:62–68.
29. Arts T, Siero JCW, Biessels GJ, Zwanenburg JJM. Automated Assessment of Cerebral Arterial Perforator Function on 7T MRI. *Journal of Magnetic Resonance Imaging.* 2020:1–9.
30. Iadecola C. The Neurovascular Unit Coming of Age: A Journey through Neurovascular Coupling in Health and Disease. *Neuron.* 2017;96:17–42.
31. Ainslie PN, Duffin J. Integration of cerebrovascular CO2 reactivity and chemoreflex control of breathing: Mechanisms of regulation, measurement, and interpretation. *American Journal of Physiology - Regulatory Integrative and Comparative Physiology.* 2009;296.
32. Arts T, Siero J, Biessels GJ, Zwanenburg J. Method for vessel selection effects the outcome and reproducibility of velocity and pulsatility measures in cerebral penetrating arteries. In: *Annual Meeting of the International Society of Magnetic Resonance* Montreal, 2019; p. #3264.
33. Geurts L, Biessels GJ, Luijten P, Zwanenburg J. Better and faster velocity pulsatility assessment in cerebral white matter perforating arteries with 7T quantitative flow MRI through improved slice profile, acquisition scheme, and postprocessing. *Magnetic Resonance in Medicine.* 2018;79:1473–1482.

34. Siero JC, Petridou N, Hoogduin H, Luijten PR, Ramsey NF. Cortical Depth-Dependent Temporal Dynamics of the BOLD Response in the Human Brain. *Journal of Cerebral Blood Flow & Metabolism.* 2011;31:1999–2008.

35. Siero JCW, Ramsey NF, Hoogduin H, Klomp DWJ, Luijten PR, Petridou N. BOLD Specificity and Dynamics Evaluated in Humans at 7 T: Comparing Gradient-Echo and Spin-Echo Hemodynamic Responses. *PLoS ONE.* 2013;8:1–8.

36. Thrippleton MJ, Shi Y, Blair G, Hamilton I, Waiter G, Schwarzbauer C, et al. Cerebrovascular reactivity measurement in cerebral small vessel disease: Rationale and reproducibility of a protocol for MRI acquisition and image processing. *International Journal of Stroke.* 2018;13:195–206.

37. Williams RJ, Goodyear BG, Peca S, McCreary CR, Frayne R, Smith EE, et al. Identification of neurovascular changes associated with cerebral amyloid angiopathy from subject-specific hemodynamic response functions. *Journal of Cerebral Blood Flow and Metabolism.* 2017;37:3433–3445.

38. Dumas A, Dierksen GA, Eng M, Gurol ME, Halpin A, Martinez-ramirez S, et al. Functional MRI detection of vascular reactivity in cerebral amyloid angiopathy. *Annals of Neurology.* 2012;72:76–81.

39. Cheema I, Switzer AR, McCreary CR, Hill MD, Frayne R, Goodyear BG, et al. Functional magnetic resonance imaging responses in CADASIL. *Journal of the Neurological Sciences.* 2017;375:248–254.

40. Peca S, Mccreary CR, Donaldson E, Kumarpillai G, Sanchez K, Charlton A, et al. Neurovascular decoupling is associated with severity of cerebral amyloid angiopathy. *Neurology.* 2013;81:1659–1665.

41. Opstal AM Van, Rooden S Van, Harten T Van, Labadie G, Fotiadis P, Gurol ME, et al. Cerebrovascular function in pre-symptomatic and symptomatic individuals with hereditary cerebral amyloid angiopathy: a case-control study. *Lancet neurology.* 2017;16:115–122.

42. Blair GW, Thrippleton MJ, Shi Y, Hamilton I, Stringer M, Chappell F, et al. Intracranial hemodynamic relationships in patients with cerebral small vessel disease. *Neurology.* 2020;94:e2258–e2269.

43. Moreton FC, Cullen B, Delles C, Santosh C, Gonzalez RL, Dani K, et al. Vasoreactivity in CADASIL: Comparison to structural MRI and neuropsychology. *Journal of Cerebral Blood Flow and Metabolism.* 2018;38:1085–1095.

44. Spence JD. Blood pressure gradients in the brain: Their importance to understanding pathogenesis of cerebral small vessel disease. *Brain Sciences.* 2019;9:1–8.

45. Kundu P, Inati SJ, Evans JW, Luh WM, Bandettini PA. Differentiating BOLD and non-BOLD signals in fMRI time series using multi-echo EPI. *NeuroImage.* 2012;60:1759–1770.

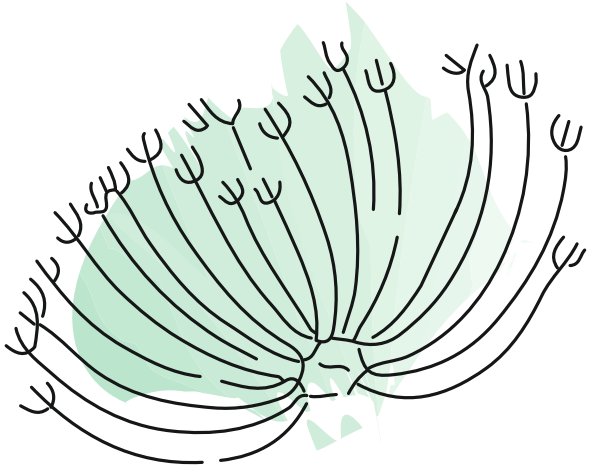

4

CADASIL affects multiple aspects of cerebral small vessel function on 7T-MRI

Hilde van den Brink*, Anna Kopczak*, Tine Arts*, Laurien Onkenhout, Jeroen C.W. Siero, Jaco J.M. Zwanenburg, Sandra Hein, Mathias Hübner, Benno Gesierich, Marco Duering, Michael S. Stringer, Jeroen Hendrikse, Joanna M. Wardlaw, Anne Joutel, Martin Dichgans, Geert Jan Biessels, on behalf of the SVDs@target group

*These authors contributed equally

Annals of Neurology: 2023;93:29-39

Abstract

Objective

Cerebral small vessel diseases (cSVDs) are a major cause of stroke and dementia. We used cutting-edge 7T-MRI techniques in patients with CADASIL, to establish which aspects of cerebral small vessel function are affected by this monogenic form of cSVD.

Methods

We recruited 23 CADASIL patients (age 51.1±10.1 years, 52% women) and 13 age- and sex-matched controls (46.1±12.6, 46% women). Small vessel function measures included: basal ganglia and centrum semiovale perforating artery blood flow velocity and pulsatility, vascular reactivity to a visual stimulus in the occipital cortex and reactivity to hypercapnia in the cortex, subcortical grey matter, white matter and white matter hyperintensities.

Results

Compared with controls, CADASIL patients showed lower blood flow velocity and higher pulsatility index within perforating arteries of the centrum semiovale (mean difference -0.09 cm/s, p=0.03 and 0.20,p=0.009) and basal ganglia (mean difference -0.98 cm/s, p=0.003 and 0.17, p=0.06). Small vessel reactivity to a short visual stimulus was decreased (BOLD mean difference -0.21%,p=0.04) in patients, while reactivity to hypercapnia was preserved in the cortex, subcortical grey matter and normal appearing white matter. Among patients, reactivity to hypercapnia was decreased in white matter hyperintensities compared to normal appearing white matter (BOLD mean difference -0.29%, p=0.02).

Interpretation

Multiple aspects of cerebral small vessel function on 7T-MRI were abnormal in CADASIL patients, indicative of increased arteriolar stiffness and regional abnormalities in reactivity, locally also in relation to white matter injury. These observations provide novel markers of cSVD for mechanistic and intervention studies.

Graphical abstract

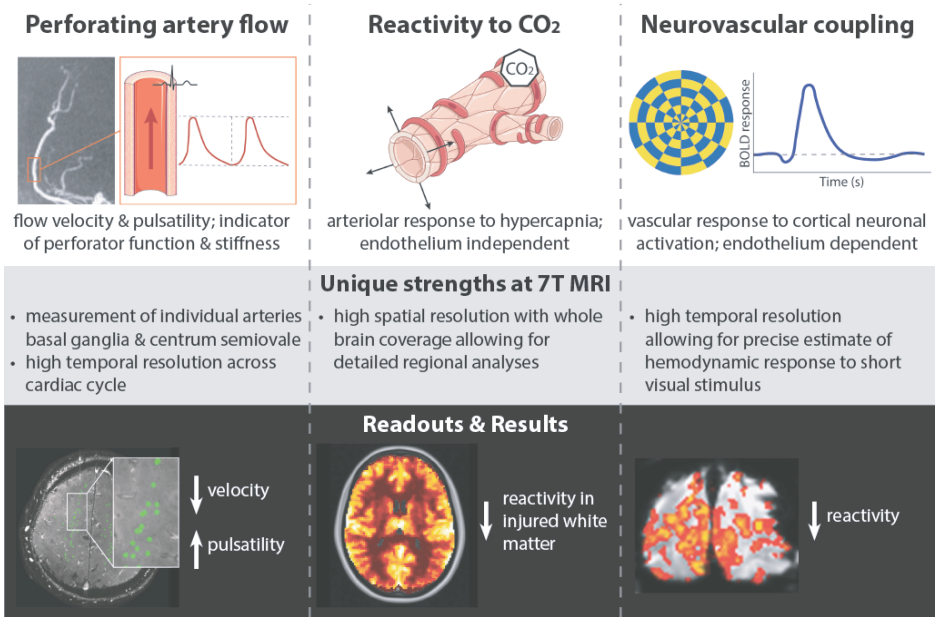

Introduction

Cerebral small vessel diseases (cSVDs) are a major cause of stroke and dementia.[1] cSVD related lesions on brain MRI can be found in roughly 70% of 65-year-old individuals and in almost all 90-year-olds.[2] Despite the profound health impact of cSVDs, there is no specific treatment, likely due to our limited understanding of underlying disease mechanisms. Because of the small diameter of affected blood vessels in cSVDs and the limited resolution of conventional techniques for in vivo imaging in humans, cSVDs have been mostly studied through markers of parenchymal injury (e.g. lacunes, white matter hyperintensities (WMH), microbleeds, enlarged perivascular spaces,[3] microstructural white matter changes,[4–6] blood based markers of neuro-axonal damage[7]). While these markers are important because of their association with major clinical outcomes including stroke, cognitive decline, and dementia, they represent downstream consequences of cSVDs. To understand underlying mechanisms of cSVDs, it is essential to study the disease at its core, the vessels themselves.

Cerebral Autosomal Dominant Arteriopathy with Subcortical Infarcts and Leukoencephalopathy (CADASIL) is a monogenic form of cSVD caused by mutations in the NOTCH3 gene. Previous studies on the brain vasculature in CADASIL have been mostly restricted to the examination of autopsy material.[8,9] Pathology in pial and small perforating cerebral arteries is an important feature, including degeneration of vascular smooth muscle cells and thickening of the arteriolar wall.[8–10] This likely has an impact on small vessel function, which has indeed been observed in pial and perforating arteries in experimental animal models[11,12] and also in small vessels outside of the brain in humans, for example in the heart.[13] Ultra-high field imaging with 7T-MRI now provides in vivo measures that inform on several aspects of cerebral small vessel function in humans, including perforating artery flow velocity and stiffness, and endothelium dependent and independent vascular reactivity in different brain regions.[14,15] These measures may provide leads on disease mechanisms in CADASIL and other forms of cSVDs.

We set out to evaluate cerebral small vessel function in CADASIL patients using 7T-MRI. Specifically, we assessed which measures of small vessel function on 7T-MRI are affected in CADASIL patients compared with controls and if small vessel dysfunction on 7T-MRI is associated with WMH in CADASIL.

Methods

Study design and participants

Participants in this study were recruited through the ZOOM@SVDs study, a prospective observational cohort study.[15] At University Hospital LMU Munich, 23 CADASIL patients and 13 individually age- and sex-matched controls were recruited between October 2017 and July 2019. CADASIL was either confirmed by mutation in the NOTCH3 gene (n=20) or by skin biopsy (n=3). Controls were recruited among partners or relatives of the patients and through flyer advertisement. Participants underwent clinical assessment and 3T brain MRI at the LMU and travelled to the UMC Utrecht in the Netherlands to undergo 7T brain MRI. Participants travelled to Utrecht through their preferred means and were offered a one night stay in a hotel. All travel expenses were covered. Participants received no further financial compensation. Detailed inclusion and exclusion criteria and study procedures are published elsewhere.[15] The Medical Ethics Review Committees of the LMU (Project Number 17-088) and UMC Utrecht (Project number NL62090.041.17) approved the study. Written informed consent was obtained from all participants. The study was registered in the Netherlands Trial Register; NTR6265.

Clinical assessment

Demographics and vascular risk profiles were recorded for all participants. Stroke, hypertension, and diabetes mellitus were recorded based on presence in medical history. Current systolic and diastolic blood pressure were based on seven-day blood pressure measurements done three times a day at home with a telemetric blood pressure device (Tel-O-Graph® GSM Plus, graded A/A by the British Hypertension Society). Smoking was based on self-report.

3T brain MRI

Participants underwent 3T brain MRI at the LMU on a Siemens Magnetom Skyra 3T scanner with a 64-channel head coil. The scan protocol included 3D T1-weighted gradient echo, 3D T2*-weighted multi-echo gradient echo, and 3D fluid-attenuated inversion recovery (FLAIR) scan (sequence details Table 1). Lacunes (on T1-weighted and FLAIR scan) and microbleeds (on longest echo time of T2*-weighted scan) were manually counted according to the STRIVE-criteria.[16] Segmentations of WMH, lacunes, intracranial volume and total brain volume, were assessed as previously published.[17]

7T brain MRI

All participants underwent 7T-MRI at the UMC Utrecht (Philips Healthcare, Best, The Netherlands) using a 32-channel receive head coil with a quadrature transmit coil (Nova Medical, MA, USA) (sequence details Table 1). Three complementary aspects of small vessel function were investigated.

1. 7T-MRI allows to assess blood flow velocity and pulsatility within perforating arteries at the level of the basal ganglia (known diameter 200-800μm) and centrum semiovale (100-300μm), indicative of perforating artery stiffness.[18–20] Flow velocity data was acquired with two single-slice 2D-Qflow velocity mapping acquisitions, and a peripheral pulse unit was used for retrospective cardiac gating. Mean blood flow velocity and pulsatility index in perforating arteries in the basal ganglia and centrum semiovale were calculated (see supplementary table for exact processing pipeline).

2. Reactivity in response to a short visual stimulus was assessed in the visual cortex with the blood-oxygen-level dependent (BOLD) response. Participants were presented with a 8Hz blue-yellow reversing checkerboard using very short (0.5s) and long blocks (16.7s) of visual stimulation, during a 10-minute experiment (for detailed parameters see design paper[15]). Neuronal activation to these stimuli induces vasodilation via neurovascular coupling and signalling from capillaries to pre-capillary arterioles to increase blood flow to the activated cortex.[21] The activation pattern in response to the long blocks of visual stimulation for each subject served as region of interest. The BOLD signal on 7T-MRI is weighted more towards signals from the microvasculature (e.g. capillaries, small venules) than on lower field strength,[22] which allows us to measure BOLD reactivity in small vessels as long as the large pial veins are removed from the region of interest.[15] In addition, the high temporal resolution on 7T-MRI provides a precise estimate of the hemodynamic response function (HRF) within the region of interest in response to very short visual stimulation (see supplementary table for exact processing pipeline). The BOLD% signal change and full width at half maximum of the HRF estimate are the main outcome variables.

3. Whole-brain reactivity to a hypercapnic stimulus was measured with the BOLD response. The participants wore a face mask to breathe medical air and premixed 6% CO2 in air in alternating blocks: three two-minute blocks of medical air with two two-minute blocks of 6% CO2 in air in between (for detailed parameters see design paper[15]). The hypercapnic stimulus causes relaxation of the vascular smooth muscle cells, primarily at the level of the arterioles, thereby causing endothelium independent small vessel vasodilation.[23,24] Monitoring equipment recorded pulse rate and end-tidal CO2 (40Hz,; CD3-A AEI Technologies, Pittsburgh, USA) (based on Thrippleton et al[25], as specified in van den Brink et al[15]). Signal from large pial veins was again excluded so the remaining BOLD signal primarily represents small vessel reactivity (see supplementary table for exact processing pipeline). The high spatial resolution of BOLD on 7T-MRI permits regional analyses. The BOLD% signal change in the cortical grey matter, subcortical grey matter, and white matter are the main outcome measures.

The order of MRI scans was strictly adhered to. After the first BOLD scan with visual stimulation, every participant was taken out of the scanner. After a short break of at least five minutes, the participant put on the breathing mask and the protocol was continued with the hypercapnic challenge.

Table 1: Brain MRI scan parameters

MR sequence	Acquired resolution mm^3	Time min:s	Parameters
3T MRI			
T1-weighted GE	1.0x1.0x1.0	05:08	FOV 256x256x192 mm^3; TR 2500 ms; TE 4.37 ms; TI 1100 ms; flip angle 7°
T2*-weighted GE	0.9x0.9x2.0	05:56	FOV 230x160x187 mm^3; TR 35 ms; TE 4.9-29.5 ms, deltaTE 4.9ms; flip angle 15°
FLAIR	1.0x1.0x1.0	06:27	FOV 250x250x176 mm^3; TR 5000 ms; TE 398 ms; TI 1800 ms
7T MRI			
T1-weighted	1.0x1.0x1.0	01:59	FOV 250x250x190 mm^3; TR 4.2 ms; TI 1297 ms; shot interval 3000 ms; flip angle 5°
2D-Qflow CSO	0.3x0.3x2.0	03:24*	FOV 230x230 mm^2; reconstructed resolution 0.18x0.18mm^2 ; TR 29 ms; TE 16 ms; Venc 4 cm/s; temporal resolution 116 ms; flip angle 50°
2D-Qflow BG	0.3x0.3x2.0	03:47*	FOV 170x170 mm^2; reconstructed resolution 0.18x0.18mm^2 ; TR 28 ms; TE 15 ms; Venc 20 cm/s ; temporal resolution 112 ms; flip angle 50°
BOLD visual cortex[a]	1.3x1.3x1.3	10:05	FOV 140x140x11 mm^3; TR 880 ms; TE 25 ms
BOLD whole-brain[b]	2.0x2.0x2.0	10:00	FOV 224x256x101 mm^3; TR 3000 ms; TE 25 ms

BG = basal ganglia; BOLD = blood-oxyen-level dependent; CSO = centrum semiovale; FOV = field of view; GE = gradient echo; TE = echo time; TI = inversion time; TR = repetition time.
*Total scan time for a heart rate of 80bpm.
[a] The participant is presented with a *short visual stimulus*.
[b] The participant undergoes a *hypercapnic challenge*. Between the two BOLD sequences the participant is taken out of the scanner for a short break and to put on the mask for the hypercapnic challenge.

Statistical analysis

Differences in characteristics between CADASIL patients and controls were tested with an independent samples t-test for continuous normally distributed data, Mann-Whitney U test for non-parametric continuous data and chi-square for categorical data. Differences between patients and controls in small vessel function measures were tested with ANCOVA. Age and sex were included as a covariate to accommodate small differences in age and sex between groups. Pulsatility index was additionally corrected for mean

blood flow velocity, and BOLD hypercapnia comparisons were additionally corrected for change in end-tidal CO2 in response to hypercapnia.

Within the patient group, mean blood flow velocity and pulsatility index in the perforating arteries in the centrum semiovale and BOLD% signal change to hypercapnia were compared in normal appearing white matter (NAWM) and WMH with a paired t-test. This comparison could not be made for perforating arteries in the basal ganglia because of limited WMH volume in that region of interest. For the same reason NAWM versus WMH comparisons for BOLD% signal change to hypercapnia could not be performed in control participants.

For measures of small vessel function that differed between patients and controls we performed explorative analyses in the patient group, where we related these measures to age and WMH volume. WMH volume was normalized to the intracranial volume and because data were skewed, we used the cube-root of the WMH volume. Given the collinearity of possible confounders (e.g. age relates to disease stage) with small vessel function measures, we did not correct for possible confounding variables in these exploratory analyses.

All statistical analyses were performed in SPSS version 25 and $p<0.05$ was considered significant.

Results

The characteristics of the 23 CADASIL patients and 13 controls are shown in Table 2. Groups were reasonably well matched with respect to age and sex (patients: mean age 51.1±10.1 years, 52% female; controls: 46.1±12.6 years, 46% female). As expected, patients more often had a history of stroke, more often used antiplatelet drugs, and showed high burden of imaging markers of cSVD on 3T MRI. None of the controls was excluded because of covert cSVD on MRI (i.e. presence of lacunes or Fazekas ≥ 2 as defined in the protocol[15]), as expected given their age. Figure 1 lists the number of 7T measures included in the final analysis. Participants with missing or failed 7T measurements were no different regarding demographics or disease severity than participants with complete 7T datasets.

Table 2: Characteristics of CADASIL patients and controls

	CADASIL n=23	**Control n=13**	***p*-value**
Demographics			
Age, M±SD	51.1±10.1	46.1±12.6	0.20
Female sex, n (%)	12 (52)	6 (46)	1.00
Vascular risk profile			
Stroke, n (%)	7 (30)	0 (0)	0.03
Hypertension, n (%)	4 (17)	1 (8)	0.63
Current 7-day systolic BP, M±SD [mmHg]	118.4±10.1	120.9±10.2	0.48
Current 7-day diastolic BP, M±SD [mmHg]	76.0±8.9	79.0±10.6	0.37
Diabetes Mellitus, n (%)	0 (0)	1 (8)	0.36
Current/ever smoker, n (%)	15 (65)	6 (46)	0.31
Medication use			
Antihypertensives, n (%)	6 (26)	1 (7)	0.23
Statins, n (%)	9 (39)	1 (7)	0.06
Antiplatelet drugs, n (%)	14 (61)	1 (7)	0.004
3T MRI SVD markers			
WMH volume, median [min-Q1-Q3-max] [% of ICV]	3.87 [0.88-2.06-5.56-7.89]	0.01 [0.00-0.00-0.03-0.12]	<0.001
Lacune presence, n (%)	13 (57)	0 (0)	0.001
Lacune count[a], median [Q1-Q3]	4 [3-8]	0 [0-0]	
Microbleed presence, n (%)	13 (57)	0 (0)	0.001
Microbleed count[b], median [Q1-Q3]	3 [2-8]	0 [0-0]	
Brain volume, M±SD [% of ICV]	78.3±5.2	77.6±3.2	0.76

BP = blood pressure; M = mean; ICV = intracranial volume; SD = standard deviation; WMH = white matter hyperintensities; Q1-Q3 = quartile 1 and quartile 3.

[a] Count for participants with ≥ 1 lacune(s). [b] Count for participants with ≥ 1 microbleed(s).

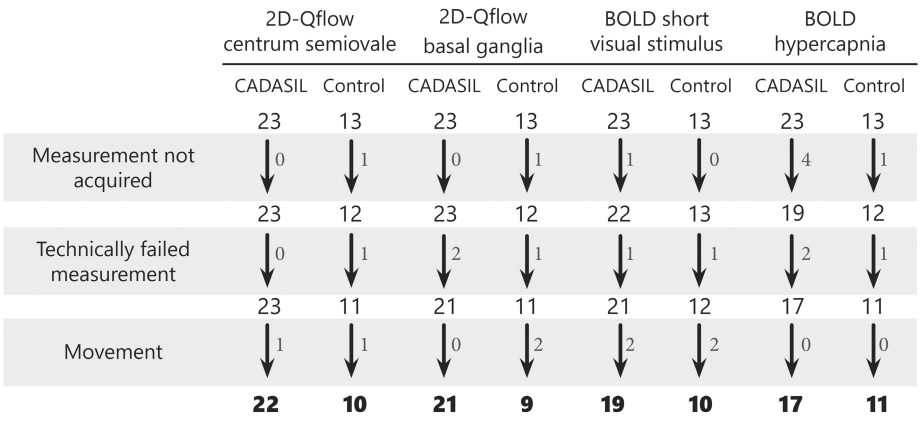

Figure 1: Flowchart showing reasons for excluded scans per small vessel function measure. Reasons for not acquired measurements are: technical failure on the scanner for the 2D-Qflow scans, glasses that would not fit in the head coil for the BOLD short visual stimulus scan, and participants unwilling or unable to do the hypercapnia challenge after first trying it outside the scanner for the BOLD hypercapnia scan.

Small vessel function in CADASIL patients and controls

Perforating artery flow velocity and pulsatility

Perforating artery density (i.e. number of perforating arteries per cm^2 of the subject specific region of interest) was similar in patients and controls both in the centrum semiovale (2.2±0.8/cm^2 and 2.2±1.0/cm^2 respectively, p=0.86) and the basal ganglia (0.9±0.3/cm^2 and 1.0±0.3/cm^2, p=0.33). Figure 2A and 2C display the mean blood flow velocity in perforating arteries in the centrum semiovale and basal ganglia respectively for CADASIL patients and controls (see Figure 2B and 2D for individual traces). Mean perforating artery blood flow velocity was lower, and pulsatility index higher in CADASIL patients than in controls, both in the centrum semiovale and basal ganglia (Table 3). When only perforating arteries in the NAWM were considered, differences between patients (blood flow velocity 0.55±0.07 cm/s and pulsatility index 0.62±0.24) and controls (blood flow velocity 0.63±0.13 cm/s and pulsatility index 0.37±0.11) were similar (p=0.05 and p=0.01 respectively). Among CADASIL patients perforating artery flow velocity and pulsatility were similarly affected in WMH (blood flow velocity 0.48±0.14 cm/s and pulsatility index 0.85±0.45) and NAWM (blood flow velocity 0.53±0.06 cm/s and 0.60±0.28, p=0.14 and p=0.07 respectively).

Small vessel reactivity in response to a visual stimulus

Figure 2E displays the mean estimate of the HRF to a visual stimulus in the visual cortex in CADASIL patients and controls respectively (see Figure 2F for individual traces). Of note, the size (i.e. number of activated voxels) of the participant-specific regions of interest

in which the HRFs were estimated was similar between patients (percentage activated voxels in scanning plane: 32.7±13.3 and controls (30.4±12.7, *p*=0.54). The peak BOLD% signal change was lower in patients compared with controls (Table 3). There was no significant group difference in response timing parameters; full width at half maximum (Table 3), onset time (patients 2.10±0.54s; controls 1.72±0.46s, *p*=0.09), and time-to-peak (4.62±1.04s; 4.39±0.38s, *p*=0.46).

Whole-brain small vessel reactivity to a hypercapnic stimulus

There were no significant group differences in BOLD% signal change to hypercapnia in any of the regions of interest (Table 3). When looking in more detail, BOLD% signal change was non-significantly higher in the cortical grey matter, total white matter and NAWM in patients versus controls (Table 3). In patients, BOLD% signal change was lower in WMH (0.24±0.40) than NAWM (0.53±0.54, *p*=0.02).

Table 3: Small vessel function on 7T MRI in CADASIL patients and controls

	CADASIL	Control	*p*-value
2D-Qflow centrum semiovale[a]	n=22	n=10	
Blood flow velocity [cm/s]	0.54±0.06	0.63±0.13	0.03
Pulsatility index[b]	0.57±0.19	0.37±0.11	0.009
2D-Qflow basal ganglia[a]	n=21	n=9	
Blood flow velocity [cm/s]	3.07±0.67	4.05±0.83	0.003
Pulsatility index[b]	0.46±0.12	0.29±0.15	0.06
BOLD short visual stimulus[c]	n=19	n=10	
BOLD % signal change	0.61±0.20	0.82±0.25	0.04
Full width at half max [s]	3.82±0.65	3.94±0.36	0.59
BOLD hypercapnic stimulus[d]	n=17	n=11	
CGM BOLD % signal change	3.66±1.24	3.07±1.20	0.26
SGM BOLD % signal change	3.37±0.98	3.45±1.43	0.77
WM BOLD % signal change	0.35±0.33	0.17±0.31	0.31
NAWM BOLD % signal change	0.53±0.54	0.17±0.31	0.18

BOLD = blood-oxygen-level dependent; CGM = cortical grey matter; NAWM = normal appearing white matter; SGM = subcortical grey matter; WM = white matter.
Data are shown as mean ± standard deviation.
[a] The region of interest is the entire centrum semiovale and basal ganglia excluding lacunes. Analyses are corrected for age and sex.
[b] Additional correction for blood flow velocity.
[c] Analyses corrected for age and sex.
[d] Analyses corrected for age, sex and change in end-tidal CO_2 to hypercapnia.

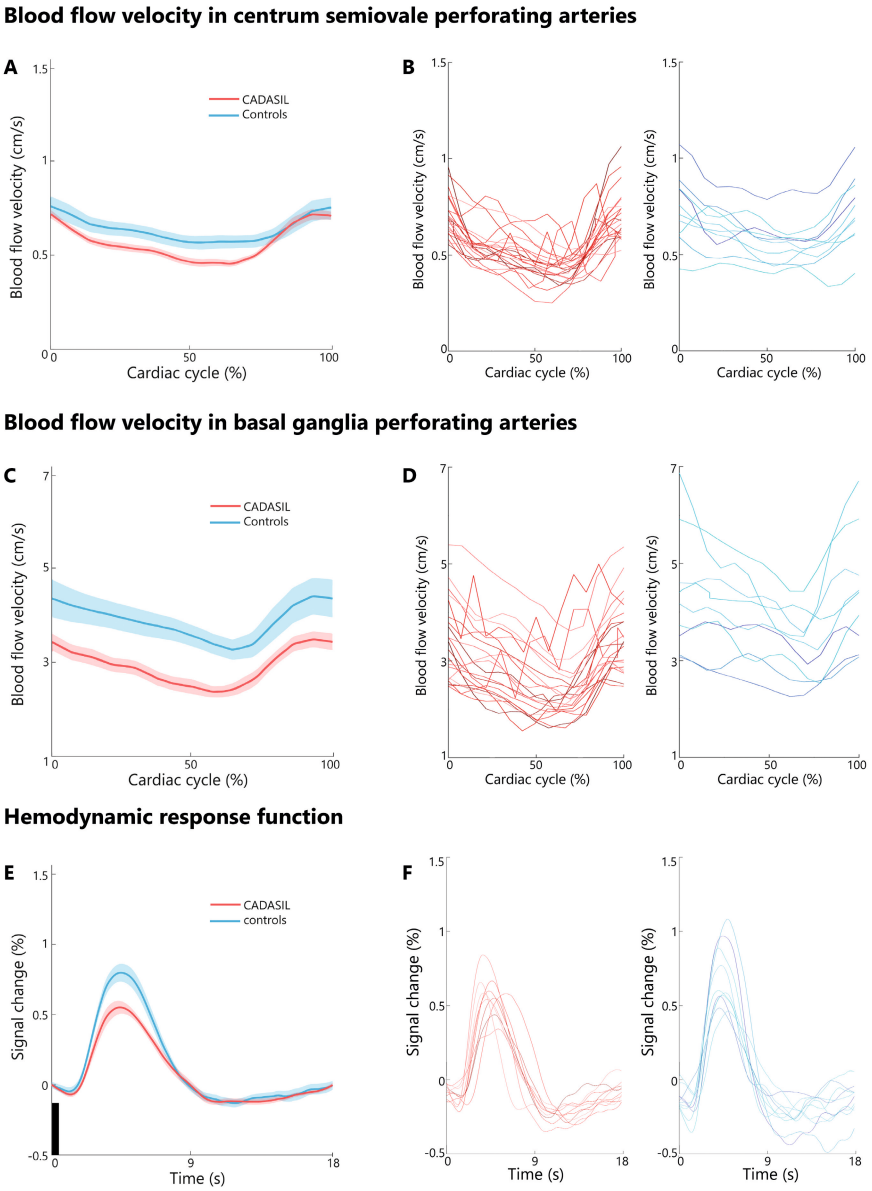

Figure 2: Mean and individual participant traces. The mean blood flow velocity (solid lines) and standard errors of the mean (shaded lines) in perforating arteries in the centrum semiovale (A) and basal ganglia (C) for CADASIL patients and controls. Individual blood flow velocity traces in perforating arteries in the centrum semiovale (B) and basal ganglia (D) for CADASIL patients in red and controls in blue. (E) The mean hemodynamic response function estimates (solid lines) and standard errors of the mean (shaded areas) after 500ms visual stimulation (black bar) for CADASIL patients and controls. (F) Individual BOLD hemodynamic response function estimates after 500ms visual stimulation for all CADASIL patients in red and controls in blue.

Small vessel function and age and WMH volume in CADASIL patients

Relations with age and WMH volume were explored for 7T measures that were affected in patients. There was a trend for a negative association between blood flow velocity within perforating arteries of the centrum semiovale and WMH volume but not age (Table 4). There was no relation between small vessel function measures and antiplatelet or antihypertensive drug use (all $p>0.05$).

Table 4: Associations of small vessel dysfunction with age and white matter hyperintensity volume in CADASIL patients

	Age	WMH volume
2D-Qflow centrum semiovale[a]		
Blood flow velocity (cm/s)	B = -51.25 p = 0.15	B = -0.57 p = 0.05
Pulsatility index	B = -9.62 p = 0.42	B = -0.10 p = 0.35
2D-Qflow basal ganglia[a]		
Blood flow velocity (cm/s)	B = -1.44 p = 0.69	B = -0.04 p = 0.18
Pulsatility index	B = 26.23 p = 0.20	B = 0.13 p = 0.48
BOLD short visual stimulus		
BOLD % signal change	B = -2.17 p = 0.87	B = -0.04 p = 0.70
BOLD hypercapnic stimulus		
WMH BOLD % signal change	B = -2.46 p = 0.74	B = 0.01 p = 0.87

BOLD = blood-oxygen-level dependent; CGM = cortical grey matter; WMH = white matter hyperintensities. Tested with linear regression without corrections. WMH volume was normalized for intracranial volume and cube-root transformed. Sensitivity analyses on non-transformed data, with Spearman correlations, produced similar results (data not shown).

[a] The region of interest is the entire centrum semiovale and basal ganglia minus lacunes.

Discussion

This study found multiple abnormalities of cerebral small vessel function in CADASIL, in a well-defined sample of prospectively recruited patients and controls, applying cutting-edge 7T-MRI technology. These abnormalities involved between group differences in blood flow velocity and pulsatility in perforating arteries, as well as in reactivity to a visual or hypercapnic stimulus, likely reflecting changes in vascular physiology in multiple small vessel populations. Moreover, among patients, cortical reactivity to a hypercapnic stimulus locally associated to white matter injury.

Reduced mean flow velocity and increased pulsatility in CADASIL patients were observed in perforating arteries both in the basal ganglia, fed by proximal intracranial arteries, and the centrum semiovale, fed by distal arterial branches. Only one previous study also reported decreased blood flow velocity in perforating arteries in CADASIL[26], albeit in the most proximal section of the lenticulostriate arteries, that have a larger diameter than the perforating arteries in our current work. We previously assessed our 7T-MRI measures of perforating artery flow velocity in a small explorative study in patients with sporadic cSVDs (i.e. with lacunar infarction or deep intracerebral haemorrhage) and observed increased pulsatility in patients compared to controls but no reduction in flow velocity.[19] Decreased blood flow velocity on 2D-Qflow velocity measures can be explained by decreased total blood flow or increase in arteriolar lumen area. The perforating arteries that we assess have a sub-voxel size diameter. Therefore we cannot actually measure lumen area or total blood flow. Of note, a previous autopsy study in CADASIL showed that lumen diameter is unchanged in the basal ganglia, but is decreased due to intimal thickening and fibrosis in perforating arteries in the white matter.[27] Therefore, given the current understanding of the disease,[28] decreased blood flow velocity in CADASIL is likely attributable to decreased total blood flow in the perforating arteries. Of note, flow velocity and pulsatility index in the perforating arteries are not independent of effect up- and downstream in the vascular tree.[29] Increased pulsatility index of perforating artery flow velocity may therefore reflect changes in upstream vessels (generating a more pulsatile perfusion pressure), enhanced stiffness of the pial or perforating arteries themselves, or changes in the downstream vascular bed including abnormal microvascular compliance. Autopsy studies in CADASIL have reported vessel changes primarily in arterioles, but also in capillaries and venules.[28,30,31] In addition to luminal narrowing in white matter arterioles, these changes include degeneration of smooth muscle cells and reduced capillary length. Moreover, although changes in small vessel function have been noted outside of the brain in CADASIL (for example in the heart[13]), indicating systemic effects of the disease, systemic perfusion pressure as reflected in blood pressure and pulse pressure, was not affected in our patients. Hence, upstream changes in larger vessels are unlikely to explain increased pulsatility in CADASIL. It seems more likely that increased pulsatility reflects vascular stiffness of the perforating arteries at the point that they are probed with the 7T measurements or downstream small arterioles. Of note, blood flow velocity and pulsatility index changes in perforating arteries in NAWM and WMH were similar. Hence, the observed changes likely reflect generalized disease effects on these perforating arteries, although it should be considered that 2D slices predominantly capture perforating arteries that are passing through the white matter at the site of measurement rather than arteries that specifically supply the white matter contained in the slice. Finally, we found indications that blood flow velocity in perforating arteries of the centrum semiovale associates negatively with WMH volume, suggesting that these measures may become progressively abnormal in patients as the disease evolves.

Both measures of small vessel reactivity were affected in CADASIL patients. The neurovascular coupling dependent response to a short visual stimulus elicited lower reactivity in the visual cortex in patients compared with controls. Additionally, reactivity to hypercapnia, which acts directly on vascular smooth muscle cells in arterioles, was decreased in WMH compared to NAWM in patients. Similar to our result, decreased reactivity within WMH to hypercapnia and acetazolamide was a consistent finding in earlier studies in CADASIL that were conducted at lower field strength.[32,33] We did observe non-significant higher reactivity to hypercapnia in the cortical grey matter, total white matter and NAWM in patients compared with controls. Whether this finding across these three different regions represents a true phenomenon or is due to chance remains to be determined, as earlier studies have not reported such results.[32,33] On the other hand, increased cortical reactivity in the visual cortex was reported in CADASIL patients versus controls in a study that used visual stimulation, with a much longer stimulus (40s),[34] compared to our study (0.5s). These differential findings are likely the result of fundamental differences in the nature and duration of the stimuli. Clearly, responses to different types of stimuli involve different physiological pathways in different vessel populations. The BOLD signal to a visual stimulus depends on neurovascular coupling, entailing activation of cortical neurons, which directly initiates an endothelium dependent response of local capillaries and upstream feeding arterioles. Hypercapnia, on the other hand, is a stimulus that according to current insight directly affects smooth muscle cells in the arterioles throughout the brain, in an endothelial independent manner.[23] In addition, the differences in stimulus duration between different paradigms will have an effect on the BOLD signal as well. Short stimuli (< 1 second, e.g. short visual stimulation) only engage blood flow changes via arteriole dilation. In contrast, prolonged stimuli (e.g. 2 minute hypercapnia) also induce notable blood volume changes on the venous side that will affect the BOLD signal as well.[35] Therefore, different stimulus durations will also probe different vascular pools and thus assess vascular reactivity and signals of different vessel populations. Our findings thus suggest that in CADASIL patients the vascular system is unable to sufficiently respond to quick, subtle and local demands in the cortex. In contrast, prolonged and global stimulation by hypercapnia can still generate vascular responses, resulting in a preserved response in the cortex, although not in WMH.

Taken together, these findings suggest that changes in small vessel blood flow velocity, pulsatility and reactivity in CADASIL patients depend on the tissue type that is assessed and the type and extent of stimulation. This likely reflects the dynamic nature of small vessel function. These findings warrant further studies, also with longitudinal design and also involving patients with sporadic cSVDs. It would be of particular interest to explore if these measures of small vessel function respond to drug therapy and as such could serve as an intermediate outcome measure in future cSVD drug trials. Reactivity to hypercapnia at 3T MRI is already evaluated in that context.[36] Yet, for the novel more detailed 7T-MRI measures presented here this will first require further characterisation.

A strength of our study is that we used three measures that probe complementary aspects of small vessel function in one patient population. The advantage of 7T-MRI is that it provides high spatial and temporal resolution, but also enhances BOLD signal properties improving signal to noise and permitting separation of the signal in small vessels from that in larger draining veins.[37] Additionally, investigating a pure, genetically-defined disease like CADASIL enables to study cSVD without confounding factors associated with aging. A limitation of our study is potential selection bias inherent to the relatively demanding study protocol, which required participants to travel from Germany to the Netherlands for 7T brain MRI. As a consequence, patients in this study were mostly in earlier disease stages with relatively limited lesion load and cognitive problems. This limited the possibilities to study the relation of small vessel function with markers of disease severity. On the other hand, the study shows that even in early stages, small vessel function changes are already apparent. In addition, the control group was age-matched and thus relatively young as well, with low burden of cSVD, which may have increased the contrasts between groups. Another limitation of the visual stimulus method is its dependence on an intact cortical neuronal response to the visual stimulus. Although we did not test this neuronal response in our study, it was previously shown to be unaffected in CADASIL patients.[34] Lastly, the temporal resolution of the Qflow sequences was relatively low, which could cause for an underestimation of the pulsatility index. The temporal resolution however needs to be balanced with a tolerable scan time[38] and we can still reliably study relative differences between patients and controls.

In conclusion, multiple aspects of cerebral small vessel function on 7T-MRI were abnormal in CADASIL patients, indicative of increased arteriolar stiffness and regional abnormalities in reactivity, locally also in relation to white matter injury. These abnormalities likely reflect dynamic changes in vascular physiology in multiple small vessel populations. These novel functional markers help to better understand disease mechanisms in CADASIL, but are likely also important for sporadic cSVDs.

References

1. Wardlaw JM, Smith C, Dichgans M. Small vessel disease: mechanisms and clinical implications. *Lancet Neurol*. 2019;18:684-696.
2. Debette S, Schilling S, Duperron MG, Larsson SC, Markus HS. Clinical Significance of Magnetic Resonance Imaging Markers of Vascular Brain Injury: A Systematic Review and Meta-analysis. *JAMA Neurol*. 2019;76:81-94.
3. Wardlaw JM, Smith EE, Biessels GJ, et al. Neuroimaging standards for research into small vessel disease and its contribution to ageing and neurodegeneration. *Lancet Neurol*. 2013;12:822-838.
4. Van Norden AGW, De Laat KF, Van Dijk EJ, et al. Diffusion tensor imaging and cognition in cerebral small vessel disease: The RUN DMC study. *Biochim Biophys Acta - Mol Basis Dis*. 2012;1822:401-407.
5. Tuladhar AM, Van Norden AGW, De Laat KF, et al. White matter integrity in small vessel disease is related to cognition. *NeuroImage Clin*. 2015;7:518-524.
6. Baykara E, Gesierich B, Adam R, et al. A Novel Imaging Marker for Small Vessel Disease Based on Skeletonization of White Matter Tracts and Diffusion Histograms. *Ann Neurol*. 2016;80:581-592.
7. Duering M, Konieczny MJ, Tiedt S, et al. Serum neurofilament light chain levels are related to small vessel disease burden. *J Stroke*. 2018;20:228-238.
8. Chabriat H, Joutel A, Dichgans M, Tournier-Lasserve E, Bousser MG. Cadasil. *Lancet Neurol*. 2009;8:643-653.
9. Di Donato I, Bianchi S, De Stefano N, et al. Cerebral Autosomal Dominant Arteriopathy with Subcortical Infarcts and Leukoencephalopathy (CADASIL) as a model of small vessel disease: Update on clinical, diagnostic, and management aspects. *BMC Med*. 2017;15:1-12.
10. Hervé D, Chabriat H. CADASIL. *J Geriatr Psychiatry Neurol*. 2010;23:269-276.
11. Joutel A, Monet-leprêtre M, Gosele C, et al. Cerebrovascular dysfunction and microcirculation rarefaction precede white matter lesions in a mouse genetic model of cerebral ischemic small vessel disease. *J Clin Invest*. 2010;120:433-445.
12. Dabertrand F, Krøigaard C, Bonev AD, et al. Potassium channelopathy-like defect underlies early-stage cerebrovascular dysfunction in a genetic model of small vessel disease. *Proc Natl Acad Sci*. 2015;112:E796-E805.
13. Argirò A, Sciagrà R, Marchi A, et al. Coronary microvascular function is impaired in patients with cerebral autosomal dominant arteriopathy with subcortical infarcts and leukoencephalopathy. *Eur J Neurol*. 2021;28:3809-3813.
14. Zwanenburg JJM, Van Osch MJP. Targeting cerebral small vessel disease with MRI. *Stroke*. 2017;48:3175-3182.
15. van den Brink H, Kopczak A, Arts T, et al. Zooming in on cerebral small vessel function in small vessel diseases with 7T MRI: Rationale and design of the “ZOOM@SVDs” study. *Cereb Circ - Cogn Behav*. 2021;2:100013.
16. Wardlaw JM, Smith EE, Biessels GJ, et al. Neuroimaging standards for research into small vessel disease and its contribution to ageing and neurodegeneration. *Lancet Neurol*. 2013;12:822-838.

17. Gesierich B, Tuladhar AM, ter Telgte A, et al. Alterations and test–retest reliability of functional connectivity network measures in cerebral small vessel disease. *Hum Brain Mapp*. 2020;41:2629-2641.
18. Bouvy WH, Geurts LJ, Kuijf HJ, et al. Assessment of blood flow velocity and pulsatility in cerebral perforating arteries with 7-T quantitative flow MRI. *NMR Biomed*. 2015;29:1295-1304.
19. Geurts L, Zwanenburg JJM, Klijn CJM, Luijten PR, Biessels GJ. Higher Pulsatility in Cerebral Perforating Arteries in Patients With Small Vessel Disease Related Stroke, a 7T MRI Study. *Stroke*. 2019;50:62-68.
20. Arts T, Siero JCW, Biessels GJ, Zwanenburg JJM. Automated Assessment of Cerebral Arterial Perforator Function on 7T MRI. *J Magn Reson Imaging*. 2021;53:234-241.
21. Iadecola C. The Neurovascular Unit Coming of Age: A Journey through Neurovascular Coupling in Health and Disease. *Neuron*. 2017;96:17-42.
22. Uludağ K, Müller-Bierl B, Uğurbil K. An integrative model for neuronal activity-induced signal changes for gradient and spin echo functional imaging. *Neuroimage*. 2009;48:150-165.
23. Ainslie PN, Duffin J. Integration of cerebrovascular CO2 reactivity and chemoreflex control of breathing: Mechanisms of regulation, measurement, and interpretation. *Am J Physiol - Regul Integr Comp Physiol*. 2009;296:R1473-R1495.
24. Sleight E, Stringer MS, Marshall I, Wardlaw JM, Thrippleton MJ. Cerebrovascular Reactivity Measurement Using Magnetic Resonance Imaging: A Systematic Review. *Front Physiol*. 2021;12:643468.
25. Thrippleton MJ, Shi Y, Blair G, et al. Cerebrovascular reactivity measurement in cerebral small vessel disease: Rationale and reproducibility of a protocol for MRI acquisition and image processing. *Int J Stroke*. 2018;13:195-206.
26. Sun C, Wu Y, Ling C, et al. Reduced blood flow velocity in lenticulostriate arteries of patients with CADASIL assessed by PC-MRA at 7T. *J Neurol Neurosurg Psychiatry*. 2021;0:1-3.
27. Miao Q, Paloneva T, Tuisku S, et al. Arterioles of the Lenticular Nucleus in CADASIL. *Stroke*. 2006;37:2242-2247.
28. Craggs LJL, Yamamoto Y, Deramecourt V, Kalaria RN. Microvascular pathology and morphometrics of sporadic and hereditary small vessel diseases of the brain. *Brain Pathol*. 2014;24:495-509.
29. Arts T, Onkenhout LP, Amier RP, et al. Non-Invasive Assessment of Damping of Blood Flow Velocity Pulsatility in Cerebral Arteries With MRI. *J Magn Reson Imaging*. 2022;55:1785-1794.
30. Rajani RM, Ratelade J, Domenga-Denier V, et al. Blood brain barrier leakage is not a consistent feature of white matter lesions in CADASIL. *Acta Neuropathol Commun*. 2019;7:1-14.
31. Pettersen JA, Keith J, Gao F, Spence JD, Black SE. CADASIL accelerated by acute hypotension: Arterial and venous contribution to leukoaraiosis. *Neurology*. 2017;88:1077-1080.
32. Chabriat H, Pappata S, Ostergaard L, et al. Cerebral hemodynamics in CADASIL before and after acetazolamide challenge assessed with MRI bolus tracking. *Stroke*. 2000;31:1904-1912.
33. Atwi S, Shao H, Crane DE, et al. BOLD-based cerebrovascular reactivity vascular transfer function isolates amplitude and timing responses to better characterize cerebral small vessel disease. *NMR Biomed*. 2019;32:1-12.
34. Cheema I, Switzer AR, McCreary CR, et al. Functional magnetic resonance imaging responses in CADASIL. *J Neurol Sci*. 2017;375:248-254.
35. Uludağ K, Blinder P. Linking brain vascular physiology to hemodynamic response in ultra-high field MRI. *Neuroimage*. 2018;168:279-295.

36. Blair GW, Janssen E, Stringer MS, et al. Effects of Cilostazol and Isosorbide Mononitrate on Cerebral Hemodynamics in the LACI-1 Randomized Controlled Trial. *Stroke*. 2022;53:29-33.
37. Siero JCW, Bhogal A, Jansma JM. Blood oxygenation level-dependent/Functional Magnetic Resonance Imaging: Underpinnings, Practice, and Perspectives. *PET Clin*. 2013;8:329-344.
38. Geurts L, Biessels GJ, Luijten P, Zwanenburg J. Better and faster velocity pulsatility assessment in cerebral white matter perforating arteries with 7T quantitative flow MRI through improved slice profile, acquisition scheme, and postprocessing. *Magn Reson Med*. 2018;79:1473-1482.

Supplementary material

Supplementary Table: Processing pipelines for the three 7T MRI measures that assess small vessel function

Sequence	Processing steps
Blood flow velocity and pulsatility index in perforating arteries	To calculate mean blood flow velocity and pulsatility index in the perforating arteries in the basal ganglia and centrum semiovale, the post processing pipeline of the 2D-Qflow scans involved: (1) generating regions of interest in the basal ganglia and centrum semiovale, (2) detecting individual perforating arteries, and (3) calculating mean blood flow velocity and pulsatility index from the velocity data.
	1. The region of interest in the basal ganglia slice was manually delineated in the 2D-Qflow magnitude image. The region of interest in the centrum semiovale was generated using an automatically delineated 2D white matter mask from a T1-weighted scan. The outside border of this mask (80 pixels = 14 mm) was excluded to be robust to small participant motion between the acquisition of the T1-weighted and the 2D-Qflow scan, which could lead to unsolicited inclusion of cortical vessels located in sulci. Separate regions of interest were also generated for white matter hyperintensities (based on 3T white matter hyperintensity masks) and normal appearing white matter in the centrum semiovale. Lastly, lacunes were excluded from all regions of interest, because no perforating arteries are expected in a cavity. 2. In the regions of interest, perforating artery detection was performed with a previously developed method which automatically excludes perforating arteries in ghosting artefacts in the centrum semiovale, and perforating arteries in the basal ganglia that are oriented non-perpendicularly to the scanning plane.[1] Additionally, apparent perforating arteries that are located within a 1.2 mm radius from each other were excluded, as these mostly are 'false detections' of larger and non-perpendicular vessels. Cerebral perforating artery density was calculated (number of perforating arteries/cm^2). 3. Perforating artery flow velocity was then assessed per participant as in earlier work.[1–3] The blood flow velocity over the cardiac cycle was averaged per participant to calculate mean blood flow velocity in cm/s per participant. To calculate the velocity pulsatility index (PI), the velocities over the cardiac cycle were first normalized and averaged. PI was then calculated per participant as $(V_{max} - V_{min})/V_{mean}$ where V_{max}, V_{min} and V_{mean} are the maximum, minimum and mean of the normalized and averaged blood flow velocity over the cardiac cycle.[2,4] Mean blood flow velocity and pulsatility index are considered the primary outcome measures.

Supplementary Table: Processing pipelines for the three 7T MRI measures that assess small vessel function *(continued)*

Sequence	Processing steps
Small vessel reactivity to a visual stimulus	The visual stimulus experiment that was used to stimulate the visual cortex and induce an increase in BOLD signal compromised two parts. Block design stimulation (33s) was used to determine the region of interest (i.e. the voxels in the scanning volume that show significant activation in response to the visual stimulus), and an event-related design stimulation (500ms) was used to make an estimate of the average hemodynamic response function in response to the visual stimulus in the participant-specific region of interest. The BOLD MRI data that was acquired during the experiment was processed according to the following steps (explained in detail below): (1) data cleaning, (2) generating a participant-specific region of interest in the visual cortex based on BOLD MRI data from the block design, and (3) estimating an average hemodynamic response function per participant based on BOLD MRI data acquired during the event-related design in the region of interest.
	1. Raw BOLD MRI data were motion corrected with the '2Dimreg' function of AFNI.5 Data were spatially smoothed using a 2-mm full width at half maximum (FWHM) Gaussian kernel, and independent component analysis was performed for denoising purposes with the MELODIC tool in FMRIB Software Library FSL (version 6.0., Oxford, UK).6 A maximum of 60 data components were computed and manually rated as signal or noise to delete noise components.7 The dataset was then cut to create a separate dataset for the event-related and the block design parts, 589 and 129 volumes respectively (note 34 baseline volumes between the event-related and the block design parts were included in both the event-related and block design datasets).

Supplementary Table: Processing pipelines for the three 7T MRI measures that assess small vessel function *(continued)*

Sequence	Processing steps
	2. Generation of the participant-specific region of interest was based on the block design data. Data were slice time corrected and temporally filtered to remove slow signal drifts using a high-pass temporal filter with a cut-off at 1/100Hz. Cluster analysis was then performed using a time-series GLM approach as implemented in FEAT of FSL. The GLM included several regressors; the regressor of interest was the time-series model consisting of the task design convolved with a gamma hemodynamic response function. A temporal derivative regressor was added to allow for slight timing differences of the stimulus model, and additional regressors for outlier time points (as detected with FSL Motion Outliers with standard settings: root mean square intensity difference to first volume) were added to remove the effects of outliers from the analysis. Estimates of brain activity magnitude in response to the stimulus were computed and converted to a *z*-statistic. The *z*-statistic images were non-parametrically thresholded using clusters determined by $z>3.1$ and a (corrected) cluster significance threshold of $p=.05$. The significantly activated clusters defined the starting point of the region of interest. From this region of interest, large draining vessels were removed in order for the region of interest to represent the activated voxels in the parenchyma and be most specific to small vessel reactivity. On 7T MRI, large vessels have a low BOLD signal and high BOLD signal variability wherefore we could calculate a temporal noise-to-signal ratio per voxel (*100%) and then apply a single fixed value threshold (of 3%) above which the voxel represented signal from a large vessel. 3. Estimation of the hemodynamic response function was performed with the event-related dataset, as in earlier published work.8 In short, the estimation was done by means of conjugate gradients for deconvolution, after normalization of the voxel's signal time-series by the baseline signal (mean of the first 45 volumes) and 8-fold Fourier interpolation (images were acquired every 880 ms, thus yielding an effective temporal hemodynamic response function resolution of 110 ms). This level of interpolation was chosen for the purpose of slice-timing correction, and thus equal to the number of slices (=8). Slice-timing correction was performed simultaneously with the hemodynamic response function estimation by shifting the stimuli model for each slice according to the slice acquisition time. BOLD % signal change (i.e. maximum amplitude), full width at half maximum, time-to-peak, and onset time were calculated from the hemodynamic response functions. Onset time was defined by the fit of a line to the slope between 20% and 80% of the peak of the hemodynamic response function and computing the intercept with the baseline.9 BOLD % signal change and full width at half maximum of the hemodynamic response function estimate are considered main outcome variables.

Supplementary Table: Processing pipelines for the three 7T MRI measures that assess small vessel function *(continued)*

Sequence	Processing steps
Small vessel reactivity to a hypercapnic stimulus	To determine cerebrovascular reactivity to a hypercapnic stimulus, the acquired BOLD MRI data post-processing pipeline involved: (1) delineation of region of interest for cortical grey matter, subcortical grey matter and white matter (including separate masks for white matter hyperintensities and normal appearing white matter), and (2) a voxel-based analysis to calculate the amplitude of the reactivity response.
	1. Several masks were used in order to make the regions of interest. The white matter and grey matter probability masks and the delineations of white matter hyperintensities and lacunes were taken from the 3T images. Lacunes were dilated with a 2D 3mm kernel to include surrounding pathology. Lacunes and white matter hyperintensities together constitute the lesion mask. With these masks, the regions of interest were calculated. First, the subcortical grey matter region of interest was defined using the FIRST tool in FSL10 and consists of the thalamus, caudaute head and putamen. The lesion mask was subtracted from this subcortical grey matter region of interest, the region of interest was eroded with a cubic kernel of 3 voxels and binarized. The cortical grey matter region of interest was defined by subtracting the subcortical grey matter from the grey matter probability mask, thresholding the result at 0.5 and binarizing. The normal appearing white matter region of interest was derived by subtraction of the lesions and large vessels around the ventricles from the white matter probability mask, thresholding at 0.9 and binarizing. These large vessels around the ventricles were deleted by means of generating a delated ventricle mask. This same mask was also used to exclude large draining vessels from the white matter hyperintensity mask, to obtain the white matter hyperintensity region of interest. The white matter region of interest is a combination of both the normal appearing white matter and white matter hyperintensity region of interest. Lastly, all regions of interest are multiplied with a binary brain mask, and the pons and cerebellum were removed from all regions of interest. The regions of interest were registered from 3T space to 7T BOLD space to be able to obtain the regional BOLD response amplitudes. In 7T BOLD space, another large vessel mask was made using the temporal noise-to-signal ratio method as described earlier, with the threshold set at 1.5* the mean noise-to-signal in the BOLD data for each participant. This large vessel mask subtracted from the cortical and subcortical grey matter masks.

Supplementary Table: Processing pipelines for the three 7T MRI measures that assess small vessel function *(continued)*

Sequence	Processing steps
	2. To obtain BOLD % signal change to the hypercapnic stimulus, BOLD data were processed with FSL. The data were motion-corrected using FSL MCFLIRT11 and smoothed (FWHM Gaussian = 3 mm), after which ICA-AROMA was applied to identify and remove motion-related components from the data.12 The 'non-aggressive' setting was used with the high-frequency content threshold adjusted from 0.35 to 0.70 because of overall high amount of high frequency content in the data. The automatic labelling of ICA-AROMA was checked and corrected as needed. In addition, FSL Motion Outliers (with standard settings) was used to identify time points in the data that showed large motion, and slice time correction was performed in FEAT. Using a general linear model in FSL FEAT, each participant's BOLD signal was regressed with the participant's end-tidal CO2 trace (the envelope of the subject-specific end-tidal CO2, derived and normalized between 0 and 1 using Matlab (R2020a, Mathworks, Natick, MA). The model trace is convolved by a canonical hemodynamic response (gamma), including a set hemodynamic delay of 6 seconds to account for delays caused by the tubing, as well as the BOLD scan number (to account for linear signal drift), and the outlier time points added as confounders. This yielded a map of the response amplitude expressed as a percentage change in BOLD in response to the stimulus. Finally, we overlaid the regions of interest on this map and performed voxel-wise averaging to obtain the region of interest specific BOLD % signal change. The BOLD % signal change in the cortical grey matter, subcortical grey matter and white matter regions of interest are considered main outcome measures.

References

1. Arts T, Siero JCW, Biessels GJ, Zwanenburg JJM. Automated Assessment of Cerebral Arterial Perforator Function on 7T MRI. *J Magn Reson Imaging*. 2021;53:234-241.
2. Bouvy WH, Geurts LJ, Kuijf HJ, et al. Assessment of blood flow velocity and pulsatility in cerebral perforating arteries with 7-T quantitative flow MRI. *NMR Biomed*. 2015;29:1295-1304.
3. Geurts L, Biessels GJ, Luijten P, Zwanenburg J. Better and faster velocity pulsatility assessment in cerebral white matter perforating arteries with 7T quantitative flow MRI through improved slice profile, acquisition scheme, and postprocessing. *Magn Reson Med*. 2018;79:1473-1482.
4. Geurts L, Zwanenburg JJM, Klijn CJM, Luijten PR, Biessels GJ. Higher Pulsatility in Cerebral Perforating Arteries in Patients With Small Vessel Disease Related Stroke, a 7T MRI Study. *Stroke*. 2019;50:62-68.
5. Cox J.S. RW. H. AFNI: Software for analysis and visualization of functional magnetic resonance neuroimages. *Comput Biomed Res*. 1996;29:162-173.
6. Jenkinson M, Beckmann CF, Behrens TEJ, Woolrich MW, Smith SM. FSL. *Neuroimage*. 2012;62:782-790.
7. Griffanti L, Douaud G, Bijsterbosch J, et al. Hand classification of fMRI ICA noise components. *Neuroimage*. 2017;154:188-205.
8. Siero JC, Petridou N, Hoogduin H, Luijten PR, Ramsey NF. Cortical Depth-Dependent Temporal Dynamics of the BOLD Response in the Human Brain. *J Cereb Blood Flow Metab*. 2011;31:1999-2008.
9. Siero JCW, Ramsey NF, Hoogduin H, Klomp DWJ, Luijten PR, Petridou N. BOLD Specificity and Dynamics Evaluated in Humans at 7 T: Comparing Gradient-Echo and Spin-Echo Hemodynamic Responses. *PLoS One*. 2013;8:1-8.
10. Patenaude B, Smith SM, Kennedy DN, Jenkinson M. A Bayesian model of shape and appearance for subcortical brain segmentation. *Neuroimage*. 2011;56:907-922.
11. Jenkinson M, Bannister P, Brady M, Smith S. Improved Optimization for the Robust and Accurate Linear Registration and Motion Correction of Brain Images. *Neuroimage*. 2002;841:825-841.
12. Pruim RHR, Mennes M, van Rooij D, Llera A, Buitelaar JK, Beckmann CF. ICA-AROMA: A robust ICA-based strategy for removing motion artifacts from fMRI data. *Neuroimage*. 2015;112:267-277.

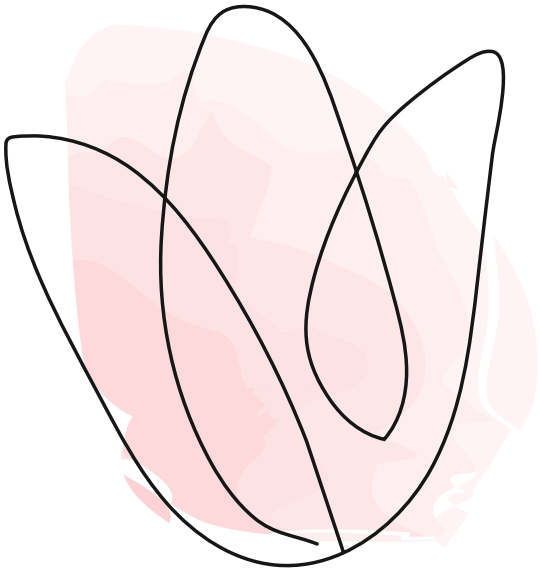

5

Cerebral small vessel function with 7T-MRI in sporadic cerebral small vessel disease: the ZOOM@SVDs study

Hilde van den Brink, Stanley D.T. Pham, Jeroen C.W. Siero, Tine Arts, Laurien Onkenhout, Hugo J. Kuijf, Jeroen Hendrikse, Joanna M. Wardlaw, Martin Dichgans, Jaco J.M. Zwanenburg, Geert Jan Biessels, on behalf of the SVDs@target group

Submitted

Abstract

Background

Cerebral small vessel disease (cSVD) is a major cause of stroke and dementia, but little is known about disease mechanisms at the level of the small vessels. 7T-MRI allows assessing small vessel function in vivo in different vessel populations. We hypothesized that multiple aspects of small vessel function are altered in patients with cSVD and that these abnormalities relate to disease burden.

Methods

46 patients with sporadic cSVD (mean age±sd 65±9 years) and 22 matched controls (64±7 years) participated in the ZOOM@SVDs study. Small vessel function measures on 7T-MRI included: perforating artery blood flow velocity and pulsatility index in the basal ganglia and centrum semiovale, vascular reactivity to visual stimulation in the occipital cortex, and reactivity to hypercapnia in the grey and white matter. Lesion load on 3T-MRI and cognitive function were used to assess disease burden.

Results

Compared with controls, patients had increased pulsatility index (mean difference 0.09, p=0.01) but similar blood flow velocity in basal ganglia perforating arteries and similar flow velocity and pulsatility in centrum semiovale perforating arteries. The duration of the vascular reponse to brief visual stimulation in the occipital cortex was shorter in patients than in controls (mean difference -0.63s, p=0.02), while reactivity to hypercapnia was not significantly affected in the grey and total white matter. Among patients, reactivity to hypercapnia was lower in white matter hyperintensities compared with normal-appearing white matter (BOLD mean difference 0.35%, p=0.001). Blood flow velocity and pulsatility in basal ganglia perforating arteries and reactivity to brief visual stimulation correlated with disease burden.

Conclusion

We observed abnormalities in several aspects of small vessel function in patients with cSVD indicative of regionally increased arteriolar stiffness and decreased reactivity. Worse small vessel function also correlated with increased disease burden. These functional measures provide new mechanistic markers of sporadic cSVD.

Introduction

Cerebral small vessel disease (cSVD) is a disorder of the small perforating arteries, capillaries and venules in the brain and a major cause of stroke and dementia in the elderly.[1] A challenge for research into the underlying disease mechanisms is that the diameter of the affected blood vessels is so small that they are difficult to investigate in vivo in humans. Therefore, previous studies of these vessels in cSVD mostly involved post-mortem neuropathology, observing loss of smooth muscle cells, fibrosis, thickening of the vessel walls and luminal narrowing or even occlusion in cerebral arterioles, but also abnormalities in capillaries and venules.[1] These structural alterations of the vessels are thought to affect their function, which was indeed observed in experimental animal models of small vessel disease.[2,3] Studying small vessel function in humans could provide insight into possible disease mechanisms at the level of the small vessels and thus contribute to the development of urgently needed treatment.

Vessel function on MRI in patients with sporadic cSVD has been the topic of previous (3T-MRI) studies, mostly involving assessment of perfusion, blood-brain barrier permeability and vascular reactivity to vasodilating effects of hypercapnia or acetazolamide as well as blood flow pulsatility in large intracranial arteries. Although the findings from these studies vary, an emerging observation is that vessel function decreases with increasing white matter hyperintensity (WMH) burden.[4–11] With technical advancements in 7T-MRI, we can now study complementary aspects of small vessel function in several vessel populations with a sensitivity and temporal and spatial resolution that was not possible before. These measures can inform on perforating artery flow velocity and stiffness, and endothelium-dependent and independent vascular reactivity in different brain regions.[12] We have recently shown abnormal small vessel function in multiple vessel populations on these 7T-MRI measures in patients with monogenic cSVD.[13] Moreover, one small previous study suggests that perforating artery stiffness may be abnormal in patients with sporadic cSVD.[14]

In this study, we used novel complementary 7T-MRI measures to explore which aspects of small vessel function are abnormal in patients with sporadic cSVD and whether small vessel function relates to disease burden.

Methods

Study design and participants

Patients with symptomatic sporadic cSVD and age- and sex-matched controls were included through the ZOOM@SVDs study at the UMC Utrecht hospital in the Netherlands between March 2017 and April 2021. A total of 54 patients were recruited from the stroke, rehabilitation and memory clinics of the UMC Utrecht and referring neighbouring clinics. Controls (N=28) were recruited among partners or relatives of the patients and through flyer advertisements within the UMC Utrecht. Detailed in- and exclusion criteria are published in the design paper,[12] but in short:

- Sporadic cSVD was defined as either having a history of a clinical lacunar stroke in the last 5 years with a compatible small subcortical infarct visible on MRI or CT, or objective cognitive impairment with Fazekas ≥ 2 WMH on MRI. Patients could not have large vessel disease or a major cardioembolic source of embolism and no other neurological condition affecting the brain.
- Controls were age- and sex- matched to the patients on a group level. Controls could not have a history of stroke or cognitive complaints, as well as "silent" cSVD on 3T brain MRI defined as confluent WMH (Fazekas ≥ 2) or lacunes.

Participants underwent extensive clinical assessment, 3T brain MRI and 7T brain MRI. Seven participants turned out to be screen failures, and seven participants could not successfully undergo 7T brain MRI (see Figure 1 for the in- and exclusion flowchart), leaving 46 patients and 22 controls for inclusion. Detailed study procedures are published elsewhere.[12] The Medical Ethics Review Committee of the UMC Utrecht (Project number NL62090.041.17) approved the study. Written informed consent was obtained from all participants. The study was registered in the Netherlands Trial Register; NTR6265.

Clinical assessment

Stroke, hypertension, hypercholesterolemia and diabetes mellitus were recorded based on presence in medical history, and smoking was based on self-report. Current systolic and diastolic blood pressure and pulse wave velocity were based on seven-day measurements done three times a day at home with a telemetric blood pressure device (Tel-O-Graph® GSM Plus, graded A/A by the British Hypertension Society).[12]

All participants underwent a standardized neuropsychological test battery (full test battery reported in design paper[12]). Individual test scores were standardized into *z*-scores using the control group as a reference. Test *z*-scores were then combined to represent specific cognitive domains. The executive function domain is composed of *z*-scores on category fluency, phonemic fluency, trail-making test (TMT) part B/A, and digit span backward. The attention and processing speed domain is composed of *z*-scores on TMT A and digit span forward. A compound score of executive function and attention and processing speed was calculated as the average of the two domain *z*-scores.[12]

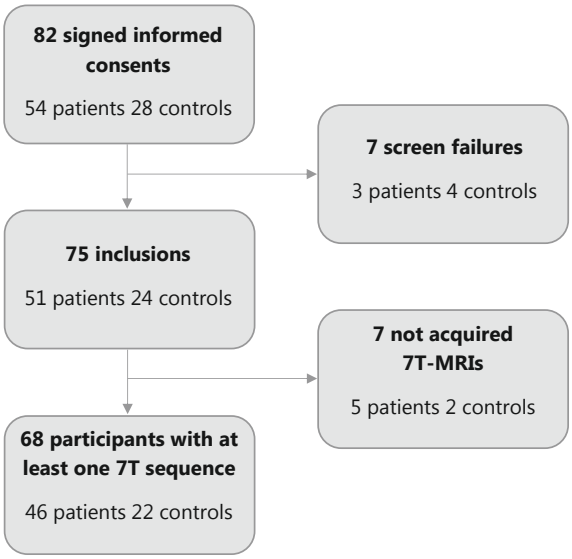

Figure 1: Flowchart of participant in- and exclusions
Reasons for screenfailures are: no lacune lesion on study MRI for three patients recruited because of a clinical diagnosis lacunar infarct, objective cognitive deficits for one control, an occlusion of the internal carotid on study MRI for one control and two controls who had signs of cSVD on study MRI. Reasons for not acquired 7T-MRIs are: scanning was too much a burden for four patients, and one patient and two controls were claustrophobic in the 7T-MRI.

3T brain MRI

Participants underwent 3T brain MRI on a Philips Achieva 3T scanner with an 8-channel SENSE head coil. The scan protocol included 3D T1-weighted gradient echo, 3D T2-weighted turbo spin echo, 3D T2*-weighted gradient echo, and 3D fluid-attenuated inversion recovery (FLAIR) scan (sequence details supplementary Table 1). Lacunes (on T1-weighted, T2-weighted and FLAIR scan) were manually counted and microbleed (on T2*-weighted scans) counting was supported by semi-automated rating software.[14] Ratings were performed according to the STRIVE-criteria.[15] Segmentations of WMH, lacunes, intracranial volume and total brain volume were acquired as previously published.[12]

7T brain MRI

Participants underwent 7T brain MRI on a Philips 7T scanner with a 32-channel receive head coil with a quadrature transmit coil (Nova Medical, MA, USA). The scan protocol included 2D-Qflow velocity mapping acquisitions and blood-oxygen-level dependent (BOLD) sequences (sequence details supplementary Table 1), with which three complementary aspects of small vessel function were measured:

1. *Perforating artery flow velocity and pulsatility index.* At the level of the centrum semiovale and basal ganglia, 2D-Qflow velocity mapping acquisitions were used

to assess flow velocity in perforating arteries. A peripheral pulse unit was used for retrospective cardiac gating. Mean blood flow velocity and pulsatility index within perforating arteries were calculated as the main outcome measures. Pulsatility index provides – among others – an indication of perforating artery stiffness.

2. *Small vessel reactivity to a brief visual stimulus.* Neurovascular coupling-dependent vascular reactivity in the visual cortex was assessed by estimating the average BOLD hemodynamic response function (HRF) to a brief (500ms) visual stimulus. The region of interest was subject-specific and was based on the activation pattern in response to long blocks (16.7s) of visual stimulation. The BOLD signal on 7T-MRI is weighted more towards signals from the microvasculature (e.g. capillaries, small venules) than on lower field strength,[17] which allows us to measure BOLD reactivity in small vessels as long as the large (pial) veins are removed from the region of interest. In addition, the high temporal resolution on 7T-MRI provides a precise estimate of the HRF, from which the peak BOLD% signal change and full-width-at-half-maximum were derived as the main outcome measures.

3. *Whole-brain small vessel reactivity to a hypercapnic stimulus.* Endothelial-independent whole-brain vascular reactivity to hypercapnia (i.e. breathing 6% CO_2 in air for 2x2 minutes) was measured with the BOLD response. Monitoring equipment recorded pulse rate and end-tidal CO_2 (40Hz, CD3-A AEI Technologies, Pittsburgh, USA) (based on Thrippleton et al.[18], as specified in the design paper[12]) . The signal from large (pial) veins was also excluded, so the remaining BOLD signal primarily represents small vessel reactivity. The high spatial resolution of BOLD on 7T-MRI permits regional analyses. The BOLD% signal change in the cortical grey matter, subcortical grey matter, white matter, and WMH were derived as the main outcome measures.

The order of MRI scans was strictly adhered to. After the first BOLD scan with visual stimulation, every participant was taken out of the scanner for a short break. Then the participant put on the breathing mask and the protocol was continued with the hypercapnic challenge. Details on data processing pipelines were published before.[13]

Statistical analyses

Differences in characteristics between patients with cSVD and controls were tested with independent samples t-tests for continuous normally distributed data, Mann-Whitney U tests for non-normally distributed data and chi-square for categorical data. Differences between patients and controls in small vessel function measures were tested with ANCOVA, with age and sex as covariates. Pulsatility index was additionally corrected for mean blood flow velocity, and BOLD hypercapnia comparisons were additionally corrected for change in end-tidal CO_2 in response to hypercapnia. Within the patients, BOLD% signal change to hypercapnia was compared in normal-appearing white matter

(NAWM) and WMH with a paired t-test. Of note, the numbers of perforating arteries that was detected in WMH in patients was too low (median 1, maximum 7 in centrum semiovale) to reliably compare perforating artery blood flow velocity and pulsatility index in NAWM versus WMH.

In secondary analyses, measures of small vessel function that differed between patients and controls were associated with age, cognitive function, WMH volume and lacune count. Blood flow velocity and pulsatility were considered together in these analyses, because of their close interrelation. WMH volume and lacune count were cube-root transformed because data were skewed, and WMH volume was additionally normalized to the intracranial volume. The associations of small vessel function with cognitive function, WMH volume and lacune count were corrected for age and the standardized betas are reported for ease of comparison between variables. The associations that were significant, we also tested in control participants, to test whether the association was unique for patients (and thus likely pathological) or not.

All statistical analyses were performed in SPSS version 25, and $p<0.05$ was considered significant.

Results

Characteristics of patients with cSVD and controls are shown in Table 1. Patients and controls were well matched with regard to age and sex. As expected, patients more often had hypertension and hypercholesterolemia, and more often used antihypertensives, statins and antiplatelet drugs. Characteristic cSVD imaging markers were also more prominent in patients than controls (details in Table 1). Figure 2 lists the number of subjects for each of the 7T measures included in the analyses. Participants with missing or failed 7T measurements did not differ from participants with complete 7T datasets with regard to demographics or disease severity (all $p>0.2$).

Table 1: Characteristics of patients with sporadic cSVD and controls

	Sporadic cSVD n=46	**Control n=22**	***p*-value**
Demographics			
Age, M±SD	65.3±9.4	63.5±6.6	0.35
Female sex, n (%)	15 (33)	8 (36)	0.79
Vascular risk profile			
Stroke, n (%)	31 (67)	0 (0)	<0.001
Hypertension, n (%)	39 (85)	3 (14)	<0.001
Current 7-day systolic BP, M±SD [mmHg]	129.7±11.6	126.3±10.7	0.25
Current 7-day diastolic BP, M±SD [mmHg]	85.3±7.9	85.8±9.7	0.83
Pulse wave velocity, M±SD	9.5±1.5	9.2±0.9	0.36
Hypercholesterolemia, n (%)	34 (74)	7 (32)	0.001
Diabetes Mellitus, n (%)	7 (15)	0 (0)	0.09
Current/ever smoker, n (%)	38 (83)	14 (64)	0.13
Medication use			
Antihypertensives, n (%)	38 (83)	4 (18)	<0.001
Statins, n (%)	32 (70)	4 (18)	<0.001
Antiplatelet drugs, n (%)	36 (78)	1 (5)	<0.001
3T MRI SVD markers			
WMH volume, median [min-Q1-Q3-max] [% of ICV]	1.03 [0.02-0.34-1.65-4.73]	0.05 [0.00-0.03-1.03-2.77]	<0.001
Lacune presence, n (%)	30 (65)	0 (0)	<0.001
Lacune count[a], median [Q1-Q3]	3 [1-6]	0 [0-0]	
Microbleed presence, n (%)	23 (50)	4 (18)	0.02
Microbleed count[b], median [Q1-Q3]	3 [2-12]	2 [1.5-2.5]	0.22
Brain volume, M±SD [% of ICV]	69.9±6.4	73.5±4.2	0.02

BP = blood pressure; M = mean; ICV = intracranial volume; SD = standard deviation; Q1-Q3= quartile 1 and quartile 3; WMH = white matter hyperintensities.

[a] Count for participants with ≥ 1 lacune(s).

[b] Count for participants with ≥ 1 microbleed(s).

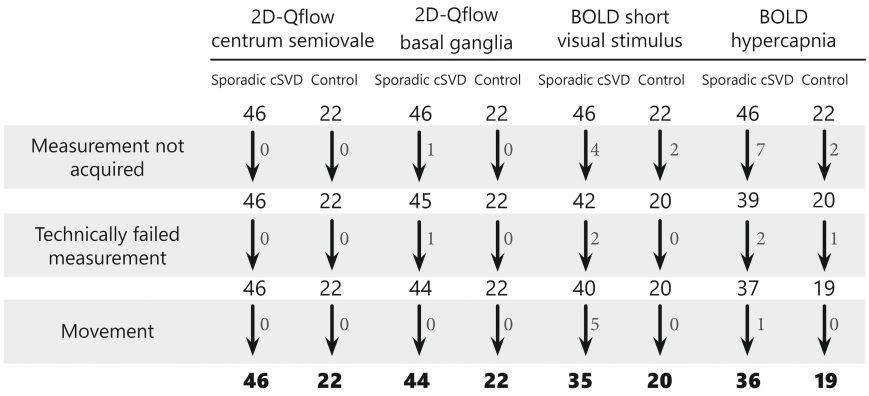

Figure 2: Flowchart showing reasons for excluded scans per small vessel function measure Reasons for not acquired measurements are: the participant could not continue the scanning session for the 2D-Qflow scan (1); glasses that would not fit in the head coil (3), very bad vision of the participant (2), or unable to finish the sequence (1) for the BOLD short visual stimulus scan; and equipment not yet available (5) or participants unwilling or unable to do or finish the hypercapnia challenge (4) for the BOLD hypercapnia scan.

Small vessel function in cSVD versus controls

Perforating artery flow velocity and pulsatility index

The number of perforating arteries included in the analyses were similar (i.e. similar density, calculated as the number of perforating arteries per cm^2 of the subject-specific region of interest) in patients with cSVD (centrum semiovale, median N=48, density mean±SD 2.23±1.13/cm^2; basal ganglia, median N=19, density mean±SD 0.91±0.27/cm^2) and controls (centrum semiovale, median N=44, density mean±SD 2.27±0.89/cm^2, p=0.92; basal ganglia, median N= 19, density mean±SD 0.92±0.29/cm^2, p=0.99). In perforating arteries in the basal ganglia, pulsatility index was increased in patients versus controls, while mean blood flow velocity was similar (Table 2). In perforating arteries in the centrum semiovale, mean blood flow velocity and pulsatility index in the two groups were similar (Table 2).

Small vessel reactivity to a brief visual stimulus

Figure 3A shows the estimates of the average hemodynamic response function (HRF) in the visual cortex in response to a brief visual stimulus in patients and controls (Figure 3B provides the individual responses per participant). Of note, the size of the participant-specific regions of interest (i.e. percentage of activated voxels in the imaging region) in which the estimates were made was similar between patients (mean±SD 25.6±12.5%) and controls (30.4±12.5%, p=0.23). The full-width-at-half-maximum of the HRF was shorter in patients compared with controls, as indicated by the dotted lines in Figure 3A (corresponding numbers are in Table 2). There were no significant group differences in peak BOLD% signal change (Table 2), onset time (patients mean±SD 1.90±0.50s; controls 1.73±0.68s, p=0.29), and time-to-peak (patients mean±SD 4.22±0.70s; controls 4.31±0.78s, p=0.66).

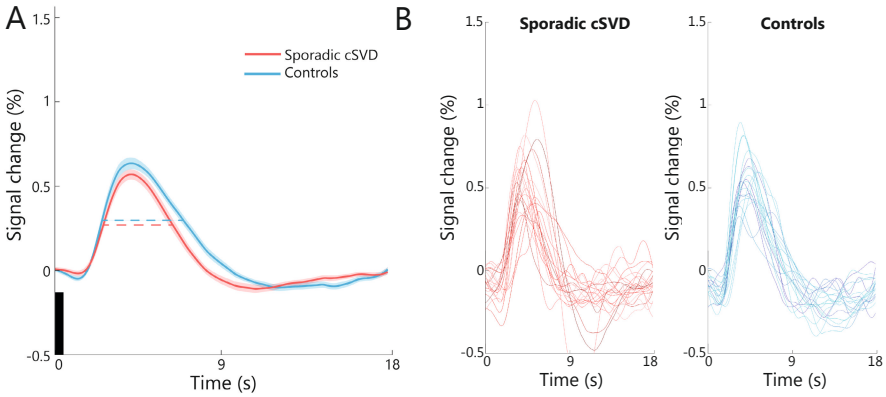

Figure 3: Hemodynamic response functions after visual stimulation (A) The average hemodynamic response function estimates (solid lines) and standard error of the mean (shaded areas) after 500ms visual stimulation (black bar) for patients with sporadic cSVD (red) and controls (blue). The horizontal dotted lines indicate the full-width-at-half-maximum which was significantly shorter in patients than in controls. (B) Individual BOLD hemodynamic response function estimates after 500ms visual stimulation for all Sporadic cSVD patients and controls.

Small vessel reactivity to a hypercapnic stimulus

In the cortical grey matter, subcortical grey matter and total white matter, BOLD% signal change to hypercapnia was similar in patients and controls (Table 2). In patients, BOLD% signal change was lower in WMH (0.31±0.34) than in NAWM (0.65±0.52, $p<0.001$). These analyses were based on 29 patients, because in seven patients the volume of WMH was too small (arbitrary cut-off at <0.3% of intracranial volume) for regional vascular reactivity assessment.

Table 2: Small vessel function on 7T-MRI in patients with sporadic cSVD and controls

	Sporadic cSVD	**Control**	***p*-value**
2D-Qflow centrum semiovale[a]	n=46	n=22	
Blood flow velocity [cm/s]	0.65±0.12	0.64±0.10	0.70
Pulsatility index[b]	0.35±0.13	0.32±0.11	0.40
2D-Qflow basal ganglia[a]	n=44	n=22	
Blood flow velocity [cm/s]	3.73±0.69	3.87±0.68	0.55
Pulsatility index[b]	0.45±0.14	0.36±0.13	0.01
BOLD short visual stimulus[c]	n=35	n=20	
Peak BOLD% signal change	0.63±0.20	0.67±0.16	0.46
Full width at half max [s]	3.37±0.97	4.00±0.80	0.02
BOLD hypercapnic stimulus[d]	n=36	n=19	
CGM BOLD% signal change	3.72±1.37	3.29±1.51	0.17
SGM BOLD% signal change	3.92±1.45	3.47±1.56	0.30
WM BOLD% signal change	0.58±0.41	0.59±0.35	0.72

BOLD = blood-oxygen-level dependent; CGM = cortical grey matter; SGM = subcortical grey matter; WM = white matter. Data are shown as mean ± standard deviation.

[a] The region of interest is the entire centrum semiovale and basal ganglia excluding lacunes. Statistical analyses included age and sex as covariates.

[b] Statistical analyses additionally included blood flow velocity as covariate.

[c] Statistical analyses included age and sex as covariates.

[d] Statistical analyses included age, sex and change in end-tidal CO_2 to hypercapnia as covariates.

Small vessel function and disease burden in patients with sporadic cSVD

Decreased blood flow velocity and increased pulsatility index in perforating arteries in the basal ganglia, and a shorter full-width-at-half-maximum of the BOLD response to a brief visual stimulus associated with disease burden. Specifically, decreased blood flow velocity was significantly associated with higher age, worse cognition, higher WMH volume and higher lacune count (Table 3). Increased pulsatility index was associated with a higher lacune count (Table 3). Lastly, a shorter full-width-at-half-maximum of the BOLD response to a brief visual stimulus was associated with worse cognition and higher WMH volume (Table 3). NB: these associations were not observed in control participants (Supplementary Table 2).

Table 3: Associations of small vessel dysfunction with age, cognition, white matter hyperintensity volume and lacune count in patients with sporadic cSVD

	Age	Cognition[b]	WMH volume	Lacune count
2D-Qflow basal ganglia[a]				
Blood flow velocity [cm/s]	β = -0.37 CI = -0.66 – -0.08 *p* = 0.02	β = 0.39 CI = 0.05 – 0.72 *p* = 0.03	β = -0.41 CI = -0.70 – -0.11 *p* = 0.01	β = -0.43 CI = -0.74 – -0.11 *p* = 0.01
Pulsatility index	β = 0.27 CI = -0.03 – 0.57 *p* = 0.08	β = -0.26 CI = -0.59 – 0.06 *p* = 0.11	β = 0.14 CI = -0.18 – 0.45 *p* = 0.39	β = 0.40 CI = 0.10 – 0.70 *p* = 0.01
BOLD short visual stimulus				
Full width at half max [s]	β = 0.05 CI = -0.31 – 0.40 *p* = 0.79	β = 0.39 CI = 0.06 – 0.72 *p* = 0.02	β = -0.49 CI = -0.77 – -0.21 *p* = 0.001	β = 0.05 CI = -0.31 – 0.41 *p* = 0.77
BOLD hypercapnic stimulus				
WMH BOLD% signal change	β = 0.19 CI = -0.20 – 0.58 *p* = 0.32	β = 0.19 CI = -0.28 – 0.66 *p* = 0.42	β = -0.06 CI = -0.44 – 0.34 *p* = 0.77	β = 0.16 CI = -0.24 – 0.56 *p* = 0.42

β = standardized beta; BOLD = blood-oxygen-level dependent; CI = 95% confidence interval; CGM = cortical grey matter; WMH = white matter hyperintensities. Tested with linear regressions, with an age correction and standardized betas are reported for ease of comparison between variables. We analysed the relation for both blood flow velocity and pulsatility index, because the two are so strongly interrelated. WMH volume was normalized for intracranial volume and cube-root transformed and lacune count was cube-root transformed.

[a] The region of interest is the entire basal ganglia minus lacunes.

[b] Compound score of executive function, and attention and processing speed.

Discussion

Using cutting-edge techniques on 7T-MRI, we found abnormalities in cerebral small vessel function in patients with sporadic cSVD compared with age- and sex-matched controls, including increased pulsatility index in perforating arteries in the basal ganglia, shorter vascular reactivity to brief visual stimulation in the occipital cortex, and decreased reactivity to hypercapnia within WMH. Among patients, blood flow velocity and pulsatility index in basal ganglia perforating arteries and reactivity to brief visual stimulation related to disease burden. These findings likely reflect regionally increased arteriolar stiffness and decreased endothelial-dependent and -independent vascular reactivity, which become increasingly affected with progression of cSVD disease severity.

Previous studies on pulsatility index of the cerebral vasculature mostly studied the internal carotid and middle cerebral arteries, where a relationship was observed between increased pulsatility of flow in these vessels and WMH volume.[10] Here we assessed pulsatility at the level of the perforating arteries. We observed increased pulsatility index in small perforating arteries within the basal ganglia in patients compared with controls, also in relation to higher disease burden. These findings seem in accordance with two small previous studies in sporadic cSVD. One study also observed increased pulsatility in perforating arteries within the basal ganglia,[14] while the other did not, possibly reflecting the relatively low disease burden in that study.[19] Interestingly, we found that pulsatility index was unaffected in perforating arteries within the centrum semiovale, whereas we previously reported increased pulsatility index in centrum semiovale perforating arteries in patients with CADASIL and patients with either lacunar infarction or deep intracerebral haemorrhage.[13,14] These findings imply that underlying pathogenesis may differ in small vessel populations throughout the brain and that these spatial differentiations may depend on the type of cSVD under study. Pulsatility index measured from the velocity trace is known to reflect local vessel stiffness,[20] but it is important to note that the measured pulsatility index is also dependent on effects up- and downstream in the vascular tree.[21] The increased pulsatility index that we observed could therefore reflect a higher pulsatile perfusion pressure transmitted through the larger upstream vessels, enhanced stiffness of the perforating arteries themselves, and/or changes in the downstream vascular bed such as abnormal microvascular compliance. Pulse wave velocity in the brachial artery was similar between patients and controls. This, in combination with what we know about the small vessel wall changes in cSVD that are known to lead to stiffened vessel walls and luminal narrowing at the level of arterioles, capillaries and venules,[1] makes that we interpret the increased pulsatility index in the present cohort as vessel stiffness of the perforating arteries at the point that we measured, or of the downstream smaller arterioles.

Vascular reactivity has previously mostly been studied using 3T-MRI, or lower field strength, with several types of stimuli probing different physiological pathways in

different vessel populations. Neuronal task-based approaches, such as motor and visual stimulation, have been used to study endothelial-dependent reactivity based on neurovascular coupling. Hypercapnia or administration of vasodilatory medication has been applied to study endothelial-*in*dependent reactivity. Task-based approaches have so far mostly been applied in patients with cerebral amyloid angiopathy, reporting decreased reactivity in response to 19-40s visual stimulation in patients compared with controls.[22–26] In our current study we assessed reactivity (i.e. the HRF response) to a brief (0.5s) visual stimulus. While the peak amplitude of the HRF estimate was similar for patients and controls, the full-width-at-half-maximum of the HRF estimate was shorter in patients (Figure 3A), which was related to a higher disease burden. A shorter full-width-at-half-maximum could reflect (a combination of) several underlying physiological changes.[27] The most likely possible explanation is disturbed blood pooling in downstream venules and veins, for example, through shorter capillary transit time[28] and/or stenosis or occlusion of arterioles and/or venules.[1] This possibly disturbed blood flow then worsens with higher disease severity. To our knowledge, a similar set-up with a brief visual stimulus on 7T-MRI has only once been used before in cSVD, in our parallel ZOOM@SVDs study in patients with CADASIL, where we observed a lower peak amplitude of the HRF estimate compared to controls, indicative of less blood flow increase in response to brief visual stimulation,[13] yet without a shorter full-width-at-half-maximum. Apparently, abnormalities in neurovascular response profiles may differ between different forms of cSVD. In our study, we also assessed vascular reactivity to (2x2min) hypercapnia. Earlier studies on lower field strength reported a relation between decreased reactivity and WMH burden in cSVD.[4–9,29,30] The spatial resolution of 7T-MRI helps to better assess vascular reactivity to hypercapnia in specific regions of interest. Between patients and controls, reactivity to hypercapnia was not altered in subcortical grey matter, cortical grey matter or white matter. Within the patient group, however, we observed lower reactivity within WMH than NAWM. In our earlier study in patients with CADASIL, we reported similar findings for all these regions of interest.[13] Our findings thus suggest that in sporadic cSVD the endothelium-dependent vascular response to quick, subtle and local demands in the cortex is altered, while longer and global stimulation with hypercapnia seems to generate a normal endothelium-independent vascular response in the cortex, although not in WMH.

This study also has some limitations. Inherent to the demanding study protocol, the participants recruited in this study were mostly not in the latest disease stages of cSVD, which poses a selection bias. This bias is however more likely to underestimate than overestimate the reported disease effects. Likewise, not all recruited participants could successfully finish the full scan protocol (Figure 2). Importantly, however, participants' demographics were similar to those for whom complete scan datasets were available, suggesting that selection bias after recruitment was likely minimal. There are limitations of the 7T-MRI measures too. To avoid prolonged scan times, the acquisition protocol for the Qflow sequences had a relatively low temporal resolution,[31] which could cause underestimation of the pulsatility index. This, however, should not affect the between

group relative differences. Also, despite the high field strength, particularly in the white matter, the contrast-to-noise ratio (i.e. sensitivity) of the BOLD signal is modest, which limits sensitivity to disease effects. Given the apparent impact of the nature (i.e. duration, intensity) of the stimulus on the deficits in vascular function observed in cSVD, stimulus protocols also need further standardisation. A limitation of the set-up of our study is the cross-sectional design. Even though we report a relation between small vessel dysfunction and disease severity, longitudinal studies are warranted to test if small vessel function predicts worsening parenchymal damage and cognitive decline. These studies are currently underway.

In conclusion, we observed that small vessel function is affected in patients with cSVD. Our findings likely reflect regionally increased arteriolar stiffness and decreased endothelial-dependent and -independent vascular reactivity, which are increasingly affected with higher cSVD disease severity. The results thus provide new biomarkers for cSVD at the level of the small vessels themselves. Longitudinal studies are warranted and underway to see if small vessel dysfunction predicts increasing tissue injury and cognitive decline in cSVD and further technical and biological validation studies are needed[32] to further establish these markers as intermediate outcome measures for future cSVD drugs trials.

References

1. Wardlaw JM, Smith C, Dichgans M. Small vessel disease: mechanisms and clinical implications. *Lancet Neurol*. 2019;18(7):684-696.
2. Schreiber S, Bueche CZ, Garz C, et al. The pathologic cascade of cerebrovascular lesions in SHRSP: Is erythrocyte accumulation an early phase. *J Cereb Blood Flow Metab*. 2012;32(2):278-290.
3. Jandke S, Garz C, Schwanke D, et al. The association between hypertensive arteriopathy and cerebral amyloid angiopathy in spontaneously hypertensive stroke-prone rats. *Brain Pathol*. 2018;28(6):844-859.
4. Blair GW, Doubal FN, Thrippleton MJ, Marshall I, Wardlaw JM. Magnetic resonance imaging for assessment of cerebrovascular reactivity in cerebral small vessel disease: A systematic review. *J Cereb Blood Flow Metab*. 2016;36(5):833-841.
5. Blair GW, Thrippleton MJ, Shi Y, et al. Intracranial hemodynamic relationships in patients with cerebral small vessel disease. *Neurology*. 2020;94(21):e2258-e2269.
6. Sam K, Crawley AP, Conklin J, et al. Development of White Matter Hyperintensity Is Preceded by Reduced Cerebrovascular Reactivity. *Ann Neurol*. 2016;80(2):277-285.
7. Sam K, Conklin J, Holmes KR, et al. Impaired dynamic cerebrovascular response to hypercapnia predicts development of white matter hyperintensities. *NeuroImage Clin*. 2016;11:796-801.
8. Reginold W, Sam K, Poublanc J, Fisher J, Crawley A, Mikulis DJ. The efficiency of the brain connectome is associated with cerebrovascular reactivity in persons with white matter hyperintensities. *Hum Brain Mapp*. 2019;40(12):3647-3656.
9. Atwi S, Shao H, Crane DE, et al. BOLD-based cerebrovascular reactivity vascular transfer function isolates amplitude and timing responses to better characterize cerebral small vessel disease. *NMR Biomed*. 2019;32(3):1-12.
10. Shi Y, Thrippleton MJ, Marshall I, Wardlaw JM. Intracranial pulsatility in patients with cerebral small vessel disease: a systematic review. *Clin Sci*. 2018;132(1):157-171.
11. Smith EE, Beaudin AE. New insights into cerebral small vessel disease and vascular cognitive impairment from MRI. *Curr Opin Neurol*. 2018;31(1):36-43.
12. van den Brink H, Kopczak A, Arts T, et al. Zooming in on cerebral small vessel function in small vessel diseases with 7T MRI: Rationale and design of the "ZOOM@SVDs" study. *Cereb Circ - Cogn Behav*. 2021;2:1-9.
13. van den Brink H, Kopczak A, Arts T, et al. CADASIL Affects Multiple Aspects of Cerebral Small Vessel Function on 7T-MRI. *Ann Neurol*. 2023;93:29-39
14. Geurts L, Zwanenburg JJM, Klijn CJM, Luijten PR, Biessels GJ. Higher Pulsatility in Cerebral Perforating Arteries in Patients With Small Vessel Disease Related Stroke, a 7T MRI Study. *Stroke*. 2019;50(1):62-68.
15. Kuijf HJ, Brundel M, Bresser J De, et al. Semi-Automated Detection of Cerebral Microbleeds on 3.0 T MRI Images. *PLoS One*. 2013;8(6):e66610.
16. Wardlaw JM, Smith EE, Biessels GJ, et al. Neuroimaging standards for research into small vessel disease and its contribution to ageing and neurodegeneration. *Lancet Neurol*. 2013;12(8):822-838.
17. Uludağ K, Müller-Bierl B, Uğurbil K. An integrative model for neuronal activity-induced signal changes for gradient and spin echo functional imaging. *Neuroimage*. 2009;48(1):150-165.

18. Thrippleton MJ, Shi Y, Blair G, et al. Cerebrovascular reactivity measurement in cerebral small vessel disease: Rationale and reproducibility of a protocol for MRI acquisition and image processing. *Int J Stroke*. 2018;13(2):195-206.
19. Perosa V, Arts T, Assmann A, et al. Pulsatility Index in the Basal Ganglia Arteries Increases with Age in Elderly with and without Cerebral Small Vessel Disease. *Am J Neuroradiol*. 2022;43(4):540-546.
20. van Tuijl RJ, Ruigrok YM, Velthuis BK, van der Schaaf IC, Rinkel GJE, Zwanenburg JJM. Velocity pulsatility and arterial distensibility along the internal carotid artery. *J Am Heart Assoc*. 2020;9:e016883.
21. Arts T, Onkenhout LP, Amier RP, et al. Non-Invasive Assessment of Damping of Blood Flow Velocity Pulsatility in Cerebral Arteries With MRI. *J Magn Reson Imaging*. 2022;55(6):1785-1794.
22. Cheema I, Switzer AR, McCreary CR, et al. Functional magnetic resonance imaging responses in CADASIL. *J Neurol Sci*. 2017;375:248-254.
23. Dumas A, Dierksen GA, Eng M, et al. Functional MRI detection of vascular reactivity in cerebral amyloid angiopathy. *Ann Neurol*. 2012;72(1):76-81.
24. Peca S, Mccreary CR, Donaldson E, et al. Neurovascular decoupling is associated with severity of cerebral amyloid angiopathy. *Neurology*. 2013;81:1659-1665.
25. Opstal AM Van, Rooden S Van, Harten T Van, et al. Cerebrovascular function in pre-symptomatic and symptomatic individuals with hereditary cerebral amyloid angiopathy: a case-control study. *Lancet Neurol*. 2017;16(2):115-122.
26. Williams RJ, Goodyear BG, Peca S, et al. Identification of neurovascular changes associated with cerebral amyloid angiopathy from subject-specific hemodynamic response functions. *J Cereb Blood Flow Metab*. 2017;37(10):3433-3445.
27. Siero JC, Petridou N, Hoogduin H, Luijten PR, Ramsey NF. Cortical Depth-Dependent Temporal Dynamics of the BOLD Response in the Human Brain. *J Cereb Blood Flow Metab*. 2011;31(10):1999-2008.
28. Østergaard L, Jespersen SN, Mouridsen K, et al. The role of the cerebral capillaries in acute ischemic stroke: The extended penumbra model. *J Cereb Blood Flow Metab*. 2013;33(5):635-648.
29. Chabriat H, Pappata S, Ostergaard L, et al. Cerebral hemodynamics in CADASIL before and after acetazolamide challenge assessed with MRI bolus tracking. *Stroke*. 2000;31(8):1904-1912.
30. Beaudin AE, McCreary CR, Mazerolle EL, et al. Cerebrovascular Reactivity Across the Entire Brain in Cerebral Amyloid Angiopathy. *Neurology*. 2022;98(17):E1716-E1728.
31. Geurts L, Biessels GJ, Luijten P, Zwanenburg J. Better and faster velocity pulsatility assessment in cerebral white matter perforating arteries with 7T quantitative flow MRI through improved slice profile, acquisition scheme, and postprocessing. *Magn Reson Med*. 2018;79(3):1473-1482.
32. Smith EE, Biessels GJ, De Guio F, et al. Harmonizing brain magnetic resonance imaging methods for vascular contributions to neurodegeneration. *Alzheimer's Dement Diagnosis, Assess Dis Monit*. 2019;11:191-204.

Supplementary material

Supplementary Table 1 3T and 7T brain MRI protocol

MR sequence	Acquired resolution mm^3	Time min:s	Parameters
3T-MRI			
T1-weighted GE	1.0x1.0x1.0	05:39	FOV 256x232x192 mm^3; TR 8 ms; TI 955 ms; shot interval 2500 ms; flip angle 7°
T2-weighted TSE	0.7x0.7x0.7	07:37	FOV 250x250x190 mm^3; TR 2500 ms; TE 298 ms
T2*-weighted GE	0.8x0.8x0.8	02:22	FOV 230x192x144 mm^3; TR 69 ms; TE 29 ms; flip angle 23°
FLAIR	1.0x1.0x1.0	06:15	FOV 250x250x180 mm^3; TR 5000 ms; TE 253 ms; TI 1700 ms
7T-MRI			
T1-weighted	1.0x1.0x1.0	01:59	FOV 250x250x190 mm^3; TR 4.2 ms; TI 1297 ms; shot interval 3000 ms; flip angle 5°
2D-Qflow CSO	0.3x0.3x2.0	03:24*	FOV 230x230 mm^2; reconstructed resolution 0.18x0.18mm^2 ; TR 29 ms; TE 16 ms; Venc 4 cm/s; temporal resolution 116 ms; flip angle 50°
2D-Qflow BG	0.3x0.3x2.0	03:47*	FOV 170x170 mm^2; reconstructed resolution 0.18x0.18mm^2 ; TR 28 ms; TE 15 ms; Venc 20 cm/s ; temporal resolution 112 ms; flip angle 50°
BOLD fMRI visual cortex[a]	1.3x1.3x1.3	10:05	FOV 140x140x11 mm^3; TR 880 ms; TE 25 ms
BOLD fMRI whole-brain[b]	2.0x2.0x2.0	10:00	FOV 224x256x101 mm^3; TR 3000 ms; TE 25 ms

BG = basal ganglia; BOLD = blood-oxyen-level dependent; CSO = centrum semiovale; fMRI = functional MRI; FOV = field of view; GE = gradient echo; TE = echo time; TI = inversion time; TR = repetition time; TSE = turbo spin echo.

*Total scan time for a heart rate of 80bpm.

[a] The participant is presented with a *visual stimulus*.

[b] The participant undergoes a *hypercapnic challenge*.

Between the two BOLD sequences the participant is taken out of the scanner for a short break and to put on the mask for the hypercapnic challenge.

Supplementary Table 2 Associations of small vessel dysfunction with age, cognition and white matter hyperintensity volume in control participants

	Age	**Cognition[a]**	**WMH volume**
2D-Qflow basal ganglia			
Blood flow velocity [cm/s]	β = -0.28	β = 0.16	β = -0.11
	CI = -0.73 – 0.16	CI = -0.35 – 0.67	CI = -0.57 – 0.34
	p = 0.20	*p* = 0.52	*p* = 0.63
Pulsatility index	β = 0.30	β = -0.39	β = 0.15
	CI = -0.15 – 0.74	CI = -0.87 – 0.09	CI = -0.33 – 0.63
	p = 0.18	*p* = 0.11	*p* = 0.53
BOLD short visual stimulus			
Full width at half max [s]	β = 0.19	β = 0.07	β = 0.29
	CI = -0.29 – 0.67	CI = -0.47 – 0.62	CI = -0.20 – 0.78
	p = 0.42	*p* = 0.78	*p* = 0.22

β = standardized beta; BOLD = blood-oxygen-level dependent; CI = 95% confidence intervals; CGM = cortical grey matter; WMH = white matter hyperintensities. Tested with linear regressions, with an age correction and standardized betas are reported for ease of comparison between variables. We analysed the relation for both blood flow velocity and pulsatility index, because the two are so strongly interrelated. WMH volume was normalized for intracranial volume and cube-root transformed and lacune count was cube-root transformed.

[a] Compound score of executive function, and attention and processing speed.

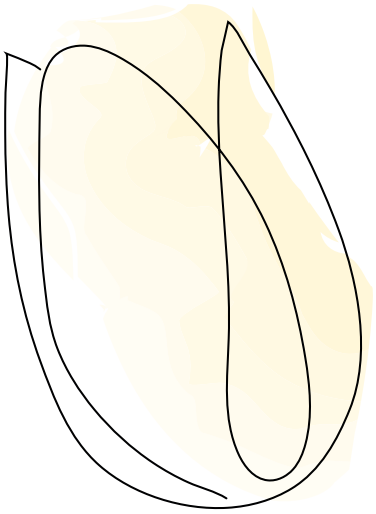

6

The relation between small vessel function and white matter microstructure in monogenic and sporadic small vessel disease - the ZOOM@ SVDs study

Naomi Vlegels*, **Hilde van den Brink***, Anna Kopczak, Tine Arts, Stanley Pham, Jeroen Siero, Benno Gesierich, Alberto de Luca, Marco Duering, Jaco Zwanenburg, Martin Dichgans, Geert Jan Biessels on behalf of the SVDs@target group
*These authors contributed equally

Manuscript in preparation for submission

Abstract

In cerebral small vessel disease, vascular dysfunction has been associated with widespread tissue injury. Here we further explore these associations and hypothesize that local variation in vascular dysfunction explains regional variance in injury. We included 23 patients with monogenic cSVD (i.e. CADASIL) and 46 patients with sporadic cSVD. With whole-brain analyses, we tested if small vessel flow velocity and reactivity measures from 7T-MRI associated with global peak-width-of-skeletonized-mean-diffusivity (PSMD). We also tested voxel-wise correlations between reactivity to hypercapnia and mean diffusivity (MD) in white matter. Whole-brain analyses showed a negative association between blood flow velocity within perforating arteries and PSMD in the centrum semiovale in CADASIL and in the basal ganglia in sporadic cSVD. Global white matter reactivity to hypercapnia was not associated with PSMD, but we did observe significant voxel-wise negative correlations between BOLD% signal change and MD both in CADASIL and sporadic cSVD. In conclusion, both in patients with CADASIL and sporadic cSVD small vessel dysfunction is associated with microstructural white matter alterations, also at voxel-level. The latter may reflect a direct causal relationship between local small vessel dysfunction and tissue injury.

Introduction

Cerebral small vessel disease (cSVD) is a major cause of stroke and dementia among the elderly.[1,2] With MRI, cSVD has mostly been studied through markers of parenchymal injury (e.g. white matter hyperintensities (WMH), lacunes, cerebral microbleeds[3]). The processes that underlie the formation of these lesions likely involve disturbances at the level of the cerebral small vessels. Due to their small size these vessels are difficult to probe *in vivo*. Previous studies on the small vessels in cSVD therefore mostly involved neuropathology of autopsy material, showing loss of smooth muscle cells, thickening of the vessel walls and luminal narrowing in cerebral arterioles, but also abnormalities in capillaries and venules.[2] Over the past years, these observations have been complemented by functional vascular measures using MRI. This included studies at common field strengths (i.e. up to 3T-MRI), showing that decreased vessel function related to increased WMH burden.[4–11] With technological advancements on 7T-MRI we can now assess small vessel flow velocity and pulsatility index as well as (small) vessel reactivity with a sensitivity and temporal and spatial resolution that was not possible before *in vivo* in humans.[12] We recently showed that these measures of small vessel function on 7T-MRI were abnormal in patients with cSVD, indicative of regional abnormalities in arteriolar stiffness and reactivity. There were similarities, but also apparent differences in the way that these measures of small vessel function were altered in patients with monogenic (i.e. CADASIL) versus sporadic cSVD (Chapter 4 and 5).

Diffusion MRI-based measures of the white matter microstructure are currently the most sensitive method for studying tissue injury in cSVD.[13,14] Diffusion MRI quantifies the diffusion properties of water molecules in brain tissue and is thereby highly sensitive in detecting subtle tissue alterations. Moreover, cSVD related diffusion alterations are associated with clinical deficits and typically outperform conventional MRI markers in terms of strength of this association.[14,15] Diffusion alterations in cSVD can be assessed locally in the white matter, at voxel level, but also with robust global measures such as *"peak width of skeletonized mean diffusivity"* (PSMD). PSMD is a sensitive and robust measure of white matter microstructure.[14]

In the current study, we tested the association between several complementary novel measures of small vessel dysfunction on 7T-MRI with diffusion MRI measures of white matter microstructure, both in patients with CADASIL and more common sporadic cSVD. We capitalized on the high spatial resolution of 7T-MRI to also directly relate small vessel function impairment to tissue injury on a voxel-by-voxel level, because we hypothesize that local variation in vascular dysfunction explains regional variance in tissue injury.

Materials and Methods

Participants and study procedure

Patients with cSVD were recruited through the ZOOM@SVDs study, a prospective observational cohort study,[12] at the Institute of Stroke and Dementia Research at Ludwig Maximilian University (LMU) Munich, Germany, and the University Medical Center Utrecht (UMCU) in the Netherlands. Detailed inclusion and exclusion criteria and study procedures are published in the design paper of ZOOM@SVDs[12] but a short description can be found below:

- Monogenic cSVD: At LMU, a tertiary national referral centre for patients with CADASIL in Germany, 23 patients with CADASIL and 13 age- and sex-matched reference participants were recruited. CADASIL was either confirmed by molecular genetic testing (n=20) or by skin biopsy (n=3). Reference participants without cSVD (defined as no history of stroke or of cognitive complaints for which the person has previously sought medical advice, and no so-called "silent" cSVD (Fazekas <2 and no lacunes) on the study MRI) were recruited among partners or relatives of the patients and through advertisement. There were no screenfailures. All participants underwent clinical assessment and 3T brain MRI at LMU and travelled to the UMCU to undergo 7T brain MRI.
- Sporadic cSVD: At the stroke and memory clinics of the UMCU and referring centres, 54 patients with symptomatic sporadic cSVD and 28 age- and sex- matched reference participants were recruited. Symptomatic sporadic cSVD was defined as having a history of clinical lacunar stroke in the last 5 years with a corresponding lesion on MRI or CT, or having cognitive impairment with confluent WMH on MRI (Fazekas ≥ 2). Reference participants without cSVD were recruited among partners or relatives of the patients and through advertisement. There were three patients for whom we could not confirm a small subcortical infarct on the study MRI, three reference participants were excluded because of signs of silent cSVD on the study MRI and one reference participant was excluded because of objective cognitive impairment. This left 51 included patients and 24 included reference participants. These participants underwent clinical assessment, 3T and 7T brain MRI at the UMCU.

For the current study we only included patients and reference participants with at least one available small vessel function measure on 7T-MRI and available diffusion MRI. We could include all patients with CADASIL (n=23) and their reference participants (n=13). We had to exclude five patients with sporadic cSVD and two of their reference participants due to missing small vessel function measures and 1 of the reference participants due to a failed diffusion scan, leaving 46 patients with sporadic cSVD and 21 reference participants for this study.

The Medical Ethics Review Committees of LMU and UMCU both approved the study, which is conducted in accordance with the declaration of Helsinki and the European law of General Data Protection Regulation. Written informed consent was obtained from all participants prior to enrolment in the study.

Brain MRI acquisition

At LMU, 3T brain MRI was acquired in patients with CADASIL and reference participants on a Siemens Magnetom Skyra 3T scanner with a 64-channel head/neck coil. At UMCU, a Philips Achieva 3T scanner with an 8-channel SENSE head coil was used for the 3T brain MRI in patients with sporadic cSVD and reference participants. The scan protocol and acquisition parameters have been previously published[12] and included a 3D T1-weighted gradient echo, a 3D T2*-weighted gradient echo, a 3D fluid-attenuated inversion recovery (FLAIR), and a diffusion-weighted MRI scan (LMU: voxel size 2x2x2m^3, TR/TE: 3800/104.8 ms, b-values: 0, 1000 and 2000 s/mm^2, 90 diffusion directions (30 for b = 1000 s/mm^2, 60 for b = 2000 s/mm^2); UMCU: voxel size 2.5x2.5x2.5mm^3, TR/TE: 8185/73 ms, b-values 0 and 1200 s/mm^2, 45 diffusion directions).

All participants underwent a 7T brain MRI on a Philips 7T scanner (Philips Healthcare, Best, The Netherlands) using a 32-channel receive head coil in combination with a quadrature transmit coil (Nova Medical, MA, USA). The scan protocol and acquisition parameters are published elsewhere[12] and included 2D-Qflow sequences to assess blood flow velocity and pulsatility index in perforating arteries in the basal ganglia and centrum semiovale as well as blood oxygen-level dependent (BOLD) sequences to assess vascular reactivity in response to a visual stimulus and hypercapnic challenge.

Conventional cSVD markers and brain volumetrics

Lacunes (on T1-weighted and FLAIR) and microbleeds (on T2*-weighted) were manually rated according to the STRIVE-criteria.[3] Volumetric measures and masks of WMH, intracranial volume, total brain volume, white matter and grey matter were acquired as previously published.[12]

Small vessel function measures

Three complementary measures of small vessel function in different small vessel populations were acquired on 7T brain MRI. A detailed description of these measures,[12] as well as the processing pipelines (Chapter 4), is provided elsewhere. In short:

1. 2D-Qflow velocity mapping acquisitions were acquired at the level of the basal ganglia and centrum semiovale to assess flow velocity in perforating arteries. Mean blood flow velocity and pulsatility index within perforating arteries of the basal ganglia and centrum semiovale were derived. In these cohorts with known small vessel alterations, we regard pulsatility index in perforating arteries as an indicator of perforating artery stiffness.

2. BOLD data were acquired in the visual cortex to assess endothelial-dependent (via neurovascular coupling) vascular reactivity in response to looking at a short visual stimulus. The average BOLD hemodynamic response function as generated by the short visual stimulus was estimated and the BOLD% signal change and full-width-at-half-maximum (FWHM) were derived.

3. Whole-brain BOLD data were acquired to assess endothelial-independent vascular reactivity in response to a hypercapnic stimulus (i.e. breathing 6% CO_2 in air for 2x2 minutes). The BOLD% signal change in the cortical grey matter, subcortical grey matter and white matter were derived.

Diffusion measures

The diffusion images for both patients with CADASIL and patients with sporadic cSVD were processed with similar pipelines. After visual inspection to exclude major artefacts, raw diffusion images were pre-processed using the MRtrix3 packages (MRtrix3)[16] and the Functional Magnetic Resonance Imaging of the Brain (FMRIB) software library (FSL[17]), v6.0.3. First, noise and Gibbs ringing artefacts were removed ('dwidenoise',[18–20] 'mrdegibbs',[21] MRtrix3), followed by correction of subject motion and distortion correction ('topup' (only for CADASIL), 'eddy',[22–25] FSL). Lastly, we corrected for bias field in the CADASIL group (ANTS[26]). Patients with CADASIL who underwent their 3T brain MRI in Munich, had a multishell diffusion MRI. After preprocessing we only selected volumes with b=0 and b=1000 s/mm^2 ('dwiextract', MRtrix3[16]) and used this single shell for further processing. Using the preprocessed diffusion images, we calculated the diffusion tensors to obtain mean diffusivity (MD) maps (which were used for the voxel-wise analyses as described below) ('dtifit', FSL). As a marker of whole-brain microstructure of the white matter, we calculated PSMD.[14] PSMD is a sensitive and robust measure of white matter microstructure[14] and was calculated using the publicly available script (http://psmd-marker.com). PSMD is an index of the dispersion of mean diffusivity (MD) values across the white matter skeleton and has been described in detail before.[14] In short: to calculate PSMD, the white matter tracts are first skeletonized using tract-based spatial statistics (TBSS[27], FSL), then to avoid CSF contamination by partial volume effects, the skeleton is masked with a custom-made mask designed to exclude regions close to CSF. Lastly, with histogram analysis of MD values within the masked skeleton the peak width is calculated as the difference between the 95th and 5th percentile. PSMD was calculated both for the total white matter and for the normal appearing white matter (NAWM). The NAWM mask was obtained by subtracting lesions (i.e. WMH and lacunes) from the total white matter mask and subsequent erosion of the mask.

Analyses

Differences in baseline characteristics between the patient groups and their respective reference groups were tested with independent sample t-tests for continuous normally distributed data, Mann Whitney U tests for non-parametric continuous data, chi-square tests for categorical data and ANOVA with age and sex correction for 7T small vessel function measures. Statistical analyses on group differences in pulsatility index were additionally corrected for mean blood flow velocity. BOLD reactivity to hypercapnia analyses were additionally corrected for change in end-tidal CO_2 in response to hypercapnia.

Whole-brain analyses on small vessel function and diffusion alterations. Within the CADASIL patient group and the sporadic cSVD patient group, we tested the association between small vessel function measures and PSMD in total white matter with simple linear regressions. All analyses were repeated with NAWM PSMD. Regression analyses were not adjusted for age. Given that age is not a confounder in CADASIL, we wanted to keep the primary analyses as harmonized as possible. In an additional sensitivity analysis in patients with sporadic cSVD we added age as a covariate in the statistical analyses.

Voxel-wise analyses on small vessel function and diffusion alterations. For these analyses, we first registered the 3T 3D-T1 weighted images to the 7T BOLD images for each participant, using FLIRT (FSL[28–30]). The resulting transformation matrix was then applied to register the 3T MD map to the 7T BOLD image. All registrations were visually checked. Per participant, we then calculated the correlation coefficient between BOLD% signal change and MD across all voxels within the white matter mask (see example in Figure 1). These within-participant assessments essentially eliminate the influence of possible confounders (i.e. shared risk factors for abnormal small vessel function and cerebral tissue injury). We performed two different analyses with these correlation coefficients. First, we tested for each group if the pooled individual correlation coefficients of the BOLD% signal change with MD significantly deviated from zero using a Wilcoxon rank sum test. Second, we tested if the group-level mean of individual correlation coefficients was different for patients and reference participants in both CADASIL and sporadic cSVD with Wilcoxon rank sum tests. These analyses were repeated for the NAWM. All statistical analyses were performed in R and a significance level of $p < 0.05$ was considered significant.

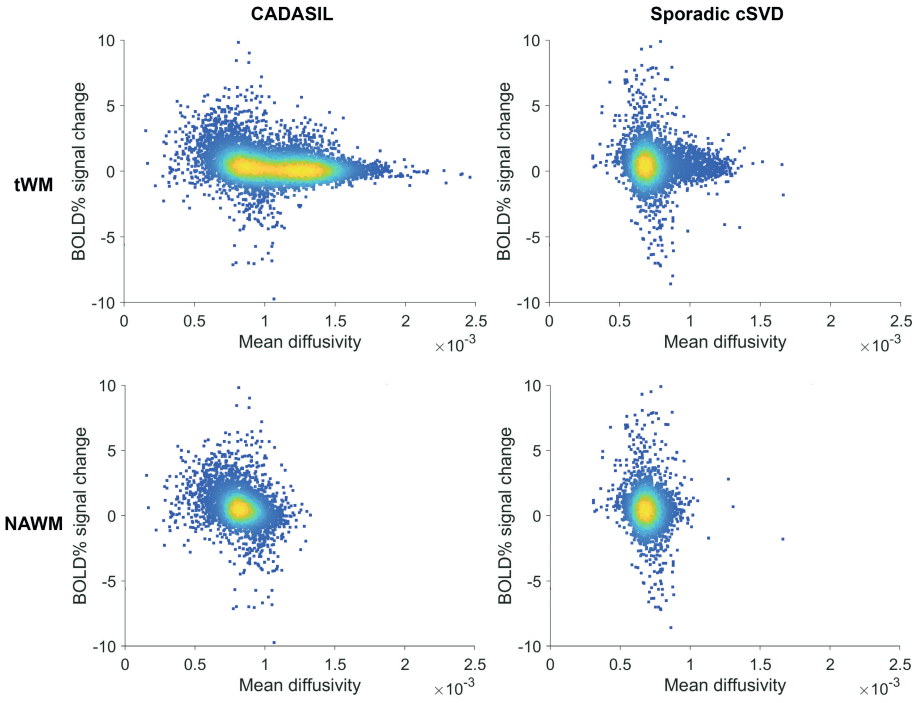

Figure 1: Example density plots for one representative CADASIL and sporadic cSVD patient. Each panel shows the relationship of each voxel in a single patient between BOLD% signal change and mean diffusivity in total white matter (tWM; upper panels) and normal appearing white matter (NAWM; lower panels). From this, we calculated the correlation coefficient between BOLD% signal change and mean diffusivity for each participant.

Results

Characteristics of the patients with CADASIL, patients with sporadic cSVD and both matched reference groups are shown in Table 1. As reported previously (Chapter 4 and 5), small vessel function measures, including blood flow velocity, pulsatility, and reactivity, were affected both in patients with CADASIL and sporadic cSVD, but with differences in the affected vessel populations and differences in the way that vascular reactivity was affected (Table 1). As expected, both patients with CADASIL and sporadic cSVD had a higher lesion load and higher PSMD (i.e. loss of white matter microstructure) than their reference groups.

Whole-brain associations between small vessel function measures and PSMD

In both patients groups, perforating artery flow velocity was associated with PSMD, albeit with differences in the arterioles involved. In CADASIL, lower blood flow velocity in the centrum semiovale was associated with higher PSMD (Table 2). In sporadic cSVD, this

negative association was observed for blood flow velocity in the perforating arteries in the basal ganglia instead. Additionally, in this group, higher pulsatility index in the perforating arteries in the basal ganglia associated with increased PSMD (Table 2).

Vascular reactivity to hypercapnia in the cortical grey matter was negatively associated with PSMD in patients with sporadic cSVD, but not in CADASIL, although the direction of the effect was the same (Table 2). Of note, in both groups reactivity to hypercapnia in the cortical grey matter tended to be higher in the patients than in the reference groups (Table 1). Subcortical grey matter and white matter reactivity to hypercapnia did not relate to PSMD (Table 2).

In sensitivity analyses using PSMD in the NAWM only, the above significant associations persisted (Supplementary Table 1). We performed additional sensitivity analyses in patients with sporadic cSVD in which we corrected for age. In these age-corrected analyses, only the association between blood flow velocity in the perforating arteries of the basal ganglia and white matter PSMD remained significant (B(CI) = -0.32 (-0.60 – -0.04), p = 0.03; Supplementary Table 2).

Voxel-wise correlations between BOLD% signal change to hypercapnia and MD

In the voxel-wise analyses we found a negative correlation between BOLD% signal change to hypercapnia and MD across voxels in the white matter both in patients with CADASIL (mean of individual correlation coefficients (r)±sd: 0.08±0.14-; Wilcoxon rank sum test p <. 0001, indicating that a significant proportion of patients showed this negative correlation) and in patients with sporadic cSVD (r = -0.10 ± 0.09; Wilcoxon p < .0001). This, mean negative correlation was stronger in the patient groups than in their respective reference groups, both in the total white matter (mean difference CADASIL and reference group -0.04, p = 0.3; mean difference sporadic cSVD and reference group -0.08, p = 0.003; Figure 2) and NAWM (mean difference CADASIL and reference group 0.01, p = 0.006, mean difference sporadic cSVD and reference group 0.06, p = 0.007; Figure 2).

Table 1: Characteristics of patients with CADASIL and sporadic cSVD and their respective reference groups

	CADASIL	**Reference**		**Sporadic cSVD**	**Reference**	
	n = 23	**n = 13**	***p***	**n = 46**	**n = 21**	***p***
Demographics						
Age [years]	51.1±10.1	46.1±12.6	0.20	65.3±9.4	63.3±6.7	0.42
Female sex	12 (52)	6 (46)	1.00	15 (33)	8 (38)	0.87
7T MRI small vessel function						
2D-Qflow centrum semiovalea	n=22	n=10		n=46	n=21	
Blood flow velocity [cm/s]	0.54±0.06	0.63±0.13	0.03	0.65±0.12	0.65±0.10	0.87
Pulsatility indexb	0.56±0.19	0.37±0.11	0.009	0.35±0.13	0.32±0.11	0.34
2D-Qflow basal ganglia	n=21	n=9		n=44	n=21	
Blood flow velocity [cm/s]	3.07±0.67	4.05±0.83	0.003	3.7±0.69	3.9±0.70	0.35
Pulsatility indexb	0.46±0.12	0.29±0.15	0.06	0.45±0.14	0.36±0.13	0.005
BOLD visual stimulus	n=19	n=10		n=35	n=19	
BOLD% signal change	0.61±0.20	0.82±0.25	0.04	0.63±0.2	0.66±0.16	0.51
Full width half max [s]	3.82±0.65	3.94±0.36	0.60	3.37±0.97	4.01±0.81	0.02
BOLD hypercapnic stimuluscd	n=17	n=11		n=36	n=18	
CGM BOLD% signal change	3.66±1.24	3.07±1.20	0.26	3.66±1.38	3.39±1.43	0.51
SGM BOLD% signal change	3.37±0.98	3.44±1.42	0.87	3.91±1.49	3.52±1.50	0.38
tWM BOLD% signal change	0.35±0.33	0.17±0.31	0.31	0.56±0.44	0.55±0.38	0.96
3T MRI cSVD markers						
PSMD [mm2/s x 10-4]	4.1 [1.87]	2.1 [0.26]	<0.001	4.1 [1.97]	2.9 [0.8]	<0.001
WMH volume [% of ICV]	4.5 [4.4]	0.01 [0.04]	<0.001	1.15 [1]	0.09 [0.08]	<0.001
Lacune presence	13 (57)	0 (0)	0.001	30 (65)	0 (0)	<0.001
Microbleed presence	13 (57)	0 (0)	0.001	23 (50)	4 (9)	0.03
Brain volume [% of ICV]	78.3±5.2	77.6±3.2	0.76	69.9±6.4	73.3±4.3	0.04

Differences were tested with an independent sample t-test for continuous normally distributed data, Mann-Whitney U test for non-parametric continuous data (i.e. PSMD and WMH volume) and chi-square for categorical data. Data presented as M±SD, n(%) or median[IQR].

[a] The ROI is the entire semioval centre and basal ganglia excluding lacunes. Analyses are corrected for age and sex. [b] Additional correction for blood flow velocity. [c] Analyses corrected for age, sex and change in end-tidal CO_2 to hypercapnia. [d] Vascular reactivity to hypercapnia was reduced in WMH (compared to NAWM in both CADASIL: mean BOLD% change difference -0.29, $p = 0.02$ and sporadic cSVD: mean BOLD% change difference -0.35, $p < 0.001$).

BOLD = Blood oxygenation level-dependent, BP = blood pressure, CGM = cortical grey matter, ICV = intracranial volume, PSMD = peak width of skeletonized mean diffusivity, Qflow = quantitative flow (velocity phase contrast MRI), SGM = subcortical grey matter, tWM = total white matter, WMH = White matter hyperintensity.

Table 2: Linear regressions between 7T small vessel function measures and PSMD in total white matter

	CADASIL			**Sporadic cSVD**		
	B	**CI95**	***p***	**B**	**CI95**	***p***
2D-Qflow centrum semiovale	N=22			N= 46		
Blood flow velocity [cm/s]	-0.42	-0.83 – -0.03	0.04	0.02	-0.28 – 0.33	0.87
Pulsatility Index	-0.18	-0.63 – 0.25	0.38	0.12	-0.19 – 0.42	0.44
2D-Qflow basal ganglia	N=21			N= 44		
Blood flow velocity [cm/s]	-0.23	-0.72 – 0.26	0.33	-0.45	-0.73 – -0.17	0.002
Pulsatility index	0.21	-0.28 – 0.70	0.38	0.31	0.01 – 0.60	0.04
BOLD visual stimulus	N=19			N=35		
BOLD% signal change	-0.25	-0.67 – 0.18	0.24	-0.04	-0.37 – 0.28	0.78
Full width half max [s]	0.36	-0.05 – 0.76	0.08	-0.23	-0.54 – 0.08	0.14
BOLD hypercapnic stimulus	N=17			N=36		
CGM BOLD% signal change	-0.27	-0.84 – 0.31	0.35	-0.35	-0.68 – -0.03	0.03
SGM BOLD% signal change	-0.30	-0.87 – 0.28	0.29	-0.25	-0.59 – 0.08	0.14
NAWM BOLD% signal change	0.26	-0.33 – 0.86	0.36	-0.01	-0.36 – 0.34	0.96

B = standardized beta, BOLD = Blood oxygenation level-dependent, CGM = cortical grey matter, CI95 = 95% confidence interval, NAWM = normal appearing white matter, PSMD = peak width of skeletonized mean diffusivity, Qflow = quantitative flow (velocity phase contrast MRI), SGM = subcortical grey matter.

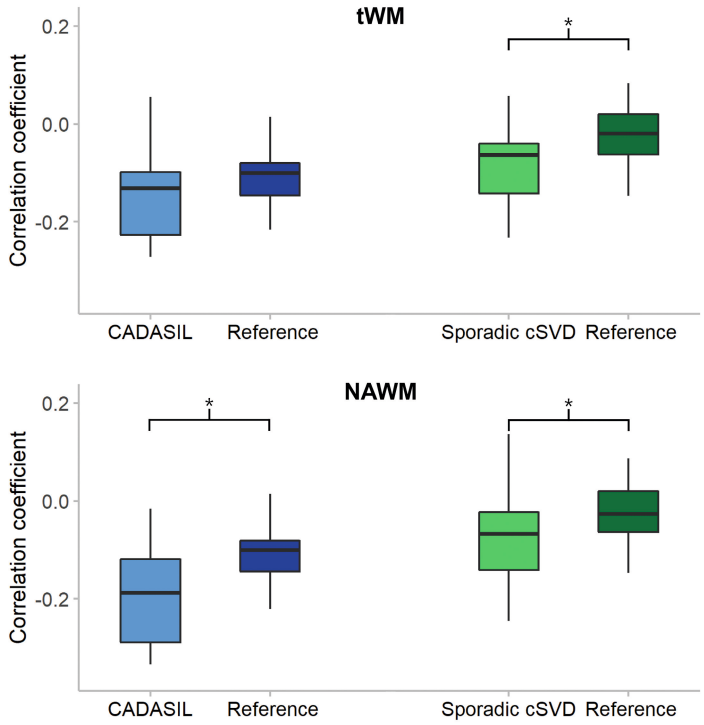

Figure 2: Boxplots showing the correlation coefficients of the voxel-wise relation between BOLD% signal change to hypercapnia and mean diffusivity in total white matter and normal appearing white matter. As mentioned in Figure 1, we calculated a correlation coefficient between BOLD% signal change and mean diffusivity across all voxels for each participant (both patient and reference groups). We tested whether the mean of these individual correlation coefficients was different between the patient groups and their respective reference groups. The negative associations are significantly stronger for the patients groups, except for the difference between CADASIL and the reference group in total white matter (see difference between light coloured and dark coloured boxes). * indicates $p < .05$.

Discussion

Here we show that small vessel dysfunction is associated with white matter alterations at a whole-brain but also at a voxel-by-voxel level. Whole-brain changes in white matter microstructure mostly related with perforating artery blood flow velocity, but with notable differences between CADASIL and sporadic cSVD in the arterioles involved. Whole-brain changes in white matter microstructure did not consistently relate with endothelial-dependent or independent reactivity, while both in CADASIL and sporadic cSVD a voxel-by-voxel level correlation was found between endothelial-independent white matter reactivity and white matter microstructure. Particularly these voxel-by-voxel

level correlations in both patient groups could support a causal relationship between small vessel dysfunction and white matter alterations.

Assessment of perforating artery blood flow velocity and pulsatility index with 7T MRI is a relatively new technique (Chapter 4 and 5). Consequently, the relation of small vessel function measures with microstructural white matter alterations has not been studied before. In this study we observed a significant association between decreased blood flow velocity and microstructural white matter alterations, with disease-specific patterns. In patients with CADASIL this relation was significant for blood flow velocity in perforating arteries in the centrum semiovale and for patients with sporadic cSVD for blood flow velocity in perforating arteries in the basal ganglia. These findings could reflect differences in the underlying physiology leading to parenchymal injury, varying between small vessel populations and types of cSVD. Even though it is plausible that small vessel dysfunction and white matter injury are causally related, these observed whole-brain associations could also reflect shared risk factors.

The whole-brain relation between endothelial-independent vessel reactivity (to hypercapnia and acetazolamide) and white matter injury has been studied previously with 3T-MRI. Findings indicated that decreased reactivity related to increased WMH burden, both in patients with CADASIL and sporadic cSVD.[4–11] In addition, one earlier study reported an association between reduced vascular reactivity and white matter alterations with diffusion MRI on 3T-MRI.[8] In the present observations from the ZOOM@ SVDs study, we extend these earlier findings with detailed reactivity measurements on 7T-MRI. We did not observe a consistent relation between endothelial-dependent or independent reactivity and white matter alterations, with the exception of a negative relation of endothelial-independent reactivity in the cortex with white matter alterations in patients with sporadic cSVD. The direction of this effect was similar in patients with CADASIL. At first, the direction of the effect may seem counterintuitive, but baseline cortical grey matter reactivity in fact tended to be *higher* in patients than in the reference groups. This might reflect a compensatory mechanism to protect the cortex. *Higher* endothelial-independent reactivity in the cortex thus relates to more microstructural white matter damage, while no relations were observed in the subcortical grey matter or white matter. Interestingly, both in patients with CADASIL and sporadic cSVD, when performing voxel-level within-subject analyses in the white matter, we observed a significant negative correlation between endothelial-independent reactivity and white matter microstructure. This correlation was stronger in patients than in the reference groups, implying that this correlation was driven by cSVD related disease processes. Even though there might be a weak correlation between vascular reactivity and white matter microstructure in healthy tissue, this correlation is apparently stronger in damaged tissue. Furthermore, we found this correlation both in total white matter as well as NAWM which suggests that disease processes are already taking place in tissue that looks healthy on conventional MRI scans. Given that these voxel-level analyses eliminate the influence of confounders, these

findings provide a more direct lead towards a possible causal relation between decreased white matter endothelial-independent reactivity and white matter microstructure, both in patients with CADASIL and sporadic cSVD.

The main strength of this study is that we used state-of-the-art 7T measures of small vessel function, which measure complementary aspects of function from distinct vessel populations. These measures provided the opportunity to not only assess whole-brain relationships, voxel-by-voxel ones as well, which are free of confounders (i.e. shared risk factors for abnormal small vessel function and cerebral tissue injury). Furthermore, we were able to study both a genetically-defined and thus pure and a sporadic form of cSVD. A limitation of the study is the relatively small sample size of both patient groups, which might have caused a lack of power in the whole-brain analyses. Furthermore, we have a selection bias in our CADASIL patient group as they were required to travel internationally to be included in the study, leaving out the more affected patients. However, we would expect disease effects to be more pronounced in more affected patients, meaning that we would expect even stronger relations in more affected patients. In our voxel-wise analyses, we could only assess reactivity to hypercapnia in the white matter in relation to loss of white matter microstructure. Other forms of small vessel function might be differentially related to white matter microstructure and this should be explored in future studies. For the CADASIL patient group, multi-shell diffusion data was acquired, which would have allowed for more complex modelling such as diffusion kurtosis and biophysical diffusion models. However, this data was not available in the sporadic cSVD group and we decided to keep the analysis harmonized between the two groups by using only the tensor model. Lastly, we only had cross-sectional data available for this study and longitudinal data is needed to establish causality in the relationship between small vessel function and tissue injury.

In conclusion, we found that whole-brain changes in white matter microstructure related with perforating artery blood flow velocity, with differences in the arterioles involved between CADASIL and sporadic cSVD. For endothelial-dependent or independent reactivity, despite absence of significant relations with whole-brain changes in white matter microstructure, we did observe local voxel-by-voxel level correlations, both in CADASIL and sporadic cSVD. These findings indicate a possible causal relationship between small vessel function and white matter microstructure that should be studied further in longitudinal studies.

References

1. Debette S, Schilling S, Duperron MG, et al. Clinical Significance of Magnetic Resonance Imaging Markers of Vascular Brain Injury: A Systematic Review and Meta-analysis. *JAMA Neurol.* 2019;76:81–94.
2. Wardlaw JM, Smith C, Dichgans M. Small vessel disease: mechanisms and clinical implications. *Lancet Neurol.* 2019;18:684–696.
3. Wardlaw JM, Smith EE, Biessels GJ, et al. Neuroimaging standards for research into small vessel disease and its contribution to ageing and neurodegeneration. *Lancet Neurol.* 2013;12:822–838.
4. Blair GW, Doubal FN, Thrippleton MJ, et al. Magnetic resonance imaging for assessment of cerebrovascular reactivity in cerebral small vessel disease: A systematic review. *Journal of Cerebral Blood Flow and Metabolism.* 2016;36:833–841.
5. Blair GW, Thrippleton MJ, Shi Y, et al. Intracranial hemodynamic relationships in patients with cerebral small vessel disease. *Neurology.* 2020;94:e2258–e2269.
6. Sam K, Crawley AP, Conklin J, et al. Development of White Matter Hyperintensity Is Preceded by Reduced Cerebrovascular Reactivity. *Ann Neurol.* 2016;80:277–285.
7. Sam K, Conklin J, Holmes KR, et al. Impaired dynamic cerebrovascular response to hypercapnia predicts development of white matter hyperintensities. *NeuroImage Clin.* 2016;11:796–801.
8. Reginold W, Sam K, Poublanc J, et al. The efficiency of the brain connectome is associated with cerebrovascular reactivity in persons with white matter hyperintensities. *Hum Brain Mapp.* 2019;40:3647–3656.
9. Chabriat H, Pappata ; S, Ostergaard ; L, et al. Cerebral Hemodynamics in CADASIL Before and After Acetazolamide Challenge Assessed With MRI Bolus Tracking. *Stroke.* 2000;31(8):635-648.
10. Atwi S, Shao H, Crane DE, et al. BOLD-based cerebrovascular reactivity vascular transfer function isolates amplitude and timing responses to better characterize cerebral small vessel disease. *NMR Biomed.* 2019;32(3):1-12.
11. Smith EE, Beaudin AE. New insights into cerebral small vessel disease and vascular cognitive impairment from MRI. *Current Opinion in Neurology.* 2018;31:36–43.
12. van den Brink H, Kopczak A, Arts T, et al. Zooming in on cerebral small vessel function in small vessel diseases with 7T MRI: Rationale and design of the "ZOOM@SVDs" study. *Cereb Circ - Cogn Behav.* 2021;2:100013.
13. Pasi M, Van Uden IWM, Tuladhar AM, et al. White Matter Microstructural Damage on Diffusion Tensor Imaging in Cerebral Small Vessel Disease: Clinical Consequences. *Stroke.* 2016;47:1679–1684.
14. Baykara E, Gesierich B, Adam R, et al. A Novel Imaging Marker for Small Vessel Disease Based on Skeletonization of White Matter Tracts and Diffusion Histograms. *Ann Neurol.* 2016;80:581–592.
15. Low A, Mak E, Stefaniak JD, et al. Peak Width of Skeletonized Mean Diffusivity as a Marker of Diffuse Cerebrovascular Damage. *Front Neurosci.* 2020;14:1–11.
16. Tournier JD, Smith R, Raffelt D, et al. MRtrix3: A fast, flexible and open software framework for medical image processing and visualisation. *Neuroimage.* 2019;202:116137.
17. Smith SM, Jenkinson M, Woolrich MW, et al. Advances in functional and structural MR image analysis and implementation as FSL. *Neuroimage.* 2004;23:208–219.

18. Veraart J, Novikov DS, Christiaens D, et al. Denoising of diffusion MRI using random matrix theory. *Neuroimage.* 2016;142:394–406.
19. Veraart J, Fieremans E, Novikov DS. Diffusion MRI noise mapping using random matrix theory. *Magn Reson Med.* 2016;76:1582–1593.
20. Cordero-Grande L, Christiaens D, Hutter J, et al. Complex diffusion-weighted image estimation via matrix recovery under general noise models. *Neuroimage.* 2019;200:391–404.
21. Kellner E, Dhital B, Kiselev VG, et al. Gibbs-ringing artifact removal based on local subvoxel-shifts. *Magn Reson Med.* 2016;76:1574–1581.
22. Andersson JLR, Sotiropoulos SN. An integrated approach to correction for off-resonance effects and subject movement in diffusion MR imaging. *Neuroimage.* 2016;125:1063–1078.
23. Andersson JLR, Graham MS, Zsoldos E, et al. Incorporating outlier detection and replacement into a non-parametric framework for movement and distortion correction of diffusion MR images. *Neuroimage.* 2016;141:556–572.
24. Andersson JLR, Graham MS, Drobnjak I, et al. Towards a comprehensive framework for movement and distortion correction of diffusion MR images: Within volume movement. *Neuroimage.* 2017;152:450–466.
25. Andersson JLR, Graham MS, Drobnjak I, et al. Susceptibility-induced distortion that varies due to motion: Correction in diffusion MR without acquiring additional data. *Neuroimage.* 2018;171:277–295.
26. Tustison NJ, Avants BB, Cook PA, et al. N4ITK: Improved N3 Bias Correction. *IEEE Trans Med Imaging.* 2010;29:1310–1320.
27. Smith SM, Jenkinson M, Johansen-Berg H, et al. Tract-based spatial statistics: Voxelwise analysis of multi-subject diffusion data. *Neuroimage.* 2006;31:1487–1505.
28. Jenkinson M, Smith S. A global optimisation method for robust affine registration of brain images. *Med Image Anal.* 2001;5:143–156.
29. Jenkinson M, Bannister P, Brady M, et al. Improved Optimization for the Robust and Accurate Linear Registration and Motion Correction of Brain Images. *Neuroimage.* 2002;17:825–841.
30. Greve DN, Fischl B. Accurate and robust brain image alignment using boundary-based registration. *Neuroimage.* 2009;48:63–72.

Supplementary material

Supplemental table 1: Linear regressions between 7T small vessel function measures and PSMD in normal appearing white matter

	CADASIL			Sporadic cSVD		
	B	**CI95**	***p***	**B**	**CI95**	***p***
2D-Qflow centrum semiovale	N=22			N=46		
Blood flow velocity [cm/s]	-0.43	-0.82 – -0.05	0.03	-0.018	-0.34 – 0.30	0.91
WM Pulsatility Index	-0.27	-0.69 – 0.14	0.19	0.047	-0.29 – 0.38	0.78
2D-Qflow basal ganglia	N=21			N=44		
Blood flow velocity [cm/s]	-0.04	-0.54 – 0.46	0.86	-0.383	-0.68 – -0.1	0.01
Pulsatility index	0.09	-0.40 – 0.59	0.69	0.305	0.01 – 0.61	0.05
BOLD visual stimulus	N=19			N=35		
BOLD% signal change	-0.37	-0.79 – 0.05	0.08	0.017	-0.29 – 0.32	0.91
Full width half max [s]	-0.15	-0.41 – 0.11	0.25	-0.154	-0.45 – 0.14	0.30
BOLD hypercapnic stimulus	N=17			N=36		
CGM BOLD% signal change	-0.37	-0.90 – 0.17	0.16	-0.36	-0.69 – -0.03	0.03
SGM BOLD% signal change	-0.34	-0.89 – 0.19	0.19	-0.27	-0.56 – 0.13	0.21
NAWM BOLD% signal change	0.04	-0.54 – 0.63	0.88	-0.168	-0.52 – 0.18	0.33

B = standardized beta, BOLD = Blood oxygenation level-dependent, CGM = cortical grey matter, CI95 = 95% confidence interval, NAWM = normal appearing white matter, PSMD = peak width of skeletonized mean diffusivity, Qflow = quantitative flow (velocity phase contrast MRI), SGM = subcortical grey matter.

Supplemental table 2: Linear regressions between 7T small vessel function measures and PSMD corrected for age in patients with sporadic cSVD

	PSMD WM (log transformed)			**PSMD NAWM (log transformed)**		
	B	**CI95**	***p***	**B**	**CI95**	***p***
2D-Qflow centrum semiovale	N= 46			N = 46		
Blood flow velocity [cm/s]	0.07	-0.20 – 0.34	0.61	0.08	-0.20 – 0.36	0.58
WM Pulsatility Index	0.09	-0.18 – 0.36	0.51	0.08	-0.21 – 0.37	0.58
2D-Qflow basal ganglia	N = 44			N = 44		
Blood flow velocity [cm/s]	-0.32	-0.60 – -0.04	0.03	-0.23	-0.51 – 0.06	0.12
Pulsatility index	0.19	-0.09 – 0.48	0.18	0.18	-0.10 – 0.46	0.21
BOLD visual stimulus	N = 35			N = 35		
BOLD% signal change	-0.05	-0.36 – 0.25	0.72	0.01	-0.28 – 0.29	0.96
Full width half max [s]	-0.25	-0.54 – 0.05	0.10	-0.17	-0.45 – 0.10	0.21
BOLD hypercapnic stimulus	N = 36			N = 36		
CGM BOLD% signal change	-0.28	-0.59 – 0.03	0.07	-0.28	-0.58 – 0.02	0.07
SGM BOLD% signal change	-0.24	-0.55 – 0.07	0.11	-0.21	-0.51 – 0.10	0.18
NAWM BOLD% signal change	-0.12	-0.43 – 0.20	0.46	-0.07	-0.41 – 0.28	0.69

B = standardized beta, BOLD = Blood oxygenation level-dependent, CGM = cortical grey matter, CI95 = 95% confidence interval, NAWM = normal appearing white matter, PSMD = peak width of skeletonized mean diffusivity, Qflow = quantitative flow (velocity phase contrast MRI), SGM = subcortical grey matter.

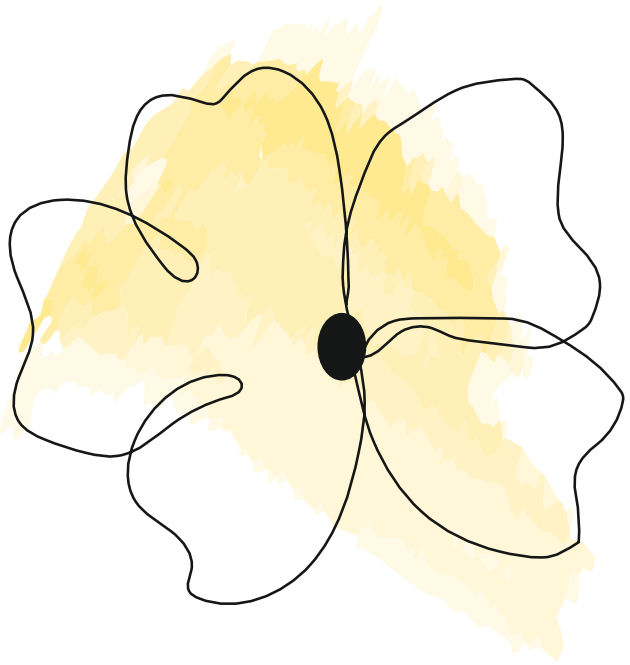

7

Cortical Microinfarcts on 3T Magnetic Resonance Imaging in Cerebral Amyloid Angiopathy

Hilde van den Brink, Angela Zwiers, Aaron R. Switzer, Anna Charlton, Cheryl R. McCreary, Bradley G. Goodyear, Richard Frayne, Geert Jan Biessels, Eric E. Smith

Stroke: 2018;49(8):1899-1905

Abstract

Background and purpose

Cerebral microinfarcts are small ischemic lesions that are found in cerebral amyloid angiopathy (CAA) patients at autopsy. The current study aimed to detect cortical microinfarcts (CMI) on in vivo 3T MRI in CAA patients, to study the progression of CMI over a one-year period, and to correlate CMI with markers of CAA-related vascular brain injury and cognitive functioning.

Methods

35 CAA patients (mean age 74.2±7.6 years), 13 Alzheimer's disease (AD) patients (67.0±5.8 years) and 26 healthy controls (67.2±9.5 years) participated in the study. All participants underwent a standardized clinical and neuropsychological assessment as well as 3 Tesla MRI. CMI were rated according to standardized criteria.

Results

CMI were present in significantly more CAA patients (57.1%) (median number: 1, range 1-9) than in AD (7.7%) or in healthy controls (11.5%) (p<0.001). Incident CMI were observed after a one-year follow-up. CMI did not correlate with any other MRI marker of CAA nor with cognitive function.

Conclusions

In vivo CMI are a frequent finding on 3-T MRI in CAA patients and incident CMI are observable after one year-follow up. CMI can be regarded as a new MRI marker of CAA, potentially distinct from other well-established markers. Future larger cohort studies with longitudinal follow-up are needed to elucidate the relationship between CMI and possible causes and clinical outcomes in CAA.

Introduction

Cerebral Amyloid Angiopathy (CAA) is characterized by beta-amyloid deposition in the walls of small arterioles and capillaries in the cerebral cortex and meninges.[1,2] CAA pathology is traditionally known as a cause of lobar intracerebral hemorrhages (ICH)[3,4] and microbleeds.[5] More recently, CAA has also been implicated as a cause of ischemic brain lesions[6] and neurodegeneration.[7] The mechanisms by which CAA causes neurodegeneration and impairs cognition are, however, poorly understood.

Cerebral microinfarcts are ischemic lesions of about 50 µm-4 mm in size that have been found in the brains of CAA and dementia patients at autopsy,[8–10] and therefore might help explain cognitive dysfunction.[11–13] Recently, it was shown that cortical microinfarcts (CMI) of about 1 to 2 mm can be detected *in vivo* with high-resolution 7-T and 3-T MRI.[14] Whether CMI can be detected *in vivo* in CAA, and whether they relate to other markers of CAA or cause cognitive impairment is currently not known.

The present explorative study aimed to examine the frequency of *in vivo* CMI on 3-T MRI images and their progression over one year in a CAA cohort, and compare it with age-matched healthy controls and persons with Alzheimer's disease (AD) dementia. Secondary objectives in CAA patients were to determine: (a) the association of age, sex, and vascular risk factors with CMI, (b) the association between CMI and cerebrovascular reactivity and other MRI correlates of CAA, and (c) to explore a relation between CMI and cognitive functioning in patients with CAA.

Material and Methods

Anonymized data created for the study are available in a persistent repository available at: http://dx.doi.org/10.5683/SP/NYR8PB.

Study participants

This study included 40 patients with CAA that were recruited as part of the Functional Assessment of Vascular Reactivity (FAVR) study, which is an observational, prospective, follow-up study.[15] All patients met the validated modified Boston criteria for probable CAA, that require MRI evidence of lobar ICH, CMBs, or superficial cortical siderosis without another evident cause.[3] Patients were recruited from an inpatient stroke service or an outpatient cognitive assessment clinic and presented with ICH (18 patients), transient focal neurological episodes (16 patients), or cognitive impairment (6 patients). To avoid acute effects of ICH, patients with recent symptomatic stroke (<90 days) were excluded. Patients with CAA-associated inflammation were only included if they were in remission, with resolution of acute cerebral edema. Furthermore, patients were excluded if they had abnormal visual acuity (<20/50 Snellen visual acuity), had moderate to severe dementia (clinical dementia rate >1.0), or were non-fluent in English.

A group of 26 healthy controls were recruited from the community through newsletter advertisement as part of FAVR. Control participants did not have a history of stroke or dementia as examined by a neurologist, and were excluded if they had silent lobar microbleeds (but not silent brain infarcts or deep microbleeds). A total of 19 AD dementia participants were recruited in FAVR from a memory clinic and had mild dementia (Folstein Minimental Status Exam ≥20[16] and Clinical Dementia Rating[17] total score ≤1.0). They were diagnosed by National Institute on Aging-Alzheimer's Association (NIA-AA) criteria for probable AD,[18] without biomarker support.

All study participants went through an extensive study visit, including clinical, physical and neuropsychological assessments as well as 3-T MRI. Five patients with CAA and six AD patients were excluded because of low-quality imaging data caused by patient motion, leaving 35 CAA patients, 13 AD patients and 26 controls for baseline analyses. One year follow-up visits consisted of a repeated study visit and MR imaging. Follow-up data were available and analyzable for 21 CAA patients, 8 AD patients and 25 controls. The follow-up imaging was done after 13.6±2.0 months. Figure 1 shows a study flow diagram, including reasons for exclusions and loss to follow up.

All study participants provided written informed consent to participate in the study, which was approved by the Institutional Review Board of the University of Calgary. The study was conducted in adherence to the Declaration of Helsinki.

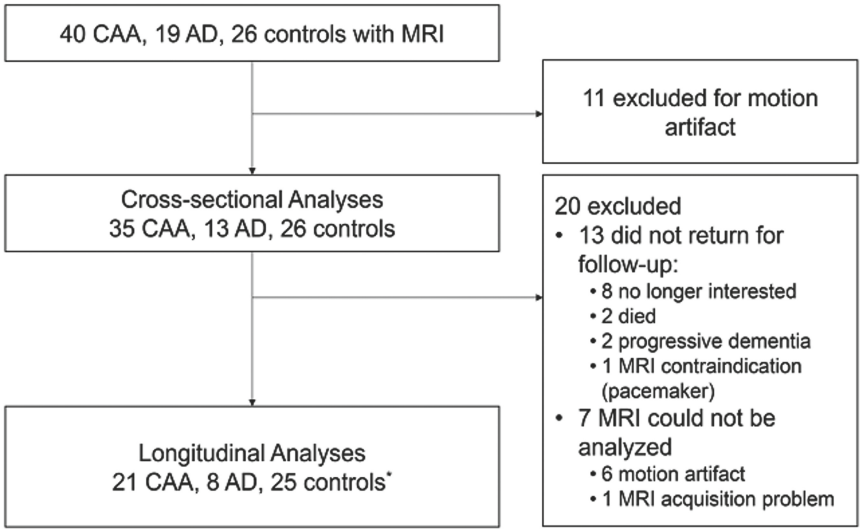

Figure 1: Flow diagram showing reasons for exclusions and loss to follow-up for participants in the study.

Measurements

The neuropsychological test battery was based on the battery proposed by the National Institute for Neurological Diseases and Stroke-Canadian Stroke Network.[19] Raw scores were standardized into z-scores based on normative data provided by the test manuals. Z-scores were then averaged in three domain-specific scores: memory, executive functioning and speed of processing. The memory domain was assessed by the California Verbal Learning Test-Delayed Recall (CVLT-DR)[20] and the Rey-Osterrieth Complex Figure Test-Delayed Recall (ROCFT-DR).[21] The domain executive functioning included scores on the Trail making B (TMT-B)[22] and Controlled Oral Word Association test-FAS (COWAT-FAS).[23] Lastly, the domain of processing speed consisted of scores on the Digit Symbol Coding (DSC) subtest of the WAIS-IV[24] and Trail Making A (TMT-A).[22]

The vascular risk profile that was recorded for all patients included hypertension, diabetes mellitus, and current smoking and past smoking. This was determined by a neurologist and based on interview, medical history and current medication use.

All imaging was performed on a 3-T GE MR scanner (either Signa Excite or Discovery 750; GE Healthcare, Waukesha, WI). Because of a scanner upgrade, 5 CAA patients and 18 controls had their baseline scan on the older (Excite) system and their one-year follow-up on the newer (Discovery) system. All other participants had both their baseline and follow-up scan on the newer system. Among other sequences, the scan protocol included T1-weighted (TR/TE/TI = 6.0/2.5/650 ms; voxel size 0.9 x 0.9 x 1 mm^3; 256 x 256 x 200_reconstructed matrix size), T2-weighted (TR/TE = 3500/86 ms; voxel size 0.9 x 0.9 x 3.5 mm^3; 256 x 256 matrix size), susceptibility-weighted (SWI) (TR/TE = 30/20 ms; voxel size 0.5 x 0.5 x 1 mm^3; 256 x 256 matrix size), fluid-attenuated inversion recovery (FLAIR) (TR/TE/TI = 9000/145/2250 ms; voxel size 0.9 x 0.9 x 3.5 mm^3; 256 x 256 matrix size) and T2*-weighted blood oxygen level (BOLD) functional MR images (fMRI) that were acquired using a GRE-EPI sequence (TR/TE = 2000/30 ms; voxel size 3.75 x 3.75 x 4 mm^3; 64 x 64 matrix). During the fMRI acquisitions, participants passively viewed 40-second blocks of an 8-Hz contrast-reversing checkerboard, activating the primary visual cortex in the occipital lobe. These activation blocks were alternated with 40-s rest blocks of a grey screen with a central fixation cross. Blocks were repeated four times.

MRI rating and analysis

CMI were rated using MeVisLab (MeVis Medical Solutions AG, Bremen, Germany, version 2.7.1), according to published autopsy-validated criteria.[25] These criteria define a CMI as a hypointense signal on the T1-weighted sequence, a hyper- or iso-intense signal on the FLAIR and T2-weighted sequences, <5 mm in diameter, perpendicular to the cortical surface, restricted to the cortex and distinct from perivascular spaces.[13] After all CMI detection, corresponding locations were checked on the SWI for susceptibility artifacts, to distinguish CMI from microbleeds. Possible CMI located in tissue affected by cortical infarcts were excluded.[25] Lobar location was assigned visually based on a

template published as part of the Cerebral Haemorrhage Anatomical RaTing instrument (CHART).[26] All baseline and follow-up MR images were analyzed simultaneously by one trained rater (H.B.). The rater was blinded to clinical participant characteristics but not scan order, because findings on baseline and follow-up were compared after initial ratings to exclude false positives (on baseline) and misses (on either baseline or follow-up). The rater could not be completely blinded for hemorrhages visible on FLAIR or T1-weighted images, as well as microbleed load during later examination of CMI on SWI images. Rater H.B. was trained for CMI detection on an official 3T MRI test set in the UMC Utrecht, with good reliability results on the exam scans (ICC = 0.96; Dice's similarity index (DSC) = 0.81). Intra-rater reliability was determined on a random subset of 20 images and was good (ICC = 0.87; DSC = 0.75).

CMBs, lacunar infarcts, large cerebral infarcts, ICH, superficial cortical siderosis, enlarged perivascular spaces (PVS) and WMHs are key neuroimaging features of CAA[12] and were rated according to the standards for reporting vascular changes on neuroimaging (STRIVE) .[27] Total numbers of CMBs, lacunar infarcts, large (>15 mm) or cortical cerebral infarcts and ICHs were recorded. Superficial cortical siderosis was recorded as present or absent. A validated scale was used to score enlarged PVS on high resolution T1-weighted images: 0 = no PVS, 1 = <10 PVS, 2 = 10-20 PVS, 3 = 21-40 PVS, and 4 = >40 PVS.[28] WMH volumes were segmented on the FLAIR images using *Quantomo*, a custom-designed software application (Cybertrials Inc; Calgary, AB, Canada).[29] To normalize for different head sizes, individual WMH volumes were analyzed as the percent of intracranial volume, where intracranial volume was obtained using FSL[30] and OptiBET.[31] Overall CAA-related small vessel disease burden was measured using a previously published scale.[32]

The change in fMRI blood oxygen level dependent (BOLD) response in the occipital cortex to a visual stimulation task was assessed as per a prior study.[33] The fMRI data were analyzed using FSL (version 5.0.1, Oxford UK).[34]

Statistical analyses

Baseline differences between groups were assessed with a one-way independent ANOVA for age and Kruskal-Wallis test for MRI correlates of CAA that were non-normally distributed continuous variables. Chi-square was used to test for differences in sex, vascular risk factors and categorical MRI variables.

CMI presence was compared between groups by a chi-square test and differences in total numbers of CMI were tested with the Kruskal-Wallis test for both baseline counts and new CMI at follow-up. The Wilcoxon rank-sum test was used to compare total numbers of new CMI at follow-up between participants with CMI at baseline versus without CMI at baseline. Logistic regression was used to determine whether CAA status (vs. controls) was associated with CMI, controlling for other differences between groups. In CAA, mean CMI counts by brain lobe were tabulated. The difference in mean CMI per lobe was tested

using a generalized linear model accounting for repeated measures within the same subject. CMI numbers were weighted for lobar volume, using weights derived from the International Consortium for Brain Mapping (ICBM) atlas "2009c Nonlinear Symmetric"[35] (frontal: 319.0 ml; parietal: 151.4 ml; temporal: 208.4 ml; occipital: 84.3 ml).

A relation of age, sex, vascular risk factors, MRI markers and cognition to CMI was studied only in patients with CAA. Differences between patients with and without CMI were assessed with independent *t*-tests for age, occipital BOLD responses, and cognitive domains; and a chi-square test for sex and vascular risk factors. A relation of CMI with other MRI markers of CAA at baseline and follow-up were tested with chi-square tests for categorical data and Mann-Whitney *U*-tests for continuous data.

Analyses were carried out in SAS version 9.4 (Cary, NC), with the significance threshold set at $p<0.05$.

Results

At baseline, we analyzed data from 35 CAA, 13 AD, and 26 controls (Table 1). Compared to CAA, patients with AD and controls were significantly younger ($p=0.001$). Hypertension was the only other variable that occurred significantly more often in patients with CAA than in AD and controls ($p<0.001$) (Table 1).

CMI were present in 57.1% of patients with CAA, which was significantly more than healthy controls (11.5%) or AD-dementia (7.7%) ($p<0.001$). CMI were also higher in number in CAA patients ($p<0.001$, Table 2). CMI presence and total number were not different in the different CAA presentations (i.e. ICH, transient focal neurological episodes, cognitive impairment). Nor were any of the following results different after excluding the CAA patients with cognitive impairment from the analyses. An example of a CMI in a CAA patient is shown in Figure 2. In a multivariable-adjusted model controlling for age and hypertension, CAA was independently associated with the likelihood of having CMI compared to controls (OR 7.8, 95% CI 1.5 to 40.8, $p=0.02$). CMI counts in each lobe are shown in Table 2. The mean number of CMI per lobe did not differ ($p=0.11$) after taking into account differences in lobe volumes.

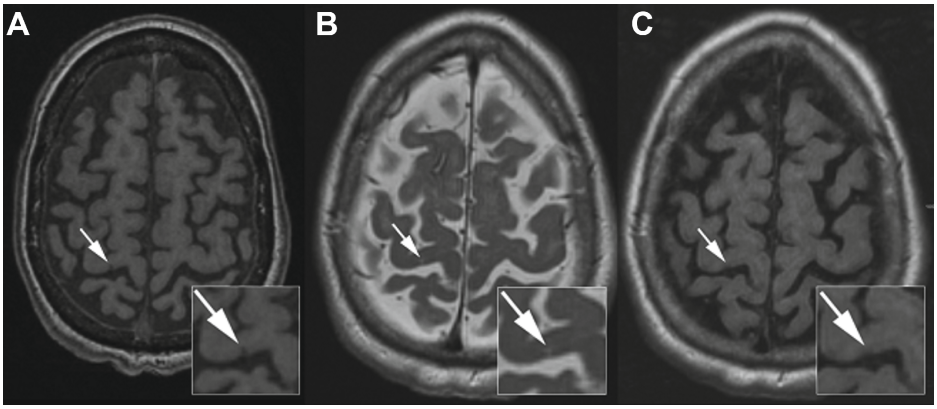

Figure 2: Example of a cortical microinfarct, seen as a hypointensity on T1-weighted (A), hyperintensity on T2-weighted (B) and isointensity on FLAIR (C) image.

Table 1: Characteristics of the Study Population

Characteristic	**CAA** ***n*=35**	**AD-dementia** ***n*=13**	**Control** ***n*=26**	***p*-value**
Age	74.5±7.5	67.0±5.8	67.2±9.5	.001
Sex (female)	15 (42.9)	6 (46.2)	16 (61.5)	0.34
Vascular risk factors				
Hypertension	24 (68.6)	4 (30.8)	2 (7.7)	<0.001
Diabetes	5 (14.3)	2 (15.4)	1 (3.8)	0.36
Smoking	1 (2.9)	1 (7.7)	1 (3.8)	0.75
MRI markers of CAA				
Microbleeds present	33 (94.3)	1 (7.7)	4 (15.4)	<0.001
Microbleed total	22.0 [5.0, 90.0]	0 [0, 0]	0 [0, 0]	<0.001
Superficial siderosis	21 (61.8)	0 (0.0)	0 (0.0)	<0.001
WMH %	1.88 [0.86, 3.65]	0.36 [0.33, 0.65]	0.18 [0.13, 0.32]	<0.001
PVS, bg	2.0 [1, 2]	1.0 [1, 1]	1.5 [1, 2]	0.04
PVS, cs	2.0 [1, 2]	1.0 [1, 1]	1.0 [1, 2]	0.07
Lacunes, bg	4 (11.4)	0 (0)	1 (3.8)	0.29
Lacunes, cs	11 (31.4)	1 (7.7)	4 (15.4)	0.13
Non-lacunar infarcts	6 (17.1)	1 (7.7)	1 (3.8)	0.24

Data are presented as mean±SD, median [25th, 75th percentiles] or number (percentage). WMH is expressed as the percent of intracranial volume. Abbreviations: AD, Alzheimer's disease; bg, basal ganglia; CAA, cerebral amyloid angiopathy; cs, centrum semiovale; PVS, perivascular spaces.

Table 2: Presence and distribution of CMI in CAA and Comparison Groups

	CAA ***n*=35**	**AD-dementia** ***n*=13**	**Control** ***n*=26**	***p*-value**
CMI present	20 (57.1)	1 (7.7)	3 (11.5)	<0.001
Number of CMI	1.0 [0, 2.0]	0.0 [0, 0]	0.0 [0, 0]	<0.001
0	15	12	23	-
1	10	1	3	-
2	6	0	0	-
3	1	0	0	-
4	2	0	0	-
≥5*	1	0	0	-
Lobar count (total number in each lobe, across all patients)				
Frontal	16 (38.1)	1 (100)	2 (66.6)	-
Parietal	14 (33.3)	0 (0.0)	0 (0.0)	-
Occipital	2 (4.8)	0 (0.0)	1 (33.3)	-
Temporal	10 (23.8)	0 (0.0)	0 (0.0)	-

*15 CAA patient had 0 CMI, 10 had 1 CMI, etc. Other data are presented as median [25th, 75th percentiles] or number (percentage). Abbreviations: AD, Alzheimer's disease; CAA, cerebral amyloid angiopathy; CMI, cortical microinfarct.
PII vessel disease.paces. ves

The characteristics of CAA patients with CMI compared with CAA patients without CMI are shown in Table 3. CAA patients with CMI did not differ in age, sex, or vascular risk factors compared to CAA patients without CMI. The presence of CMI was not associated with any of the other CAA neuroimaging markers or overall CAA small vessel disease burden. Also, baseline CMI did not predict progression of neuroimaging markers at follow-up. Cognitive domain scores did not differ between patients with CMI and patients without CMI.

In participants who had follow-up, new CMI were identified in 9/21 with CAA (total of 16 new CMI), 1/8 with AD-dementia (total of 2 new CMI), and 0/25 controls (p<0.001). For 10/46 participants with CMI at baseline, 1 baseline CMI (total of 10) was not visible at follow-up. New CMI were more likely to be seen in participants with CMI at baseline (new CMI at follow-up were seen in 7/18 with CMI at baseline vs. 3/36 without CMI at baseline, p=0.006). Follow-up scanner model (Excite vs Discovery) was not associated with new CMI detection. Compared to CAA patients without new CMI (n=12), patients with new CMI (n=9) had no evidence of different WMH progression (median 0.44% of intracranial volume [interquartile range -0.04% to 0.68%] vs. 0.10% of intracranial volume [-0.03% to 0.45%], p=0.59), frequency of new microbleeds (5/9 vs 4/11, p=0.39), number of new microbleeds (median 1.0 [range 0-87] vs. 0.0 [range 0-4] p=0.13), or change in fMRI BOLD amplitude (mean -0.02±0.70 vs. -0.37±0.50, p=0.26).

Table 3: Characteristics of CAA patients with vs. without CMI

Characteristic	CAA CMI+ *n*=20	CAA CMI- *n*=15	*p*-value
Age	74.3±6.8	74.8±8.8	0.84
Sex (female)	8 (40.0)	7 (46.7)	0.69
Vascular risk factors			
Hypertension	15 (75.0)	9 (60.0)	0.34
Diabetes	3 (15.0)	2 (13.3)	0.89
Smoking	1 (5.0)	0 (0.0)	0.38
MRI markers of CAA			
Occipital BOLD change	1.83±0.77	2.00±0.79	0.52
Microbleeds present	19 (95.0)	14 (93.3)	0.25
Microbleed total	23.00 [6.00;123.00]	10.00 [5.00;58.00]	0.49
Superficial siderosis	10 (52.6)	11 (73.3)	0.22
WMH %	1.75 [0.88, 3.92]	2.05 [0.75, 2.90]	0.63
PVS, bg	2.0 [1, 2]	1.0 [1, 2]	0.14
PVS, cs	2.0 [1, 2]	1.5 [1, 2]	0.21
Lacunes, bg	4 (20.0)	0 (0.0)	0.07
Lacunes, cs	5 (25.0)	6 (40.0)	0.34
Non-lacunar infarcts	4 (20.0)	2 (13.3)	0.60
CAA small vessel disease burden score	3.0 [2.5, 4.0]	3.5 [2.0, 4.0]	0.97
Progression of MRI markers			
Occipital BOLD change	-0.11±0.57	-0.61±-0.55	0.26
Number with new microbleeds	7 (50.0)	4 (44.4)	0.79
Median new microbleeds	0.50 [0.00;2.25]	0.00 [0.00;13.50]	0.82
WMH change	0.36 [0.00;0.61]	0.05 [-0.05;0.37]	0.21
Cognitive functioning			
Memory	-0.72±1.07	-0.50±0.85	0.54
Speed of processing	-1.15±1.14	-1.02±1.09	0.74
Executive functioning	-1.07±1.19	-1.21±0.96	0.71

Data are presented as mean±SD, median [25th, 75th percentile] or number (percentage). WMH is expressed as the percent of intracranial volume. At baseline, one patient had missing microbleed and superficial siderosis information because the SWI sequence was not obtained. Three patients had missing bg PVS scores and four patients had missing cs PVS scores because the scans were affected by motion. For follow-up, MRI data were available for 14 patients with baseline CMI and 9 patients without baseline CMI. Abbreviations: AD, Alzheimer's disease; bg, basal ganglia; CAA, cerebral amyloid angiopathy; cs centrum semiovale; PVS, perivascular spaces; SVD, small vessel disease.

Discussion

CMI were frequently detected on 3-T MRI in CAA patients (57.1%), and significantly more than in AD patients (7.7%) and healthy controls (11.5%). After one year follow-up, new CMI appeared in CAA. Surprisingly, CMI in CAA did not relate with any of the other neuroimaging markers of the disease and CMI did not significantly explain cognitive dysfunction in CAA.

Our findings show that CMI are a significant new MRI marker of CAA. Moreover, compared to earlier *in vivo* studies, CMI appear to be much more prevalent in CAA than in healthy elderly and other patient populations. Whereas current findings show a CMI prevalence of 57.1% in CAA, earlier studies report CMI in 6.3-11.5% of healthy elderly,[36,37] 20% of patients with vascular cognitive impairment[37] and 32% of memory clinic patients.[25] Also, in our study CMI were seen significantly more often in CAA than in AD (7.7%). Residual confounding by differences in age and hypertension between CAA patients versus AD patients and controls can however not be excluded, while *in vivo* CMI detection is also limited in only capturing larger CMI.[38] Despite these limitations our prevalence is in line with neuropathological findings that report CMI in 33.3-87.5% of CAA patients.[8–10,39]

The much higher prevalence of *in vivo* CMI in CAA than in healthy elderly and other patient populations suggests that vascular beta amyloid plays a role in the etiology of CMI in CAA. Amyloid deposition might impair normal vessel function, causing decreased cerebral blood flow regulation and mismatched blood supply versus demand during brain activation. The resulting oxygen shortage might cause ischemic tissue damage, like CMI. Although we did not find that CMI were associated with fMRI BOLD reactivity, our BOLD measurement was limited to primary visual cortex whereas the majority of CMI were found in other brain regions. In ongoing work, we are addressing this limitation by measuring vascular reactivity to carbon dioxide across the whole brain.

Interestingly, follow-up data show that in CAA a substantial number of incident CMI develop in one year or less. To our knowledge, our study is the first to report follow-up data on CMI detection in any condition. By showing that accumulating CMI burden can be detected with *in vivo* MR methods, it becomes possible to study a causal relationship between CMI and clinical outcomes in future larger longitudinal studies. It must be noted however that not all baseline CMI were found at follow-up. Since intra-rater reliability was good, this discrepancy is most likely caused by scan-related factures, such as different head positioning during MRI.

Even though our findings show that CMI are a marker of CAA, we did not find relationships between CMI and other key neurovascular imaging markers of CAA pathology.[12] This suggests that CMI may reflect unique pathways of CAA-related injury that are distinct from those that lead to hemorrhages, white matter changes, or perivascular space

enlargement. However, given our relatively small sample size we cannot exclude mild to moderate strength associations between CMI and other CAA markers, which merit further investigation in larger studies. Also, it must be noted that *in vivo* chronic CMI detection is only possible in the cortex, whereas subcortical CMI, undetectable by current imaging methods, might be more closely related to WMH. As a marker of CAA that is distinct from other markers, CMI could be a possible *in vivo* diagnostic aid for CAA. Although further studies, also controlling for brain atrophy, are necessary, CMI might increase diagnostic certainty when observed in the context of other well-recognized MR markers of CAA.

The main limitation of this study is the small sample size, that limited the power to study causes and consequences of CMI in CAA. This may be the reason we failed to find an association between CMI and worse cognition that has been demonstrated in non-CAA cohorts.[25,36,37,40] MRI detects only the larger CMI and thus offers only a loose approximation of the total CMI burden, which may limit the statistical power to detect associations. Also, even though rater H.B. was trained extensively, the absence of inter-rater reliability for CMI detection in our dataset poses a second limitation. Lastly, vascular reactivity was only studied in the visual cortex, whereas CMI were rarely found in the occipital lobe. This complicated the study of a relationship between vascular reactivity and CMI. Ongoing work addresses this limitation by measuring BOLD reactivity using carbon dioxide inhalation. This yields a measure of vascular reactivity that covers the whole brain, and therefore is a better surrogate to study decreased vascular reactivity as a possible cause for CMI in CAA.

This explorative study shows that *in vivo* CMI are a frequent finding on 3T MRI in CAA and that incident CMI are already observed after one year follow-up. CMI can be regarded as a new marker of CAA pathology. Additional larger, adequately powered studies with longitudinal follow-up are warranted to determine possible causes and clinical outcomes in CAA.

References

1. Chen Y, Lee M, Smith EE. Cerebral amyloid angiopathy in East and West. *Int. J. stroke*. 2010;5:403–411.
2. Vinters H V. Cerebral Amyloid Angiopathy A Critical Review. *Stroke*. 1987;18:311–324.
3. Knudsen KA, Rosand J, Karluk D, Greenberg SM. Clinical diagnosis of cerebral amyloid angiopathy: Validation of the Boston Criteria. *Neurology*. 2001;56:2000–2002.
4. Smith EE, Rosand J, Greenberg SM. Imaging of Hemorrhagic Stroke. *Magn. Reson. Imaging*. 2006;14:127–140.
5. Rooden S Van, Grond J Van Der, Boom R Van Den, Haan J, Linn J, Greenberg SM, et al. Descriptive Analysis of the Boston Criteria Applied to a Dutch-Type Cerebral Amyloid Angiopathy Population. *Stroke*. 2009;40:3022–3027.
6. Reijmer YD, Veluw SJ Van, Greenberg SM. Ischemic brain injury in cerebral amyloid angiopathy. *J. Cereb. Blood Flow Metab*. 2016;36:40–54.
7. Smith EE. Cerebral amyloid angiopathy as a cause of neurodegeneration. *J. Neurochem*. 2017;1–8.
8. Haglund M, Passant U, Sjobeck M, Ghebremedhin E, Englund E. Cerebral amyloid angiopathy and cortical microinfarcts as putative substrates of vascular dementia. *Int. J. Geriatr. psychiatry*. 2006;681–687.
9. Reuck J De, Deramecourt V, Cordonnier C, Leys D, Maurage CA, Pasquier F. The impact of cerebral amyloid angiopathy on the occurrence of cerebrovascular lesions in demented patients with Alzheimer features: a neuropathological study. *Eur. J. Neurol.* 2011;18:913–918.
10. Soontornniyomkij V, Lynch MD, Mermash S, Pomakian J, Badkoobehi H, Clare R, et al. Cerebral Microinfarcts Associated with Severe Cerebral b -Amyloid Angiopathy. *Brain Pathol.* 2010;20:459–467.
11. Brundel M, Bresser J De, Dillen JJ Van, Kappelle LJ, Biessels GJ. Cerebral microinfarcts: a systematic review of neuropathological studies. *J. Cereb. Blood Flow Metab*. 2012;32:425–436.
12. Charidimou A, Boulouis G, Gurol ME, Ayata C, Bacskai BJ, Frosch MP, et al. Emerging concepts in sporadic cerebral amyloid angiopathy. *Brain*. 2017;1–22.
13. van Veluw SJ, Shih AY, Smith EE, Chen C, Schneider JA, Wardlaw JM, et al. Detection, risk factors, and functional consequences of cerebral microinfarcts. *Lancet Neurol.* 2017;16:730–740.
14. van Veluw SJ, Zwanenburg JJM, Engelen-Lee J, Spliet WGM, Hendrikse J, Luijten PR, et al. In vivo detection of cerebral cortical microinfarcts with high-resolution 7T MRI. *J. Cereb. blood flow Metab*. 2013;33:322–9.
15. Peca S, Mccreary CR, Donaldson E, Kumarpillai G, Sanchez K, Charlton A, et al. Neurovascular decoupling is associated with severity of cerebral amyloid angiopathy. *Neurology*. 2013;81:1659–1665.
16. Folstein MF, Folstein SE, McHugh PR. "Mini-mental state". A practical method for grading the cognitive state of patients for the clinician. *J. Psychiatr. Res.* 1975;12:189–198.
17. Morris JC. The Clinical Dementia Rating (CDR): Current version and scoring rules. *Neurology*. 1993;43:2412–2412.
18. McKhann GM, Knopman DS, Chertkow H, Hyman BT, Jack CR, Kawas CH, et al. The diagnosis of dementia due to Alzheimer's disease: Recommendations from the National Institute on Aging-Alzheimer's Association workgroups on diagnostic guidelines for Alzheimer's disease. *Alzheimer's Dement*. 2011;7:263–269.

19. Hachinski V, Iadecola C, Petersen RC, Breteler MM, Nyenhuis DL, Black SE, et al. National Institute of Neurological Disorders and Stroke-Canadian Stroke Network vascular cognitive impairment harmonization standards. *Stroke*. 2006;37:2220–2241.

20. Delis, D., Kramer, J., Kaplan, E., & Ober B. California Verbal Learning Test-Second Edition. San Antonio, TX: The Psychological Corporation; 2000.

21. Osterrieth P. Le test de copie d'une figure complexe. *Arch Psychol.* 1944;30:206–356.

22. Corrigan JD, Hinkeldey NS. Relationships Between Parts A and B of the Trail Making Test. *J. Clin. Psychol.* 1987;43:402–410.

23. Benton, A.L., & Hamsher K. Multilingual Aphasia Examination. Iowa: University of Iowa Press; 1976.

24. Wechsler D. Wechsler Adult Intelligence Scale-Fourth Edition. San Antonio, TX: Pearson; 2008.

25. van Veluw SJ, Hilal S, Kuijf HJ, Ikram MK, Xu X, Tan BY, et al. Cortical microinfarcts on 3T MRI: Clinical correlates in memory-clinic patients. *Alzheimer's Dement*. 2015;1–10.

26. Charidimou A, Schmitt A, Wilson D, Yakushiji Y, Gregoire SM, Fox Z, et al. The Cerebral Haemorrhage Anatomical RaTing inStrument (CHARTS): Development and assessment of reliability. *J. Neurol. Sci.* 2017;372:178–183.

27. Wardlaw JM, Smith EE, Biessels GJ, Cordonnier C, Fazekas F, Frayne R, et al. Neuroimaging standards for research into small vessel disease and its contribution to ageing and neurodegeneration. *Lancet Neurol.* 2013;12:822–838.

28. Maclullich AMJ, Wardlaw JM, Ferguson KJ, Starr JM, Seckl JR, Deary IJ. Enlarged perivascular spaces are associated with cognitive function in healthy elderly men. *J. Neurol. Neurosurg. Psychiatry*. 2004;75:1519–1523.

29. Kosior JC, Idris S, Dowlatshahi D, Alzawahmah M, Eesa M, Sharma P, et al. Quantomo: validation of a computer-assisted methodology for the volumetric analysis of intracerebral haemorrhage. *Int. J. Stroke*. 2011;6:302–305.

30. Smith SM. Fast Robust Automated Brain Extraction. *Hum. Brain Mapp.* 2002;155:143–155.

31. Lutkenhoff ES, Rosenberg M, Chiang J, Zhang K. Optimized Brain Extraction for Pathological Brains (optiBET). *PLoS One*. 2014;1–13.

32. Charidimou A, Martinez-Ramirez S, Reijmer YD, Oliveira-Filho J, Lauer A, Roongpiboonsopit D, et al. Total magnetic resonance imaging burden of small vessel disease in cerebral amyloid angiopathy an imaging-pathologic study of concept validation. *JAMA Neurol.* 2016;73:994–1001.

33. Switzer AR, Mccreary C, Batool S, Stafford RB, Frayne R, Goodyear BG, et al. Longitudinal decrease in blood oxygenation level dependent response in cerebral amyloid angiopathy. *NeuroImage Clin*. 2016;11:461–467.

34. Smith SM, Jenkinson M, Woolrich MW, Beckmann CF, Behrens TEJ, Johansen-berg H, et al. Advances in functional and structural MR image analysis and implementation as FSL. *Neuroimage*. 2004;23:208–219.

35. Fonov VS, Evans AC, McKinstry RC, Almli CR, Collins DL. Unbiased nonlinear average age-appropriate brain templates from birth to adulthood. *Neuroimage*. 2009;47:S102.

36. Hilal S, Sikking E, Amin SM, van Veluwe S, Vrooman H, Cheung CY, et al. Cortical Cerebral Microinfarcts on 3 Tesla Magnetic Resonance Imaging: a Novel Marker of Cerebrovascular Disease. *Neurology*. 2016;P524–P525.

37. Ferro DA, van Veluw SJ, Koek HL, Exalto LG, Biessels GJ, Utrecht Vascular Cognitive Impairment (VCI) study group. Cortical Cerebral Microinfarcts on 3 Tesla MRI in Patients with Vascular Cognitive Impairment. *J. Alzheimer's Dis*. 2017;60:1443–1450.

38. Van Veluw SJ, Charidimou A, Van Der Kouwe AJ, Lauer A, Reijmer YD, Costantino I, et al. Microbleed and microinfarct detection in amyloid angiopathy: A high-resolution MRI-histopathology study. *Brain*. 2016;139:3151–3162.

39. Lauer A, Veluw SJ Van, William CM, Charidimou A, Roongpiboonsopit D, Vashkevich A, et al. Microbleeds on MRI are associated with microinfarcts on autopsy in cerebral amyloid angiopathy. *Neurology*. 2016;87:1488–1492.

40. Wang Z, Veluw SJ Van, Wong A, Liu W, Shi L, Yang J, et al. Risk Factors and Cognitive Relevance of Cortical Cerebral Microinfarcts in Patients With Ischemic Stroke or Transient Ischemic Attack. *Stroke*. 2016;2450–2455.

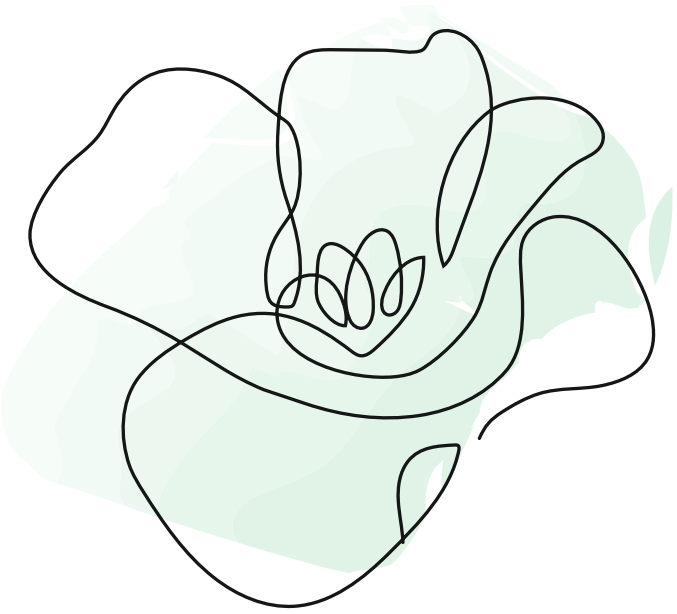

8

Cerebral cortical microinfarcts in patients with internal carotid artery occlusion

Hilde van den Brink*, Doeschka A Ferro*, Jeroen de Bresser, Esther E. Bron, Laurien P. Onkenhout, L Jaap Kappelle, Geert Jan Biessels, Heart-Brain Connection Consortium

*These authors contributed equally

Journal of Cerebral Blood Flow & Metabolism: 2021;41(10):2690-2698

Abstract

Cerebral cortical microinfarcts (CMI) are small ischemic lesions that are associated with cognitive impairment and probably have multiple etiologies. Cerebral hypoperfusion has been proposed as a causal factor. We studied CMI in patients with internal carotid artery (ICA) occlusion, as a model for cerebral hemodynamic compromise. We included 95 patients with a complete ICA occlusion (age 66.2±8.3, 22% female) and 125 reference participants (age 65.5±7.4, 47% female). Participants underwent clinical, neuropsychological, and 3T brain MRI assessment. CMI were more common in patients with an ICA occlusion (54%, median 2, range 1-33) than in the reference group (6%, median 0; range 1-7; OR 14.3; 95% CI 6.2-33.1; p<.001). CMI were more common ipsilateral to the occlusion than in the contralateral hemisphere (median 2 and 0 respectively; p<.001). In patients with CMI compared to patients without CMI, the number of additional occluded or stenosed cervical arteries was higher (p=.038), and cerebral blood flow was lower (B -6.2 ml/min/100ml; 95% CI -12.0:-0.41; p=.036). In conclusion, CMI are common in patients with an ICA occlusion, particularly in the hemisphere of the occluded ICA. CMI burden was related to the severity of cervical arterial compromise, supporting a role of hemodynamics in CMI etiology.

Introduction

Cerebral cortical microinfarcts (CMI) are small ischemic lesions that are a common finding in patients with stroke and dementia.[1,2] CMI can be visualized on brain autopsy and recently also with in vivo high-resolution MRI.[3] Studies have shown associations between CMI and cognitive impairment, emphasizing their clinical relevance.[2]

CMI can have multiple underlying causes that are linked to large vessel disease, small vessel disease or cardiac disease.[2] Hypoperfusion is proposed as a possible underlying mechanism. We recently showed a relation between reduced global brain perfusion and CMI in a memory clinic population.[4] However, because of the heterogeneous nature of the etiology of cerebral pathologies inherent to this population, the question remains if this observed association could be causal, where low perfusion induces CMI, or just reflects shared risk factors.

In the current study we further investigated hypoperfusion as a possible cause for CMI. We studied CMI in patients with an internal carotid artery (ICA) occlusion, as a model for cerebral hemodynamic compromise. An ICA occlusion causes an altered, more vulnerable, hemodynamic brain state. Although only some patients with permanent (i.e. non-acute) ICA occlusion have resting state hypoperfusion, they are clearly at risk of hypoperfusion (temporary cerebral ischemia) in case of temporary drops in perfusion pressure.[5] We studied if CMI occur more often in patients with an ICA occlusion than in a reference group without ICA occlusion. Among patients with a unilateral ICA occlusion, we examined if CMI occurred more often in the ipsilateral hemisphere than in the contralateral hemisphere. Lastly, within the patient group we examined if occurrence of CMI is associated with the severity of collateral steno-occlusive disease, and with lower cerebral blood flow.

Materials and Methods

Study population

Participants took part in the Heart-Brain Connection study, a Dutch multicenter study focusing on cardiovascular and hemodynamic contributions to cognitive impairment.[6] Data collection took place in four university medical centers (UMCs) in The Netherlands (Leiden UMC, Maastricht UMC, Amsterdam UMC and UMC Utrecht). Reference participants were recruited among spouses of patients and through advertising leaflets in the four UMCs.

Generic inclusion criteria for both patients and reference participants in the Heart-Brain Connection study were age of 50 years or older, being independent in daily life and able to undergo cognitive testing and MRI. Exclusion criteria for all participants were a life expectancy of less than three years, current atrial fibrillation, and neurologic or psychiatric disease affecting cognitive performance other than vascular injury or possible co-occurring Alzheimer's disease. Additional criteria applied for patients with an ICA occlusion.

Before inclusion, an ICA occlusion had to be confirmed either with ultrasound, magnetic resonance angiography or computed tomography angiography. Also, patients with an ICA occlusion should not have had a brain infarct or transient ischemic attack in the three months prior to inclusion, and should have no planned carotid surgery or participation in an intervention trial. There were no additional criteria regarding the occlusion being symptomatic or asymptomatic.

For the current study five patients with an ICA occlusion and one reference participant were excluded because brain MRI was not available. In addition, two patients and two reference participants were excluded because of missing MRI sequences and three patients due to insufficient MRI scan quality for the sequences necessary to rate CMI. This resulted in a study population of 95 patients and 125 reference participants.

The Heart-Brain Connection study was approved by the Medical Ethics Review Committee of the Leiden UMC (number P.14.002) and local boards of the other UMCs. The study was conducted in accordance with the declaration of Helsinki and the Medical Research Involving Human Subjects Act (WMO). Written informed consent was obtained from all participants prior to enrolment in the study. The data that support the findings of this study are available from the corresponding author upon reasonable request.

Clinical characteristics

For the patients with an ICA occlusion we recorded the side of the occlusion and whether the ICA occlusion had been symptomatic, which we defined as an ipsilateral transient ischemic attack (TIA) or ischemic stroke. This was based on medical records. Possible occlusions and stenosis in other cervical arteries (i.e. left and right internal carotid arteries and left and right vertebral arteries) were recorded from medical records as well (i.e. duplex ultrasound, computed tomography angiography and/or magnetic resonance angiography).

Demographics and vascular risk factors were recorded for both patients and reference participants. Hypertension was based on presence in medical history. Current office hypertension was defined as a mean systolic tension >140mm/Hg or diastolic tension >90mm/Hg measured during the research day. Hypercholesterolemia was defined as presence in medical history or medication use. Diabetes mellitus was based on medical history. Smoking was defined as current or previous smoking and obesity was defined as a body mass index over 30.

All participants underwent a standardized neuropsychological test battery. Raw test-scores were corrected for age, sex and education relative to the reference group and a mean composite cognitive z-score was calculated for every patient with an ICA occlusion.[6]

MRI protocol and analysis

Brain MRI was acquired at 3T Philips Ingenia, Philips Achieva and Philips Gemini MRI scanners (Philips, Best, the Netherlands). The brain protocol included a 3D T1-weighted image (TR/TE/TI=8.2/4.5/990 ms; shot interval 3000 ms; flip angle 8°; voxel size 1.0x1.0x1.0 mm^3), fluid-attenuated inversion recovery (FLAIR) image (TR/TE/TI=4800/313/1650 ms; TSE factor 182; voxel size 1.11x1.11x1.11 mm^3), susceptibility-weighted image (SWI) (TR/TE=45/31 ms; flip angle 13°; EPI factor 3; voxel size 0.8x0.8x1.6 mm^3) and phase-contrast flow measurement (TR/TE=12/8.2 ms; flip angle 10°; Venc 200 cm/s; untriggered; 10 averages; voxel size 1.17x1.17x5 mm^3).

CMI were rated in the cortex according to previously established criteria for 3T MRI.[2] In short, CMI had to be hypointense lesions on T1-weighted MRI with a corresponding hyper- or isointense signal on FLAIR and SWI, <4 mm in diameter, and located strictly intracortical. Of note, these criteria can currently not be used to identify subcortical CMI.[2] CMI had to be distinct from perivascular spaces and visible in at least two planes (i.e. sagittal, transversal, coronal). Lesions neighboring a larger stroke (i.e. <1 cm in the same gyrus) were excluded.[2] CMI were rated by three experienced raters (HvdB, DF, RvdB) with the use of an in-house developed tool in MeVisLab (MeVis Medical Solutions AG, Bremen, Germany). Raters were blind to the clinical condition of the participants. Interrater agreement was good (interclass correlation = 0.97 in a random subset of 31 scans).

Infarcts, microbleeds, enlarged perivascular spaces and white matter hyperintensities (WMHs) were rated by a neuroradiologist (JdB) according to the STRIVE-criteria.[7] Small vessel disease (SVD) presence was then summed in a previously developed SVD burden score for all patients.[8] Total brain volume, grey matter volume and WMH volume were segmented with an automated pipeline (Quantib brain, Rotterdam, the Netherlands), taking into account manually segmented infarcts and other pathologies. Blood flow in the basilar artery and ICAs was quantified (ml/min) based on phase-contrast flow scans. The arteries were manually contoured using the flow analysis tool of Mass software (Division of Image Processing, Department of Radiology, Leiden University Medical Center, Leiden, the Netherlands). We then calculated total cerebral blood flow by summing blood flow in all arteries, dividing this by the individual's brain volume and multiplying the result by 100 (thus obtaining total blood flow in ml/min/100ml).

Statistics

Differences in baseline characteristics between patients and the reference group were assessed with an independent t-test for age and cerebral blood flow, $\chi 2$ for sex and vascular risk factors, and Mann-Whitney U test for education. Logistic regression was used to determine whether an ICA occlusion (versus reference group) was associated with CMI presence, also when controlling for differences in baseline characteristics between the groups. Total numbers of CMI for patients and the reference group where compared with a Mann-Whitney U test.

Further analyses were only carried out in the group of patients with an ICA occlusion. Differences between patients with and without CMI were assessed with an independent t-test for age and cognition, χ2 for sex, and Mann-Whitney U test for education. CMI count in the ipsilateral and contralateral hemispheres was compared with a Wilcoxon signed rank test. The relation between number of occluded or stenosed cervical arteries and CMI was tested with a Mann Whitney median test and the relation of cerebral blood flow with CMI presence was tested with regression analysis. The relations of risk factors and MRI markers with CMI presence were analyzed with logistic regression for categorical data and Mann-Whitney U test or regression for continuous data. Brain volumes were corrected for age, sex and intracranial volume and white matter hyperintensity volume was log transformed additionally.

Analyses were carried out in SPSS Statistics version 25 with the significance threshold set at $p<.05$.

Results

Comparison between patients with an ICA occlusion and the reference group

ICA occlusion was confirmed for all patients and ruled out for all reference participants on the research MRI scan. The characteristics of patients with an ICA occlusion and participants from the reference group are shown in Table 1. Patients with an ICA occlusion were of similar age as the reference group, but more often male, and lower educated. As expected, the burden of vascular risk factors was higher among patients. Cerebral blood flow was 14% lower in patients with an ICA occlusion (average 47.6 ml/min/100ml; SD 12.8) than in the reference participants (average 55.5 ml/min/100ml; SD 13.6; $p<.001$).

Table 1: Demographics and vascular risk factors of patients and reference group

	ICA occlusion (n=95)	Reference (n=125)	*p*-value
Demographics			
Age (y)	66.2 ± 8.3	65.5 ± 7.4	.552
Sex (female)	21 (22)	59 (47)	<.001
Education (7 levels)	5 [4-6]	6 [5-6]	.010
Vascular risk factors			
Hypertension (medical history)	73 (77)	34 (27)	<.001
Hypertension (office hypertension)[a]	64 (67)	61 (49)	.006
Hypercholesterolemia	87 (92)	38 (30)	<.001
Diabetes	28 (30)	2 (2)	<.001
Smoking	89 (94)	70 (56)	<.001
Obesity	24 (25)	19 (15)	.062

Abbreviations: ICA= internal carotid artery. Data are presented as mean ± SD, median [25th–75th percentile], or number (percentage).

[a] Office hypertension: systolic tension >140mmg/Hg or diastolic tension >90mm/Hg.

CMI were present in 54% of the patients with an ICA occlusion and in 6% of the reference group (crude OR 17.0; 95% CI 7.5-38.6; *p*<.001; OR corrected for sex and education 14.3; 95% CI 6.2-33.1; *p*<.001; additional correction for all defined vascular risk factors OR 6.9; 95% CI 2.4-20.0; *p*<.001). Among the participants with CMI, 69% of the patients and 25% of the reference participants had multiple CMI (range 2-33 and 2-7 respectively). The total number of CMI per participant was significantly higher in patients than in the reference group (*p*<.001).

Analyses within the patient group

The characteristics of patients with an ICA occlusion with CMI and without CMI are shown in Table 2. Only hypertension and hypercholesterolemia were associated with CMI presence in patients.

In patients with an ICA occlusion, 80% had one or more CMI in the hemisphere ipsilateral to the occlusion and 48% had one or more CMI in the contralateral hemisphere. The number of CMI was significantly higher in the hemisphere ipsilateral to the occlusion (median 2, interquartile range 3) than in the contralateral hemisphere (median 0, interquartile range 1) (*p*=.001). Figure 1 shows the 3D distribution of CMI relative to an ICA occlusion. CMI were preferentially located in the cranial part of the frontal and parietal lobes. The vast majority of CMI were located in the perfusion territory of the ICA, with an apparent predilection for watershed areas. The distribution of CMI in the ipsilateral hemisphere was not different from that in the contralateral hemisphere.

Table 2: Demographics and vascular risk factors for patients with and without CMIs

	ICA occlusion CMI present (n=51)	**ICA occlusion CMI absent (n=44)**	**OR [95% CI]**	***p*-value**
Characteristics				
Age (y)	67.1 ± 8.4	65.1 ± 8.3	-	.238
Sex (females)	11 (22)	10 (22)	-	.892
Education (7 levels)	5 [4-6]	5 [5-6]	-	.166
Cognitive function[a]	-0.51 ± 0.69	-0.52 ± 0.58	-	.943
Symptomatic occlusion	42 (82)	39 (89)	0.6 [0.2; 1.9]	.392
Vascular risk factors				
Hypertension (medical history)	45 (88)	28 (64)	4.3 [1.5; 12.2]	.007
Hypertension (office hypertension)[b]	31 (61)	33 (75)	0.5 [0.2; 1.3]	.143
Hypercholesterolemia	50 (98)	37 (84)	9.5 [1.1; 80.2]	.039
Diabetes	18 (35)	10 (23)	1.9 [0.7; 4.6]	.183
Smoking	49 (96)	40 (91)	2.5 [0.4; 14.1]	.315
Obesity	16 (31)	8 (18)	2.1 [0.8; 5.4]	.144

Abbreviations: ICA= internal carotid artery; CMI= cortical microinfarct

Data are presented as mean ± SD, median [25th–75th percentile], or number (percentage).

[a] Cognitive function is measured as a composite z-score, corrected for age, sex, and education.

[b] Office hypertension: systolic tension >140mmg/Hg or diastolic tension >90mm/Hg.

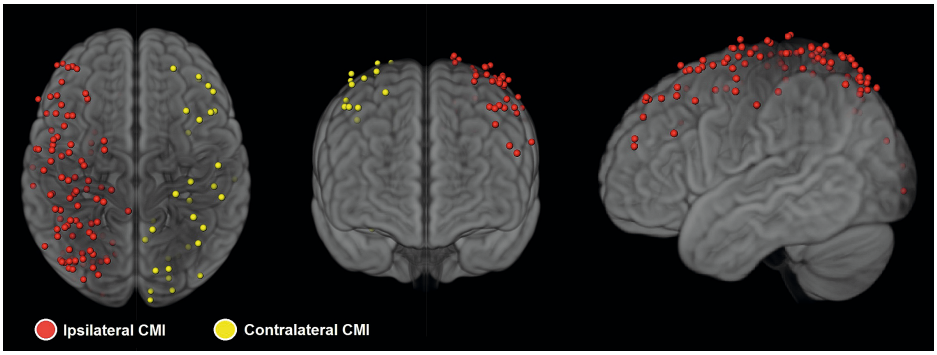

Figure 1: 3D distribution across the cortex on an MNI-standard brain of all CMI in 40 patients with a unilateral ICA occlusion and CMI. For patients with a right ICA occlusion the CMI distribution was flipped to create this image where CMI are presented ipsilateral (red) and contralateral (yellow) to the occlusion. An atlas based representation of the watershed areas is included in blue.[20] CMI burden is higher in the hemisphere ipsilateral to the occlusion (p=.001). From visual inspection CMI appear to have a predilection for watershed areas. This distribution was not evaluated by formal statistical testing, because sensitivity of CMI detection may vary by brain region and because the actual watershed region varies between individuals. Note: for visualization of both the CMI and the watershed areas, the cortex was shrunk and made translucent. This may give the false impression that some CMI were located outside of the brain

By design, all patients had at least one occluded carotid artery. An occlusion of the other carotid was present in 15 (15%) and >50% stenosis in 1 (1%) of the patients. Moreover, an occlusion or >50% stenosis of one or both vertebral arteries was present in 10 (11%) and 19 (20%) respectively. Figure 2 shows that a higher number of occluded or >50% stenosed cervical arteries (i.e. left and right carotid arteries, and left and right vertebral arteries) was associated with CMI presence (*p*=.038). In patients with a unilateral ICA occlusion, decreased cerebral blood flow also related with CMI presence. Total cerebral blood flow was 12% lower in patients with CMI than in patients without CMI (B -6.2 ml/min/100ml; 95% CI -12.0:-0.41; *p*=.036). This was mainly due to lower flow in the contralateral ICA (B -62.3 ml/min; 95% CI -117.5:-7.1; *p*=.028), rather than the basilar artery (B 13.5 ml/min; 95% CI -30.0:56.8; *p*=.54), see Figure 3.

Table 3 shows the relations between CMI presence in patients with an ICA occlusion and other MRI-markers of cerebral small vessel and large vessel disease. Lacunar infarcts and microbleeds were more common among patients with CMI and SVD burden score was positively associated with CMI presence. There were no significant associations between CMI presence and any of the other MRI markers. Also, there was no correlation between large artery infarcts or lacunar infarcts ipsilateral to the ICA occlusion and ipsilateral CMI (τ_b = .13; *p*=.30).

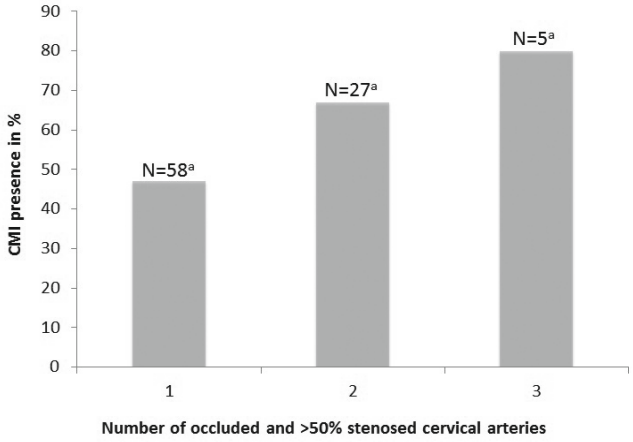

Figure 2: CMI presence in patients with 1-3 occluded or >50% stenosed cervical arteries (i.e. left and right internal carotid arteries and left and right vertebral arteries). None of the patients had occlusions or >50% stenosis in all 4 cervical arteries. [a] Number of patients with 1, 2 or 3 occluded or >50% stenosed cervical arteries. N=90 because of 5 missings.

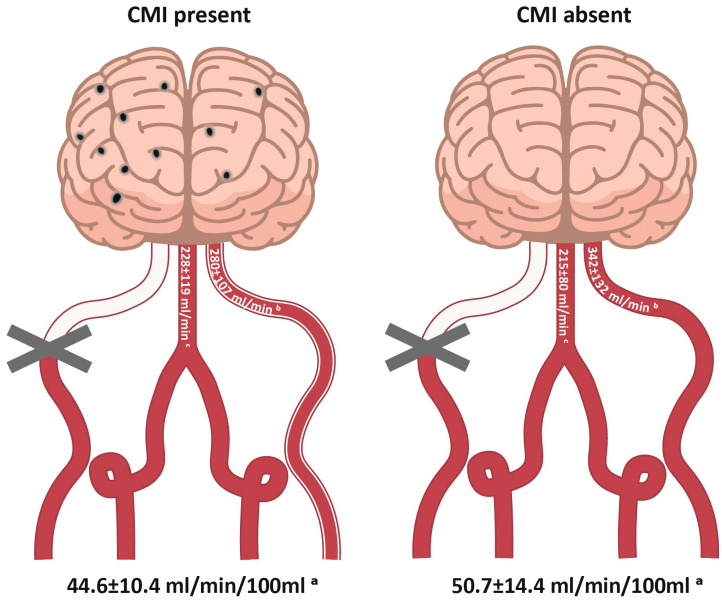

Figure 3: Total cerebral blood flow (mean ± SD, ml/min/100ml) to the brain and blood flow through the non-occluded ICA and basilar artery (mean ± SD, ml/min). [a] Total cerebral blood flow was significantly lower in patients with CMI than in patients without CMI. [b] This difference was attributable to a lower flow in the contralateral ICA [c] not in the basilar artery. N=75 (CMI present N=38, CMI absent N=37) because of 5 missings and because 15 patients were excluded from this analysis due to a double-sided ICA occlusion.

Table 3: Cerebral MRI-markers in patients with and without CMIs

	ICA occlusion CMI present (n=51)	**ICA occlusion CMI absent (n=44)**		***p*-value**
Brain volumes			**B [95% CI]**	
Total brain volume (ml)[a]	1073.4 ± 111.2	1086.8 ± 114.9	-14.2 [-32.0; 3.6]	.12
Total grey matter volume (ml)[a]	639.9 ± 62.9	641.2 ± 67.5	-1.0 [-13.4; 11.4]	.87
CeVD markers			**OR [95% CI]**	
Large artery infarct	38 (75)	31 (71)	1.2 [0.5; 3.0]	.61
Lacunar infarct	34 (67)	19 (43)	2.6 [1.1; 6.1]	.02
Microbleeds	15 (29)	6 (14)	2.6 [0.9; 7.5]	.07
			B [95% CI]	
WMH volume (ml)[ab]	0.69 [0.3-1.0]	0.63 [0.3-1.4]	-0.1[-0.4.; 0.2]	.48
SVD burden score	1 [1-2]	1 [0-1]	-	.03

Abbreviations: ICA= internal carotid artery; CMI= cortical microinfarct; CeVD= cerebrovascular disease; WMH= white matter hyperintensity; SVD burden score= Small vessel disease burden score, ranging between 0 (no SVD) to 4 (severe SVD).
Data are presented as mean ± SD, median [25th–75th percentile], or number (percentage).
[a] Brain volume analyses are corrected for age, sex and intracranial volume; [b] WMH volume was log transformed.

Discussion

CMI are common in patients with an ICA occlusion and occur more frequently in the hemisphere ipsilateral to the occlusion. Within the patient group, the severity of arterial compromise, in terms of number of vessels affected by severe atherosclerosis and blood flow, is related to CMI occurrence, suggesting that hemodynamics indeed play a role in CMI etiology.

To the best of our knowledge this is the first study to examine CMI in patients with a complete ICA occlusion. CMI burden in terms of occurrence and total number is much higher in the patients (54%) than in our reference group and control participants from previous studies (6-12% [9–11]). Earlier studies in patients with ICA stenosis also reported high CMI prevalence. Specifically, CMI prevalence was 26% in a 3T MRI study in patients with a >30% ICA stenosis,[12] and 67% in a 7T MRI study in patients with a >50% ICA stenosis.[13] Of note, the prevalence of this last study is not readily comparable due to higher sensitivity of CMI detection on 7T MRI.[3]

We considered patients with an ICA occlusion as a model for hemodynamic compromise. Accordingly, we hypothesized that CMI would be more common in patients with an ICA occlusion than in the reference group, that CMI would be more common in the

hemisphere ipsilateral than contralateral to the occlusion, and that the severity of cervical arterial compromise among patients with an ICA occlusion (i.e. worse collateral steno-occlusive disease and worse collateral blood supply) would relate to CMI presence. All these hypotheses were supported by the study data, and there appeared to be a higher occurrence of CMI in watershed areas, which seems to support the notion that worse hemodynamics indeed contribute to CMI etiology. The causal pathway that links hypoperfusion to CMI could be direct, with temporary hypoperfusion directly causing small ischemia in the most distal and smallest vessels.[14] Alternatively, hypoperfusion could be associated with washout disturbances in insufficiently perfused arterioles and/or venules which could lead to embolisms that produce CMI.[14,15] Additionally there is evidence for an interaction of hypoperfusion with small vessel disease, specifically cerebral amyloid angiopathy (CAA). A study with a CAA mouse model showed markedly higher CMI burden in CAA mice that were subjected to chronic hypoperfusion than in CAA mice with normal brain perfusion.[16] Yet, additional explanations for the high CMI occurrence in our patient population with high vascular burden need to be considered. Vascular risk factors could contribute to CMI, since we found a relation of CMI presence with hypertension and hypercholesterolemia. However, vascular risk factors cannot explain all our findings, particularly not the within patient between hemisphere differences in CMI occurrence. Moreover, patients with an ICA occlusion are strongly affected by large vessel disease which could give rise to microemboli through different mechanisms. Microemboli could for example have originated from large thrombi that caused ischemic stroke. Of note, we excluded CMI that were located in tissue directly adjacent to large artery infarcts. We did not find that CMI occurred more often in patients that had been symptomatic (versus asymptomatic) and we did not find a relation of CMI with large artery infarcts on MRI, but microemboli could also have originated from pre-occlusive stenosis in earlier disease stages. Indeed it has previously been reported that CMI are related with vulnerable ICA plaques.[12] Yet, this possible mechanism cannot explain that *current* cerebral blood flow was lower in patients with CMI compared to patients without CMI. We encourage future research to study acute CMI on diffusion weighted imaging in clinically stable patients with an ICA occlusion. If acute CMI would be observed in the hemisphere of the occluded ICA, this would provide further support for hemodynamics as cause of CMI.

The findings of this study may be of clinical relevance to patients with an ICA occlusion, or patients that are in other ways vulnerable to hemodynamic compromise. In other settings, acute CMI have been associated with increased risk of poor clinical outcome after two years,[17] and with (vascular) cognitive impairment.[2] Since patients with an ICA occlusion are known to be at risk of cognitive impairment,[18] the prognostic relevance of CMI in this setting should be topic of future research. Moreover, CMI might be a marker of future stroke risk, even in patients with apparently stable ICA occlusion, but this should be explored in longitudinal studies.

An important strength of this study is the relatively large sample size of patients with an ICA occlusion that were examined in a stable disease phase. Also, due to the high CMI occurrence in the cohort, we had enough power to investigate the relation of CMI with vascular risk factors and measures of collateral compromise. A limitation of our study is that we cannot exclude microemboli from large vessel disease as (partly) cause of CMI in our cohort. We therefore encourage future research to study acute CMI in patients with a clinically stable ICA occlusion. Another limitation of our study is that we studied CMI with 3T MRI which can only image the largest CMI. Therefore we may have missed smaller CMI that might have a different distribution and pathophysiology. Lastly, we did not measure perfusion at tissue level, but used a measure derived from the main feeding arteries of the brain. We preferred this approach over arterial spin labeling (ASL), because transit time effects in patients with arterial occlusive disease is a well-known source of quantification errors in ASL.[19] Yet, a limitation of our method is that we cannot provide local measures of cortical perfusion and for the analysis presented in figure 3 we cannot take possible collateral flow through the external carotid artery into account.

In conclusion, in this study we explored hypoperfusion as possible cause for CMI, in patients with an ICA occlusion as a model condition of hemodynamic compromise. We found that CMI are common in patients with an ICA occlusion, even more so in the hemisphere of the occluded ICA. Moreover, CMI presence related with the severity of cervical arterial compromise. These findings support a role for hemodynamics in the pathophysiology of CMI.

Acknowledgements

We want to acknowledge Roos van den Berg for assistance in microinfarct ratings. We acknowledge the contribution of Heart-Brain Study researchers and employees.

References

1. Smith EE, Schneider JA, Wardlaw JM, et al. Cerebral microinfarcts: the invisible lesions. *Lancet Neurol*. 2012;11:272-282.
2. van Veluw SJ, Shih AY, Smith EE, et al. Detection, risk factors, and functional consequences of cerebral microinfarcts. *Lancet Neurol*. 2017;16:730-740.
3. van Veluw SJ, Zwanenburg JJM, Engelen-Lee J, et al. In vivo detection of cerebral cortical microinfarcts with high-resolution 7T MRI. *J Cereb blood flow Metab*. 2013;33:322-329.
4. Ferro DA, Mutsaerts HJJM, Hilal S, et al. Cortical microinfarcts in memory clinic patients are associated with reduced cerebral perfusion. *J Cereb Blood Flow Metab*. 2020;40:1869-1878.
5. Klijn CJM, Kappelle LJ. Haemodynamic stroke: clinical features, prognosis, and management. *Lancet Neurol*. 2010;9:1008-1017.
6. Hooghiemstra AM, Bertens AS, Leeuwis AR, et al. The missing link in the pathophysiology of vascular cognitive impairment : Design of the Heart-Brain Study. *Cereb Cortex*. 2017;7:140-152.
7. Wardlaw JM, Smith EE, Biessels GJ, et al. Neuroimaging standards for research into small vessel disease and its contribution to ageing and neurodegeneration. *Lancet Neurol*. 2013;12:822-838.
8. Staals J, Makin SDJ, Doubal FN, et al. Stroke subtype, vascular risk factors, and total MRI brain small-vessel disease burden. *Neurology*. 2014;83:1228-1235.
9. Ferro DA, van Veluw SJ, Koek HL, et al. Cortical cerebral microinfarcts on 3 Tesla MRI in patients with vascular cognitive impairment. *J Alzheimer's Dis*. 2017;60:1443-1450.
10. Hilal S, Sikking E, Amin SM, et al. Cortical cerebral microinfarcts on 3 Tesla Magnetic Resonance Imaging: a novel marker of cerebrovascular disease. *Neurology*. 2016;87:1583-1590.
11. van den Brink H, Zwiers A, Switzer AR, et al. Cortical microinfarcts on 3T Magnetic Resonance Imaging in cerebral amyloid angiopathy. *Stroke*. 2018;49:1899-1905.
12. Takasugi J, Miwa K, Watanabe Y, et al. Cortical cerebral microinfarcts on 3T Magnetic Resonance Imaging in patients with carotid artery stenosis. *Stroke*. 2019;50:1-6.
13. Rotte AAJ De, Koning W, Den Hartog AG, et al. 7.0 T MRI detection of cerebral microinfarcts in patients with a symptomatic high-grade carotid artery stenosis. *J Cereb Blood Flow Metab*. 2014;34:1715-1719.
14. Caplan LR, Wong S, Hennerici MG. Is hypoperfusion an important cause of strokes? If so, how? *Cerebrovasc Dis*. 2006;21:145-153.
15. Hartmann DA, Hyacinth HI, Liao FF, et al. Does pathology of small venules contribute to cerebral microinfarcts and dementia? *J Neurochem*. 2018;144:517-526.
16. Okamoto Y, Yamamoto T, Kalaria RN, et al. Cerebral hypoperfusion accelerates cerebral amyloid angiopathy and promotes cortical microinfarcts. *Acta Neuropathol*. 2012;123:381-394.
17. Ferro DA, van den Brink H, Exalto LG, et al. Clinical relevance of acute cerebral microinfarcts in vascular cognitive impairment. *Neurology*. 2019;92:1558-1566.
18. Oudeman EA, Kappelle LJ, Van den Berg-vos RM et al. Cognitive functioning in patients with carotid artery occlusion; a systematic review. *J Neurol Sci*. 2018;394:132-137.
19. Alsop DC, Detre JA, Golay X, et al. Recommended implementation of ASL perfusion MRI for clinical applications: a consensus of the ISMRM perfusion study group and the European consortium for ASL in dementia. *Magn Reson Med*. 2015;73:102-116.

20. Hartkamp NS, Petersen ET, Chappell MA, et al. Relationship between haemodynamic impairment and collateral blood flow in carotid artery disease. *J Cereb Blood Flow Metab*. 2018;38:2021-2032.

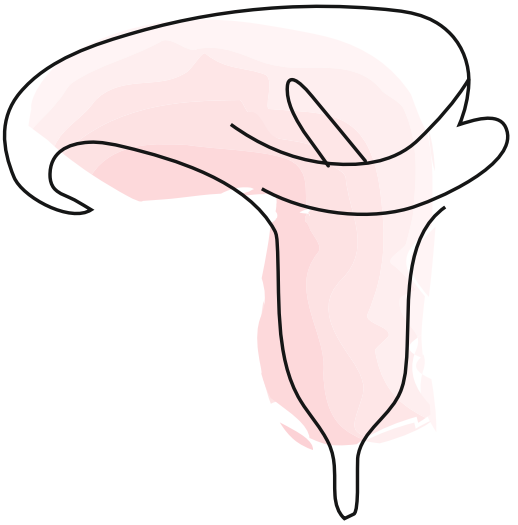

9

Clinical relevance of acute cerebral microinfarcts in vascular cognitive impairment

Doeschka A. Ferro*, **Hilde van den Brink***, Lieza G. Exalto, Jooske M.F. Boomsma, Frederik Barkhof MD, Niels D. Prins, Wiesje M van der Flier Geert Jan Biessels, on behalf of the TRACE-VCI study group.

* these authors contributed equally

Neurology: 2019;92(14):e1558-e1566

Abstract

Objective

To determine the occurrence of acute cerebral microinfarcts (ACMIs) in memory clinic patients and relate their presence to vascular risk and cognitive profile, CSF and neuroimaging markers, and clinical outcome.

Methods

The TRACE-VCI study is a memory clinic cohort of patients with vascular brain injury on MRI (i.e. possible vascular cognitive impairment (VCI)). We included 783 patients (mean age 67.6 ±8.5, 46% female) with available 3 tesla diffusion-weighted imaging (DWI). ACMIs were defined as supratentorial DWI hyperintensities <5mm with a corresponding hypo/isointense ADC signal and iso/hyperintense T2*-weighted signal.

Results

23 ACMIs were found in 16 of the 783 patients (2.0%). Patients with ACMIs did not differ in vascular risk or cognitive profile, but were more often diagnosed with vascular dementia (odds ratio (OR) 5.1; 95% CI 1.4-18.9, *p*=.014). ACMI presence was associated with lower levels of amyloid beta (*p*<.004) and with vascular imaging markers (lacunar infarcts; OR 3.5; 1.3-9.6, *p*=.015, non-lacunar infarcts; OR 4.1; 1.4-12.5, *p*=.012, severe white matter hyperintensities; OR 4.8; 1.7-13.8, *p*=.004, microbleeds; OR 18.9; 2.5-144.0, *p*=.0001). After a median follow up of 2.1 years, the risk of poor clinical outcome (composite of marked cognitive decline, major vascular event, death and institutionalization) was increased among patients with ACMIs (HR 3.0; 1.4-6.0, *p*=.005).

Conclusion

In patients with possible VCI, ACMI presence was associated with a high burden of cerebrovascular disease of both small and large vessel etiology and poor clinical outcome. ACMIs may thus be a novel marker of *active* vascular brain injury in these patients.

Introduction

Cerebral microinfarcts are small ischemic lesions that are increasingly recognized as an important contributor to cognitive decline and dementia.[1] Until recently microinfarcts were only considered to be detectable on brain autopsy, but they can now be visualized in vivo on MRI.[2,3] *Acute cerebral microinfarcts* (ACMIs) are detectable on diffusion-weighted MRI (DWI) for up to two weeks after their onset[1]. Despite this narrow window, ACMI detection provides valuable information on microinfarct occurrence and may help identify individuals at risk for ongoing vascular brain injury.

ACMIs, previously referred to as small DWI hyperintense lesions, have been reported in patients with cerebral amyloid angiopathy (CAA),[4,5] hemorrhagic stroke[6–11] and memory clinic patients.[12,13] These studies -with modest sample sizes- demonstrated an association between ACMIs and other small vessel disease (SVD) imaging markers, but not a link with a specific vascular risk profile. The relation with CSF biomarkers has not yet been investigated, despite the known association between microinfarcts and CAA. Studies assessing the correlation between ACMIs and cognitive performance have yielded inconclusive results.[12,13]

Follow up studies of patients with acute hemorrhagic stroke found that ACMIs were associated with increased disability after 3 months[8,14] and stroke and vascular death after 3 years.[7] However, no studies have focused on the long-term cognitive consequences of ACMIs.

This study investigated the occurrence of ACMIs in a memory clinic cohort with possible vascular cognitive impairment (VCI) and their association with vascular risk and cognitive profile, CSF and neuroimaging markers and clinical outcome.

Methods

Population

This study involved patients from the TRACE-VCI study, an observational prospective cohort study of 861 consecutive memory clinic patients with vascular brain injury on MRI (i.e. possible VCI).[15] Patients were included from VU Medical Center (n=665) and the University Medical Center Utrecht (n=196) between September 2009 and December 2013. All patients had evidence of vascular brain injury on MRI, operationalized as the presence of at least one of the following neuroimaging markers (note that multiple criteria could apply to a single patient): a) white matter hyperintensities (WMH) Fazekas scale grade ≥2 (46% of included patients)[16] b) Fazekas scale 1 and two vascular risk factors (e.g. hypertension, diabetes etc) (36%) c) ≥1 lacunar infarcts (22%) d) ≥1 non-lacunar infarct (10%) e) ≥1 cerebral microbleed (43%) f) ≥1 intracerebral hemorrhage (2%). Presence of co-existing neurodegenerative disorders (such as Alzheimer dementia) was accepted in line

with earlier proposed VCI criteria.[17] Patients with primary non-vascular/non-degenerative causes of cognitive dysfunction (such as traumatic brain injury, inflammatory disease and brain tumors), psychiatric disease (other than depression) and patients with monogenetic (non-) vascular causes were excluded from the cohort. Extensive details on the inclusion and exclusion criteria of the cohort have been previously published.[15] For the present study only the patients with available DWI and ADC sequences on 3.0 Tesla MRI were selected (n=788). A further 4 patients were excluded due to insufficient scan quality and one patient because revision of the MRI revealed a tectum glioma. This resulted in a study population of 783 patients. All study patients underwent a standardized, one-day assessment, including clinical interview, physical examination, neuropsychological testing and MRI.

Standard protocol approvals, registrations and patient consents

All study patients provided written informed consent prior to research related procedures. Ethical approval was granted by the institutional review board of the two hospitals. The study was conducted in adherence to the Declaration of Helsinki.

Vascular risk factors

Hypertension was defined as a blood pressure above 140/90 mmHg, use of antihypertensive medication or reported in medical history. *Hypercholesterolemia* was identified based on medical history or use of cholesterol lowering medication. *Diabetes mellitus* was identified based on medical history or use of appropriate medication. *Obesity* was defined as a body mass index (BMI) ≥ 30, calculated as weight in kilograms divided by height in meters squared. *History of stroke* was based on a history of clinical hemorrhagic or ischemic stroke. *History of atrial fibrillation* was based on a history of paroxysmal and permanent atrial fibrillation and *history of ischemic cardiac disease* was based on a history of myocardial infarction, surgery, or endovascular treatment for coronary artery disease.

Level of cognitive impairment and clinical diagnosis

Patients were divided in three levels of cognitive impairment; *Dementia* was diagnosed if there was a deficit in two or more cognitive domains at neuropsychological testing and interference with daily living. Further etiological diagnoses of dementia were made based on internationally established diagnostic criteria (without knowledge of CFS biomarkers) into *vascular dementia*,[18] *Alzheimer's disease (AD),*[19] other neurodegenerative (e.g. Lewy body, frontotemporal dementia) or unknown origin. *Mild cognitive impairment* (MCI) was defined as complaints or deterioration from prior functioning and objective impairment in at least one cognitive domain, with no or mild impairment of activities in daily living. Patients with complaints but without objective cognitive impairment on neuropsychological testing were classified as "*No objective cognitive impairment*" (NOCI).

Neuropsychological assessment and level of education

The education level of patients was rated according to the 7-point Verhage criteria.[20] The Clinical Dementia Rating (CDR; 0-3) was used to assess the severity of cognitive symptoms and associated functional deficits.[21] A Dutch version of the mini-mental state examination (MMSE) was used as a measure of global cognitive performance.[22] An extensive neuropsychological test battery was carried out covering the following domains: *working memory*, *memory*, *attention and executive functioning*, *perception and construction* and *processing speed*. Detailed information on the tests comprising these cognitive domains has been previously reported.[15] Domain scores per patient were created by averaging individual z-scores per subtest and then standardized again into z-scores.

MRI acquisition and neuroimaging markers

All participants underwent an elaborate brain MRI protocol that included at least 3D T1, 2D T2 and T2*-weighted/susceptibility-weighted and fluid-attenuated inversion recovery (FLAIR) sequences, as well as DWI and ADC. Details on the MRI sequence parameters were previously published.[15] Brain volumetric measurements were carried out using automated segmentation using Computational Anatomy Toolbox - CAT12.[23] The automated CAT 12 segmentations for *total brain, grey and WMH volume* were subsequently corrected for by hand segmentation of stroke lesion volume (e.g. lacunes, non-lacunar infarcts, hemorrhages). Neuroimaging markers were analyzed by visual inspection. Microbleeds, lacunar and non-lacunar infarcts were rated according to the STRIVE criteria,[24] WHM were rated according to the modified Fazekas scale[16] and medial temporal lobe atrophy (MTA) according to the Scheltens scale (scores for both hemispheres averaged).[25]

ACMI rating

ACMIs were rated in accordance with criteria proposed by a group of international collaborators[1] as hyperintense lesions on DWI <5mm along the longest diameter with a corresponding hypo- or isointense signal on ADC and hyper- or isointense signal on T2*-weighted image. Following these criteria ACMIs within the first week (hyperintens DWI; ADC hypointensity) and thereafter up to approximately two weeks (hyperintens DWI; isointense ADC) were detected.[26] An example of two ACMIs is displayed in Figure 1. ACMI screening procedure started with assessment of the DWI sequence of the supratentorial brain in the axial followed by the sagittal plane. In case a hyperintense DWI lesion was found, ADC and T2*-weighted images were examined as well to confirm the finding. The total number of ACMIs per patient, as well as size and location was recorded. Location was classified as either cortical, subcortical white matter or deep grey matter (basal ganglia, thalamus). All scans were rated using MeVisLab (MeVis medical solutions, Bremen, Germany) by one trained rater (H.B.) blinded to the clinical condition of the patient. There was a good intrarater agreement (test set 50 scans; k =.85; Dice's similarity index (DSC) =.86) and interrater agreement (test set 50 scans; k =.83; DSC=.80 to a second trained rater (D.F.)).

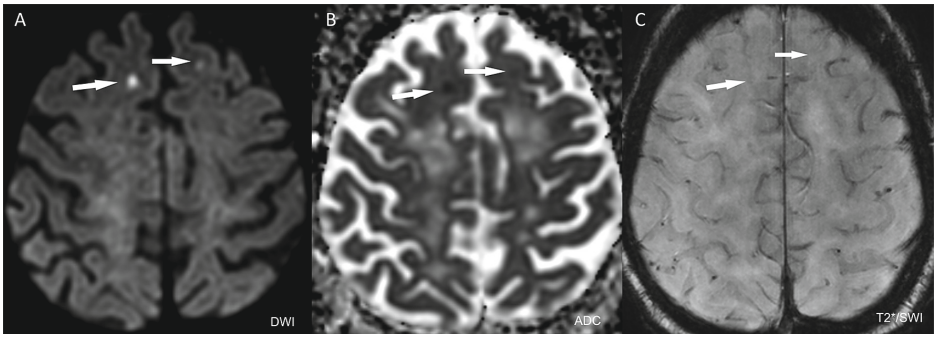

Figure 1: Example of two ACMIs in a single patient. Two ACMIs (arrows left and right frontal lobe) in one patient. (A) There is a hyperintens signal on DWI, (B) corresponding hypointens signal on ADC and (C) isointens (i.e. not distinctly visible) signal on T2*-weighted image (right).

CSF biomarkers

Lumbar puncture to collect CSF was carried out in a subset of the patients at the physician's and patient's discretion. CSF concentrations of amyloid beta 1-42 (Aβ) (n=499), tau (Tau) and total tau phosphorylated at threonine 181 (p-Tau) (n=492) were determined.[27]

Follow up data

Follow up data was collected approximately 2 years after baseline inclusion. According to the predefined TRACE-VCI protocol, only patients with a MMSE score≥20 or a CDR≤1 at baseline were eligible for follow up (n=648; i.e. 83% baseline population). Data was collected from patients and care-givers during a visit at the outpatient clinic. Patients who were not able to attend the clinic where contacted by phone. If patients or relatives could not be reached, the general practitioner or doctor of the nursing home was contacted, but only if patients had provided informed consent at baseline visit. 14 Patients were lost to follow up and 5 patients had withdrawn their consent, resulting in a follow up population of 629 patients. Information was collected regarding death (including vascular cause), stroke, cardiovascular events and institutionalization (due to either somatic or cognitive decline). Cognitive symptoms were rated using the CDR.[21] *Poor clinical outcome* was defined as a composite of (1) marked cognitive decline (operationalized as change in CDR of ≥1 and/or institutionalization due to cognitive dysfunction, (2) occurrence of a major vascular event (stroke (TIA excluded) or myocardial infarctions), (3) death and (4) institutionalization due to reasons other than cognitive decline.

Statistical analysis

Differences between patients with and without ACMIs were analyzed with independent T-tests for normally distributed data (age, log transformed CSF biomarkers), χ-square test for categorical data (sex, vascular risk factors) and Mann-Whitney U tests for non-normally distributed continuous data (education, CDR, microbleed count, MTA). Binary logistic regression was used to analyze the odds (with 95% confidence interval) of ACMI

presence given the clinical diagnosis (odds ratio (OR) reflects "severity steps" in clinical diagnosis) and presence of imaging markers. Linear regression was used to analyze the association between ACMI presence and cognitive functions (adjusted for age, sex and education) and brain volumetrics (adjusted for intracranial volume).

Follow up data was analyzed using Cox proportional hazard model, to assess the risk of ACMI presence on the time to event for the composite *poor clinical outcome*, and separately for each component (death, stroke, cardiovascular events and institutionalization). Results are presented with and without adjustment for age, sex and level of cognitive impairment and also for other vascular imaging markers. *Change in CDR* was analyzed using a Mann-Whitney U test. IBM SPSS statistics (version 22) was used for data analysis, a p-value < .05 was considered significant.

Data availability statement
Any data on the TRACE-VCI cohort used in these analyses that is not published within this article is available by request from any qualified investigator.

Results

ACMI occurrence in the cohort
A total of 23 ACMIs was found in 16 of the 783 patients (2%). Another 6 larger DWI positive lesions were found, but disregarded due to size (between 6-10mm). Thirteen patients had a single ACMI and 3 patients had multiple ACMIs (range 2-5). The majority of the ACMIs was located in the subcortical white matter (n= 16, 70%), 4 ACMIs (17%) were located in the cortical grey matter and 3 ACMIs (13%) were located in the deep grey matter.

Demographics and vascular risk factors in patients with and without ACMIs
The mean age of patients in the study population was 67.6 (SD 8.5) years and 46% was female. No differences in demographics or vascular risk factors were observed between patients with ACMIs compared to patients without ACMIs (Table 1).

Table 1: Demographics and vascular risk factors in patients with and without ACMIs

	No ACMI (n = 767)	**ACMI Present (n=16)**	***p***
Demographics			
Age (y)	67.5 ±8.5	69.4 ±9.6	.386
Sex (female)	352 (46)	6 (38)	.505
Education	5 [1-7]	4.5 [2-7]	.310
Vascular risk factors			
Hypertension	646 (84)	14 (88)	.722
Hypercholesterolemia	342 (45)	6 (38)	.573
Diabetes mellitus	139 (18)	2 (13)	.565
Current smoking (n=775)	156 (21)	2 (13)	.435
Obesity (n=773)	158 (21)	3 (19)	.836
History of reported stroke	68 (9)	3 (19)	.186
History of ischemic heart disease	55 (7)	1 (6)	.862
Atrial fibrillation (n=777)	31 (4)	1 (6)	.667

Abbreviations: ACMI=Acute cerebral microinfarct. Data presented as group mean ±SD, n (%) and median [range]. All comparisons between groups with and without ACMIs were performed with a χ-square test, except age (T-test) and education (Mann-Whitney U).

Cognitive performance in patients with and without ACMIs

Patients with and without ACMIs did not differ with respect to clinical diagnosis, severity of cognitive impairment or cognitive profile (i.e. scores on the five domains) (Table 2). However, patients with ACMIs were more likely to have received the etiological diagnosis vascular dementia (4% ACMI absent vs 8% in the ACMI present, OR 5.1 [1.4-18.9], *p*=.014), but not Alzheimer's disease (35% ACMI absent vs 25% ACMI present, OR 0.6 [.2-2.0], *p*=.418).

Table 2: Clinical diagnosis and cognitive performance in patients with and without ACMIs.

	No ACMI (n=767)	**ACMI Present (n=16)**	**OR (95% CI)**	***p***
Clinical diagnosis			1.2 [.61-2.18]	.450
NOCI	178 (23)	2 (13)		
MCI	195 (25)	6 (38)		
Dementia	394 (51)	8 (50)		
Cognitive functions			**Mean estimated differences [95% CI]**	
CDR	0.5 [0-3]	0.5 [0-2]		.542
MMSE (n=779)	24.3 ±4.8	25.1 ±4.9	-1.12 [-3.46; 1.21]	.346
Memory (n=778)	.002 ±1.006	-.077 ±.676	-.08 [-.57; .40]	.733
Working memory (n=761)	.004 ±1.002	-.189 ±.899	.12 [-.35; .58]	.627
Processing speed (n=761)	.000 ±1.008	-.020 ±472	.13 [-.62; .35]	.588
AEF (n=771)	.005 ±1.002	-.264 ±.885	.14 [-.35; .64]	.568
PC (n=645)	-.002 ±1.004	.105 ±.807	-.17 [-.70; .36]	.521

Abbreviations: ACMI=Acute cerebral microinfarct; OR=odds ratio; NOCI=No objective cognitive impairment; MCI=mild cognitive impairment; CDR=Clinical Dementia Rating; AEF=attention and executive functioning; PC=perception and construction.
Data are presented as mean ±SD, n (%) or median [range]. Statistical testing. Clinical diagnosis: Logistic regression with the odds of ACMI presence given diagnosis (odds ratio reflects "severity steps" in clinical diagnosis). Cognitive functions: Linear regression with estimated mean differences adjusted for age and sex of groups with and without ACMIs. CDR compared between group with and without ACMIs with Mann-Whitney U.

Neuroimaging markers in patients with and without ACMIs

The presence of ACMIs was associated with WMH (both WMH volume and presence of Fazekas score 3), presence of lacunar and non-lacunar infarcts and microbleeds (all $p<.05$, Table 2). In patients with ACMIs compared to those without ACMIs, microbleeds were present both in a higher proportion of cases and in larger numbers per case (both $p=.0001$). Moreover the spatial distribution of microbleeds was different in patients with ACMIs, with relatively more microbleeds in deep and mixed (i.e. both deep and lobar) locations than in patients without ACMIs (both $p<.05$). No association was found between ACMIs and total brain volume, grey matter volume or MTA (Table 2). Regarding the CSF biomarkers, the presence of ACMIs was associated with a lower level of CSF Aβ ($p=.011$), with marginally higher levels of Tau or p-Tau ($p=.065$ and $p=.062$, respectively, Table 3).

Table 3: Neuroimaging and CSF biomarkers patients with and without ACMIs

	No ACMI (n = 767)	**ACMI Present (n=16)**	**Mean estimated difference [95% CI]**	***p***
Brain volumetrics				
Total brain volume (ml) (n=768)	1034 ±116	1031 ±100	8.9 [-23.8; 41.6]	.592
Total grey matter volume (ml) (n=768)	565 ±76	557 ±60	10.0 [-23.3; 43.2]	.557
WMH volume (ml) (n=768)	11.8 ±15.3	30.0 ±27.5	na*	.0001
Imaging markers			**OR [95% CI]**	
WMH (Fazekas 3)	88 (12)	6 (38)	4.8 [1.7; 13.8]	.004
Non-lacunar infarcts	71 (9)	5 (31)	4.1 [1.4; 12.5]	.012
Lacunar infarcts	163 (21)	8 (50)	3.5 [1.3; 9.6]	.015
Microbleeds number (n=776)	0 [0-500]	12 [0-200]		.0001
All microbleed presence (n=776)	330 (43)	15 (94)	18.9 [2.5; 144.0]	.005
Strictly lobar	214 (65)	6 (40)	1.5 [.5 ;4.1]	.467
Strictly deep	42 (13)	3 (20)	3.9 [1.1; 14.3]	.040
Mixed	73 (22)	6 (40)	5.5 [2.0; 15.7]	.001
MTA (n=758)	1 [0-4]	1 [0-2.5]		.928
CSF biomarkers				
Aβ ng/L (n=499)	721.3 ±303.2	470.8 ±174.3	na*	.011
Tau ng/L (n=492)	471.4 ±329.5	715.6 ±445.3	na*	.065
p-Tau ng/L (n=492)	63.7 ±34.1	96.6 ±69.1	na*	.062

Abbreviations: ACMI=Acute cerebral microinfarct; OR=odds ratio; WMH=White matter hyperintensities; MTA =medial temporal lobe atrophy; Aβ= amyloid beta; p-Tau=phosphorylated tau. Data are presented as group mean ±SD, n (%) and median [range]. Statistical testing: Brain volumetrics and CSF biomarkers: Lineair regression between group with and without ACMIs. * WMH volume and CSF biomarkers log transformed. Imaging markers: Logistic regression with the odds of the imaging marker given ACMI presence. MTA and Microbleed number analyzed with Mann-Whitney U test.

Follow up

Follow up data was obtained from 629 of 648 eligible (97%) patients (n=615 (97%) of patients without ACMIs; n=14 (100%) from patients with ACMIs) after a median follow up of 2.1 years [range 0.2-3.0]. Patients with ACMIs had a higher risk of *poor clinical outcome*, also after adjusting for age, sex and cognitive impairment at baseline and additionally for vascular imaging markers (Table 4, all *p<.02).* ACMI presence also increased the risk of stroke (mainly driven by the occurrence of ischemic stroke) and institutionalization (both *p*<.01, also in fully adjusted models) but not death (Table 4). The increase in CDR at follow up (i.e. more cognitive symptoms) tended to be higher for patients with ACMIs at baseline, (*p*=.128, Table 4).

Table 4: Events during follow up for patients with and without ACMIs

	ACMI absent (n=615)	ACMI present (n=14)	Model 1 HR [95% CI]	*p*	Model 2 HR [95% CI]	*p*	Model 3 HR [95% CI]	*p*
Poor clinical outcome*	148 (24)	7 (50)	3.0 [1.4-6.0]	.005	2.8 [1.3-6.0]	.010	2.6 [1.2-5.8]	.017
Death (n=629)	58 (9)	2 (14)	1.9 [.5-7.7]	.379	1.5 [.4-6.1]	.600	1.1 [.3-4.8]	.879
Stroke (n=612)	16 (3)	3 (21)	9.3 [2.7-31.9]	.0001	6.6 [1.8-23.5]	.004	7.5 [1.8-31.3]	.006
Ischemic	14 (2)	3 (21)						
Hemorrhage	2 (.3)	0						
Cardiovasc event (n=599)	12 (2)	0		(..)		(..)		(..)
Institutionalization (n=609)	51 (9)	4 (29)	3.9 [1.4-10.8]	.009	4.9 [1.7-14.2]	.003	3.6 [1.2-10.6]	.019
Due to cognitive decline	34 (6)	3 (21)						
Change CDR* (n=535)	0 [-1 ;2]	.5 [0 ;2]		.128				

Abbreviations: ACMI=Acute cerebral microinfarct; OR=odds ratio; CDR=Clinical Dementia Rating. *Poor clinical outcome defined as cognitive decline, major vascular events (including stroke), death or institutionalization. Data are presented as n (%) and median [range]. (..) insufficient data to perform statistical analysis. HR was calculated with Cox proportional hazard model. Model 1: unadjusted; Model 2: adjusted for age, sex and level of cognitive impairment at baseline; Model 3: adjusted for vascular imaging markers at baseline (presence of Fazekas 3, microbleeds lacunar and non-lacunar infarcts). Change in CDR was analyzed with a Mann-Whitney U test.

Discussion

In this large cohort of memory clinic patients with possible VCI, ACMIs were detected in 2% of patients and located predominantly in the subcortical white matter. The presence of ACMIs was associated with a high burden of both small and large vessel disease on MRI and the diagnosis of vascular dementia. Moreover, patients who presented with ACMIs at baseline had 3-fold increased risk of poor clinical outcome after two years.

This study extends an emerging literature from previous studies, few of them in a memory clinic setting, on the occurrence and clinical correlates of ACMIs. ACMI occurrence was in agreement with previously smaller studies assessing ACMIs in a memory clinic setting (incidences 3-4%),[12,13],whereas higher occurrence rates have been described in patients with CAA (15-35%)[4,5] and hemorrhagic stroke (12-44%).[6–10] In contrast, in a population based cohort of elderly persons ACMIs were more rare (0-0.3%).[28] Of note, even low occurrence rates of ACMIs may reflect substantial disease burden. A mathematical model, which considered the limited spatial and temporal resolution of ACMI detection on DWI, estimated that detecting one ACMI suggests an annual incidence of several hundreds of microinfarcts.[13] Thus in contrast to chronic microinfarcts that represent cumulative damage over time, ACMIs provide a measure of very recent and thus “active” vascular brain injury that may predict further vascular injury.

We found an association between ACMIs and CSF biomarkers. Previously, elevated CSF tau without changes in Aß, has been observed for months after acute clinical ischemic stroke.[29] Yet, given the tiny volume of the affected tissue in ACMI, we expect that the currently observed CSF changes more likely reflect the underlying pathology of ACMIs rather than the tissue injury due to the ACMIs themselves. The reduced – i.e. more abnormal - CSF Aβ levels in patients with ACMIs, may thus suggest a relation with more widespread CAA or other AD pathology.[30] A link with prototypical AD pathologies – i.e. plaques and tangles - appears less likely, as no association was found between ACMIs and the clinical diagnosis AD and the CSF biomarkers pattern was not typical for AD. The CSF pattern we found, with reduced Aβ and slightly elevated Tau and p-Tau, has recently been reported in a meta-analysis of patients with clinically diagnosed CAA.[31] In CAA primarily Aβ 40, but Aβ 42 also to a lesser extent, accumulates in the walls of leptomeningeal and cortical vessels and leads to structural vessel wall changes.[32] These CAA-laden vessels cause both hemorrhagic and ischemic stroke, including lobar microbleeds and microinfarcts.[33] Paradoxically, we found that ACMIs were associated specifically with deep and mixed microbleeds, rather than lobar microbleeds which are considered to be CAA-related. Also, the question arises how CAA, which predominantly occurs in leptomeningeal and cortical vessels, can be linked to the preferential subcortical localization of ACMIs. A further challenge to the interpretation of the CSF pattern is that different underlying pathologies frequently coexist. How these pathologies interact and contribute biomarker profile certainly warrants further investigation.

No relationship was established between ACMI presence and conventional vascular risk factors, which has been a relatively common finding throughout ACMI literature.[1] The observed association of ACMIs with imaging markers of both SVD (i.e. microbleeds, lacunar infarcts and WMHs) and large vessel disease (i.e. non-lacunar infarcts) is also in line with currently evolving literature on MRI detected microinfarcts.[1] A remarkably strong relationship was observed between ACMIs and microbleeds, which appeared both in higher numbers and relatively more often in deep and mixed locations. These locations suggest that multiple etiologies contribute to ACMIs, as occurrence of deep microbleeds is considered to be driven by hypertensive arteriolopathy rather than CAA related pathology.[34] The association with non-lacunar infarcts is also in line with this multiple etiology concept.

ACMIs have shown to evolve into chronic lesions, appearing on follow up imaging as WMH,[35] cavitated lesions and cortical microinfarcts.[5] It has been proposed that ACMIs damage network integrity and therefore result in worsening of cognitive performance.[36] No correlation was found between ACMI presence and cognitive impairment at baseline. However, patients with ACMIs were four times as likely to be institutionalized at follow-up, mostly due to cognitive decline, and tended to have a faster deterioration of their CDR score. These findings support the notion that ACMIs should be considered a risk factor for cognitive deterioration.

Follow up data from this study showed that ACMI presence at baseline predicted *poor clinical outcome*, future stroke and institutionalization. One previous study of acute hemorrhagic stroke patients with adequate follow up established a similar result with respect to recurring stroke and vascular death.[7] These findings emphasize the important clinical implications of ACMIs as a marker of active vascular disease. Future studies should explore if ACMI may guide targeted prevention strategies.

Strength of this study is the large cohort with high quality MRI, cognitive data, CSF biomarker availability and follow up in the large majority of eligible participants. Limitations concern the limited spatial and temporal resolution of ACMI detection on DWI, which provides a “snapshot” of ischemic injury from the past two weeks. Longitudinal studies with frequent repeat MRIs and cognitive testing could provide more detail on these lesions, their evolution over time and cumulative effect on cognitive performance. Another issue is the relatively arbitrary proposed cut off of 5mm,[1] as this and many other studies found DWI lesions measuring up to 10mm. Whether these slightly larger lesions represent a different cerebrovascular pathology is unclear. Finally, it is still unclear whether our findings are generalizable to chronic microinfarcts and other types of (non) vascular cohorts. It may be argued that the acute stage of a microinfarct should have the same risk factors and clinical correlates as its chronic stage. Yet, the DWI lesion does represent an acute stage in the process, whereas the chronic lesions may reflect events that have occurred even decades ago. Moreover, not all ACMIs evolve into a lesion that

is detectable as a chronic.[5] With regard to generalizability to other cohorts, it should be noted that the etiology, burden comorbidities of ACMI may markedly differ between cohorts[1] which may be relevant to their clinical correlates.

This study found that ACMIs in memory clinic patients with possible VCI are associated with an increased burden of mixed vascular brain pathology, especially SVD and reduced levels of CSF Aβ. Our findings highlight that ACMIs, despite being relatively rare, are an important imaging marker of active vascular brain injury that carry prognostic value with regards to poor clinical outcome.

Acknowledgements

Contributors to the TRACE-VCI cohort (in alphabetical order, per department):
Amsterdam UMC, Amsterdam, Netherlands:
Alzheimer Center and Department of neurology: M.R. Benedictus, J. Bremer, J. Leijenaar, B.M. Tijms.
Department of Radiology and Nuclear Medicine: M.P. Wattjes.
University Medical Centre Utrecht, Utrecht, The Netherlands:
Department of Neurology: S.M. Heringa, L.J. Kappelle, Y.D. Reijmer,
Hospital Diakonessenhuis Zeist, the Netherlands: M. Hamaker, R. Faaij, M. Pleizier, E. Vriens.
Onze Lieve Vrouwe Gasthuis (OLVG) West, Amsterdam, The Netherlands:
Department of Neurology: H.M. Boss, H.C. Weinstein.

References

1. Van Veluw SJ, Shih AY, Smith EE, et al. Detection, risk factors, and functional consequences of cerebral microinfarcts. *Lancet Neurol.* 2017;16:730–740.
2. Smith EE, Schneider JA, Wardlaw JM, Greenberg SM. Cerebral microinfarcts: The invisible lesions. *Lancet Neurol.* 2012;11:272–282.
3. Van Veluw SJ, Zwanenburg JJM, Engelen-Lee J, et al. In vivo detection of cerebral cortical microinfarcts with high-resolution 7T MRI. *J. Cereb. Blood Flow Metab.* 2013;322–329.
4. Kimberly WT, Gilson a., Rost NS, et al. Silent ischemic infarcts are associated with hemorrhage burden in cerebral amyloid angiopathy. *Neurology.* 2009;72:1230–1235.
5. van Veluw SJ, Lauer A, Charidimou A, et al. Evolution of DWI lesions in cerebral amyloid angiopathy. *Neurology.* 2017;89:2136–2142.
6. Auriel E, Gurol ME, Ayres A, et al. Characteristic distributions of intracerebral hemorrhage-associated diffusion-weighted lesions. *Neurology.* 2012;79:2335–2341.
7. Kang DW, Han MK, Kim HJ, et al. New ischemic lesions coexisting with acute intracerebral hemorrhage. *Neurology.* 2012;79:848–855.
8. Garg RK, Liebling SM, Maas MB, Nemeth AJ, Russell EJ, Naidech AM. Blood pressure reduction, decreased diffusion on MRI, and outcomes after intracerebral hemorrhage. *Stroke.* 2012;43:67–71.
9. Prabhakaran S, Gupta R, Ouyang B, et al. Acute brain infarcts after spontaneous intracerebral hemorrhage: A diffusion-weighted imaging study. *Stroke.* 2010;41:89–94.
10. Gregoire SM, Charidimou A, Gadapa N, et al. Acute ischaemic brain lesions in intracerebral haemorrhage: Multicentre cross-sectional magnetic resonance imaging study. *Brain.* 2011;134:2376–2386.
11. Wu B, Yao X, Lei C, Liu M, Selim MH. Enlarged perivascular spaces and small diffusion-weighted lesions in intracerebral hemorrhage. *Neurology.* 2015;85:2045–2052.
12. Saini M, Suministrado MSP, Hilal S, et al. Prevalence and risk factors of acute incidental infarcts. *Stroke.* 2015;46:2722–2727.
13. Auriel E, Westover MB, Bianchi MT, et al. Estimating Total Cerebral Microinfarct Burden From Diffusion-Weighted Imaging. *Stroke.* 2015;46:2129–2135.
14. Tsai YH, Lee MH, Weng HH, Chang SW, Yang JT, Huang YC. Fate of diffusion restricted lesions in acute intracerebral hemorrhage. *PLoS One.* 2014;9.
15. Boomsma JMF, Exalto LG, Barkhof F, et al. Vascular Cognitive Impairment in a Memory Clinic Population: Rationale and Design of the "Utrecht-Amsterdam Clinical Features and Prognosis in Vascular Cognitive Impairment" (TRACE-VCI) Study. *JMIR Res Protoc.* 2017;6:e60.
16. Fazekas F, Chawluk J, Alavi A, Hurtig H, Zimmerman R. MR signal abnormalities at 1.5 T in Alzheimer's dementia and normal aging. *Am J Roentgenol.* 1987;149:351–356.
17. Gorelick PB, Scuteri A, Black SE, et al. Vascular Contributions to Cognitive Impairment and Dementia: A Statement for Healthcare Professionals From the American Heart Association/American Stroke Association. *Stroke.* 2011;42:2672–2713.
18. Román GC, Tatemichi TK, Erkinjuntti T, et al. Vascular dementia: diagnostic criteria for research studies. Report of the NINDS-AIREN International Workshop. *Neurology.* 1993;43:250–260.

19. McKhann G, Drachman D, Folstein M, Katzman R, Price D, Stadlan EM. Clinical diagnosis of Alzheimer's disease: report of the NINCDS-ADRDA Work Group under the auspices of Department of Health and Human Services Task Force on Alzheimer's Disease. *Neurology.* 1984;34:939–944.

20. Verhage F. Intelligentie en leeftijd : onderzoek bij Nederlanders van twaalf tot zevenenzeventig jaar. 1964.

21. Hughes CP, Berg L, Danziger WL, Coben LA, Martin RL. A new clinical scale for the staging of dementia. *Br J Psychiatry.* 1982;140:566–572.

22. Folstein MF, Folstein SE, McHugh PR. "Mini-mental state." *J Psychiatr Res.* 1975;12:189–198.

23. Gaser, C., Dahnke R. CAT - a computational anatomy toolbox for the analysis of structural MRI data. Pap Present 22nd Annu Meet Organ Hum Brain Mapping, Geneva, Switzerland. 2016.

24. Wardlaw JM, Smith EE, Biessels GJ, et al. Neuroimaging standards for research into small vessel disease and its contribution to ageing and neurodegeneration. *Lancet Neurol.* 2013;12:822–838.

25. Scheltens P, Launer LJ, Barkhof F, Weinstein HC, Gool WA. Visual assessment of medial temporal lobe atrophy on magnetic resonance imaging: Interobserver reliability. *J Neurol.* 1995;242:557–560.

26. Lansberg MG, Thijs VN, Brien MWO, et al. Evolution of Apparent Diffusion Coef cient, Diffusion-weighted, and T2-weighted Signal Intensity of Acute Stroke. *Stroke.* 2001;22:637–644.

27. Duits FH, Prins ND, Lemstra AW, et al. Diagnostic impact of CSF biomarkers for Alzheimer's disease in a tertiary memory clinic. *Alzheimer's Dement.* 2015;11:523–532.

28. Batool S, O'Donnell M, Sharma M, et al. Incidental magnetic resonance diffusion-weighted imaging-positive lesions are rare in neurologically asymptomatic community-dwelling adults. *Stroke.* 2014;45:2115–2117.

29. Hesse C, Rosengren L, Vanmechelen E, et al. Cerebrospinal fluid markers for Alzheimer's disease evaluated after acute ischemic stroke. *J Alzheimer's Dis.* 2000;2:199–206.

30. Strozyk D, Blennow K, White LR, Launer LJ. CSF A 42 levels correlate with amyloid-neuropathology in a population-based autopsy study. *Neurology.* 2003;60:652–656.

31. Charidimou A, Friedrich JO, Greenberg SM, Viswanathan A. Core CSF biomarker profile in cerebral amyloid angiopathy. *Neurology.* 2018;90:e1–e9.

32. Pantoni L. Cerebral small vessel disease: from pathogenesis and clinical characteristics to therapeutic challenges. *Lancet Neurol.* 2010;9:689–701.

33. Reijmer YD, van Veluw SJ, Greenberg SM. Ischemic brain injury in cerebral amyloid angiopathy. *J Cereb Blood Flow Metab.* 2015:1–10.

34. Poels MMF, Vernooij MW, Ikram MA, et al. Prevalence and Risk Factors of Cerebral Microbleeds: An Update of the Rotterdam Scan Study. *Stroke.* 2010;41:S103–S106.

35. Conklin J, Silver FL, Mikulis DJ, Mandell DM. Are acute infarcts the cause of leukoaraiosis? Brain mapping for 16 consecutive weeks. *Ann Neurol.* 2014;76:899–904.

36. Auriel E, Edlow BL, Reijmer YD, et al. Microinfarct disruption of white matter structure: A longitudinal diffusion tensor analysis. *Neurology.* 2014;83:182–188.

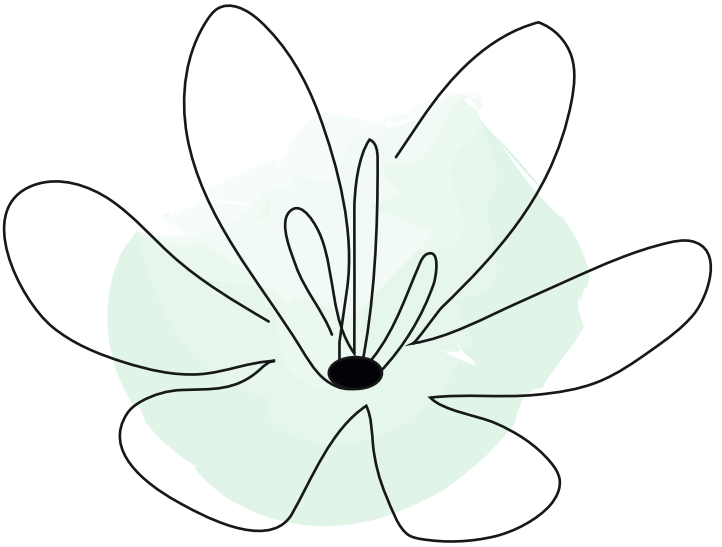

10

Advanced MRI in cerebral small vessel disease

Hilde van den Brink, Fergus N Doubal, Marco Duering

International Journal of Stroke: 2023;18(1):28-35.

Abstract

Cerebral small vessel disease (cSVD) is a major cause of stroke and dementia. This review summarizes recent developments in advanced neuroimaging of cSVD with a focus on clinical and research applications. In the first section we highlight how advanced structural imaging techniques, including diffusion MRI, enable improved detection of tissue damage, including characterization of tissue appearing normal on conventional MRI. These techniques enable progression to be monitored and may be useful as surrogate endpoint in clinical trials. Quantitative MRI, including iron and myelin imaging, provides insights into tissue composition on the molecular level. In the second section, we cover how advanced MRI techniques can demonstrate functional or dynamic abnormalities of the blood vessels, which could be targeted in mechanistic research and early-stage intervention trials. Such techniques include the use of dynamic contrast enhanced MRI to measure blood-brain barrier permeability, and MRI methods to assess cerebrovascular reactivity. In the third section we discuss how the increased spatial resolution provided by ultra-high field MRI at 7T allows imaging of perforating arteries, and flow velocity and pulsatility within them. The advanced MRI techniques we describe are providing novel pathophysiological insights in cSVD and allow improved quantification of disease burden and progression. They have application in clinical trials, both in assessing novel therapeutic mechanisms, and as a sensitive endpoint to assess efficacy of interventions on parenchymal tissue damage. We also discuss challenges of these advanced techniques and suggest future directions for research.

Introduction

Cerebral small vessel disease (cSVD) is a major cause of ischemic and hemorrhagic stroke, and vascular cognitive impairment.[1] It is typically characterized by multiple tissue alterations visible on MRI, including but not limited to white matter hyperintensities (WMH), lacunes, cerebral microbleeds and enlarged perivascular spaces.[2] These cSVD lesions on MRI can be useful in clinical practice for diagnosis and some, in particular WMH, can be reliably segmented, e.g. using deep learning-based algorithms.[3] However, a lesion-based MR imaging approach has limitations as the lesion-based concept dichotomizes tissue alterations into normal and abnormal, which does not reflect the gradual-onset of tissue damage found in cSVD.[3] Quantitative imaging approaches provide a continuous (rather than dichotomized) measure of brain abnormalities, allowing increased granularity in assessment of pathology. In the first section of this review, we highlight quantitative MRI and how these advanced structural imaging techniques enable better assessment of cSVD severity and progression as well as how they provide insights into tissue composition on the molecular level.

Parenchymal lesions are a downstream consequence of vessel pathology and allow only an indirect assessment of cSVD. As such, tissue alterations do not capture early pathological changes in vascular integrity and function, which could be targeted in mechanistic research and early-stage intervention trials.[4] Recent advances in image acquisition and processing techniques have allowed investigation of vascular function and direct imaging of the small vessels to further elucidate cSVD pathogenesis and to facilitate assessment of prognosis and treatment effects.[5,6] In the second section of this review, we focus on blood brain barrier permeability and cerebrovascular reactivity. The small vessels themselves are the focus of the third section in which we cover how increased resolution provided by ultra-high field MRI allows imaging of structure as well as flow in perforating arteries.

Scope of the review

We aim to summarize the use of advanced MRI in cSVD for clinicians and researchers. We address potential future applications, technical feasibility, status of technical and clinical validation[7] and challenges (summarized in the table). Details on acquisition and analysis are beyond the scope of this review.

Table: Technical validation status in cSVD patients, strengths, and weaknesses of advanced MRI techniques

Technique	Potential applications	Technical validation	Strengths	Weaknesses
Advanced structural imaging				
Diffusion MRI (in particular DTI metrics)	Monitoring disease progression over time, endpoint in clinical trials[15,16] Prediction of dementia[14]	High scan-rescan repeatability in cSVD patients High inter-site reproducibility when using harmonized acquisition[18]	Widely available and straightforward to implement Short acquisition time when using multiband imaging Fully automated analysis possible (e.g., PSMD)[15]	Especially prone to motion artifacts and CSF contamination[62] High degree of harmonization needed for comparability across sites[63]
Quantitative MRI (relaxometry, iron, myelin)	Measuring tissue composition[25,26,31] and repair[42]	Limited data in cSVD patients	Post-mortem validation[27,28]	Typically needs long acquisition time or research sequences[64]
Cerebrovascular integrity and function				
DCE-MRI	Monitoring disease progression, improve prognosis, personalize medications[48,51]	Limited data concerning repeatability and reproducibility in cSVD patients	Ability to detect small changes in permeability with good spatial resolution	Complicated technique with low signal-to-noise ratio
CVR-MRI			Excellent spatial resolution in detection of vascular reactivity Good tolerability	Care needed in image registration. High degree of harmonization needed for comparability across sites
Imaging of small perforating arteries				
Perforating artery morphology and flow velocity	Provide insight in cSVD pathogenesis[59,60] Potential (treatable) endpoint in clinical trials at the level of the small vessels	Scan-rescan repeatability and inter-scanner reproducibility are topic of ongoing studies	Imaging at the level of small vessel pathology itself Potential to identify small vessel changes before permanent parenchymal damage occurs	Limited availability of 7T systems Potentially more claustrophobic than 3T scanner Prone to motion, given the high resolution and relatively long scan time

Search strategy and selection criteria

To focus on recent developments, PubMed was searched for articles between January 1st 2018 and November 1st 2021. Titles and abstracts were screened for relevance and full-text of relevant articles reviewed. Further relevant studies were identified from recent reviews.[5,6,8-11] Search terms used were for cSVD: "cerebral small vessel disease", "Cerebral Small Vessel Diseases"[MeSH], "small vessel disease" and microangiopathy. Diffusion MRI: diffusion AND MRI, "diffusion tensor imaging" and "diffusion tensor imaging"[MeSH]. Quantitative MRI: "quantitative MRI", relaxometry, "magnetization transfer", "myelin water" and "quantitative susceptibility mapping". Dynamic contrast enhanced MRI: "dynamic contrast enhanced" AND MRI, "blood brain barrier" AND MRI, "blood-brain barrier" AND MRI, "permeability imaging". Cerebrovascular reactivity: cerebrovascular reactivity", "blood oxygen level dependent ", vasodilatation AND MRI, vasoconstriction AND MRI, "carbon dioxide challenge". Flow velocity imaging: "blood flow velocity" AND MRI, "blood flow pulsatility" AND MRI, 7T.

Advanced structural imaging

Quantitative MRI (qMRI) measures physical properties of tissue, supposedly largely independently from the acquisition technique or scanner hardware. In a strict sense, qMRI comprises techniques to estimate relaxation times, called relaxometry, generating quantitative maps for T1, T2 and T2*. In a broader sense, techniques measuring other physical properties are also considered qMRI, such as diffusion MRI as well as iron- and myelin-sensitive acquisitions.

Diffusion MRI

Diffusion MRI indirectly probes tissue microstructure by quantifying water movement, which appears increased in cSVD.[12] Most previous work studied metrics from the diffusion tensor imaging (DTI) model. While not specific for a particular pathology, DTI alterations in the elderly seem mostly driven by cSVD and not neurodegenerative pathology, such as Alzheimer's disease.[13] In terms of clinical validation, multiple cross-sectional and longitudinal studies have shown strong associations with clinical deficits in cSVD, as highlighted by a recent systematic review.[8] DTI can detect early tissue alterations even in white matter appearing normal on conventional imaging. The precise assessment of disease burden allows prediction of the clinical course, e.g. determining the risk of dementia.[14] High reliability and high sensitivity to subtle tissue alterations make DTI analysis especially suited to capture change over time. This is best reflected in small sample size estimates for clinical trials using change in DTI metrics as endpoint.[15,16]

Recent studies explore diffusion MRI models more sophisticated than DTI, but they typically require more elaborate acquisition, e.g. with sampling of more directions and higher/multiple diffusion-weights, and thus longer scan time. Studies using free water imaging suggested that increased extracellular water is a key factor underlying tissue

alterations[12] and associated with altered haemodynamics.[17] One study highlighted a benefit of diffusion kurtosis imaging for characterizing the very subtle white matter alterations in early-stage cSVD patients.[18]

There are multiple analysis strategies for diffusion MRI with different levels of complexity (Figure 1A). A simple but powerful approach is to study global white matter metrics. This can be fully automated, as in the publicly available peak width of skeletonized mean diffusivity pipeline (PSMD, www.psmd-marker.org).[15] This fully integrated analysis solution is tailored to cSVD research and easy to implement also in clinical trials.[19] The most sophisticated analysis approach is to reconstruct structural brain networks using tractography and atlas-based brain parcellations, with analysis of network structure through graph-theoretical metrics. Structural network analysis is much more reliable than (resting-state) functional network analysis in cSVD[20,21] and can provide pathophysiological insight, such as the importance of central hub connections.[22,23] However, for quantifying disease burden and progression, the added value of network analysis over simpler analysis approaches seems limited.[24]

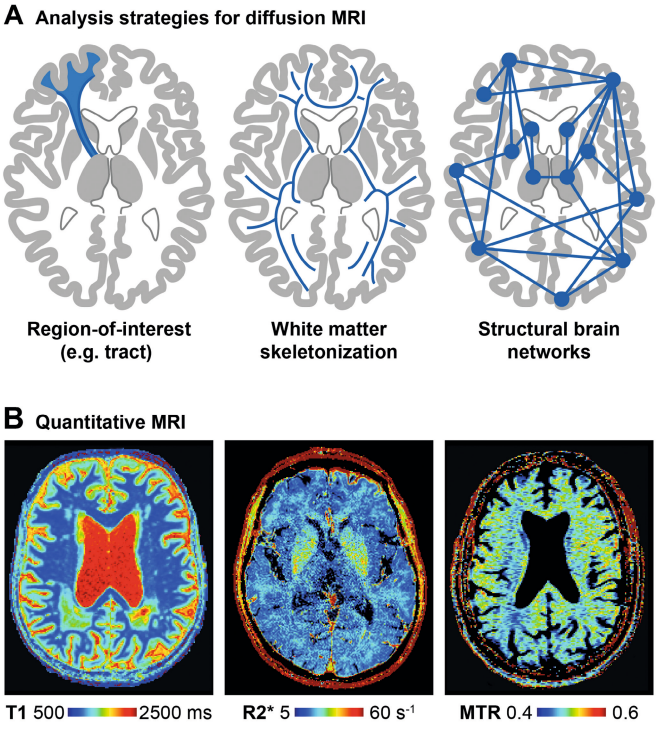

Figure 1: Quantitative MRI: (a) Analysis strategies for diffusion MRI can vary greatly in their complexity. (b) Relaxometry maps for T1 and R2* (1/T2*). Magnetization transfer ratio map as a proxy of myelin content.

Iron and myelin imaging

Apart from better assessment of disease burden, qMRI enables the study of the molecular composition of tissue. The combination of T1 and R2* relaxometry (Figure 1B) has been used to further characterize tissue alterations[25] and to identify heterogeneity in the composition of white matter hyperintensities depending on location, suggesting different pathophysiology across brain regions.[26]

T2* (or its inverse R2*) mapping is used as a proxy for iron concentration, supported by post-mortem validation.[27] Iron is found in multiple brain cell types and its deposition is considered a marker of degeneration. Quantitative susceptibility mapping also quantifies iron and has been validated for deep grey matter.[28] Using these techniques, studies have shown increased iron deposition in cSVD,[29] which was associated with other cSVD markers,[30] disability[31] and regional blood-brain barrier permeability.[32] Further studies are needed to explore the added value of iron quantification in cSVD, potentially as a marker of (secondary) neurodegeneration.[33]

Quantifying myelin in cSVD is appealing for mechanistic research and clinical trials, potentially enabling assessment of tissue repair in the form of remyelination. The best-established and still state-of-the-art myelin-sensitive technique is based on magnetization transfer, with first studies in cSVD dating back more than 20 years.[34] A correlation with myelin has been validated for magnetization transfer ratio by post-mortem studies in multiple sclerosis.[35] Recent studies showed associations between magnetization transfer ratio and gait velocity[36] as well as cognitive function,[37] although with limited added value over age. With longitudinal studies suggesting the possibility of cSVD burden regression in some patients,[38] re-myelination is a compelling imaging target that needs to be further established in future studies.

In general, qMRI parameters should be interpreted cautiously, the main issue being lack of specificity. Changes in iron can also affect magnetization transfer ratio and R2*/QSM measurements seem not only determined by iron concentration but also oxygenation state.[39] Newer developments with potentially higher sensitivity and specificity for myelin are inhomogeneous magnetization transfer[40] and myelin water imaging.[41] The latter is based on the short T2 relaxation time of compartmentalized water in myelin sheaths and has been validated post-mortem in multiple sclerosis.[42] Ultimately, the choice of qMRI method needs to be tailored to the application, as sensitivity and specificity vary between techniques.[43]

Imaging of cerebrovascular integrity and function

This review has focused thus far on parenchymal changes in cSVD, but advanced MRI techniques can also demonstrate functional or dynamic abnormalities of the blood vessels.[44] There is increasing evidence that endothelial cell dysfunction plays a key role in cSVD pathophysiology, leading to increased permeability of the blood-brain barrier (BBB). This subacute failure of maintenance of homeostasis may lead to damage to and thickening of the basement membrane with accompanying increase in stiffness of blood vessel walls. Measuring this initial leakiness and subsequent vasoreactivity (or stiffness) is key to understanding this pathophysiological pathway.[44]

Dynamic contrast-enhanced MRI to assess blood-brain barrier permeability

Gross brain pathology such as brain tumors or acute stroke lead to a lack of a functioning BBB with extravasation of fluids and contrast agents easily seen on routine clinical brain imaging. The increased BBB permeability in cSVD is of several orders of magnitude smaller and accordingly more difficult to demonstrate, but can be measured with dynamic contrast-enhanced MRI (DCE-MRI). DCE-MRI involves injection of a paramagnetic gadolinium-based contrast agent (preferably a slow bolus injection) with subsequent serial T1-weighted scanning over a period ranging from 20–30 minutes.[6] Contrast accumulates in the blood and the extravascular, extracellular space. Signal enhancement occurs as contrast agent shortens the longitudinal relaxation times of tissue water.

Following image segmentation, data are analyzed to produce a vascular input function and tissue signal-time curves. Semi-quantitative (linear modelling of signal enhancement) or quantitative methods adopting pharmacokinetic methods calculate the blood to brain transfer constant K^{trans}, a measure of the rate at which contrast agent is delivered to the extravascular space per volume of tissue and agent concentration.[6] The Patlak model is recommended to assess the pharmacokinetics of signal enhancement.[45]

BBB permeability is increased in cSVD and there is some evidence that the increased permeability is associated with cSVD-related stroke, white matter disease and vascular cognitive impairment.[45-47] Future studies will address if characterizing BBB permeability allows improved prognostication and/or stratified management, e.g., developing BBB permeability stabilizing drugs for those with the highest degree of baseline BBB permeability.

Cerebrovascular reactivity imaging

It is proposed that the leaky blood-brain barrier leads to vessel stiffness and impaired cerebrovascular reactivity (CVR), contributing to tissue damage seen in cSVD.[44,48] There are varying methods of provoking vasodilation ranging from non-invasive task-based methods (e.g., visual flicker stimuli), to breath-holding to raise CO2 levels and pharmacological methods (administration of acetazolamide). Assessment of CVR with

block administration of the potent vasodilator CO_2 however (at a concentration of 6% for 1-3 minutes) with blood oxygenation level dependent (BOLD) MRI produces excellent spatial resolution. Preliminary data in patients post minor stroke and healthy controls suggest good repeatability and reproducibility at 1.5T and 3T.[49] Repeatability though was poorer between days than within day and lower in white than grey matter (due to lower signal-to-noise ratio).[48] Overall, this technique is highly tolerable, even in older patient populations.[9,48,49]

Lower CVR is associated with worsened WMH in patients following minor stroke.[50] Baseline CVR may predict subsequent cSVD worsening or may even be used to predict response to certain medications allowing for stratification and personalized medication use.[51,52] Higher field strength MRI may yield promising results as the change in BOLD signal is larger and more weighted towards the cerebral small vessels[53], and because the higher spatial resolution allows for more local CVR assessment.

Measuring BBB permeability with DCE-MRI and CVR with BOLD are complicated techniques – there are several associated pitfalls, largely related to the small effect size and low signal-to-noise ratio but recent advances can alleviate some of the systematic errors. The effect of even small amounts of motion can be mitigated by registration,[54] care needs to be taken with scan segmentation (with appropriate masking of lesions) and determining the vascular input function. Standardizing scanning across different scanners is possible but needs careful attention to detail including regular quality assurance and scanning of phantoms to identify and minimize signal drift.[51,55]

Imaging of small perforating arteries

With the development of ultra-high field imaging at 7T in humans, exciting new possibilities emerge for cSVD research. With 7T MRI, we can now image the small vessels themselves *in vivo*. Being able to zoom in to the small vessels will play an important role in developing a better understanding of disease mechanisms.

In cSVD, individual lenticulostriate arteries (LSA) were first visualized 12 years ago with 7T time of flight MRA.[56] Studies have shown fewer LSA branches in patients with cSVD, previous lacunar stroke and CADASIL compared with controls, which also seemed to relate to cognitive impairment.[56-58] Over recent years, this study of perforating artery morphology has not translated into morphology-based applications. Instead, in an effort to capture even earlier pathological alterations, focus has shifted towards studying the functioning of these small perforating arteries. Blood flow velocity can now be measured directly in these vessels with 7T phase contrast MRI. A recent study reported reduced blood flow velocity in LSA in patients with inherited cSVD compared with controls, which was also associated with MRI lesions of cSVD and cognitive function.[59] From these blood flow velocity measures, a next step is to calculate velocity pulsatility, mostly done with

Gosling's pulsatility index, calculated as (peak systolic velocity–peak diastolic velocity)/mean velocity. Normally, pulsatile blood flow should be dampened as blood travels along the arterial tree, with little remaining pulsatility in arterioles. As already described in the second section of this review, small vessel pathology is hypothesized to cause stiffened vessel walls. Stiff vessels may insufficiently dampen arterial pulse pressure, leading to transmission of higher pulsatility in arterioles where it causes additional damage. Velocity pulsatility measurements in perforating arteries in the basal ganglia and centrum semiovale (Figure 2) in patients with sporadic cSVD indeed showed increased pulsatility compared to controls, despite no difference in flow velocity.[60] Measuring pulsatility in these small vessels and linking with other dynamic measures such as CVR will help unravel the pathways underpinning cSVD. First efforts on lower field strength show that these assessments can be performed in the basal ganglia with 3T MRI as well, although with an approximately 5-fold lesser sensitivity and therefore only in the relatively larger perforating arteries.[61]

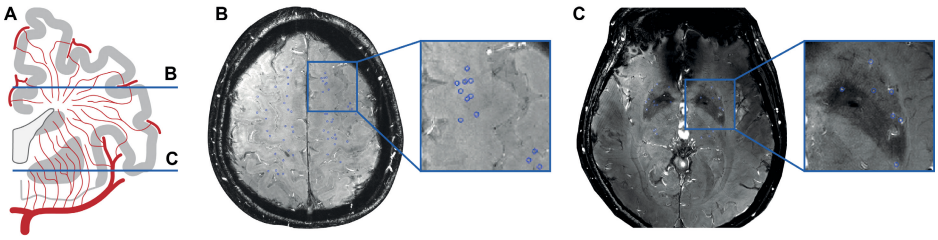

Figure 2: Flow velocity imaging in perforating arteries: (a) Coronal view of perforating artery anatomy. 2D slices in the centrum semiovale (b) and basal ganglia (c) with the perforating arteries marked in blue.

By imaging at the level of the small vessels, 7T MRI allows the study of cSVD from a new perspective and potentially captures early pathological changes before more permanent parenchymal damage occurs. Therefore, apart from the need for more validation, the main open question that needs to be addressed in future longitudinal studies is whether *in vivo* small vessel changes in cSVD are merely another consequence of small vessel pathology or causally linked to cSVD parenchymal lesions and cognitive decline. Ultimately, this might enable direct assessment of the effect of new early-stage treatments that target vascular function. With increased installation of 7T systems and further technical developments, ultra-high field MRI will undoubtedly play an important role in future cSVD research.

Conclusions

Advanced MRI contributes to a better characterization of cSVD and has the potential to provide new mechanistic insights. As more complex methods and paradigms are introduced, it is crucial to demonstrate an added benefit over established techniques to justify the increased effort. None of the reviewed advanced techniques is currently in routine clinical use, but diffusion MRI and cerebrovascular reactivity have been used as endpoints in randomized clinical trials. Still, missing technical validation and high instrumental effort are the most apparent challenges for more widespread (clinical) application, which should be the focus of future studies.

References

1. Iadecola C, Duering M, Hachinski V, et al. Vascular Cognitive Impairment and Dementia: JACC Scientific Expert Panel. *J Am Coll Cardiol.* 2019;73:3326-3344.
2. Wardlaw JM, Smith EE, Biessels GJ, et al. Neuroimaging standards for research into small vessel disease and its contribution to ageing and neurodegeneration. *Lancet Neurol.* 2013;12:822-838.
3. Kuijf HJ, Biesbroek JM, De Bresser J, et al. Standardized Assessment of Automatic Segmentation of White Matter Hyperintensities and Results of the WMH Segmentation Challenge. *IEEE Trans Med Imaging.* 2019;38:2556-2568.
4. Smith EE and Markus HS. New Treatment Approaches to Modify the Course of Cerebral Small Vessel Diseases. *Stroke.* 2020;51:38-46.
5. Blair GW, Hernandez MV, Thrippleton MJ, et al. Advanced Neuroimaging of Cerebral Small Vessel Disease. *Curr Treat Options Cardiovasc Med.* 2017;19:56.
6. Thrippleton MJ, Backes WH, Sourbron S, et al. Quantifying blood-brain barrier leakage in small vessel disease: Review and consensus recommendations. *Alzheimers Dement.* 2019;15:840-858.
7. Smith EE, Biessels GJ, De Guio F, et al. Harmonizing brain magnetic resonance imaging methods for vascular contributions to neurodegeneration. *Alzheimers Dement.* 2019;11:191-204.
8. Raja R, Rosenberg G and Caprihan A. Review of diffusion MRI studies in chronic white matter diseases. *Neurosci Lett.* 2019;694:198-207.
9. Sleight E, Stringer MS, Marshall I, et al. Cerebrovascular Reactivity Measurement Using Magnetic Resonance Imaging: A Systematic Review. *Front Physiol.* 2021;12:643468.
10. Smith EE and Beaudin AE. New insights into cerebral small vessel disease and vascular cognitive impairment from MRI. *Curr Opin Neurol.* 2018;31:36-43.
11. Benjamin P, Viessmann O, MacKinnon AD, et al. 7 Tesla MRI in cerebral small vessel disease. *Int J Stroke.* 2015;10:659-664.
12. Duering M, Finsterwalder S, Baykara E, et al. Free water determines diffusion alterations and clinical status in cerebral small vessel disease. *Alzheimers Dement.* 2018;14:764-774.
13. Finsterwalder S, Vlegels N, Gesierich B, et al. Small vessel disease more than Alzheimer's disease determines diffusion MRI alterations in memory clinic patients. *Alzheimers Dement.* 2020;16:1504-1514.
14. Egle M, Hilal S, Tuladhar AM, et al. Prediction of dementia using diffusion tensor MRI measures: the OPTIMAL collaboration. *J Neurol Neurosurg Psychiatry.* 2022;93:14-23.
15. Baykara E, Gesierich B, Adam R, et al. A Novel Imaging Marker for Small Vessel Disease Based on Skeletonization of White Matter Tracts and Diffusion Histograms. *Ann Neurol.* 2016;80:581-592.
16. Benjamin P, Zeestraten E, Lambert C, et al. Progression of MRI markers in cerebral small vessel disease: Sample size considerations for clinical trials. *J Cereb Blood Flow Metab.* 2016;36:228-240.
17. Maillard P, Mitchell GF, Himali JJ, et al. Aortic Stiffness, Increased White Matter Free Water, and Altered Microstructural Integrity: A Continuum of Injury. *Stroke.* 2017;48:1567-1573.
18. Konieczny MJ, Dewenter A, Ter Telgte A, et al. Multi-shell Diffusion MRI Models for White Matter Characterization in Cerebral Small Vessel Disease. *Neurology.* 2021;96:e698-e708.
19. Ganesh A, Barber P, Black SE, et al. Trial of remote ischaemic preconditioning in vascular cognitive impairment (TRIC-VCI): protocol. *BMJ Open.* 2020;10:e040466.

20. Gesierich B, Tuladhar AM, Ter Telgte A, et al. Alterations and test-retest reliability of functional connectivity network measures in cerebral small vessel disease. *Hum Brain Mapp.* 2020;41:2629-2641.
21. Lawrence AJ, Tozer DJ, Stamatakis EA, et al. A comparison of functional and tractography based networks in cerebral small vessel disease. *Neuroimage Clin.* 2018;18:425-432.
22. van Leijsen EMC, van Uden IWM, Bergkamp MI, et al. Longitudinal changes in rich club organization and cognition in cerebral small vessel disease. *Neuroimage Clin.* 2019;24:102048.
23. Tuladhar AM, Lawrence A, Norris DG, et al. Disruption of rich club organisation in cerebral small vessel disease. *Hum Brain Mapp.* 2017;38:1751-1766.
24. Dewenter A, Gesierich B, Ter Telgte A, et al. Systematic validation of structural brain networks in cerebral small vessel disease. *J Cereb Blood Flow Metab.* 2021:271678X211069228.
25. Iordanishvili E, Schall M, Loucao R, et al. Quantitative MRI of cerebral white matter hyperintensities: A new approach towards understanding the underlying pathology. *Neuroimage.* 2019;202:116077.
26. De Guio F, Vignaud A, Chabriat H, et al. Different types of white matter hyperintensities in CADASIL: Insights from 7-Tesla MRI. *J Cereb Blood Flow Metab.* 2018;38:1654-1663.
27. Langkammer C, Krebs N, Goessler W, et al. Quantitative MR imaging of brain iron: a postmortem validation study. *Radiology.* 2010;257:455-462.
28. Langkammer C, Schweser F, Krebs N, et al. Quantitative susceptibility mapping (QSM) as a means to measure brain iron? A post mortem validation study. *Neuroimage.* 2012;62:1593-1599.
29. Liem MK, Lesnik Oberstein SA, Versluis MJ, et al. 7 T MRI reveals diffuse iron deposition in putamen and caudate nucleus in CADASIL. *J Neurol Neurosurg Psychiatry.* 2012;83:1180-1185.
30. Bauer CE, Zachariou V, Seago E, et al. White Matter Hyperintensity Volume and Location: Associations With WM Microstructure, Brain Iron, and Cerebral Perfusion. *Front Aging Neurosci.* 2021;13:617947.
31. Sun C, Wu Y, Ling C, et al. Deep Gray Matter Iron Deposition and Its Relationship to Clinical Features in Cerebral Autosomal Dominant Arteriopathy With Subcortical Infarcts and Leukoencephalopathy Patients: A 7.0-T Magnetic Resonance Imaging Study. *Stroke.* 2020;51:1750-1757.
32. Uchida Y, Kan H, Sakurai K, et al. Iron leakage owing to blood-brain barrier disruption in small vessel disease CADASIL. *Neurology.* 2020;95:e1188-e1198.
33. Duering M and Schmidt R. Remote changes after ischaemic infarcts: a distant target for therapy? *Brain.* 2017;140:1818-1820.
34. Iannucci G, Dichgans M, Rovaris M, et al. Correlations between clinical findings and magnetization transfer imaging metrics of tissue damage in individuals with cerebral autosomal dominant arteriopathy with subcortical infarcts and leukoencephalopathy. *Stroke.* 2001;32:643-648.
35. Schmierer K, Scaravilli F, Altmann DR, et al. Magnetization transfer ratio and myelin in postmortem multiple sclerosis brain. *Ann Neurol.* 2004;56:407-415.
36. Seiler S, Pirpamer L, Gesierich B, et al. Lower Magnetization Transfer Ratio in the Forceps Minor Is Associated with Poorer Gait Velocity in Older Adults. *AJNR Am J Neuroradiol.* 2017;38:500-506.
37. Seiler S, Pirpamer L, Hofer E, et al. Magnetization transfer ratio relates to cognitive impairment in normal elderly. *Front Aging Neurosci.* 2014;6:263.
38. van Leijsen EMC, van Uden IWM, Ghafoorian M, et al. Nonlinear temporal dynamics of cerebral small vessel disease: The RUN DMC study. *Neurology.* 2017;89:1569-1577.

39. Birkl C, Birkl-Toeglhofer AM, Kames C, et al. The influence of iron oxidation state on quantitative MRI parameters in post mortem human brain. *Neuroimage.* 2020;220:117080.
40. Varma G, Girard OM, Prevost VH, et al. In vivo measurement of a new source of contrast, the dipolar relaxation time, T1D , using a modified inhomogeneous magnetization transfer (ihMT) sequence. *Magn Reson Med.* 2017;78:1362-1372.
41. Dao E, Tam R, Hsiung GR, et al. Exploring the Contribution of Myelin Content in Normal Appearing White Matter to Cognitive Outcomes in Cerebral Small Vessel Disease. *J Alzheimers Dis.* 2021;80:91-101.
42. Laule C and Moore GRW. Myelin water imaging to detect demyelination and remyelination and its validation in pathology. *Brain Pathol.* 2018;28:750-764.
43. Granziera C, Wuerfel J, Barkhof F, et al. Quantitative magnetic resonance imaging towards clinical application in multiple sclerosis. *Brain.* 2021;144:1296-1311.
44. Wardlaw JM, Smith C and Dichgans M. Small vessel disease: mechanisms and clinical implications. *Lancet Neurol.* 2019;18:684-696.
45. Chagnot A, Barnes SR and Montagne A. Magnetic Resonance Imaging of Blood-Brain Barrier permeability in Dementia. *Neuroscience.* 2021;474:14-29.
46. Kerkhofs D, Wong SM, Zhang E, et al. Blood-brain barrier leakage at baseline and cognitive decline in cerebral small vessel disease: a 2-year follow-up study. *Geroscience.* 2021;43:1643-1652.
47. Stringer MS, Heye AK, Armitage PA, et al. Tracer kinetic assessment of blood-brain barrier leakage and blood volume in cerebral small vessel disease: Associations with disease burden and vascular risk factors. *Neuroimage Clin.* 2021;32:102883.
48. Thrippleton MJ, Shi Y, Blair G, et al. Cerebrovascular reactivity measurement in cerebral small vessel disease: Rationale and reproducibility of a protocol for MRI acquisition and image processing. *Int J Stroke.* 2018;13:195-206.
49. Stringer MS, Blair GW, Shi Y, et al. A Comparison of CVR Magnitude and Delay Assessed at 1.5 and 3T in Patients With Cerebral Small Vessel Disease. *Front Physiol.* 2021;12:644837.
50. Blair GW, Thrippleton MJ, Shi Y, et al. Intracranial hemodynamic relationships in patients with cerebral small vessel disease. *Neurology.* 2020;94:e2258-e2269.
51. Blair GW, Stringer MS, Thrippleton MJ, et al. Imaging neurovascular, endothelial and structural integrity in preparation to treat small vessel diseases. The INVESTIGATE-SVDs study protocol. Part of the SVDs@Target project. *Cerebral Circulation - Cognition and Behavior.* 2021;2:100020.
52. van den Brink H, Kopczak A, Arts T, et al. Zooming in on cerebral small vessel function in small vessel diseases with 7T MRI: Rationale and design of the "ZOOM@SVDs" study. *Cerebral Circulation - Cognition and Behavior.* 2021;2:100013.
53. Siero JC, Bhogal A and Jansma JM. Blood Oxygenation Level-dependent/Functional Magnetic Resonance Imaging: Underpinnings, Practice, and Perspectives. *PET Clin.* 2013;8:329-344.
54. Bernal J, Valdes-Hernandez MDC, Escudero J, et al. A four-dimensional computational model of dynamic contrast-enhanced magnetic resonance imaging measurement of subtle blood-brain barrier leakage. *Neuroimage.* 2021;230:117786.
55. Manning C, Stringer M, Dickie B, et al. Sources of systematic error in DCE-MRI estimation of low-level blood-brain barrier leakage. *Magn Reson Med.* 2021;86:1888-1903.
56. Kang CK, Park CA, Park CW, et al. Lenticulostriate arteries in chronic stroke patients visualised by 7 T magnetic resonance angiography. *Int J Stroke.* 2010;5:374-380.
57. Seo SW, Kang CK, Kim SH, et al. Measurements of lenticulostriate arteries using 7T MRI: new imaging markers for subcortical vascular dementia. *J Neurol Sci.* 2012;322:200-205.

58. Ling C, Fang X, Kong Q, et al. Lenticulostriate Arteries and Basal Ganglia Changes in Cerebral Autosomal Dominant Arteriopathy With Subcortical Infarcts and Leukoencephalopathy, a High-Field MRI Study. *Front Neurol.* 2019;10:870.

59. Sun C, Wu Y, Ling C, et al. Reduced blood flow velocity in lenticulostriate arteries of patients with CADASIL assessed by PC-MRA at 7T. *J Neurol Neurosurg Psychiatry.* Epub ahead of print 28 Sep 2021. DOI: 10.1136/jnnp-2021-326258.

60. Geurts LJ, Zwanenburg JJM, Klijn CJM, et al. Higher Pulsatility in Cerebral Perforating Arteries in Patients With Small Vessel Disease Related Stroke, a 7T MRI Study. *Stroke.*

61. Arts T, Meijs TA, Grotenhuis H, et al. Velocity and Pulsatility Measures in the Perforating Arteries of the Basal Ganglia at 3T MRI in Reference to 7T MRI. *Front Neurosci.* 2021;15:665480.

62. Metzler-Baddeley C, O'Sullivan MJ, Bells S, et al. How and how not to correct for CSF-contamination in diffusion MRI. *Neuroimage.* 2012;59:1394-1403.

63. Croall ID, Lohner V, Moynihan B, et al. Using DTI to assess white matter microstructure in cerebral small vessel disease (SVD) in multicentre studies. *Clin Sci.* 2017;131:1361-1373.

64. Mussard E, Hilbert T, Forman C, et al. Accelerated MP2RAGE imaging using Cartesian phyllotaxis readout and compressed sensing reconstruction. *Magn Reson Med.* 2020;84:1881-1894.

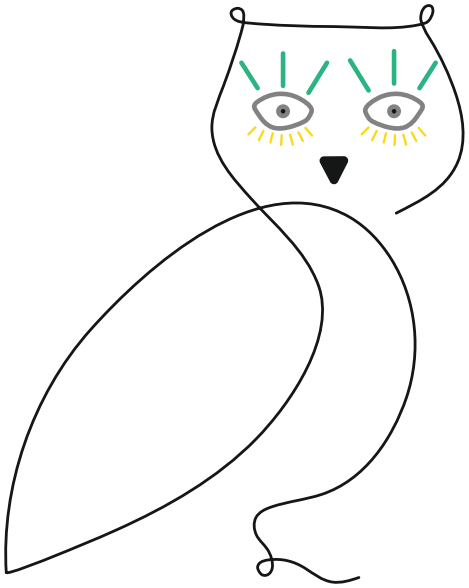

11

General discussion

The aim of this thesis was to characterize new *in vivo* MRI markers of cerebral small vessel disease, where I particularly focussed on small vessel function and cerebral microinfarcts. To be honest, during my PhD my idea of the general concept 'biomarker' still had to grow a lot. I have come to better understand how a biomarker only derives meaning from a given context and that a biomarker is usually only ideal for certain aspects e.g. diagnosis, prognosis, therapeutic efficacy. This understanding mostly grew during my weekly meetings with my promotor that almost never went without (challenging!) questions like: "what are you actually measuring?, what is the specific question that these results answer?, what is the domain?". The BEST (Biomarkers, EndpointS, and other Tools) resource of the FDA-NIH biomarker working group provides a framework for harmonized biomarker terminology and validation, and distinguishes: diagnostic, monitoring, response, predictive, prognostic, safety and susceptibility/risk biomarkers,[1] that helped me to place my findings in perspective. In this general discussion I will reflect upon the findings in this thesis and how they relate to other available literature. Also, I will reflect on the current status of MRI measures of small vessel function and cerebral microinfarcts as biomarkers in cerebral small vessel disease (cSVD), and provide suggestions on which steps I think should be addressed next. I will limit myself to a reflection of these biomarkers that were topic of my thesis, but do wish to acknowledge that other biomarkers are also under development: we provided a review of the currently most advanced *in vivo* MRI markers of cSVD in Chapter 10 of this thesis. Finally, I will end this general discussion with my idea of future perspectives on biomarkers in cSVD.

Small vessel function

In an effort to examine cSVD at the level of the small vessels themselves, we studied novel measures of small vessel function on 7T-MRI in patients with monogenic (i.e. CADASIL) and sporadic cSVD. Patients were recruited in the ZOOM@SVDs study, as described in Chapter 3. Specifically, we assessed basal ganglia and centrum semiovale perforating artery blood flow velocity and pulsatility, vascular reactivity to a short visual stimulus in the occipital cortex, and vascular reactivity to hypercapnia throughout different areas in the brain. Importantly, these measures probe complementary aspects of small vessel function in different small vessel populations. We determined if these novel measures could detect disease effects at the level of the small vessels, we identified which aspects of small vessel function were altered, and how these alterations related with markers of tissue injury and cognitive function.

In Chapter 4 and 5 we reported on the measures that reflect aspects of small vessel function that were altered in patients with CADASIL and sporadic cSVD respectively. Table 1 provides an overview of the measures that were altered in patients compared to their age- and sex-matched controls. I think that the first and most straightforward, yet very most important, finding from this part of my thesis is that we can detect disease effects with novel *in vivo* small vessel function measures on 7T-MRI, both in CADASIL

and sporadic cSVD. This allows for a paradigm shift, where we can start to study cSVD at the level of the cerebral small vessels themselves *in vivo*. When looking at what these measures represent, we found that both in CADASIL and sporadic cSVD multiple aspects of small vessel function were abnormal, indicative of increased arteriolar stiffness and regional abnormalities in endothelial-dependent and independent vascular reactivity. Vascular reactivity to quick, subtle and local demand in the cortex was altered, while prolonged and global stimulation with hypercapnia seemed to generate a normal vascular response in the grey matter, although not in white matter hyperintensities (WMH). To my knowledge there are two previous studies that also looked at pulsatility index in small perforating arteries in patients with cSVD. One of these studies reported increased pulsatility index, also indicative of increased arteriolar stiffness[2], while the second study did not, which could be explained by the fact that disease burden in the patients of that study was low.[3] Others are also assessing blood flow velocity and pulsatility in the somewhat larger lenticulostriate arteries.[4,5] These studies reported decreased blood flow velocity in patients with CADASIL[4] and a relation between higher pulsatility index and age.[5] Most previous work on vascular reactivity on MRI in patients with cSVD has been performed with BOLD MRI as well, but mostly on lower field strengths. Not all findings from these studies are directly comparable to our results, given that 7T-MRI provides a higher sensitivity and spatial and temporal resolution, which likely means that we are measuring in different (i.e. smaller) vessel populations than studies on lower field strength.[6] Because of this high temporal resolution, we could assess vascular reactivity to very short visual stimulation, which, to my knowledge, has not been studied before in cSVD. In addition, because of the high spatial resolution, we could assess vascular reactivity to hypercapnia in separate regions of interest. Earlier studies have, like us, reported decreased endothelial-independent reactivity within WMH, both in monogenic[7] and sporadic cSVD[8,9], but less is known about the grey matter. Only two previous studies in patients with CADASIL studied either the grey matter as a whole[10] or the cortex specifically[7], and did not report differences in reactivity to hypercapnia[10] or acetazolamide[7] in patients compared with controls. Future studies need to determine to what extent reactivity measured with BOLD on 7T-MRI is directly comparable to these measurements on 3T or even 1.5T-MRI.

Table 1: Small vessel dysfunction in the ZOOM@SVDs study in CADASIL and sporadic cSVD

Small vessel function measure	CADASIL	Sporadic cSVD
2D-Qflow centrum semiovale		
Blood flow velocity [cm/s]	↓	↔
Pulsatility index	↑	↔
2D-Qflow basal ganglia		
Blood flow velocity [cm/s]	↓	↔
Pulsatility index	↑	↑
BOLD short visual stimulus		
BOLD % signal change	↓	↔
Full width at half max [s]	↔	↓
BOLD hypercapnic stimulus		
CGM BOLD % signal change	↔	↔
SGM BOLD % signal change	↔	↔
WM BOLD % signal change	↔	↔
WMH BOLD % signal change[a]	↓	↓

The arrows indicate whether the measure was higher (↑), lower (↓), or unaltered (↔) in patients compared to their respective age- and sex-matched controls.

[a] WMH was compared with normal appearing white matter within the patient group.

In Chapters 4, 5 and 6 we related the novel measures of small vessel function to tissue injury and cognition. These findings are summarized in Table 2. We found that some aspects of affected small vessel function are also related to worse tissue injury and worse cognition. Similar analyses were performed in earlier 3T-MRI hypercapnia studies in cSVD, also reporting relations of decreased reactivity to WMH volume.[8–13] In addition to the global associations that are summarized in Table 2, in Chapter 6 we also made use of the high spatial resolution of 7T-MRI to study the voxel-by-voxel relation of vascular reactivity to hypercapnia and white matter integrity. Within subjects, we found a local relation between decreased vascular reactivity to hypercapnia and loss of white matter integrity, both in patients with CADASIL and sporadic cSVD. These findings provide more direct indications for a possible causal relationship between small vessel function and white matter integrity, although shared risk factors can of course not be excluded from these cross-sectional analyses. Of note, white matter integrity in this study was assessed with diffusion tensor imaging metrics from diffusion MRI. This is currently the most sensitive tissue injury measure of white matter damage in cSVD.[14,15]

Table 2: The global associations of small vessel dysfunction with tissue injury and cognition in the ZOOM@SVDs study in CADASIL and sporadic cSVD

	CADASIL		Sporadic cSVD	
Small vessel function measure	**Tissue injury[a]**	**Cognition[b]**	**Tissue injury[a]**	**Cognition[b]**
2D-Qflow centrum semiovale				
Blood flow velocity [cm/s]	↓	↔	*	*
Pulsatility index	↔	↔	*	*
2D-Qflow basal ganglia				
Blood flow velocity [cm/s]	↔	↔	↓	↑
Pulsatility index	↔	↔	↑	↔
BOLD short visual stimulus				
BOLD % signal change	↓	↔	*	*
Full width at half max [s]	*	*	↓	↑
BOLD hypercapnic stimulus				
CGM BOLD % signal change	*	*	*	*
SGM BOLD % signal change	*	*	*	*
WM BOLD % signal change	*	*	*	*
WMH BOLD % signal change	↔	↔	↔	↔

The arrows indicate whether there was a positive (↑), negative (↓), or no significant association (↔) between the specific small vessel function measure and tissue injury or cognition.

* = not analysed, because this small vessel function measure was not altered in patients compared with controls (see Table 1). Given the relatively small sample size, we only related affected measures of small vessel function with tissue injury and cognition. However, because blood flow velocity and pulsatility are closely interrelated, we considered these together in these analyses.

[a] Tissue injury was measured as WMH volume, lacune count or global WM integrity.

[b] Cognition was a compound score of executive function and attention and processing speed.

Despite some similarities, Table 1 and Table 2 show that there were also apparent differences between CADASIL and sporadic cSVD regarding the way that small vessel function was altered and how these alterations related to disease severity. We observed spatial differences in the perforating artery populations that had altered blood flow velocity and pulsatility. These differences are likely to be meaningful. It likely implies that underlying small vessel pathogenesis is different in small vessel populations throughout the brain and between types of cSVD. Such spatial differentiations have been reported before on histology and structural MRI.[16,17] An autopsy study in CADASL for example showed that lumen diameter is unchanged in the basal ganglia, but is decreased due to intimal thickening and fibrosis in perforating arteries in the centrum semiovale.[16] Also, a study looking at enlarged perivascular spaces in cSVD in the basal ganglia and centrum semiovale showed that clinical correlates of enlarged perivascular spaces in these two brain regions are different as well. This study reported that enlarged perivascular spaces in the basal ganglia were associated with an increased risk of recurrent ischemic stroke, whereas enlarged perivascular spaces in the centrum semiovale were not.[17]

In addition to these spatial differences in blood flow velocity and pulsatility, another relevant observation is how vascular reactivity was affected differently, apparently depending on the type of stimulus that was used to trigger vasodilation. Both in CADASIL and sporadic cSVD, vascular reactivity to very short visual stimulation was affected in the occipital cortex, whereas we did not observe decreased reactivity in the cortex in response to prolonged hypercapnia. In fact the type and extent of stimulation determines which aspects of vascular reactivity are assessed and where. Visual stimulation is neurovascular coupling dependent, whereas hypercapnia has a direct vasodilatory effect on the small vessel wall and is thereby endothelial independent.[18,19] Also, the fact that visual stimulation was very short (<1 second) means that we are likely measuring blood flow changes via arteriole dilation, whereas longer hypercapnia also induces notable blood volume changes on the venous side that influence the signal.[20] Different stimulus durations thus probe vascular reactivity through different effector pathways in different vessel populations. I think that these differential findings again emphasize that it is an important strength that we have assessed complementary aspects of small vessel function in different small vessel populations within one study. These complementary aspects are also the reason that I cannot choose one favourite measure when colleagues ask me to choose what I regard as the best small vessel function measure. It all depends on your research question. However, I am convinced that in order to understand underlying disease mechanisms, the combination of assessments will be key.

Given that the studies in my thesis are first efforts in characterizing small vessel function measures on 7T-MRI in cSVD, I understand that the findings in my thesis may generate more questions than they actually answer. A first important question that needs to be addressed is whether the *in vivo* small vessel function changes in cSVD are indeed causally linked to cSVD parenchymal lesions and cognitive decline, or are merely another consequence of small vessel pathology. If there is a causal relation, this would mean that the small vessel function measures can assess small vessel disease in earlier, possibly even reversible, disease stages. A stage where (further) parenchymal damage and cognitive decline could still be prevented. Ultimately, this might enable direct monitoring of the response to new early-stage treatments that target vascular function, at least in a research setting. Such a surrogate endpoint biomarker for clinical trials is currently lacking, so its development would provide a unique biomarker to the cSVD research field.[21] In order to start this validation process, longitudinal analyses are necessary. In fact, the ZOOM@SVDs study has a follow-up visit where parenchymal damage and cognitive decline are again assessed after two years, so the answer to some of these questions is already underway. In addition to a need for longitudinal analyses, I think that we should also make more use of the high spatial resolution of the whole-brain BOLD images. So far we have mostly studied relatively large regions of interest, although of course in Chapter 6 we already showed how local analyses can provide additional new insights. It would be of particular interest to see if vascular reactivity in more specific brain areas may be affected. For example, two previous studies on 3T-MRI in CADASIL showed that

areas that later developed to become WMH had lower vascular reactivity at baseline.[8,9] I would be interested to see if such local measures will provide meaningful results in sporadic cSVD as well. Particularly because the BOLD signal is pretty weak in the white matter (compared to grey matter) and also because we saw that there is a big variability in the white matter BOLD signal. We will need to see if this variability is meaningful or merely reflects noisy data. This further research is necessary to understand the use of the small vessel function measures as biomarker in cSVD. As has likely become clear from this reflection, I see most potential as a possible prognostic, monitoring and response biomarker, but I am excited to learn to what extent these markers of small vessel function will live up to this potential.

Cerebral microinfarcts

At the start of my PhD it was already clear that cerebral microinfarcts are a very common form of vascular brain injury. Also, we already knew that these lesions were related to cSVD and thus a marker of tissue injury in cSVD.[26] With the, back then relatively new, opportunity to study cortical microinfarcts *in vivo* in humans, there were new angles to study remaining uncertainties. In this thesis I aimed to improve the understanding of underlying mechanisms that lead to microinfarcts, in particular the potential role of cerebral amyloid angiopathy (CAA) and hypoperfusion. Also I aimed to assess the prognostic value of cerebral microinfarcts for long-term clinical outcome.

Neuropathology studies already showed an association between cerebral microinfarcts and CAA.[27–29] In Chapter 7 of my thesis, we were the first to explore *in vivo* occurrence of cerebral microinfarcts in the cortex in patients with CAA. We found that cortical microinfarcts occurred frequently in CAA, that new microinfarcts can be detected after one year follow-up and that microinfarct presence did not relate with other MRI markers of tissue injury or cognitive function in CAA. From these results, we concluded that cortical microinfarcts were distinct from other well-established markers of CAA and may therefore increase diagnostic certainty when observed in the context of the well-recognized MRI markers of CAA. During my PhD, three additional studies performed *in vivo* assessment of cortical microinfarcts in CAA.[30–32] These studies reported a lower frequency of cortical microinfarct presence in their cohorts; 16-39% versus 57% in our study. Even though microinfarct frequency is known to vary also between cohorts in neuropathology studies, I think we cannot exclude the possibility that this difference is (partly) explained by interrater variability, because cortical microinfarct detection is challenging. Another discrepancy between the studies is that we did not observe a relation of microinfarcts with other known MRI markers in CAA, whereas all three other studies reported such associations.[30–32] These different observations could be explained by the difference in rating sensitivity between studies, but could also mean that cortical microinfarcts are not distinct from other well-established MRI markers in CAA despite what we suggested in Chapter 7, also meaning that they may have little specific value as

diagnostic biomarker in CAA. From both the available *ex vivo* and *in vivo* studies, we can conclude that CAA causes cerebral microinfarcts. Less clear is the mechanism that would drive microinfarct formation in CAA. It is hypothesized that vessel wall alterations caused by β-amyloid deposition are directly involved. Indeed, a neuropathology study found that microinfarcts were often found close to vessels with β-amyloid deposition and that these vessels had prominent luminal narrowing.[33] Another possible pathophysiological mechanism could be that vessel stiffness could lead to reduced vascular reactivity, which may contribute to ischemic events and cerebral microinfarcts. We studied this hypothesis in Chapter 7. We did not find an association between reduced vascular reactivity and microinfarct presence, similar to one of the other *in vivo* studies.[30] It should be noted however that vascular reactivity was only assessed in the visual cortex, whereas cerebral microinfarcts were rarely found in the occipital lobe. This of course complicates the study of a relationship between the two. Studies that use a hypercapnia challenge to assess whole-brain vascular reactivity might be better suited to study decreased vascular reactivity as a possible cause for microinfarcts in CAA. It does, however, seem intuitive that occlusion or hypoperfusion due to vessel wall changes play a direct role.

In addition to CAA pathology, hypoperfusion is hypothesized as an underlying mechanism in cerebral microinfarct pathophysiology. This hypothesis emerged from the observation that cerebral microinfarcts were often seen in watershed areas in neuropathology studies.[34–36] With MRI, a 3D-distribution of cerebral microinfarcts throughout the entire brain can be made. Doing this, *in vivo* studies also tend to show some predilection for microinfarcts in watershed areas.[37,38] Stronger evidence of a role for hypoperfusion comes from studies that looked at a relation with cerebral perfusion. One previous study found that cortical microinfarct presence related to reduced global brain perfusion in a memory clinic population.[39] However, the question remained whether this reflected shared risk factors for cortical microinfarcts and reduced cerebral perfusion, or whether the two were causally related. Therefore, in Chapter 8 of this thesis, we studied cortical microinfarcts in patients with an internal carotid artery occlusion as a model for cerebral hemodynamic compromise. We found that cortical microinfarcts were very common (present in 54%) in patients with an internal carotid artery occlusion. Importantly, microinfarcts were more common in the hemisphere of the occluded internal carotid artery, which means that cortical microinfarcts are likely to be directly related to the occlusion and unlikely to be caused by other underlying factors (such as vascular risk factors) in this population. Moreover, cortical microinfarct presence related to the severity of cervical arterial compromise, in terms of the number of vessels affected by severe atherosclerosis and *current* cerebral blood flow. Together, these findings provide strong support for a role of hypoperfusion in microinfarct aetiology. The causal pathway could be direct, with temporary hypoperfusion directly causing small ischemia in the most distal and smallest vessels.[40] Alternatively, hypoperfusion could cause washout disturbances where insufficiently perfused arterioles or venules could lead to microemboli that produce microinfarcts.[40,41]

From these findings, I think we can conclude that both CAA pathology and hypoperfusion are likely causes of cerebral microinfarcts. It is however important to note that, outside the scope of this thesis, further *in vivo* studies have also confirmed other likely causes of microinfarcts; such as arteriolosclerosis and embolisms from large vessel disease and cardiac disease.[26] Like large artery infarcts, also microinfarcts can thus have multiple causes. Also, in this general discussion I focussed on *in vivo* findings in humans because of the relatively new possibility of studying cortical microinfarcts *in vivo,* which allowed for new angles to study microinfarcts. It is however important to acknowledge that animal studies and neuropathology studies also allow for unique ways to untangle the pathophysiological mechanisms of cerebral microinfarcts. For example, a mouse model study that induced hypoperfusion showed that this hypoperfusion led to increased CAA pathology as well as an increase in microinfarct incidence.[42] Also, a neuropathology study showed that in the presence of β-amyloid or tangle pathology, arteriolosclerosis was associated with greater cerebral microinfarct burden.[43] These findings underline the complex interplay between different pathological processes.

Because cerebral microinfarcts relate to several disease processes and are known to often (but not in all cohorts/studies), relate to baseline cognitive function[26], they may mark clinically relevant outcomes in cSVD and may have potential as prognostic biomarker. Initial studies indeed reported that cortical microinfarct presence predicts future cognitive decline in a memory clinic and stroke cohort.[44,45] Whereas these chronic lesions could be reflective of events that may have occurred up to decades ago, acute microinfarcts on diffusion-weighted imaging could be regarded as markers of active cerebrovascular disease. In Chapter 9 we therefore studied acute microinfarcts in patients from the memory clinic and we found that acute microinfarcts at baseline increase the two-year risk of poor clinical outcome (a composite of marked cognitive decline, major vascular event, institutionalization and death). Similar findings have been reported in patients with haemorrhagic or ischemic stroke.[46,47] These findings highlight the potential prognostic value of acute microinfarcts. The underlying mechanisms that could explain this relation are yet unclear. Microinfarcts may directly cause clinical symptoms by exerting effects also beyond their lesions boundaries, but it seems more likely that microinfarcts are a proxy of the severity or instability/activity of other underlying pathological processes. Even if the microinfarcts themselves turn out to not directly cause follow-up symptoms, the acute nature of these lesions makes that they may still guide targeted prevention strategies. However, more longitudinal studies are still necessary to reliably identify in whom an acute microinfarct marks a risk for clinical decline. A challenge with these studies is that the incidence of acute microinfarcs is low, so that large sample sizes are necessary to have statistical power to relate these lesions to clinically relevant outcomes. Therefore the consortium DIAGNOSE (Diffusion-weighted ImAGiNg pOSitive lEsion consortium) was formed, which aims to pool data in meta-analyses to determine the prevalence, risk factors and clinical relevance of “diffusion-weighted imaging positive lesions” in cSVD populations.

After cortical microinfarcts were first visualized *in vivo* with 7T and 3T-MRI, the number of studies examining these lesions grew rapidly, also providing more insight into their possible use as biomarker. Although *in vivo* studies add to the notion that cerebral microinfarcts are a marker of cSVD, findings also point to many other possible causes of microinfarcts.[26] Cerebral microinfarct presence is thus very unspecific to the specific underlying aetiology, making cerebral microinfarcts unsuitable as diagnostic biomarker. I currently see most potential for use as a prognostic biomarker in cSVD, but more validation is necessary. Even though microinfarcts are known to relate with cognition in many cohorts, this is not the case in every study/cohort. Also, more longitudinal studies are necessary to conclude whether microinfarcts indeed predict (specific aspects of) clinical decline, and in whom. At a recent microinfarct symposium that I co-organised, we concluded that the most important way forward is to study microinfarcts on a much larger epidemiological scale. This larger scale is necessary to get a better understanding of what cerebral microinfarcts mark in specific populations in given circumstances. Research groups are more and more willing to provide data for such large-scale collaborative projects. The problem is, however, that microinfarct rating is difficult, thereby observer dependent and very time-consuming, taking up to 30 minutes per scan for 3T-MRI images. To be able to perform larger scale studies, we would need computer assisted rating to speed up and optimise ratings. By applying machine learning algorithms to already marked microinfarcts, the computer could "learn" what a microinfarct looks like. Such methods have been successfully developed for aided microbleed rating.[48] Developing such a tool for microinfarcts proved to be more difficult though. Given that microinfarcts are so small, they are also hard to detect for the computer, and interrater variability makes it hard to determine a ground truth. Larger already-rated datasets are necessary to input into the algorithms, still requiring a lot of manual rating work. Efforts are however underway, which will be aided by the fast developments of machine learning methods. Very briefly I would like to mention that other techniques are potentially valuable in understanding the use of microinfarcts as biomarker as well. *Ex vivo* MRI-guided histopathologic investigations are for example a powerful tool to bridge the gap between the *in vivo* observable lesions and understanding the underlying presumed causes and potential pathophysiological mechanisms.[49] Such assessments will be topic of the postdoc position that I start at Massachusetts General Hospital.

The future of biomarker research in cerebral small vessel disease

In addition to the markers that I studied in my thesis, there are of course other developments in biomarker research in cSVD. We provided an overview of the currently most advanced *in vivo* MRI markers of cSVD in a review in Chapter 10 of this thesis, including diffusion MRI, iron and myelin imaging, and dynamic contrast enhanced MRI to assess blood-brain barrier permeability. When reading the review, one may notice that markers of tissue injury are studied the most and are currently developed furthest. However, with advancements of imaging techniques, I think focus will (need to also) shift toward measures that can assess functional and/or dynamic abnormalities in the blood vessels. I think such measures will be key in providing mechanistic insights and thereby help develop an understanding of underlying pathophysiological pathways. These insights are needed to find leads for urgently needed treatment. Subsequently, if such treatment strategies were found, these biomarkers could then instantly be used as the surrogate endpoints to test the treatment. The important asset of such mechanistic markers compared to tissue injury markers, is that they should theoretically speaking be reversible. If, in addition, such a mechanistic marker would causally relate with later tissue injury and clinical decline, this would mean that with such new markers we may be able to submit treatment before (further) tissue damage occurs, thereby preventing clinical symptoms (from worsening). Of course there are still a lot of "ifs" in this line of reasoning. In addition to these "ifs", a specific limitation of the small vessel function measures from this thesis are that they are assessed at 7T-MRI, which is not widely available, limiting the applicability in larger and diverse cohorts. It is however not unreasonable to think that measures could (partly) be translated to 3T-MRI. We have already seen such a translation for cortical microinfarct detection. Importantly, the techniques to assess small vessel function are already used on 3T-MRI,[12,23,24] but performing these measures on 3T-MRI likely means that we are measuring a different (small) vessel population. Future studies would need to determine whether measurements on 3T-MRI may still represent alterations as we observe them with 7T-MRI. Lastly, more advanced biomarkers also come with complex techniques. We would at least need to put substantial effort into finding the optimal image acquisition and analyses protocols, as complex techniques usually come with many possible challenges. Adequate validation is important to ensure that we do not start a treatment trial for which too much noise is introduced by the outcome marker, which could lead to wrong conclusions about the effect of the treatment. If these efforts are successful for the small vessel function measures, it would be quite unique for a response biomarker to be clinically meaningful, closely representative of underlying biological progression and also be efficient for short trials because of the reversibility of the measure.[21,50]

References

1. FDA-NIH Biomarker Working Group. *BEST (Biomarkers, EndpointS, and Other Tools) Resource*. Silver Spring (MD); 2016.
2. Geurts L, Zwanenburg JJM, Klijn CJM, Luijten PR, Biessels GJ. Higher Pulsatility in Cerebral Perforating Arteries in Patients With Small Vessel Disease Related Stroke, a 7T MRI Study. *Stroke*. 2019;50(1):62-68.
3. Perosa V, Arts T, Assmann A, et al. Pulsatility Index in the Basal Ganglia Arteries Increases with Age in Elderly with and without Cerebral Small Vessel Disease. *Am J Neuroradiol*. 2022;43(4):540-546.
4. Sun C, Wu Y, Ling C, et al. Reduced blood flow velocity in lenticulostriate arteries of patients with CADASIL assessed by PC-MRA at 7T. *J Neurol Neurosurg Psychiatry*. 2022;93(4):451-452.
5. Schnerr RS, Jansen JFA, Uludag K, et al. Pulsatility of lenticulostriate arteries assessed by 7 Tesla flow MRI-Measurement, reproducibility, and applicability to aging effect. *Front Physiol*. 2017;8:1-10.
6. Siero JCW, Bhogal A, Jansma JM. Blood oxygenation level-dependent/Functional Magnetic Resonance Imaging: Underpinnings, Practice, and Perspectives. *PET Clin*. 2013;8(3):329-344.
7. Chabriat H, Pappata S, Ostergaard L, et al. Cerebral hemodynamics in CADASIL before and after acetazolamide challenge assessed with MRI bolus tracking. *Stroke*. 2000;31(8):1904-1912.
8. Sam K, Crawley AP, Conklin J, et al. Development of White Matter Hyperintensity Is Preceded by Reduced Cerebrovascular Reactivity. *Ann Neurol*. 2016;80(2):277-285.
9. Sam K, Conklin J, Holmes KR, et al. Impaired dynamic cerebrovascular response to hypercapnia predicts development of white matter hyperintensities. *NeuroImage Clin*. 2016;11:796-801.
10. Atwi S, Shao H, Crane DE, et al. BOLD-based cerebrovascular reactivity vascular transfer function isolates amplitude and timing responses to better characterize cerebral small vessel disease. *NMR Biomed*. 2019;32(3):1-12.
11. Blair GW, Thrippleton MJ, Shi Y, et al. Intracranial hemodynamic relationships in patients with cerebral small vessel disease. *Neurology*. 2020;94(21):e2258-e2269.
12. Blair GW, Doubal FN, Thrippleton MJ, Marshall I, Wardlaw JM. Magnetic resonance imaging for assessment of cerebrovascular reactivity in cerebral small vessel disease: A systematic review. *J Cereb Blood Flow Metab*. 2016;36(5):833-841.
13. Reginold W, Sam K, Poublanc J, Fisher J, Crawley A, Mikulis DJ. The efficiency of the brain connectome is associated with cerebrovascular reactivity in persons with white matter hyperintensities. *Hum Brain Mapp*. 2019;40(12):3647-3656.
14. Pasi M, Van Uden IWM, Tuladhar AM, De Leeuw FE, Pantoni L. White Matter Microstructural Damage on Diffusion Tensor Imaging in Cerebral Small Vessel Disease: Clinical Consequences. *Stroke*. 2016;47(6):1679-1684.
15. Baykara E, Gesierich B, Adam R, et al. A Novel Imaging Marker for Small Vessel Disease Based on Skeletonization of White Matter Tracts and Diffusion Histograms. *Ann Neurol*. 2016;80(4):581-592.
16. Miao Q, Paloneva T, Tuisku S, et al. Arterioles of the Lenticular Nucleus in CADASIL. *Stroke*. 2006;37(9):2242-2247.
17. Lau KK, Li L, Lovelock CE, et al. Clinical Correlates, Ethnic Differences, and Prognostic Implications of Perivascular Spaces in Transient Ischemic Attack and Ischemic Stroke. *Stroke*. 2017;48(6):1470-1477.

18. Iadecola C. The Neurovascular Unit Coming of Age: A Journey through Neurovascular Coupling in Health and Disease. *Neuron*. 2017;96(1):17-42.

19. Ainslie PN, Duffin J. Integration of cerebrovascular CO2 reactivity and chemoreflex control of breathing: Mechanisms of regulation, measurement, and interpretation. *Am J Physiol - Regul Integr Comp Physiol*. 2009;296(5):R1473-R1495.

20. Uludağ K, Blinder P. Linking brain vascular physiology to hemodynamic response in ultra-high field MRI. *Neuroimage*. 2018;168:279-295.

21. Smith EE, Biessels GJ, De Guio F, et al. Harmonizing brain magnetic resonance imaging methods for vascular contributions to neurodegeneration. *Alzheimer's Dement Diagnosis, Assess Dis Monit*. 2019;11:191-204.

22. Opstal AM Van, Rooden S Van, Harten T Van, et al. Cerebrovascular function in pre-symptomatic and symptomatic individuals with hereditary cerebral amyloid angiopathy: a case-control study. *Lancet Neurol*. 2017;16(2):115-122.

23. Arts T, Meijs TA, Grotenhuis H, et al. Velocity and Pulsatility Measures in the Perforating Arteries of the Basal Ganglia at 3T MRI in Reference to 7T MRI. *Front Neurosci*. 2021;15:1-10.

24. Blair GW, Stringer MS, Thrippleton MJ, et al. Imaging neurovascular, endothelial and structural integrity in preparation to treat small vessel diseases. The INVESTIGATE-SVDs study protocol. Part of the SVDs@Target project. *Cereb Circ - Cogn Behav*. 2021;2:100020.

25. Beaudin AE, McCreary CR, Mazerolle EL, et al. Cerebrovascular Reactivity Across the Entire Brain in Cerebral Amyloid Angiopathy. *Neurology*. 2022;98(17):E1716-E1728.

26. van Veluw SJ, Shih AY, Smith EE, et al. Detection, risk factors, and functional consequences of cerebral microinfarcts. *Lancet Neurol*. 2017;16(9):730-740.

27. Lauer A, Veluw SJ Van, William CM, et al. Microbleeds on MRI are associated with microinfarcts on autopsy in cerebral amyloid angiopathy. *Neurology*. 2016;87(14):1488-1492.

28. Kövari E, Herrmann FR, Hof PR, Bouras C. The relationship between cerebral amyloid angiopathy and cortical microinfarcts in brain ageing and Alzheimer's disease. *Neuropathol Appl Neurobiol*. 2013;39(5):498-509.

29. Ringman JM, Sachs MC, Zhou Y, Monsell SE, Saver JL, Vinters H V. Clinical predictors of severe cerebral amyloid angiopathy and influence of APOE genotype in persons with pathologically-verified Alzheimer's disease. *JAMA Neurol*. 2014;7(71):878-883.

30. Gokcal E, Horn MJ, van Veluw SJ, et al. Lacunes, Microinfarcts, and Vascular Dysfunction in Cerebral Amyloid Angiopathy. *Neurology*. 2021;96(12):e1646-e1654.

31. Xiong L, Van Veluw SJ, Bounemia N, et al. Cerebral cortical microinfarcts on magnetic resonance imaging and their association with cognition in cerebral amyloid angiopathy. *Stroke*. 2018;49(10):2330-2336.

32. Ii Y, Ishikawa H, Shindo A, et al. Association between cortical microinfarcts and total small vessel disease burden in cerebral amyloid angiopathy on 3-Tesla magnetic resonance imaging. *Eur J Neurol*. 2021;28(3):794-799.

33. van Veluw SJ, Scherlek AA, Freeze WM, et al. Different microvascular alterations underlie microbleeds and microinfarcts. *Ann Neurol*. 2019;86(2):279-292.

34. Suter O christina, Sunthorn T, Kraftsik R, et al. Cerebral Hypoperfusion Generates Cortical Watershed Microinfarcts in Alzheimer Disease. *Stroke*. 2002;33(8):1986-1992.

35. Kapasi A, Leurgans SE, James BD, et al. Neurobiology of Aging Watershed microinfarct pathology and cognition in older persons. *Neurbiology of aging*. 2018;70:10-17.

36. Strozyk D, Dickson DW, Lipton RB, et al. Contribution of vascular pathology to the clinical expression of dementia. *Neurbiology of aging*. 2010;31(10):1710-1720.

37. Riba-Ilena I, Koek M, Verhaaren BFJ, et al. Small cortical infarcts: prevalence, determinants, and cognitive correlates in the general population. *World Stroke Organ*. 2015;10(October):18-24.

38. Ferro DA, van Veluw SJ, Koek HL, Exalto LG, Biessels GJ. Cortical Cerebral Microinfarcts on 3 Tesla MRI in Patients with Vascular Cognitive Impairment. *J Alzheimer's Dis*. 2017;60:1443-1450.

39. Ferro DA, Mutsaerts HJJM, Hilal S, et al. Cortical microinfarcts in memory clinic patients are associated with reduced cerebral perfusion. *J Cereb Blood Flow Metab*. 2020;40(9):1869-1878.

40. Caplan LR, Wong S, Hennerici MG. Is Hypoperfusion an Important Cause of Strokes? If So, How? *Cerebrovasc Dis*. 2006;21:145-153.

41. Hartmann DA, Hyacinth HI, Liao FF, Shih AY. Does pathology of small venules contribute to cerebral microinfarcts and dementia? *J Neurochem*. 2018;144(5):517-526.

42. Okamoto Y, Yamamoto T, Kalaria RN, et al. Cerebral hypoperfusion accelerates cerebral amyloid angiopathy and promotes cortical microinfarcts. *Acta Neuropathol*. 2012;123(3):381-394.

43. Kapasi A, Leurgans SE, Arvanitakis Z, Barnes LL, Bennett DA, Schneider JA. Aβ (Amyloid Beta) and Tau Tangle Pathology Modifies the Association between Small Vessel Disease and Cortical Microinfarcts. *Stroke*. 2021;52(3):1012-1021.

44. Wang Z, Veluw SJ Van, Wong A, et al. Risk Factors and Cognitive Relevance of Cortical Cerebral Microinfarcts in Patients With Ischemic Stroke or Transient Ischemic Attack. *Stroke*. 2016;47:2450-2455.

45. Hilal S, Tan CS, Veluw SJ Van, et al. Cortical cerebral microinfarcts predict cognitive decline in memory clinic patients. *J Cereb Blood Flow Metab*. 2020;40(1):44-53.

46. Fu R, Wang Y, Wang Y, et al. The Development of Cortical Microinfarcts Is Associated with Intracranial Atherosclerosis: Data from the Chinese Intracranial Atherosclerosis Study. *J Stroke Cerebrovasc Dis*. 2015;24(11):2447-2454.

47. Kang DW, Han MK, Kim HJ, et al. New ischemic lesions coexisting with acute intracerebral hemorrhage. *Neurology*. 2012;79(9):848-855.

48. Kuijf HJ, Brundel M, Bresser J De, et al. Semi-Automated Detection of Cerebral Microbleeds on 3.0 T MRI Images. *PLoS One*. 2013;8(6):e66610.

49. van Veluw SJ, Arfanakis K, Schneider JA. Neuropathology of Vascular Brain Health: Insights from Ex Vivo Magnetic Resonance Imaging-Histopathology Studies in Cerebral Small Vessel Disease. *Stroke*. 2022;53(2):404-415.

50. Greenberg SM, Al-Shahi SR, Biessels GJ, et al. Outcome Markers for Clinical Trials in Cerebral Amyloid Angiopathy. *Lancet Neurol*. 2014;13(4):419-428.

Appendices

Nederlandse samenvatting
About the author
List of publications
Dankwoord

Nederlandse samenvatting

Ziekte aan de kleine hersenvaatjes, cerebral small vessel disease (cSVD) in het Engels, verwijst naar ziekteprocessen die de kleinste vaatjes in de hersenen aantasten. cSVD veroorzaakt ongeveer een kwart van alle beroertes en draagt bij aan ongeveer de helft van alle gevallen van dementie. Ondanks deze ernstige gevolgen is er nog geen specifieke behandeling voor cSVD. Dit komt waarschijnlijk doordat we nog onvoldoende begrijpen waardoor de ziekte aan de kleine vaten ontstaat en via welke ziektemechanismen de ziekte vervolgens leidt tot de schade aan het hersenweefsel en de klinische symptomen. Hoofdstuk 2 van mijn proefschrift illustreert met een patiëntcasus dat ons begrip van de oorzaken van cSVD nog verre van compleet is. In dat hoofdstuk beschrijven wij eeneiige tweelingbroers van wie één wel en één geen cSVD heeft, terwijl de broers dezelfde genen en dezelfde (bekende) risicofactoren hebben. Met de huidige kennis zijn wij niet in staat om te verklaren waarom de ene broer de ziekte wél heeft en de andere broer niet.

cSVD wordt veel onderzocht met behulp van MRI-scans van de hersenen. De hersenschade die we op de MRI-scans zien heeft ons iets geleerd over de mogelijke oorzaken en gevolgen van cSVD. Toch hebben markers van hersenschade die we tot nu toe beschikbaar hadden de nodige beperkingen. Ten eerste hadden we nog geen markers om de aangedane vaatjes zelf bij levende mensen te onderzoeken, omdat de diameter van de vaatjes zo klein is dat we ze met een normale scanner niet kunnen afbeelden. Ten tweede kunnen de beschikbare bekende schade-markers niet alle klinische symptomen van de ziekte verklaren. Dat betekent dat we een deel van de schade waarschijnlijk nog misten. We zouden dus graag nieuwe markers hebben die (1) dichter bij de ziekteprocessen in de aangedane vaatjes liggen en (2) gevoeliger zijn of aanvullende informatie geven over weefselschade in de hersenen. In mijn proefschrift heb ik onderzoek gedaan naar twee nieuwe markers die hierop inhaken: (1) maten voor het functioneren van de kleine hersenvaten en (2) een relatief nieuwe en subtiele marker van hersenschade; cerebrale microinfarcten. Het doel was om te onderzoeken of, en zo ja welke, rol deze markers kunnen spelen in het beter begrijpen van oorzaken en gevolgen van cSVD.

Functioneren van de kleine vaten

Vanuit onderzoek in diermodellen weten we dat de pathologische veranderingen aan de kleine hersenvaatjes bij cSVD een effect hebben op het functioneren van die vaatjes, maar we waren lange tijd nog niet in staat om dit in mensen te onderzoeken. Een sterkere MRI scanner, de zogenaamde 7T-MRI scanner, maakt het nu mogelijk om verder op de hersenvaten in te zoomen. Onderzoekers vóór mij hebben methoden ontwikkeld waarmee we twee verschillende aspecten van vaatfunctie kunnen onderzoeken. Allereerst kunnen we nu de snelheid en pulsatiliteit van de bloedstroom meten in hersenvaatjes die kleiner dan 1 mm in diameter zijn. Met name de pulsatiliteit van de bloedstroom is interessant, omdat wij vermoeden dat cSVD de kleine hersenvaatjes stijf maakt, wat middels deze

techniek tot uiting zou moeten komen als een verhoogde pulsatiliteit. Ook kunnen we de reactiviteit van de kleine hersenvaten meten. Vaatreactiviteit verwijst naar het vermogen van de vaten om bloedtoevoer in de hersenen aan te passen, bijvoorbeeld naar gelang de zuurstofbehoefte. Om vaatreactiviteit te kunnen meten is een stimulus nodig die ervoor moet zorgen dat er meer bloed naar (een deel van) de hersenen gaat stromen. Daarbij kunnen we onderscheid maken tussen twee typen stimuli. Er zijn stimuli die hersencellen activeren, wat vervolgens (via zogenaamde neurovasculaire koppeling) leidt tot een toename van bloed naar het geactiveerde hersendeel. Een voorbeeld daarvan is het kijken naar een visuele stimulus terwijl iemand in de scanner ligt. Ook zijn er stimuli die direct effect hebben op de vaatwand door te zorgen voor vaatverwijding en dus voor een toename in bloed naar de hersenen. Een voorbeeld daarvan is het inademen van CO2 in lucht terwijl iemand in de scanner ligt. In dit proefschrift hebben we vaatreactiviteit onderzocht in reactie op een korte (500 ms) visuele stimulus en het meer langdurige (2 min) inademen van CO2 in lucht.

Hoofdstuk 3 beschrijft de opzet van de ZOOM@SVDs studie waarin we de nieuwe maten van vaatfunctie op 7T-MRI hebben onderzocht in twee patiëntgroepen met cSVD. De eerste groep patiënten heeft CADASIL, wat een erfelijke vorm van cSVD is en veroorzaakt wordt door een afwijking in één kritisch gen. De tweede groep patiënten heeft sporadische cSVD, wat zowel door (nog onbekende) risicogenen alsook door vasculaire risicofactoren (d.w.z. hypertensie, diabetes, roken etc.) veroorzaakt wordt. De bevindingen van de ZOOM@SVDs studie staan in hoofdstuk 4 en 5. Allereerst zijn we met de technieken op 7T-MRI inderdaad in staat gebleken om effecten van de ziekte op het functioneren van de kleine vaatjes in beeld te brengen. We kunnen aantonen dat de vaatjes stijver lijken en dat vaatreactiviteit plaatselijk is aangedaan. De korte en snelle vaatreactiviteit in reactie op de visuele stimulus was verminderd, terwijl tragere en langdurige vaatreactiviteit in reactie op het inademen van de CO2 in lucht niet was verminderd in gezond hersenweefsel, maar wel in aangedane witte stof. Hoewel er subtiele verschillen zijn in de precieze manier waarop en waar het functioneren van de kleine vaatjes is aangedaan, zijn de bevindingen in grote lijnen vergelijkbaar voor patiënten met CADASIL en sporadische cSVD. Vervolgens hebben wij in hoofdstuk 4, 5 en 6 gevonden dat de ernst van de functiestoornissen gedeeltelijk samenhangt met de ernst van de schade aan het hersenweefsel en de klinische symptomen. Dit kan erop wijzen dat verminderde vaatfunctie, zoals we al vermoedden, een oorzaak zou kunnen zijn van de hersenweefsel schade in cSVD. Echter, een oorzakelijk verband kunnen we alleen aantonen als we patiënten voor langere tijd volgen om te zien hoe de ziekte zich ontwikkelt. De ZOOM@SVDs studie gaat dan ook door en ziet patiënten terug na 2 jaar. Dit deel van het onderzoek wordt nog uitgevoerd.

Met deze bevindingen hebben we nu markers beschikbaar waarmee we afwijkingen kunnen aantonen op het level waar de ziekte cSVD zich primair bevindt; de kleine hersenvaatjes. Deze maten helpen om ziektemechanismen in cSVD beter te begrijpen.

Ook hebben ze potentie als biomarker, met name als biomarker die latere symptomen zou kunnen helpen voorspellen, als biomarker die ziekte-ernst zou kunnen helpen monitoren en tenslotte als biomarker die gebruikt zou kunnen worden als uitkomstmarker wanneer we de effectiviteit van nieuwe medicijnen voor cSVD willen testen.

Cerebrale microinfarcten

Cerebrale microinfarcten zijn herseninfarctjes van maximaal een paar millimeter groot. Een microinfarct ontstaat wanneer een klein bloedvat niet voldoende doorbloed wordt en een kleine stukje hersenweefsel afsterft door zuurstofgebrek. Microinfarcten geven in principe geen directe uitvalsverschijnselen (zoals bijvoorbeeld verlamming), maar worden wel veel gezien in patiënten met dementie. Microinfarcten zijn zo klein dat we ze lange tijd alleen onder de microscoop konden waarnemen, maar met de verbeterde kwaliteit van MRI scans kunnen we ze nu ook op MRI scans in levende mensen zien. Daardoor kunnen we op grotere schaal onderzoek doen. In mijn proefschrift onderzochten we twee mogelijke oorzaken van microinfarcten en of de aanwezigheid van microinfarcten het ziektebeloop van patiënten met cSVD over de tijd kan voorspellen.

In hoofdstuk 7 deden we onderzoek naar cerebrale amyloid angiopathie (CAA) als mogelijke oorzaak van microinfarcten. CAA is een ziekte waarbij de kleine hersenvaatjes worden aangetast doordat het amyloid-beta eiwit ophoopt in de wand van die vaatjes. Microinfarcten werden al veel waargenomen in het hersenweefsel van overleden patiënten met CAA. Wij onderzochten microinfarcten met MRI in (levende) patiënten en vonden dat ze voorkwamen bij 57% van de patiënten. Dezelfde patiënten hadden na één jaar bovendien al nieuwe microinfarcten gekregen. Ook drie andere onderzoeken vonden, hoewel minder vaak, microinfarcten op de MRI scans in patiënten met CAA. Wij concluderen daarom dat CAA zeer waarschijnlijk een oorzaak is van microinfarcten. In hoofdstuk 8 onderzochten we of hypoperfusie ook een oorzaak van microinfarcten kan zijn. Hypoperfusie betekent dat (een deel van) de hersenen gedurende langere tijd te weinig bloed krijgt. Hierdoor kan schade aan het hersenweefsel ontstaan, wellicht ook in de vorm van microinfarcten. In overleden patiënten werd al gezien dat microinfarcten een neiging hebben om meer voor te komen in gebieden in de hersenen die gevoeliger zijn voor hypoperfusie. Wij hebben met MRI onderzocht of microinfarcten voorkomen in (levende) patiënten bij wie er een verstopping is van één van de grote bloedvaten die de hersenen van bloed moet voorzien. Ondanks dat andere bloedvaten de doorbloeding van de hersenen overnemen, hebben deze patiënten een grotere kans op hypoperfusie van (een deel van) de hersenen. Wij vonden dat microinfarcten in 54% van deze patiënten voorkwamen en dan met name in het deel van de hersenen dat eigenlijk via het verstopte bloedvat doorbloed had moeten worden. Bovendien zagen we dat microinfarcten vaker voorkwamen in de patiënten die meerdere verstoppingen hadden en in patiënten bij wie er sprake was van een netto minder bloedstroom naar de hersenen. Samen vormen deze bevindingen sterk bewijs dat hypoperfusie ook een oorzaak is van microinfarcten. Uit onderzoek van anderen is gebleken dat microinfarcten, naast CAA en hypoperfusie,

meer mogelijke oorzaken kunnen hebben. Omdat microinfarcten bij veel verschillende patiënten voorkomen, concludeer ik dat microinfarcten niet specifiek genoeg zijn om te helpen bij het stellen van een diagnose.

In hoofdstuk 9 onderzochten we of microinfarcten kunnen voorspellen hoe het twee jaar later met patiënten gaat. Specifieker, hebben we gekeken naar acute microinfarcten. Dat zijn microinfarcten die, op het moment van de MRI-scan, tot maximaal twee weken geleden zijn ontstaan. Deze acute microinfarcten markeren dat er actief, op dit moment, sprake is van een ziekteproces in de hersenen. We vonden dat de aanwezigheid van een acuut microinfarct in een patiënt een voorspeller was voor een slechtere gezondheid twee jaar later. Achteruitgang van de denkfuncties, een beroerte, opgenomen moeten worden in een verzorgingshuis of overlijden, kwam bij mensen met acute microinfarcten vaker voor. Twee andere onderzoeken in andere patiëntgroepen kwamen tot eenzelfde conclusie. Omdat de microinfarcten zo klein zijn, lijkt het mij onwaarschijnlijk dat de schade van het microinfarct zelf de oorzaak is van een verslechterde gezondheid. Ik denk dat de aanwezigheid van een acuut microinfarct signaleert dat er sprake is van een actief ziekteproces. Zodra er een behandeling beschikbaar zou komen voor cSVD, zou de aanwezigheid van een acuut microinfarct in een patiënt dus mogelijk het signaal kunnen zijn om nú behandeling in te zetten.

Hoe nu verder?

In mijn proefschrift heb ik twee nieuwe markers van cSVD onderzocht om te ontdekken of deze markers kunnen helpen in het beter begrijpen van de oorzaken en gevolgen van cSVD, maar er gebeurt uiteraard meer in het onderzoeksveld. In hoofdstuk 10 heb ik een overzicht gegeven van andere veelbelovende markers en methoden. Wat opvalt is dat we met name veel markers hebben om schade aan het hersenweefsel te bepalen. Deze schade reflecteert een onomkeerbaar eindstadium van de ziekte. Ik denk dat de focus, met verdere technische ontwikkelingen op MRI, zal (moeten) verschuiven naar maten waarmee we verandering in het functioneren van de hersenen en bloedvaten meten vóórdat schade aan het hersenweefsel ontstaat. Ook moeten we onderzoeken welke processen de functie van de vaatjes verstoren. In het kader van dit proefschrift zie ik dan ook de meeste potentie in de markers van vaatfunctie die ik heb onderzocht. Wanneer we oorzaken en ziekteprocessen beter begrijpen, kunnen we nieuwe behandelingen ontwikkelen. Belangrijk is dat we met behulp van een dergelijke behandeling (verdere) schade aan het hersenweefsel en (verdere) klinische symptomen dan mogelijk kunnen voorkomen. In mijn nieuwe functie aan Harvard Medical School en Massachusetts General Hospital in Boston in de Verenigde Staten zal ik verder blijven werken aan het beter begrijpen van oorzaken en ziekteprocessen in cSVD.

About the author

Hendrikje (Hilde) van den Brink was born on December 1st 1991 in Harderwijk and was raised in Putten, the Netherlands. She graduated from high school in 2010, where her final research project about “memory in the elderly” already alluded to her later research interests.

Hilde studied Psychology at Utrecht University, with a focus on neuropsychology. She graduated cum laude in 2013. She then went on to do a Master’s program in Neuropsychology at Utrecht University. For her clinical training she did an internship at GGZ-Centraal Juliana-Oord, where she saw patients with neurological and psychiatric diseases as well as alcohol and drug addiction for (neuro) psychological examination and treatment. She finished this Master’s program with a research internship at the psychiatry department of the UMC Utrecht, where she studied whether transcranial direct current stimulation could help treat auditory hallucinations in patients with schizophrenia. In parallel with her studies, Hilde explored more of the world of science by working as a research assistant at Utrecht University and as project worker at the Brain foundation (*de Hersenstichting*). These experiences got her excited about scientific research and made her pursue a second Master’s degree in Neuroscience and Cognition, again at Utrecht University. During this Master’s program she did two internships which focused on studying cerebral microinfarcts. Her first internship she performed under supervision of dr. Doeschka Ferro and Professor Geert Jan Biessels at the UMC Utrecht. She went to Calgary in Canada to perform a second internship in the research group of Professor Eric Smith.

After graduating, Hilde thankfully accepted the opportunity to return to the research group of Professor Geert Jan Biessels to pursue a PhD. She was additionally supervised by dr. Jaco Zwanenburg and dr. Jeroen Siero. The results of this PhD journey are currently in the hands of the reader. During her PhD, Hilde coordinated multiple research studies and she was a student representative on the executive board of the VasCog society.

Hilde continues her scientific career as a postdoctoral researcher in the research group of dr. Susanne van Veluw at Harvard Medical School/Massachusetts General Hospital in Boston, USA.

List of publications

In this thesis

van den Brink H*, Kopczak A*, Arts T*, et al. CADASIL affects multiple aspects of cerebral small vessel function on 7T-MRI. *Annals of Neurology*. 2023;93:29-39. doi: 0.1002/ana.26527. **contributed equally*

van den Brink H, Doubal F, Duering M. Advanced MRI in cerebral small vessel disease. *International Journal of Stroke*. 2023;18(1):28-35. doi: 10.1177/17474930221091879.

van den Brink H*, Ferro DA*, de Bresser J, et al. Cerebral cortical microinfarcts in patients with internal carotid artery occlusion. *Journal of cerebral blood flow & Metabolism*. 2021;41(10):2690-2698. doi:10.1177/0271678X211011288. **contributed equally*

van den Brink H, Kopczak A, Arts T, et al. Zooming in on cerebral small vessel function in small vessel diseases with 7T MRI: Rationale and design of the "ZOOM@SVDs" study. *Cerebral Circulation – Cognition and Behavior.* 2021;2:100013. doi: 10.1016/j.cccb.2021.100013

van den Brink H, Weaver N, Biessels GJ. A case of sporadic cerebral small vessel disease in an identical twin. *Case reports in neurology*. 2020;12:416-421. doi: 10.1159/000511027.

Ferro D A, **van den Brink H**, Exalto LG, et al. Clinical relevance of acute cerebral microinfarcts in vascular cognitive impairment. *Neurology.* 2019;92(14);e1558-e1566. doi: 10.1212/WNL.0000000000007250.

van den Brink H, Zwiers A, Switzer AR, et al. Cortical microinfarcts on 3T magnetic resonance imaging in cerebral amyloid angiopathy: relations with other magnetic resonance imaging markers of cerebral amyloid angiopathy and cognition. *Stroke*. 2018:49;1899-1905. doi: 10.1161/STROKEAHA.118.020810

Other

Kopczak A, Stringer MS, **van den Brink H**, et al. The EffecTs of Amlodipine and other Blood PREssure Lowering Agents on Microvascular FuncTion in Small Vessel Diseases (TREAT-SVDs) trial: Study protocol for a randomised crossover trial. *European Stroke Journal.* 2022. doi: 10.1177/239698732211435. Online ahead of print.

Lam BYK, Cai Y, Akinyemi R, Biessels GJ, **van den Brink H**, et al. The global burden of cerebral small vessel disease in low- and middle-income countries: A systematic review and meta-analysis. *International Journal of Stroke*. 2022. doi:10.1177/17474930221137019. Online ahead of print.

De Brito Robalo BM, de Luca A, Chen C, ..., **van den Brink H**, Biessels GJ. Improved sensitivity and precision in multicentre diffusion MRI network analysis using thresholding and harmonization. *NeuroImage: Clinical*. 2022;36:103217. doi: 10.1016/j.nicl.2022.103217.

De Brito Robalo BM, Biessels GJ, Chen C, ..., **van den Brink H**, de Luca A. Diffusion MRI harmonization enables joint-analysis of multicentre data of patients with cerebral small vessel disease. *NeuroImage: Clinical*. 2021;32:102886. doi: 10.1016/j.nicl.2021.102886.

Blair GW, Stringer MS, Thrippleton MJ, ..., **van den Brink H**, et al. Imaging neurovascular, endothelial and structural integrity in preparation to treat small vessel diseases. The INVESTIGATE-SVDs study protocol. Part of the SVDs@Target project. *Cerebral Circulation – Cognition and Behavior.* 2021;2:100020. doi: 10.1016/j.cccb.2021.100020.

Ferro DA, **van den Brink H**, Amier R, et al. Cerebral cortical microinfarcts: A novel MRI marker of vascular brain injury in patients with heart failure. *International Journal of Cardiology*. 2020;310:96-102. doi: 10.1016/j.ijcard.2020.04.032.

Koops S, **van den Brink H**, Sommer IEC. Transcranial direct current stimulation as a treatment for auditory hallucinations. *Frontiers in psychology*. 2015;6:244. doi: 10.3389/fpsyg.2015.00244.

Dankwoord

Dit proefschrift heeft mijn naam op de omslag, maar is werkelijk een krachtenbundeling van vele mensen samen. Het vormt een herinnering aan de contacten die ik in de afgelopen jaren heb opgedaan en de vele ervaringen die ik tijdens dit traject rijker ben geworden. Ik wil hier graag mijn dank uitspreken aan hen die in dit geweldige avontuur een belangrijke rol hebben gespeeld.

Achter alle scans en getallen in dit proefschrift zitten echte mensen met echte verhalen. Daarom allereerst heel veel dank aan **alle participanten van de Hart-Brein studie en de ZOOM@SVDs studie**. Veel van u heb ik persoonlijk begeleid op de onderzoeksdagen. Ik heb veel bewondering voor uw onbaatzuchtige inzet voor onze onderzoeken, uw doorzettingsvermogen tijdens de lange MRI scans en ik ben u dankbaar voor uw interesse en openheid.

Beste **Geert Jan**, zonder de kansen die jij mij geboden hebt was dit proefschrift er zeker niet gekomen. Heel veel dank voor jouw vertrouwen! Dat je een ontzettend goede onderzoeker bent staat buiten kijf. Ik wil daarom juist benadrukken dat je voor mij ook een heel waardevolle mentor bent. Je ziet en creëert kansen, je stimuleert, je uit vertrouwen, je bent back-up waar nodig en je bent er voor advies. Mede daardoor heb ik durven groeien als onderzoeker. Maar, geen zorgen, ook je wetenschap inhoudelijke opvoeding lijkt geslaagd: ik hoor mijzelf (soms iets té) vaak afvragen “maar wat is nou de vraag?!”. Geert Jan, dankjewel voor alles.

Beste **Jaco**, na iedere nieuwe uitleg poging van jou begreep ik de MRI, de sequenties en je “kleine vaten maat” weer een beetje beter. De fysica blijft voor mij een grote uitdaging, maar dank voor je geduld! Dank ook voor je hands-on hulp wanneer we vastliepen bij de scanner. Samen scannen gaf ook gelegenheid om elkaar persoonlijk beter te leren kennen, zoals ook tijdens je schrijfretraites. Super leuk dat ik daarbij aan mocht sluiten!

Beste **Jeroen**, wat ben ik blij dat je in de loop van mijn PhD ook bij mijn promotieteam bent gekomen! Ik zie mezelf nog zitten in je kantoor samen met Tine, smoesjes zoekend om maar niet te hoeven coderen omdat ik dacht dat ik het niet kon. Totdat ik er achter kwam dat ik het eigenlijk hartstikke leuk vond. Jouw hulp en vertrouwen hebben hier zeker aan bijgedragen, dus onwijs bedankt daarvoor! Je enthousiasme was elke week weer een feestje.

Ik had het geluk om mijn promotietraject samen met de “Frietjes op Vrijdag” te beleven. Lieve **Naomi, Chloë, Bruno** en **Nick**, we hebben onze PhD van begin tot eind samen beleefd en dit avontuur was oprecht zo anders geweest zonder jullie! Lieve **Naomi**, van Master-buddies naar PhD-buddies naar vriendinnen! Ik ben benieuwd hoe vaak wij elkaar al gevraagd hebben “of je even mee wilt kijken”. Wat is het heerlijk dat ik bij jou altijd

ongegeneerd de domste vragen kan stellen, keihard kan lachen, kan klagen en kan aankloppen voor eerlijk advies. Ik ben super blij dat wij onze online hotline gewoon voortzetten, waardoor we soms even vergeten dat er inmiddels letterlijk een oceaan tussen ons in zit. Lieve **Chloë**, wij delen (onder andere) onze liefde voor oude mensen en de neuropsychologie! Dankjewel voor het meedenken met vele NPO's, maar vooral het heerlijke lachen, je lieve zachte g, je peptalks en bedankt dat je altijd een oogje in het zeil houdt zodat ik goed voor mezelf blijf zorgen. Ondertussen zetten we onze zoektocht naar de nieuwe perfect witte wijn voort! Lieve **Bruno**, aan jou hebben we de naam van onze groep te danken! Het eerste Nederlandse zinnetje dat je van ons geleerd hebt is "Frietjes op Vrijdag", en er zouden nog vele nuttige uitspraken volgen ("Of je worst lust?!" blijft mijn favoriet). Bijna ieder werkend Matlab script heb ik in meer of mindere mate aan jou te danken, bedankt voor je geduld! We hebben bovendien genoten van het mooie Utrecht*, saudade*! Bedankt voor heel veel gedeelde concerten, ijsjes, pizza's, biertjes. Lieve **Nick**, tijdens VasCog in Amsterdam werden we vrienden en sindsdien kan ik altijd bouwen op je relativering, flauwe grappen, positiviteit en je blik op menig MRI scan. Jij hebt een tomeloze energie en ik ben er zeker van dat dat je in de toekomst nog veel moois gaat brengen. Lieve Frietjes, jullie waren in de afgelopen 5 jaar al allemaal mijn paranimf; bedankt voor alles!

Er zijn natuurlijk veel meer collega's, waarvan ik er een aantal in het bijzonder wil bedanken. Lieve **Tine**, wat hebben wij een uren samen bij de scanner gespendeerd en menig chocoladereep weggewerkt terwijl wij elkaar steeds beter leerde kennen. Uiteindelijk waren we zo'n geoliede machine dat we aan één blik genoeg hadden. Dank voor alle tranen met tuiten, gelukkig meestal van het lachen, maar toch ook regelmatig om de falende scanner. Die relatietherapie met de scanner vind ik overigens nog steeds geen slecht idee ;-). In dit kader moet ik ook zeker **Fredy** en **Hans** noemen. Heel veel dank voor onnoemelijk vaak bijspringen wanneer Tine en ik met de handen in het haar naar een niet werkende 7T staarden. Als wij met ons karretje bij de scanner aan kwamen rollen begonnen de grappen al: "eens kijken waar de dames en de scanner nu weer ruzie over krijgen". Dat zelfs júllie ons scanprotocol een uitdaging vonden was in elk geval een troost. Lieve **Manja**, onze gezamenlijke behoefte aan orde maakte ons een topteam voor de SVDs@target studies! Ontzettend bedankt voor al je (gezellige!) hulp bij de participant visites en datamanagement. Prachtig om te zien hoe jij genoot van het contact met de participanten. Lieve **Stanley**, jij nam het stokje van Tine over en ook wij waren al snel een topteam bij de 7T. Door de corona maatregelen hebben wij menig avond en weekend in het UMC gespendeerd, zelfs al moesten we onze fietsen over twee boomstammen tillen om bij het UMC te komen na storm Eunice. Veel dank voor je gezelligheid, je hulp met de ZOOM@SVDs studie en voor het dealen met mijn regeldwang ;-). Lieve **Angela**, als VCI-moeder overzie je als geen ander de agenda van Geert Jan, maar zorg je ook dat alle promovendi een basiscursus bloemen en Italië doorlopen. Bedankt dat je altijd een oogje in het zeil houdt. Het thuiswerken tijdens de corona pandemie was niet aan mij besteed, bedankt voor je steun en luisterend oor! Dames van de Hart-Brein, lieve **Doeschka,**

Laurien, Sanne en **Eline**, bedankt voor het fijne samenwerken op de Hart-Brein studie, jullie hulp bij al mijn "dokters-vragen", maar bovenal voor de zovele gezellige etentjes! Lieve **Doeschka**, jou moet ik een in het bijzonder bedanken. Jouw begeleiding tijdens mijn master stage was onmisbaar als springplank naar mijn PhD. Bedankt dat je zoveel tijd en moeite wilde nemen om mij bij alle aspecten van onderzoek te betrekken en dank voor je aanmoediging en vertrouwen! Super leuk dat onze namen samen shinen op een aantal van de hoofdstukken in dit proefschrift. Lieve **Hugo**, uiteraard dank voor je hulp bij menig MeVisLab script, maar eigenlijk veel meer dank voor je adviezen, je gezelligheid en enthousiasme, de biertjes en je vertrouwen in mij op een racefiets. **Jantine** en **Esmée**, dank voor jullie vertrouwen in mij als jullie stage begeleider en veel dank voor jullie hulp bij het scannen en de BOLD analyses. Tenslotte, dank aan **Alberto, Floor, Jacob Jan, Jurre, Lieza, Malin, Matthijs, Mirthe, Naomi, Onno, Rutger, Willem, Yael** en **Yoni**. We hadden allemaal onze eigen specifieke projecten, maar er was altijd wel iemand beschikbaar voor feedback, koffie, een wandeling of biertje. Bedankt voor de gezelligheid op C3Oost en in het W-gebouw!

*I had the great pleasure to be part of the SVDs@target consortium, which was such a valuable experience in my PhD. The consortium taught me a great deal about working together over country boundaries. Dear **Prof. Dichgans**, thank you for allowing me to be part of it! Thank you also to all colleagues in the consortium. It was lovely to work with such motivated people and I much enjoyed getting to know everybody during our yearly consortia meetings in your beautiful cities. A special thank you to **Anna**, my partner in crime for the ZOOM@SVDs study. We spent endless hours on the phone trying to make any aspect of the study or our papers better. We work really well together and I think we can be proud of the results so far. I will miss our weekly Thursday morning updates, although I think that your office mates may think differently ;-).*

Al mijn **lieve vrienden** wil ik bedanken voor hun interesse in mijn onderzoek. De rationale, hypotheses en betekenis van de resultaten aan jullie uitleggen is altijd een goede en welkome test om mijzelf scherp te houden! Er zijn een aantal vrienden die ik specifiek in het kader van dit proefschrift wil bedanken. Lieve **Annemarie**, als huisgenoot heb je misschien wel het meeste van mijn PhD avontuur meekregen, vooral bij het thuiswerken tijdens de corona pandemie. Bedankt voor het meevieren van mijn feestjes, het drogen van tranen bij vreugde en verdriet en voor je oprechte interesse. Ik ben ontzettend dankbaar voor de mooie herinneringen in ons huisje aan de Cremerstraat. Lieve "cognitieve bazen", **Carlien, Eline, Elle, Kayla, Nienke** en **Rosyl**. Jullie zijn mijn onderzoeks-buddies sinds we samen onze Master doorliepen. Wat fijn dat jullie altijd snappen waar ik even advies bij nodig heb of even over moet klagen. Dank ook voor alle gezellige etentjes, wanneer ik in Nederland ben doen we snel weer dansjes! *Dear **Ricardo**, sometimes you seem to believe in me more than I believe in myself. Thank you for always being available to test my ability to explain my research to somebody outside the medical sciences. Thank you also for talking through so many thought experiments and considerations with me.*

Lieve **Wout**, na een intensieve werkdag moet je hoofd soms even geleegd worden en hoe beter dan tijdens onze zwem- of wandeldates! Bedankt voor je luisterend oor, maar met name voor je relativering. Bedankt dat je mijn PostNL punt wilt zijn en ik zie uit naar mijn logeerpartijtjes bij jou in ons stadsie. Liefste **Mattia**, door samen elke zondag de week door te nemen hebben we vele (te) ambitieuze planningen aangescherpt. Ook jij lijkt soms meer in mij te geloven dan ik in mijzelf. Ik ben super dankbaar dat je mij altijd onzelfzuchtig aanmoedigt om al mijn dromen na te jagen. Waar op de wereld ik ook ben, van mij kom je niet meer af!

Lieve **Bas**, lieve broer, we kunnen niet met en niet zonder elkaar. Je cynisme, je droge humor en je "maar Hil, je gaat er niet dood aan als het niet lukt"-reactie, werken immer relativerend in tijden van werkstress. Broertje, je bent een van de slimste en meest goeiige mensen die ik ken en ik gun je meer van het goede in de wereld (en een beetje meer peper in je achterste ;-)). Ik zie uit naar onze roadtrip samen in de VS!

Lieve **pap en mam**, als ik het met jullie over wetenschap heb dan spreken we vaak in termen van puzzelen. We weten niet hoeveel puzzelstukjes er gelegd moeten worden, of hoe de puzzel eruit moet komen te zien (net als bij die leuke Wasgij puzzels!), maar nu jullie dit lezen hebben jullie mijn bundeling van puzzelstukjes in handen! Ik wil jullie bedanken voor jullie trots en vertrouwen en dat jullie mij altijd aanmoedigen om te doen waar ik zelf blij van word. Ik vind het super bijzonder dat jullie altijd het volste vertrouwen hebben in het pad dat ik kies.

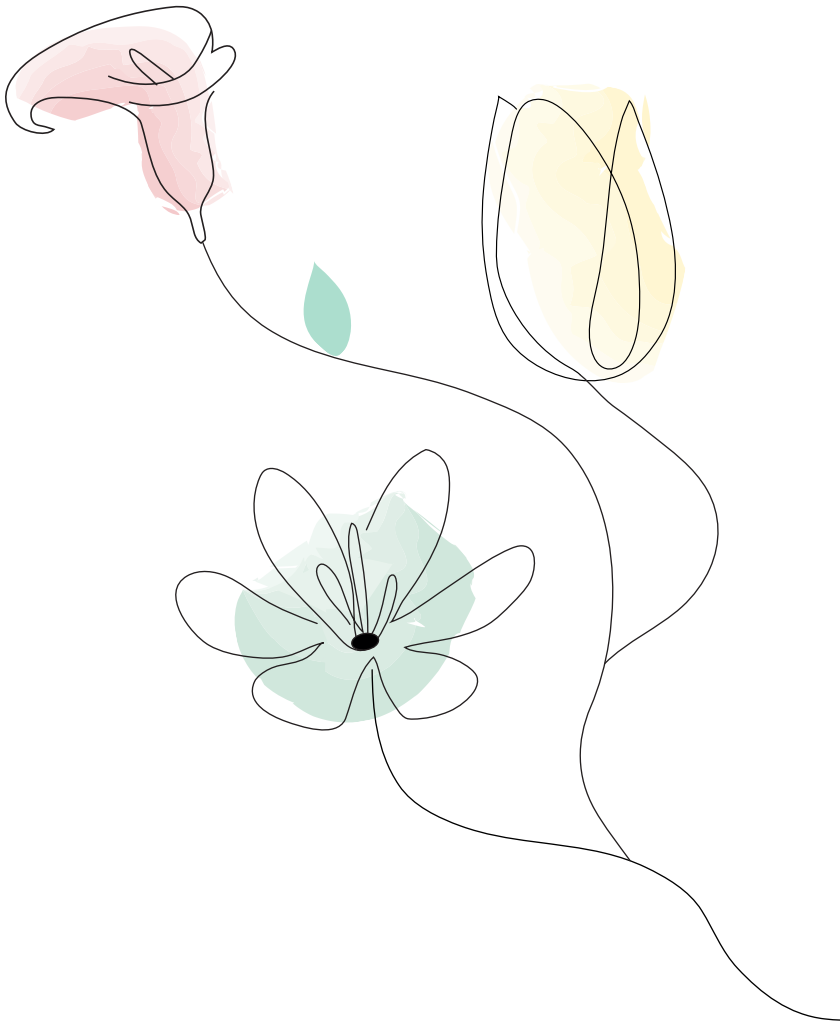

UMC Utrecht
Universiteit Utrecht
ISBN 978-94-6458-907-8